HERIOT-WATT UNIVERSITY, EDINBURGH

DEPARTMENT OF CIVIL ENGINEERING

A MODEL STUDY OF NEGATIVE SKIN FRICTION ON A FIXED BASE PILE IN SOFT CLAY

A THESIS PRESENTED TO THE

DEPARTMENT OF CIVIL ENGINEERING

FOR THE DEGREE

OF

DOCTOR OF PHILOSOPHY

AT

HERIOT-WATT UNIVERSITY

BY

TAHSIN MUNIR TOMA

BSc., MSc.

T.M.TOMA NOVEMBER 1989

ABSTRACT

In this research programme, a small-scale laboratory test was carried out to investigate the phenomenon of negative skin friction through studying the interaction between a pile and the surrounding soil and to obtain, by means of an instrumented 50mm diameter model pile, an expression for the magnitude and distribution of negative skin friction for an end-bearing pile in soft clay. The programme included measurements of pore water pressures using miniature piezometers, both vertically along the pile shaft and laterally from it, as the pattern of dissipation of this pressure controls the distribution of negative skin friction along pile length at any given time.

Two testing programmes were conducted. Each testing programme consisted of applying load increments on the soil up to 90 kPa as surcharge pressures. Pore pressures, settlements and pile loads were monitored until 90% consolidation had been achieved.

From test results, expressions relating the surcharge pressure and soil shear strength with the developed negative skin friction have been established.

The study has been extended to include predictions of negative skin friction and pore water pressures by the use of Numerical Methods such as the Finite Element Method and the Finite Difference Method. Results obtained by these methods have been compared with those measured.

DEDICATION

To The Memory Of My Father

CONTENTS

NOTATION

a	width of pile group
A_p	pile cross-sectional area
b	length of pile group
B_o	the Bessel function of order zero
c	circumference of pile
c'	cohesion intercept
C_a	unit adhesion between pile and soil
C_c	compression index
C_r	coefficient of consolidation in radial direction
Cu	undrained shear strength
C_v	coefficient of consolidation in vertical direction
C_{uo}	initial undrained shear strength
d	diameter of pile
dU	excess pore pressure
$d_{pc'}$	increment of consolidation pressure
dr	increment of radial distance
dt	increment of time
dz	increment of depth
$d_{\sigma h'}$	average change in horizontal effective stress
D	depth from ground surface to neutral point

E	Young's modulus of soil
E_p	Young's modulus of pile
f_n	partial factor of safety on the drag load
f_{ns}	shear stress mobilized as negative skin friction
f_p	partial factor of safety on the permanent load
f_Q	partial factor of safety on the ultimate bearing capacity of the pile
f_s	frictional stress along pile shaft
f_t	partial factor of safety on the transient load
G	rigidity modulus
G_s	specific gravity of soil
H	thickness of compressible soil layer
H_f	height of fill
h_i , h_j	height from incompressible stratum to elements i,j respectively
i,j	arbitrary elements along pile length
I_{ij} , I'_{ij}	influence factors for the displacement at element i due to shear stresses on the real element j and the imaginary element j', respectively
I_n	influence factor for maximum downdrag
Ip	plasticity index
J_n	the n^{th} root of the equation $B_o(J) = 0$
k	coefficient of lateral earth pressure
K	$Ep. R_A / E$

k_o	coefficient of lateral earth pressure at rest
k_m	permeability coefficient
L	depth of embedment of pile
m	factor relating negative skin friction (n.s.f) with the undrained shear strength (Cu), m=n.s.f/Cu
M	friction factor for the soil acting on the pile surface; M=tanδ'/tanø'
m_v	coefficient of compressibility
n	number of piles in a group
N_T	correction factor for effects of delayed installation
P_a	axial force on pile head
P_c'	consolidation pressure
P_o'	initial effective overburden pressure
P_j	uniform vertical shear stress
P_n	maximum downdrag load
P_{oz}'	initial effective vertical pressure at depth z
P_p	permanent load
P_{pos}	positive skin friction resistance
P_t	transient load
P_{vz}'	reduced effective vertical pressure at depth z
q	surcharge pressure
Q1	downdrag force caused by the fill
Q2	downdrag force due to pierimeter shear within the fill and the clay

Qu	ultimate bearing capacity of a pile
Qu_{tip}	pile tip resistance
Qu,a_{skin}	positive skin resistance in the non-settling soil
Qu,b_{skin}	positive skin resistance in the settling soil
r	radial distance from pile surface
R	$(1-2\mu)(1+\mu) / (1-\mu)$
R_A	$4 A_p / \pi d^2$
s	spacing of piles, centre to centre
S_i	consolidation settlement at element i
S_o	maximum (final) consolidation settlement at soil surface
SS_i	settlement at element i due to shear stresses at the pile surface
S_{ult}	displacement required to reach the ultimate shear strength value
t	time between commencement of consolidation and the time being considered
t_e	elapsed time since pile driving
t_i	thickness of interface element
t_o	time between commencement of consolidation and installation of pile
Tr	time factor for radial consolidation
Tv	time factor for vertical consolidation corresponding to (t)
Tv_o	time factor for vertical consolidation corresponding to (t_o)

Uav	average degree of consolidation
U_n	degree of development of downdrag
Ur	degree of consolidation for radial drainage only
Uz	degree of consolidation for vertical drainage only
V_{ij}	$4.L.h_j/n.d$ for $i \leq j$ $4.L.h_i/n.d$ for $i < j$
W	moisture content
Wl	liquid limit
Wp	plastic limit
z	depth below ground surface

α	adhesion factor
$\alpha_{initial}$	adhesion factor corresponding to initial undrained shear strength
$\alpha_{calculated}$	adhesion factor corresponding to the calculated undrained shear strength

α_H	minimum depth of clay beyond which no downdrag exists	pages 30 and 31
α_{Pc}	downdrag due to consolidation under self weight of clay	
α_W	minimum water content beyond which no downdrag exists	
$\alpha_{\gamma d}$	coefficient relating P_n with γ_d	

β	effective stress coefficient, $\beta=k.\tan\phi'$	
β_H'	slope of P_n-H relation	pages 30 and 31
β_{Pc}'	slope of P_n-P_c' relation	
β_W	slope of P_n-W relation	
$\beta\gamma_d$	coefficient relating P_n with γ_d	
δ'	effective friction angle between pile and soil	
ϕ'	effective friction angle of the soil	
γ_d	dry unit weight of soil	
γ_f	unit weight of fill	
γ_{sub}	submerged unit weight of soil	
γ_w	wet unit weight of soil	
μ	Poisson's ratio of soil	
μ_p	Poisson's ratio of pile	
σ_h'	effective horizontal stress	
σ_{ho}'	minimum principal effective stress	
σ_v'	effective vertical stress	
τ	shear stress	
τ_{p-s}	ultimate frictional resistance between pile and soil	
Θ	$C_v.dt/(dz)^2$	
Ω	r/dr	
Φ	$\gamma_d.H/P_c'$	

LIST OF FIGURES

LIST OF TABLES

ACKNOWLEDGEMENTS

Whatever achievement this work represents, it would be meaningless and empty without the love of my father and mother, their constancy, patience and encouragement. To them I give my thanks and love.

I would like to thank Dr. John Little for his supervision, guidance and valuable ideas which helped completing this work.

I would also wish to thank Mr. Evan Pole, my previous supervisor, for the continous assistance and guidance which he provided throughout his supervision period.

My thanks are given to Professor A.D. Edwards, formerly Head of the Department of Civil Engineering for the provision of facilities to enable the research completion.

Sincere regards are due also to the Departments' workshop Technicians for the manufacture, to exacting standards, for all the elements contained in the experiments described herein. Special thanks go to Mr. Hugh Barras for his unfailing assistance throughout the course of the study.

The author is grateful to the University of Edinburgh/Civil Engineering Department in providing their computer facilities for use of LUSAS. Special thanks are given to Mr Khalid El-Deeb for his valuable advice and assistance in this aspect of the work.

Many thanks go to my friends and colleagues particularly to Khuloud Totah and Nourredine Benlakehal for their sincere help.

The author wishes to express his gratitude to the Iraqi Government - Ministry of Higher Eduacation for financial support during the course of the study.

CHAPTER (1)

INTRODUCTION

It is well known that if a good bearing stratum does not exist near the ground surface or at a reasonably shallow depth, the load from the superstructure is quite often transmitted to a deeper dense or hard stratum by means of piles. As a general procedure for pile load calculations, one part of the load acting on a pile is transferred to the soil along the shaft and the other part is resisted by the soil located beneath the pile point. The subsequent consolidation modifies the primary load distribution as well as the stress-strain characteristics of the soils located along the pile shaft and in the zone of influence under the point. This phenomenon may be caused either by an increase of the total pressure in the case of external surcharge loads ,or by changes in the pore pressure in the soil mass after driving, or by phreatic level variations or pumping from wells under practically constant total pressure. In both cases the effective pressure varies with time. The magnitude and direction of a load transference along the pile shaft depends on the relative movements between soil and pile. These movements are influenced by the nature of the soil

strata located under the point of the pile. When a pile moves downward with respect to the soil then the shear stresses act in a way to resist this movement induced between the pile and the soil (positive skin friction). On the other hand negative skin friction or downdrag occurs when the soil moves downwards with respect to the pile shaft. Negative skin friction can therefore, be defined as a downward force acting on a pile as a result of a relative vertical displacement between the pile and the surrounding soil. Downdrag load on piles can be quite high and in some cases may exceed the load resulting from the superstructure. The commonest cause of negative skin friction is ground subsidence due to an increase in the vertical effective stress resulting from the addition of surcharge pressure but may also be induced by the lowering of the natural ground water table. Consolidation of the soil around a pile caused by the remouldind of the clay during pile installation may also create downdrag forces.

The realisation and importance of such drag loads on piles dates back to 1914 (ALDRICK, 1970), but investigations into this problem have attracted serious attention only in the past two decades. Because it reduces the safe working load of the piles and increases their settlement, the phenomenon has even been referred to as the "Silent Enemy" of pile foundations (Van Weels, 1964).

1.1 Case Records :

Negative skin friction, when not recognised or sufficiently accounted for in design has led to foundation failures (Chellis, 1961). A number of failures in different parts of the world attributed to negative skin friction have been described in the literature. The following are some of the examples which were encountered:

(1) A case in Holland where a factory building was damaged due to negative skin friction has been described by Miller (1938). Wooden piles with a length of 20m were driven through 5m of fill (sand) and 13m of clay and peat into a layer of fine sand. The building settled 700mm in four years. The increase of the load in the piles due to negative skin friction was estimated to be 150 kN/pile. The building had to be underpinned.

(2) The well-known large magnitude of the regional subsidence of the subsoil of the Mexico Valley makes negative skin friction an important factor to be considered in deep foundation design in that region. An entire Special Session was devoted to discussions on the investigations of this particular problem in the 7th International Conference of Soil Mechanics and Foundation Engineering held at Mexico in 1969. Zeevaert (1973) described several cases in Mexico city where the effect of negative skin friction had caused damage to several

buildings due to large differential settlement. The piles along the perimeter of the pile groups caused the buildings to tilt because of uneven settlement. The settlement was caused by a lowering of the ground water level due to water extraction by pumping.

(3) A concrete structure supported on composite piles (concrete and timber) in Thailand had been damaged by the effect of negative skin friction, as described by Brand and Luangdilok (1975). The 18m to 21m long piles were driven through 15m of soft clay. A 1.5m thick sand fill had been placed around the structure. It was concluded that the differential settlements of the structure were caused by negative skin friction induced by the surcharge effect of the fill and from a lowering of the ground water level.

In general negative skin friction has two major effects. First, it increases the axial load in piles. Secondly, it reduces the overburden pressure both along the pile shaft and at the level of the pile point and thereby affects the bearing capacity, (Zeevaert,1973). Among the various factors that would affect the ultimate drag load are : (a) the properties of the soil around the pile or pile group, i.e, compressibility, permeability, shear strength and thickness of compressible layers. (b) the surcharge load and the change of the ground water level. (c) the properties of the pile, i.e, roughness of the pile surface, configuration of the pile group, length

and spacing of piles, and compressibility of pile material. (d) the end-bearing conditions at the pile tip. (e) the influence of pile installation on the soil.

Driven piles in general and displacement piles in particular tend to destroy the soil fabric and remould the soil near the periphery of the pile, inducing excess pore pressures. This affected zone, on dissipation of the pore pressure, consolidates and induces a drag load the amount of which depends, among other factors, on the amount of consolidation which takes place in the remoulded layer, on the width of the remoulded zone, and on the stress-strain relationship in shear for the soil or soils in which the piles are embedded.

1.2 Negative Skin Friction And Estimation Theories :

As an outcome of a symposium on negative skin friction held in 1973 at the Massachussettes Institute of Technology, Garlanger and Lambe indicated that one of the greatest uncertainties in the design of piled foundations is the calculation of the load transfer on piles subjected to negative skin friction. The purpose of the symposium was to compare different methods of predicting negative skin friction on a steel H-pile for the Cutler Circle Bridge, Massachusetts. Different methods were used by seven prominent engineers. The negative skin friction was evaluated by measuring the rebound of the pile when an electric current was passed through the pile(electro-

osmosis) and the pile was freed from the surrounding soil. A substantial difference amounting to 100%-300% between the calculated and the measured downdrag loads was reported. These wide variations of the predicted results strongly suggest, as described by Garlanger and Lambe, that the fundamentals concerning downdrag are not well understood and the symposium put the proper perspective on the difficulty of predicting pile load values with confidence.

Chapter 2 offers a detailed discussion on the symposium along with the comparisons of both predicted and measured results.

In spite of the difficulty in predicting pile load values with confidence, there are still some conservative methods which are used in this context, namely 1) the total stress method, and 2) the effective stress method. These have and still are used in estimating negative skin friction for both single and groups of piles.

Elastic and elasto-plastic analyses using finite element procedures have also been used for the same purpose by Poulos and Davis (1972) and Walker and Dravall (1973) among others. Summaries of available methods for predicting negative skin friction or downdrag on piles are given by Fellenius (1969). The literature indicates, as will be shown in Chapter 2, that very simple to highly complex theoretical approaches have been suggested for the calculation of downdrag on piles and at the present time there is no ideal solution available.

1.3 Aim and Scope of The Study:

The main objective of this research study is to investigate the negative skin friction phenomenon and to provide a better understanding of the problem. A prediction method to be used in the design of piled foundations is always needed together with the effect of various parameters on the prediction procedures. It was therefore proposed to conduct a small-scale laboratory test on a model pile to study the interaction between a pile and the surrounding consolidating soil and to obtain, by means of an instrumented model pile, an expression for the magnitude and distribution of negative skin friction. The specific problem studied in this research was that of a fixed based pile surrounded by a remoulded soft clay which was consolidating under a uniform vertical pressure applied at the top of the clay. Extensive test results obtained from two testing programmes were presented and analysed.

Regarding the application of numerical analysis to the study of negative skin friction, a finite element programme was adopted to investigate the phenomenon through a model pile surrounded by a consolidating soil layer. Predictions obtained by the finite element analysis were compared with the measured results.

CHAPTER (2)

LITERATURE REVIEW

2.1 Introduction

During the last two decades a number of contributions to the subject of negative skin friction have been made in order to measure downdrag forces on piles and to provide a better understanding of the phenomenon.

In general, the effects of negative skin friction and the conditions under which drag forces are likely to develop are well recognised. However, there are still no standard or accepted procedures whereby one can estimate the amount of drag to be anticipated. This chapter therefore reviews the investigations carried out by many authors on both full-scale and model piles designed to provide new knowledge in this area.

2.2 Field Investigations

The simplest and one of the earliest methods of making an allowance for downdrag in the calculation of bearing

capacity was given by Terzaghi and Peck (1948). They suggested that the shear strength of the soil is mobilised along the full length of the individual piles or along the perimeter of pile groups thus assuming that the neutral point (a point where both pile and soil deflect the same amount) is located at the bearing stratum. Fig. 2.1 illustrates the application of this method to both a single pile and a group of piles.

In the case of a single pile, the downdrag is taken as the perimeter area multiplied by the shear strength of the soil, i.e, $P_n = f_s . \pi . d . L$, where f_s is the frictional stress along the pile shaft. For a group of piles, it is assumed that the entire weight of the fill within the cluster is taken by the piles and this is added to the perimeter shear within the fill and the clay, Fig. 2.1b.

$$Q1_{group} = \gamma_f . a . b . H_f / n$$

$$Q2_{group} = f_s . 2(a+b) . L/n$$

$$Q_{total} = Q1+Q2$$

Where

Q1: downdrag force caused by the fill

Q2: downdrag force due to perimeter shear within the fill and the clay

L : depth of embedment of pile

n : number of piles in a group

H_f : height of fill

γ_f : unit weight of fill

In order to reduce negative skin friction the spacing of the piles should be as small as permissible. A maximum value of 2.5d centre to centre of piles was suggested by the authors.

It is interesting to note that in the period between 1948 and 1969 (the year in which an international conference was devoted to the problem of negative skin friction), few publications were cited in the literature, by Gant et al (1958) and Johanessen & Bjerrum (1965). These investigations emphasized the importance of considering negative skin friction in the design of piled foundations.

Hansen (1968) proposed a method to calculate the skin friction for single piles and pile groups. A general theory was derived concerning skin friction of a floating pile being loaded and caused to settle a finite amount sufficient to mobilise friction. A review of the basic conditions and derivations of the dimensionless coefficients used can be found in the original paper. This theory was extended to cover negative skin friction. The case of a surcharge (q) being placed on the compressible layer after the piles were placed was considered. The presence of this load increased the effective vertical stress throughout the layer due to hang-up tendency caused by the presence of the pile. The vertical effective stress

was accordingly reduced close to the pile shaft and the reduction in stress was given by the expression : $4f_s$ where f_s is the frictional stress along the pile shaft for a single pile determined from a dimensionless coefficient. For a pile within a group, Hansen proposed the relation: $4f_s(1+1.7\ d/s)$, where d and s are the diameter of the pile and the centre to centre spacing of the piles respectively. Since the compression of the soil would change to expansion/ if the resulting vertical stress decreased/, the actual negative skin friction at any point of the pile will be limited by the expression : $f_s \leq q/(4+6.8\ d/s)$.

Concerning the effects of pore water pressure change on negative skin friction, Hansen postulated that a ground water lowering of "q" metres in clay will have the same effect as a surface load q t/m^2. Consequently the resulting negative friction can be calculated by means of the preceding expression. Excess pore pressures, dU, existing before the execution of the piles(or reduced by the driving of the piles) will, by their dissipation, increase the effective stresses correspondingly, and may thus produce negative friction. However, a negative friction will reduce the vertical stresses, and when this reduction is everywhere equal to dU, the negative friction cannot increase further, thus giving an upper limit of f_s as $dU/(4+6.8\ d/s)$.

The existence of a neutral point was cited by Endo, et al (1969), Fig. 2.2 who conducted tests on unloaded piles at a site at Tokyo. The soil was approximately 43m thick alluvium whose undrained shear strength varied from 89 kPa to 178 kPa at -40m. Four types of piles were used in order to determine the downdrag load difference between open and closed, friction and end-bearing piles.

Piles of 609.6mm diameter were driven at 10m spacing to avoid group action. It was reported that driving stresses were measured using wire strain gauges, yet under the test conditions "differential transformer type gauges" were used because of reliability for long durations.

Settlement records, started after the piles were driven, indicated the maximum surface settlements of 120mm/yr reducing to 30mm/yr after 3 ½ years (from time of piling). Considerable settlement, as explained by the authors, must have occurred during pile driving because of the loose fine sand stratum (Standard Penetration Test N-value of 10). Test results showed that the soil at each pile settled 118mm as compared with 172mm which was measured at a distance of 1.0m from the pile surface. That difference in settlement was attributed to the hanging-up effect of the soil around the pile. Pile head settlements were given, but no record was made of the settlement of the sand at toe level.

It would have been interesting to have known the settlements in the lower soil deposits. The settlements at toe level are of great interest when considering the

relative displacement of the pile-soil interface. Initially one would have expected a neutral point to have existed almost at that level and then decreased in depth as the low region became more compressed due to the process of consolidation.

Fellenius (1972) carried out a test programme in Sweden on two instrumented precast concrete piles driven through 40m of soft clay and 15m into underlying silt and sand. The programme consisted of two phases of study:

1) The influence of the driving and the following reconsolidation of the clay. The duration of this phase was 495 days started immediately after pile driving and up to the stage of pile loading.
2) The influence of load applied on the head of the pile which took 800 days started after load application up to the end of the measurements.

It was noticed that immediately after driving, the forces in the pile increased rapidly and the rate of load increase became linear after 5-7 months. The total downdrag load after 495 days was 55 tonnes, 30 tonnes of which corresponded only to reconsolidation of the clay due to pile driving and the rest due to regional settlement. The negative friction was compared with the shear strength as being 30% of the undrained shear strength or about 10% of the effective overburden pressure, Fig. 2.3.

After completion of the 495 days, the piles were loaded

by 44 tonnes and this was followed, a year later, by an additional 36 tonnes thus making a total load of 80 tonnes. In both load increments the negative skin friction in the upper two thirds of the piles was eliminated while the load at the bottom of the clay layer was only slightly affected. The force at the pile tip was not affected and that was attributed to the existence of positive skin friction near the pile tip in the silt and sand layers. Fellenius therefore presented a design approach which takes negative skin friction into consideration in determining the allowable load on single piles. The main feature of the recommended approach is that the permanent and transient working loads should be treated separately in connection with negative skin friction.

The bearing capacity of a single pile consists of a tip resistance, $Q_{u\ tip}$ and a positive skin resistance, $Q_{u\ skin}$ in the non-settling soil layer as shown in Fig. 2.4. After determining the ultimate bearing capacity, Q_u, the maximum drag load, P_n, can be estimated from the known strength properties of the settling soil without applying the usual reduction of the shear strength. If a transient load, P_t, on the pile head is smaller than twice the drag load, P_n; $P_t < 2\ P_n$, the transient load will not be added to the load in the lower portion of the pile, thus only the permanent load, P_p, on the pile head has to be considered. The following equation applies:

$$P_p \leq Q_{u\ tip} + Q_{u,a\ skin} - P_n \qquad (2.1)$$

Partial factors of safety were recommended by Fellenius to apply due to the different nature of the factors in the equation which therefore becomes:

$$f_p . P_p \leq (1/f_Q) . (Q_{u\ tip} + Q_{u,a\ skin}) - f_n . P_n \qquad (2.2)$$

where

f_p : partial factor of safety on the permanent load, P_p.

f_n : partial factor of safety on the drag load, P_n.

f_Q : partial factor of safety on the ultimate bearing capacity of the pile, Q_u.

When the transient load is larger than twice the drag load, positive skin friction will then develop along the entire length of the pile and Equation 2.2 becomes:

$$f_t . P_t + f_p . P_p \leq (1/f_Q) . Q_u \qquad (2.3)$$

where

f_t : partial factor of safety on the transient load, P_t.

As the drag load is normally calculated on the safe side, its partial factor of safety should on most occasions not exceed 1.0. The other partial factors of safety must be chosen according to the requirements in each case.

Bozozuk (1972) carried out an investigation using a 300mm diameter and 49m deep hollow steel pipe pile which was instrumented and driven vertically on the centre-line of a 9m high by 27m wide granular approach fill into an underlying marine clay. The size and distribution of skin friction generated in the floating pile over a period of 5 years was reported and compared with predicted values based on insitu horizontal effective stresses and the influence of embankment loading. The unit skin friction exerted along the surface of the pile was determined from the load distribution curve and compared with the strength of the surrounding soil. Assuming plane strain conditions and using the linear elastic theory proposed by Perloff et al (1967), both vertical and horizontal stresses exerted on the foundation clay under the centerline of the embankment were determined, Fig. 2.5. Observations on the behaviour of the foundation soil under the embankment were made with six settlement gauges and four piezometers which provided measurements of settlement from the ground surface to a depth of 44m and excess pore water pressures from 6m to 27m respectively. In carrying out the prediction analysis, Bozozuk introduced the following equations:

$$f_s = M.k_o.\sigma_v'.\tan\phi' \qquad (2.4)$$

where

f_s : frictional stress along pile shaft

M : friction factor for the soil acting on the pile surface, $M=\tan\delta'/\tan\phi'$ (a value of 0.7 was selected for the type of soil at site).

k_o : coefficient of earth pressure at rest.

σ_v' : vertical effective stress.

ϕ' : effective friction angle of the soil.

δ' : effective friction angle between pile and soil

At the end of consolidation, the total negative skin friction load to depth D from the ground surface will be,

$$P_n = \beta_1 . c . D^2/2 \qquad (2.5)$$

where

D = depth from ground surface to neutral point

$\beta_1 = M . k_o . \gamma_{sub} . \tan\phi'$

γ_{sub} = submerged unit weight of soil

c = circumference of pile

The above load will be resisted by positive friction generated in the pile from D to L, where L is the depth of embedment of pile, hence

$$P_{pos} = \beta_2 . c . (L^2 - D^2)/2 \qquad (2.6)$$

where

$$\beta_2 = \beta_1 / [(L/D)^2 - 1] \qquad (2.7)$$

To determine the location of the neutral point, Bozozuk assumed that the pile carried no load in end-bearing, then for equilibrium conditions, $P_{neg} = P_{pos}$, moreover and letting $\beta_1 = \beta_2$, then

$$D = L/\sqrt{2} \qquad (2.8)$$

Regarding skin friction loads generated by the embankment, the following expressions were obtained :

$$P_n = M.\tan\phi'.c.D.d\sigma_h' \qquad (2.9)$$

$$P_{pos} = M.\tan\phi'.c.(L-D).d\sigma_h' \qquad (2.10)$$

where

$d\sigma_h'$: average change in horizontal effective stress due to the embankment load for the required depth, Fig. 2.5b

The total load generated in the floating pile was obtained by adding the values of both Equations 2.5 and 2.9 and Equations 2.6 and 2.10 for negative and positive skin friction respectively.

Field Measurements : During the 5 years period, the ground surface settled 540mm reducing to 18mm at 44m depth. The excess pore water pressure had completely dissipated to a depth of 15 m but was still quite large at 27 m. The relative movements of the pile compared with

those of the soil indicated small values in the upper part where the excess pore pressures had dissipated, reducing to zero at a depth of 15 m. Below 21 m where the excess pore pressures were high, relative movements were very large increasing to 430 mm at the bottom of the pile.

Fig. 2.6 compares the predicted with the observed distribution of load in the test pile. A good agreement was found between the predicted load of 135 tons occuring 23 m from the top of the pile with the measured 140 tons at 22 m after 5 years. It can be seen from Fig. 2.6, at 23-30 m from the top of pile, the loads were dissipated in positive skin friction at a greater rate than was predicted, indicating that the values assumed for M and ϕ' were probably too small. However, Bozozuk attributed this to the 100 % consolidation assumed in the prediction analysis, i.e., as the 100% consolidation condition is approached, the family of positive skin friction curves will fan out and reach the predicted curves.

A comparison made between the skin friction and soil strength analysis indicated that there was little relation between the negative skin friction exerted on the pile and the insitu shear strength of the soil. In fact, where relative movements between pile and soil were small and excess pore pressure had dissipated, skin friction approached but did not exceed the drained strength. On the other hand, where relative movements and excess pore pressures were large, skin friction had decreased to the remoulded strength.

A symposium on negative skin friction was conducted by the Massachusetts Institute of Technology (Garlanger and Lambe, 1973). The purpose of the symposium was to compare different methods of predicting negative skin friction on a steel H-pile for the Cutler Circle Bridge in Revere, Massachusetts. The foundation piles of one of the abutments was under duress from downdrag due to the compression of soft soils beneath the approach fill behind the abutment. Evidence that the piles had been subjected to downdrag included a 46mm differential settlement of the approach slab, settlement and cracking of the slope protection beneath the bridge and backward tilting of the abutment. The soil profile consisted of 7.6m high approach fill overlying 4.0m of sand followed by 15.2m of soft clay and a dense to very dense glacial till.

Because the piles had not been instrumented prior to driving, a detailed programme was planned and carried out to measure the downdrag load indirectly. One of the foundation piles was cut from the pile cap, the negative skin friction in the pile was released by breaking the soil-pile bond through electro-osmosis. The elastic rebound of the pile was recorded and used to back-figure the downdrag that had been in the pile.

Given the data that were available regarding the project, and before the pile downdrag was measured, six engineers of outstanding reputation were asked to predict

the elastic rebound and downdrag load and the total load in the pile at several levels. These were : Dr. D.J. D'Appolonia, Dr. M.I. Esrig, Mr. G. Perez Guerra, Dr. E.H. Davis (with Dr. H.G. Poulos), Dr. J.E. Garlanger and Mr. J.A. Focht. The field results had been sealed and were not revealed until after the predictions had been presented at the symposium. It was noticed that all of the predictors used the same approach, however, there were differences of opinion related to determination of the structural load, determination of the maximum negative skin friction, determination of the vertical effective stress and behaviour of the bearing layer. Results of the predictions were as follows :

1. The measured load at the pile top was two to three times as great as the predicted loads. Other predictions agreed more closly with the measured results.

2. The predictions of the structural and the downdrag loads were substantially different from the measured results.

3. Regarding the predictions of movements, a wide variation as much as ±100% from the measured value was noticed.

4. The effect of the till bearing layer was only considered by two of the predictors, and none of the predictors considered horizontal movements.

Tables 2.1 and 2.2 present a summary of comparisons of both predicted and measured results.

Tomlinson (1975) proposed a design method concerning negative skin friction of single piles. Two cases were reported as shown in Fig. 2.7. The first case, where a pile is driven into a relatively incompressible layer, is shown in Fig. 2.7a, while in Fig. 2.7b, into a compressible layer. The settlement at the ground surface is assumed to be of an appreciable amount in order that the maximum negative skin friction can be mobilised. The relative movement between the soil and the pile, for soft clays, required to initiate maximum negative skin friction is, as stated by Tomlinson, approximately 1% of the pile diameter. The maximum negative skin friction in Fig. 2.7a is assumed to be fully mobilised at a distance 0.1H above the incompressible stratum.

The pile in Fig. 2.7b has been driven into a compressible stratum, e.g. stiff clay. Only the top part of the pile will then be subjected to negative skin friction. Tomlinson suggested that a pile should be designed for negative skin friction down to a depth where the settlement of the soil corresponds to the axial displacement of the pile, i.e., down to the neutral point.

It should be noted here that the work described by Tomlinson was based on the mobilisation of skin friction with depth due to the relative movement between pile and soil and this can be visualised as follows:

When surcharge pressure is applied to the soil, the movement of the ground surface will mobilise the peak skin

friction whereas the movements at lower levels would not have been such as to mobilise the peak value. Now if a load is superimposed on the pile above ground level the pile will compress elastically and the peak skin friction, at the top, will then drop into a "residual" value. This suggests that the peak value of negative skin friction will not at any time act on the whole length of the pile. However, as the magnitude of downdrag mobilised along the pile shaft is time dependent, it is in the present writer's view that the method described above can be used as a first guess of predicting downdrag forces depending on the calculated settlements of both the pile and the soil, assuming 100% consolidation.

An observation of the development of negative skin friction and its variation with time during four years period has been carried out in Mexico by Auvinet and Hanell (1981). The well known regional subsidence of the subsoil of the Mexico valley and the large settlement registered, mainly due to water pumping, makes negative skin friction an important factor to be considered in deep foundations design in that region.

Instrumented precast concrete piles were driven through 32m of highly compressible clay affected by intense pumping-induced consolidation. Two piles were used, a 30.5m friction pile and a 32m point-bearing pile which rested on a thin sandy layer. The piles, which comprised

three sections each, of triangular cross section, were built and instrumented with eleven load cells. The load cells consisted of steel pipes 152mm in diameter welded to two triangular 16mm steel plates. On the pipes, strain gauges were welded as shown in Fig. 2.8. Instrumentation of the subsoil, installed before the piles were driven, included benchmarks for recording vertical settlement at different elevations and piezometers. Test results showed that each year, during the rainy season, a significant heave of the surface was observed which caused the soil to move upwards with respect to the upper part of the piles. The authors argued that this would affect the negative skin friction distribution by developing a second neutral point. Fig. 2.9 shows two different friction distributions which were expected by the authors depending on the period of the year. Regarding the friction pile, the effect of the periodic behaviour was observed as the downdrag loads increased during the dry seasons and decreased during the rainy seasons. A maximum downdrag load of 210kN was registered in the middle of the pile nearest to the neutral point. It is interesting to note that a small but clear reduction of downdrag loads (about 20% of the maximum load) was registered as a consequence of an earthquake.

Concerning the point-bearing pile, and as shown by settlement records, the pile penetrated through the sand layer and behaved as a friction pile. A maximum downdrag load of 320kN was registered, however the authors

indicated that a great similarity existed between the behaviour of the point bearing pile and the friction pile. The periodic reductions and final vanishing of the downdrag loads were also similar for both piles. The reduction of downdrag loads due the effect of the earthquake was larger for the point bearing pile.

The maximum friction per unit area in both piles was registered during the dry seasons and the figures were compared to three different formulas by different authors, for negative skin friction estimation, i.e., 1) Kerisel (1965), 2) Zeevaert (1973) and 3) Kerisel (1976). It was concluded that when predicting negative skin friction values according to the total stress method, $f_s = \alpha Cu$, an adhesion factor value (α) of 0.8 would be in good agreement with the measured values.

In his paper "Bearing Capacity Of Pile Preloaded By Downdrag", Bozozuk (1981) reported further work relating to that first published in 1972. In the first paper he reported the results of an instrumented 49m long steel pipe pile driven through a highway embankment into a deep compressible marine clay. Ten years after pile driving the accumulated peak downdrag load was 1.52MN. After the pile was filled with concrete, a comprehensive load-testing programme was carried out to examine the load-carrying capability of the pile. Bozozuk suggested, and then showed, that the locked-in negative skin friction can

be considered as stored energy that can support transient or short-term live loads. The test programme was divided into three phases :

(1) Investigation of the performance of the prestressed friction pile loaded to Pn/3, 2Pn/3, and Pn (Pn=1.52MN), over a period of 11 days.

(2) Investigation of the performance of the pile loaded to 2Pn/3, 4Pn/3, and 2Pn over a period of 7 days.

(3) Subjecting the pile to a series of cyclic loads to investigate the effect on shaft friction.

Considering (1) above the first and second loading increments were applied and maintained for only 17 and 19 hours respectively since no additional settlements were detected over those periods of times. The third loading increment was applied and maintained for 6 days. Results showed that all the load increments were carried by the prestress in the pile. For the 3rd load (1.52MN), there was an indication of development of positive skin friction in the upper portion, Fig. 2.10. It should be noted here that the rate of settlement, at this last load, was greatly increased indicating that if this load was applied for a long period of time, positive skin friction could eventally be mobilised along the whole length of the pile. On applying the load increments in (2) above, it was noticed that the last load increment of 2Pn=3.06MN could not be maintained without causing excessive settlement of the pile. At this stage of loading it was also clear that positive skin friction was mobilised down to the neutral

point, Fig. 2.10. Regarding the third loading phase, (3) above, it appeared that cycling the load about 10 times within a stress range of ± 1/3 of Pn had very little destructive effect on the load carrying capacity of the preloaded friction pile.

Based on these observations Bozozuk concluded the following:

(1) The 1.52MN downdrag load which developed in the floating friction pile over a period of 10 years could be considered as a prestress that is capable of responding to transient, cyclic and short-term live loads.

(2) Applied axial loads equal to or less than Pn, where Pn is the maximum downdrag carried by the pile, can be supported for one month if a displacement to pile diameter ratio of 1.2% is acceptable.

(3) To support applied loads varying from Pn to 2Pn, positive skin friction must be mobilised in the upper consolidating soil.

Bozozuk therefore presented an interesting investigation into negative skin friction by considering downdrag on piles as a stored energy which is capable of supporting transient or short-term live loads for different .times depending on the magnitude of the applied load on the pile.

A field testing programme was established in Honolulu by Clement (1984) to investigate negative skin friction

and downdrag on prestressed concrete piles in highly plastic underconsolidated silty-clay. The ability of bitumen coating to reduce negative skin friction was also investigated. The clays were soft and compressible to a depth of 43m. The rate of ground settlement due to self weight of soil was about 12-18 mm/year.

Five, 420mm dia. piles were employed in a comparative field study. Three of the piles were coated with different grades and thicknesses of bitumen to reduce downdrag while the other two piles acted as uncoated reference piles to measure the full downdrag. A 3.7m high embankment was placed over the piles to accelerate the consolidation process. Pile compression data were obtained from multi-rod extensometers installed in a central hole in each pile. From these data the distribution of downdrag forces acting along each pile was established. After six months of observations the peak downdrag values on the uncoated piles were 1620 kN. After 42 months the peak values were 3335 kN and 3380 kN. These values exceeded predictions based on a total stress analysis utilising the undrained strength and on an effective stress analysis, (the Beta method). The bitumen coatings were very effective in minimising the development of negative skin friction. In one pile with 4.8mm thick coating, the increase in downdrag load in the coated length of the pile through the soft clay was nearly zero. Another pile with 1.6mm coating also exhibited a low rate of load increase with depth. On a third pile, a less viscous coating,

3.2mm thick, was also effective in reducing downdrag. The results from the uncoated piles exceeded the predictions of negative skin friction based on the semi-empirical Beta method. Values of β of 0.47 and 0.31 were calculated from the measured load distribution.

The wide variation of β values (about 52%) was attributed to the difference in the two piles considered with respect to their lengths, location of neutral points, different average pore pressures and effective stresses acting on the piles. However, Clement summarises his conclusions by reporting that β values may vary significantly from one site to another and even within the same site. Regarding the effectiveness of the bitumen on downdrag reduction, the author recommended bitumen coating thicknesses ranging from 1.6mm to 5.0mm depending on the environmental conditions above and below ground provided that the coating remains on the pile during installation.

2.3 Model Tests:

Relatively few model tests on negative skin friction have been carried out. Below is a discussion of the work reported in the literature :

The first reported tests using model piles were conducted by Elmasry (1963) and published in his Ph.D.

thesis from the Swiss Federal Institute of Technology, Zurich. The experimental apparatus consisted of a 320mm dia. steel tank to contain an instrumented 50mm dia. steel pipe pile. The pile was driven through 500mm of silty clay and its toe was embedded in a sand layer. The clay was surcharged by means of a plate on its upper surface. A series of twelve tests were carried out with several parameters changed in order to achieve a formula for the determination of the net downdrag load.

The downdrag load was shown to be dependent upon the following parameters:-

-Surcharge pressure or consolidation pressure, P_c'

-Pile perimeter, c

-Thickness of the clay layer, H

-The Ratio $\gamma_d . H/P_c' = \Phi$

-Dry unit weight of soil, γ_d

-Moisture content, W

The value of downdrag was found to be a linear function of the following four parameters as shown:-

(a) Relating to surcharge pressure, P_c' - Fig. 2.11a:

$$P_n = \alpha_P c' + \beta_P c' . P_c' \qquad (2.11)$$

Where $\alpha_P c'$ was the magnitude of downdrag P_n due to consolidation under self weight of clay, i.e, $P_c'=0$

This linear expression was obtained from a graph of P_n

versus P_c' with corresponding values of P_n for three values of P_c', as shown in Fig. 2.11a.

(b) Relating to the thickness of clay, H - Fig. 2.11b:

$$P_n = \beta'_H (H - \alpha_H) \qquad (2.12)$$

If $H < \alpha_H$ there is no downdrag.
In all tests α_H was five times the height of the pile shoe.

(c) Relating to the dry unit weight of clay, γ_d - Fig. 2.11c:

$$P_n = \alpha\gamma_d - \beta\gamma_d \cdot \gamma_d \qquad (2.13)$$

The drag force thus decreased with increasing γ_d.

(d) Relating to the moisture content, W - Fig.(2.11d):

$$P_n = \beta_W (W - \alpha_W) \qquad (2.14)$$

Below a certain moisture content no downdrag was recorded as shown in Fig. 2.11d.

Combining the above four relations and by using dimensional analysis and π-theory, Elmasry developed an empirical formula for determination of the total downdrag force on a pile, P_n. His equation is in the form,

$$P_u = \alpha_P c' + 0.416(2.P_c'.H.c - 0.7.\Phi^2.(W.P_c'^3/Gs.\gamma_d)) \quad .. \quad (2.15)$$

Where

$\alpha_P c'$: drag force due to consolidation under self weight and is determined by the equation $\alpha_P c' = c.H.\tau_{P-S}$ where τ_{P-S} is the frictional resistance between the pile and soil, and was given as 30% of the shear strength of the clay at the final stage of consolidation.

The work described by Elmasry provides a useful relationships between downdrag forces and various soil parameters. However, as one type of soil was used, it is unlikely that Equation 2.15 and the parameters obtained from the experimental tests can be universally applied to problems involving different soils.

Silva (1966), used a 76mm diameter thin walled aluminium tube which was placed at the centre of a 1.17m diameter steel tank, Fig. (2.12). A remoulded clayey silt was used as the consolidating medium. The effective depth of clay was approximately 1.19m. Drainage was provided at the top and bottom by means of sand layers and drain outlets. A uniform pressure was applied to the upper surface of the soil medium by means of a large pressurised rubber balloon bearing against a steel cover which in turn was held by a tension rod system to the base of the tank.

In order to measure pore water pressure, twelve pore pressure piezometers were embedded in the soil at two different levels. The piezometer tips were attached to the ends of 3mm outside diameter saran tubes which were placed horizontally by penetrating the tank side through small holes. Three settlement plates were also installed at the top of the clay to detect the soil surface settlement. These plates were attached to 1.6mm rods which passed through the bottom of the tank to micrometer dial indicators. The pile was cut longitudinally on one side and opened up with clamps in order to get access to the inside surface for the strain gauges to be installed. The pile was then closed up and welded at certain positions between gauge stations. The remaining cut was filled with epoxy adhesive. SR-4 type strain gauges were applied to the inside surface of the pile at 13 locations at approximately 100mm centres. A full bridge circuit was used to gain maximum sensitivity.

Before starting the test programme, the clay was remoulded at a moisture content well in excess of its liquid limit (W= 38% , WL= 31.6%) and placed by hand. The pile and settlement rods were installed prior to filling the tank with clay. The test programme included loading the soil in three stages. The 1st stage started 10 days after clay placement. The surcharge pressure was 17.3 kPa and was maintained for 28 days, then the surcharge pressure increased to 55.3 kPa and was maintained for 35 days. The last surcharge pressure was 124.4 kPa which was

maintained at this level for 52 days. After each loading stage the tank cover was lowered by tightening the tie rods.

An extensive soil testing programme was carried out after completion of the 3rd loading stage. This included classification tests, moisture content, triaxial tests, consolidation tests,...etc. Graphs of total downdrag loads at various depths were obtained from the values recorded by the strain gauges. These total drag load curves were numerically integrated to obtain frictional stresses versus depth relationships, Figs. 2.13a, 2.13b and 2.13c.

Plots of pore pressure versus distance from the pile surface at different times did not reveal any significant lateral variations. As some of the readings became unreliable especially at the upper level, pressure readings at many stations were omitted. (As explained by the author, this was due to crimping of the piezometer tubes near the tank wall caused by the vertical movement of the soil).

It was shown by Silva that the neutral point tended to move upwards as consolidation continued. It also appeared that a positive frictional zone at the bottom was created by the settlement of the pile toe. The author indicated that it was possible for the pile toe to have settled 0.22mm due to the load cell itself and the sub-tank load bearing structure, and yet only about 0.025mm of relative movement was required between pile and clay to cause

significant values of adhesion.

On the basis of these findings, Silva proposed a method for calculating downdrag which makes allowance for the existence of positive frictional stresses. The method requires that the neutral point be estimated and the approximate drag load calculated, assuming a linear relationship between effective stresses and depth. The pile compressions and soil displacements are computed from the data and the portion or element where the relative displacement is near to zero locates the neutral point.

The above work by Silva was examined in some detail by the present writer since in his view this work represents a realistic model assessment of downdrag.

Laboratory investigations using 25mm diameter model piles have also been carried out by Koerner and Mukhopadhyay (1972) in an attempt to evaluate various aspects of negative skin friction. The influences of pile batter, pile group spacing, soil water content, and pile material on negative skin friction were included in the investigation. A medium plasticity clayey silt was placed into a 0.9m diameter by 0.9m deep steel tank, Fig. 2.14. A jacking system was used for surcharge load application. Dial gauges were placed on the load plate for measuring surface deflections. The 25mm diameter steel pile, which was instrumented with 10 strain gauges, was placed through

a centre hole in the surcharge plate and was fixed to a proving ring and then to the reaction frame. The test programme comprised the following:

(i) Negative Skin Friction Behaviour:

The results of this phase of study showed that at low surcharge, hence low surface deflections, the entire downdrag force was carried in the upper portion of the pile. As surcharge increased, this force descended deeper along the pile until it reached the bottom, Fig. 2.15.

(ii) Effect of Pile Batter:

Fig. 2.16a shows the results of this study. It was shown that an increase in the amount of batter increased the average negative skin friction. That response, as described by the authors, is contrary to the only known comparison made in the field. Endo et al (1969) have compared a vertical pile to one placed at a 1:7 batter, and the result was a 16% reduction in negative skin friction in the case of the battered pile. No discussion as to the reason for this response was offered.

(iii) Effect of Pile Group Spacing:

Nine concrete piles in a 3 x 3 group were used. Spacing to diameter ratio (s/d) was varied at 1, 1.5, 2, 3, and 5. The results shown in Fig. 2.16b are for average negative skin friction at maximum, 1/2 maximum, and 1/4 maximum surface deflections. A distinct break in the

curves at about s/d = 2.5 was noticed. For smaller s/d ratios, the negative skin friction values rapidly decrease. The three curves showed that this trend is consistent over the entire range of average negative skin friction values and does not just occur at the limiting value. The value of s/d = 2.5 was in fact suggested by Terzaghi and Peck (1948) as being the recommended pile group spacing that is practical and yet would minimise negative skin friction.

(iv) Effect of Water Content and Pile Material:

Piles made of three common pile-forming materials (wood, concrete, and steel) were installed and tested simultaneously. All pile materials showed increased average negative skin friction with decreasing water content. On the other hand, tests on the effects of pile material on negative skin friction were not conclusive.

Nicholls (1973) carried out several tests using model piles, end-bearing in a sand stratum, within a compressible layer of clay surcharged with a layer of loose sand. The compressible clay layer causing negative friction on the piles was a remoulded kaolin clay installed at a water content of 55% (liquid limit=64%) and of a depth of 457mm. Surcharge loading was achieved by placing 305mm of loose dry sand on the top surface of the clay. The test programme included testing four single

piles and also a group of 13 piles to investigate the axial load distribution within the group. The single piles were constructed of brass and were of diameters 25.4mm, 31.7mm, 38.1mm, and 50.8mm. In all cases the pile toes were embedded in the lower sand layer to a depth of 175mm. With the exception of the compound pile, all piles had three axial load measurement cells. The load cells were positioned at the bottom of the surcharge sand, the bottom of the clay layer and at the pile toe. They consisted of hollow cylindrical shells with slotted walls 19mm diameter and 38mm long. Each shell had eight electrical strain gauges cemented on the outer wall.

The compound 38.1mm diameter pile contained 16 load cells and was developed to investigate the load depth relationship and to attempt a further understanding of the development of a neutral point with time by measuring the axial loads in the pile shaft throughout the complete length of the pile. Soil settlement was measured by using small wire mesh plates at the required depths. Thin fibre glass cord was attached to the plates and taken vertically to the overhead beam. Single pile tests were conducted in 763mm internal diameter pipe sections each 610mm high. Two sections were used and placed together so that the top of the clay coincided with the top of the upper pipe section. Pile group tests were carried out in a 1.25m internal diameter set of rings also 610mm high. A surcharge was placed within a split steel ring 305mm high which was placed, with suitable clamps, on top of the

concrete rings. Fig. 2.17 shows the testing arrangement.

Five series of tests were conducted in the research programme. Test No.1 included testing of three single piles, 25.4mm, 31.8mm, and 38.1mm in diameter. The sand surcharge pressure was 5.1 kPa. Forty one days after placing the fill an additional surcharge (cast iron weights) was placed, thus increasing the consolidation pressure to 9.0 kPa. The duration of the test was 66 days.

Test No.2 included testing of two single piles: a 50.8mm diameter pile and a 38.0mm diameter compound pile. The initial consolidation pressure was 4.3 kPa. After 22 days the surcharge pressure was increased to 8.2 kPa. Fig. 2.18 shows the axial loads recorded in the compound pile for different time intervals. The duration of the test was 86 days.

Test No.3 included testing of three single piles, 25.4mm, 31.8mm, and 38.0mm diameter. The consolidation pressure of 4.5 kPa was increased after 106 days to 8.4 kPa. The duration of that test was 164 days.

Test No.4 was devoted to testing a group of 13 piles each 31.8mm in diameter and at spacing of three pile diameters. The group configuration is shown in Fig. 2.19.

Test No.5 included testing of 31.8mm, 38.0mm, and 50.8mm diameter piles together with a 38.0mm compound pile. The consolidation pressure was 4.4 kPa and no additional surcharge was applied. The test duration was 49 days.

The test results are presented below :

(1) Downdrag- Sand Surcharge :

The majority of piles recorded a rapid build up of load and then a much reduced rate of increase as a limiting value was reached. A summary of downdrag loads caused by the sand surcharge is shown in Table 2.3. It is quite apparent that the piles in test No.1 recorded higher loads. That was attributed by the author to the fact that the sand had been compacted by rodding twice (presumably instead of just once). Regarding the relationship between pile diameter and magnitude of downdrag loads, results showed an increase of load with a large pile diameter.

(2) Downdrag- Clay :

In this series of tests all loads recorded on the piles were only due to the effects of downdrag within the sand surcharge and the clay layer; there was no pile head loading. The downdrag caused by the clay itself was obtained by deducting the contribution due to the sand surcharge. All piles, except the compound one, did not register the maximum axial loads apart from those existing at the bottom of the clay layer. Results from the compound pile tests, Fig. 2.18, revealed a maximum load occurred above the base of the clay layer. Table 2.4 shows the results of downdrag in the clay layer. It was observed that the increased consolidation pressure, caused by the addition of surcharge, yielded a significant

increase in the total downdrag recorded. For an increase in consolidation pressure of 82% the total downdrag load increased by 18% for piles in test No.1, 65% for piles in test No.3, and 67% for piles in test No.2.

(3) Downdrag with Depth- Compound Pile :

The compound pile was tested in tests No.2 and 5. Within the clay layer itself both tests yielded similar relationships between axial load and depth, and indicated peak axial loading just below the mid-plane area of the clay layer. Moreover, the build up of clay downdrag does not appear to be linear. The increase of loading with depth followed a curve which achieved a significant maximum value as the mid-plane position of the clay was approached. The relationship between downdrag and depth within the clay was closely associated with the relationship between excess pore water pressure and depth which itself was considered to be essentially non-linear.

(4) Distribution of Downdrag Within the Group :

The configuration of the pile group used by Nicholls is shown in Fig. 2.19. Curves representing the total downdrag within the group is shown in Fig. 2.20. These curves clearly indicate that piles within a group are not subjected to the same amount of downdrag loading. The variation of total downdrag between the centre pile and outer corner piles was quite significant. It can be seen from Fig. 2.20 that corner piles in the group recorded the

highest total downdrag loads followed by the middle piles in the outer ring. The average total downdrag on the outer ring of piles exceeded the loading on the centre pile by 52%. The curve of sand surcharge, on the other hand, showed a reverse trend to that indicated by a total downdrag distribution. The centre pile recorded the highest sand surcharge loading followed by the pile ring. A possible explanation, given by the author, was the occurrence of arching within the group. The differential settlement within the group allows different degrees of arching to build up. The area of sand within the inner ring was subjected to less settlement than the outer ring. The increased settlement on the outer ring may reduce the arching effect on those piles, thus recording lower values of downdrag. The sand rodding showed a reduction in axial load within the sand surcharge and consequently an increase in the clay downdrag.

Some of the concluding remarks drawn from this work can be summarised below:

1. The downdrag loads increased with additional surcharge loading but there was not a simple relationship between vertical effective stress within the soil mass and the distribution of negative skin friction with depth.

2. It was assumed, for calculation purposes, that a uniform pressure was present at the clay surface when additional surcharge was applied, and that might not be the case since the additional loading was rather irregular

with respect to uniformity of pressure distribution.

3. The sand surcharge in all the tests displayed the phenomenon of arching which affected the consolidation pressure within the clay and was, on several occasions, reduced by rodding. The effects of arching were particularly noticeable in the pile group.

Model aluminium pipe piles of 38mm in diameter, 1.05m long and 2mm wall thickness were used by Narasimha and Krishnamurthy (1982) in an experimental work on negative skin friction. The piles were instrumented with electrical resistance strain gauges mounted on the inner surface of the pipes at 100mm centres. Tests were conducted in a steel tank of size (0.6 x 0.6 x 0.6)m. The central portion of the area, only 0.35m x 0.26m, was filled with clay and the remaining portion was filled with sand. A 20mm thick sand layer was provided at the bottom. The sand surrounding the clay packing was introduced to speed up the consolidation of the clay layer. A schematic diagram of the experimental set up is shown in Fig. 2.21.

In the first set-up the negative skin friction on a pile embedded in a homogeneous clay deposit was measured. A surcharge pressure of 5 kPa was applied at the top of the clay layer. It was found that nearly 60 hrs were required to achieve full mobilisation of negative skin friction. The maximum value of the force measured was 15 kN. In this set up the ratio of negative skin friction to

overburden pressure, calculated for the depths at which maximum negative friction was mobilised, was 0.33.

During the 2nd set up, the drag force on the pile in a two layer deposit with sand overlying was investigated. Two different surcharge loading conditions were conducted. The ultimate values of negative skin friction were realised much faster in this series with the time taken being 26 hrs. The rate of increase of drag force was much more in the overlying sandy layer than in the clay layer. The maximum force being recorded by the gauge located at the bottom of the sand layer. The settlements measured at the maximum drag forces were of the order of 1.9mm and 3.4mm for 2.5 kN and 5.0 kN surcharge loads respectively.

2.4 Analyses Based on Theory of Elasticity :

In calculating negative skin friction by the elastic method it is assumed that the soil behaves either as an ideal elastic material or as an elasto-plastic material. Early elastic analysis based on integral equation methods were provided by Salas and Belzunce (1965) and Begemann (1969). Since then more extensive work regarding the application of numerical techniques on pile foundations has been conducted by Poulos and Mattes (1969), Poulos and Davis (1972, 1975), and Butterfield and Banerjee (1978) amongst others.

Below is a discussion of the elastic solutions presented by Poulos and Mattes (1969) and Poulos and Davis (1975) regarding downdrag analysis in end-bearing piles.

Poulos and Mattes (1969) performed an analysis of the effects of negative skin friction on a single compressible pile of circular cross-section. The tip of the pile was assumed to rest on a perfectly rigid base, and the surrounding soil was assumed to be an homogeneous isotropic elastic material. A pile of length L and outer diameter d was considered and divided into n equal cylindrical elements, Fig. 2.22a. The area of the pile section is A_p, and element j is acted upon by a uniform vertical shear stress P_j on the periphery. The surrounding soil layer was assumed to have constant elastic parameters E and μ, where E is the Young's modulus and μ is the Poission's ratio. It was also assumed that the consolidation settlement of the soil remote from the pile varied linearly with depth from S_o at the surface to zero at the base of the layer, Fig. 2.22b.

The problem was solved by equating the displacement of the soil adjacent to the pile to that of the pile itself at various points along the pile. The settlement of the soil is determined from both the shear stresses along the pile and from the consolidation of the soil itself.

From Fig. 2.22a, the settlement at element i (SS_i) due to the shear stresses along the pile was expressed as:

$$SS_i = \frac{d}{E} \sum_{j=1}^{n} P_j \, (I_{ij} - I'_{ij}) \qquad (2.16)$$

where

I_{ij} , I'_{ij} = Influence factors for the displacement at element i due to shear stresses on the real element j and the imaginary element j', respectively.

Both I_{ij} and I'_{ij} are obtained by integration of the Mindlin equation (Mindlin, 1936) for the vertical displacement of a point within a semi-infinite mass.

Referring to Fig. 2.22b, the displacement at element i due to consolidation of the soil is S_i, therefore, the net downward displacement of the soil at element i is :

$$SS_i\,(soil) = S_i - \frac{d}{E} \sum_{j=1}^{n} P_j \, (I_{ij} - I'_{ij}) \qquad (2.17)$$

In calculating the displacement of the pile itself, the authors considered pure axial compression only. From Fig. 2.22c, the displacement of the pile at element i is expressed as :

$$SS_i\,(pile) = \frac{1}{E_p \, . \, R_A} \sum_{j=1}^{n} P_j \, . \, V_{ij} \qquad (2.18)$$

where

R_A = $4A_p / \pi d^2$

= the area ratio (for the case of a solid pile, R_A=1)

A_p = area of pile section

$V_{ij} = 4L.h_j/n.d$ for $i \leq j$

$= 4L.h_i/n.d$ for $i < j$

E_p = Young's modulus of pile material

h_i & h_j are defined in Fig. 2.22c

If no local yield occurs between the pile and the soil, the displacements of the pile and soil at any point are equal, and thus from equations 2.17 and 2.18,

$$\sum_{j=i}^{n} P_j.d.(V_{ij}/K.d + I_{ij} - I'_{ij}) = E.S_i \qquad (2.19)$$

where

$K = E_p.R_A/E$

= the pile stiffness factor

Equation 2.19 is written in a matrix form for all n elements of the pile as follows:

$$d[D/K.d + I - I'] \cdot [P_j] = E.[S] \qquad (2.20)$$

In obtaining the subsequent solutions, the pile was divided into 10 arbitrary elements. This number, as reported by the authors, was found to give results of satisfactory accuracy. In Fig. 2.23 the influence factor

I_n for the maximum downdrag force P_n is plotted against K, $K=E_p/E$, for various values of L/d and for $\mu=0$ and $\mu=0.5$. The actual downdrag force is related to the influence factor I_n as follows:

$$P_n = I_n . E . S_o . L . R . N_T + Pa \qquad (2.21)$$

where

S_o = maximum settlement at the soil surface

$R = (1-2\mu)(1+\mu)/(1-\mu)$

μ = Poisson's ratio of the soil

N_T = correction factor for effects of delayed installation

Pa= axial force on pile head

The correction factor (N_T) depends on the time between pile installation and surcharge application (t_o). It's values range between 0.8 and 1.0 when the time factor $Tv_o = C_v . t_o / (L/2)^2$, regarding pile installation, decreases from 0.05 to zero.

It can be seen in Fig. 2.23 that both L/d and K have a significant effect on P_n, i.e., for a pile of given length L, the downdrag force P_n increases as L/d decreases, also P_n increases from zero for K=1 (a pile of equal stiffness with the soil) to a maximum for $K=\infty$ (an incompressible pile). It is also shown that the effect of Poisson's ratio of the soil μ has less effect on P_n when compared to the effect of L/d and K.

The variation of the downdrag force with depth, from zero at the surface (z/L=0) to P_n at the pile toe (z/L=1.0), is plotted in Fig. 2.24 for the case L/d=25. As shown from Fig. 2.24, for very compressible piles (K=50), the downdrag force is constant over the lower half of the pile, reflecting the very small shear stresses developed over that portion of the pile.

Poulos and Davis (1975) extended the analysis described by Poulos and Mattes (1969) to account for the development of downdrag force with time during consolidation. They presented solutions for the magnitude and rate of development of maximum downdrag force of an end-bearing pile in a consolidating soil layer subjected to surface loading.

A large number of parameters were investigated such as L/d, K, μ, C_a/q, $\gamma.L/q$ and $k.\tan\delta'$ where

C_a = unit adhesion between pile and soil

q = surcharge pressure

γ = unit weight of soil

k = coefficient of lateral earth pressure

δ' = effective friction angle between pile and soil

Drainage conditions in the soil were also considered which included two time parameters, 1) the time, t_o, between the commencement of consolidation of the soil and installation of the pile, and 2) the time, t, between the

commencement of consolidation of the soil and the time being considered. These parameters were expressed as dimensionless time factors T_{v_o} and T_v corresponding to t_o and t respectively as follows:

$$T_{v_o} = \frac{N.C_v.t_o}{L^2} \quad , \quad T_v = \frac{N.C_v.t}{L^2}$$

in which

C_v = coefficient of consolidation of the soil

N = 1 (one-way drainage)

= 4 (two-way drainage)

The rate of development of the maximum downdrag force with time thus predicted for L/d=50, K=1000 is shown in Fig. 2.25. The term U_n is the ratio of the maximum downdrag due to negative friction, at any time, to the final maximum value at $T_v=\infty$.

Poulos and Davis noted that Fig. 2.25 may be used approximately for all values of T_{v_o} provided that the time factor is defined in terms of the elapsed time, $t_e = t - t_o$, since installation of the pile. Thus the downdrag force, P_{n_t}, at any time after installation of the pile, may be expressed as:

$$P_{n_t} = U_n (P_n - P_a) + P_a \qquad (2.22)$$

in which

P_n = final maximum downdrag force calculated from equation 2.21

U_n = degree of development of downdrag for

$Tv = N.C_v.t_e/L^2$

P_a = axial force on pile head

The analysis shows that the time of installation of piles after the placement of a fill has a large influence on the magnitude and distribution of negative skin friction. The drag load is reduced considerably if the piles are driven after the fill has been placed particularly if the compressible layer is drained both top and bottom.

The theoretical investigation presented by Poulos and Mattes (1969), and Poulos and Davis (1975) provided important predictions of downdrag forces for cases where full slip between soil and pile occurs. The analyses were justified by comparing the solutions obtained with field measurements.

2.5 Summary

The literature indicates that a considerable amount of work has been carried out in the last 20 years to provide quantitative data on the effects of downdrag generated by the consolidation of soft clay deposits.

The importance of the downdrag phenomenon as a factor to be taken into account in deep foundation design has

been confirmed by both full-scale tests and model or scaled-down laboratory tests.

Field observations for piles bearing on a hard stratum have shown that negative skin friction along the pile surface can be very large and may exceed the design load from the superstructure. Friction piles are not commonly considered when negative skin friction is involved since their use is not recommended when significant soil settlements are expected.

It has been suggested that single piles and pile groups subjected to negative skin friction should be designed for maximum skin friction above the neutral point (a point at which the relative displacement between the pile and the soil is zero) and that the downdrag can be modelled by the effective stress method and by the total stress method (the Beta and Alpha methods, see Sections 6.4.1 and 6.4.5 in Chapter 6). Parameters obtained by these methods, for negative skin friction prediction, have been reported in the literature by various authors.

Theoretical methods based on elastic theory show good agreement with field measurements only when representative elasticity parameters of the media considered are known.

It is believed that verification of any proposed technique to investigate the downdrag phenomenon requires field test results that are difficult to obtain in the field because of the long time and expense involved. The alternative to full-scale field testing are scaled-down

model tests that can be conducted in the laboratory under controlled conditions. It then becomes possible to experiment with the variables that affect the process.

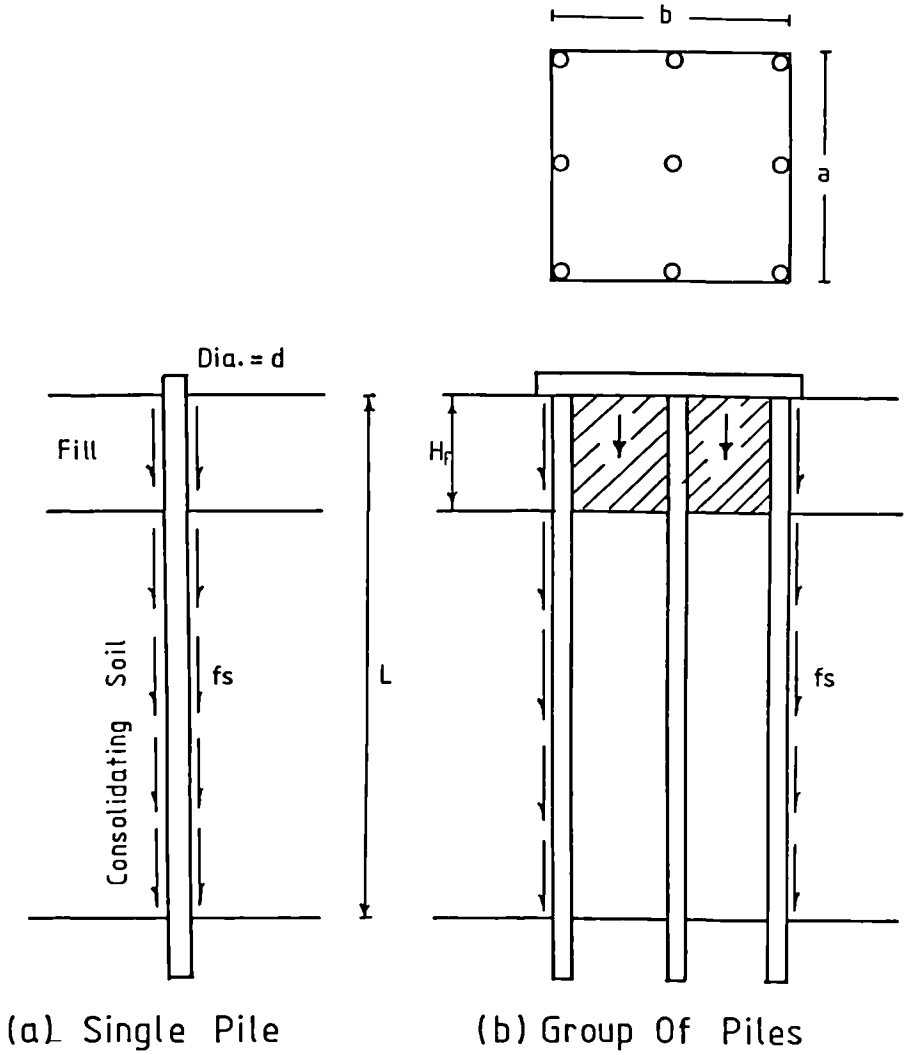

FIG. 2.1 NEGATIVE SKIN FRICTION ON PILES

(After TERZAGHI AND PECK, 1948)

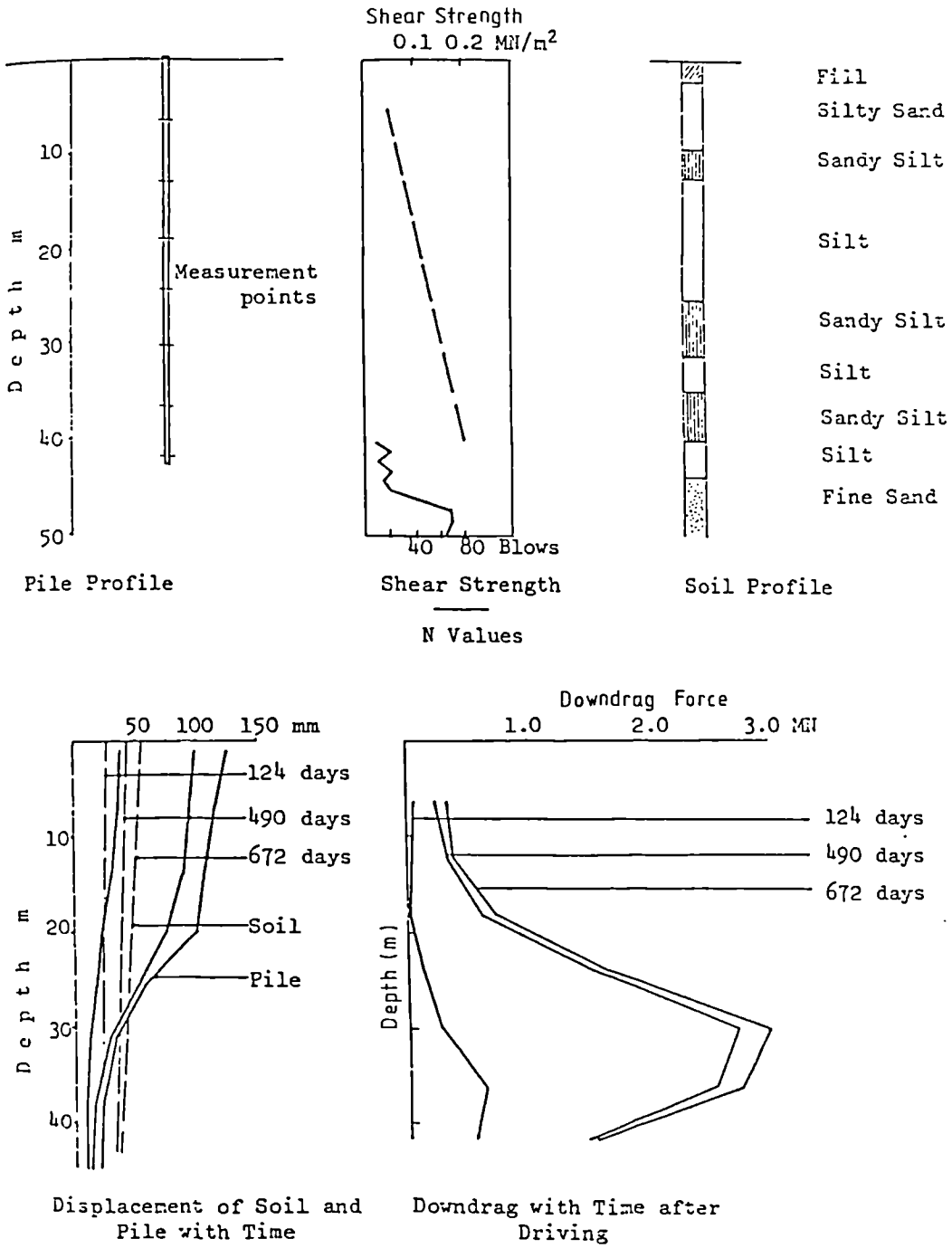

FIG. 2.2 PILE TEST AT TOKYO (After ENDO ET AL, 1969)

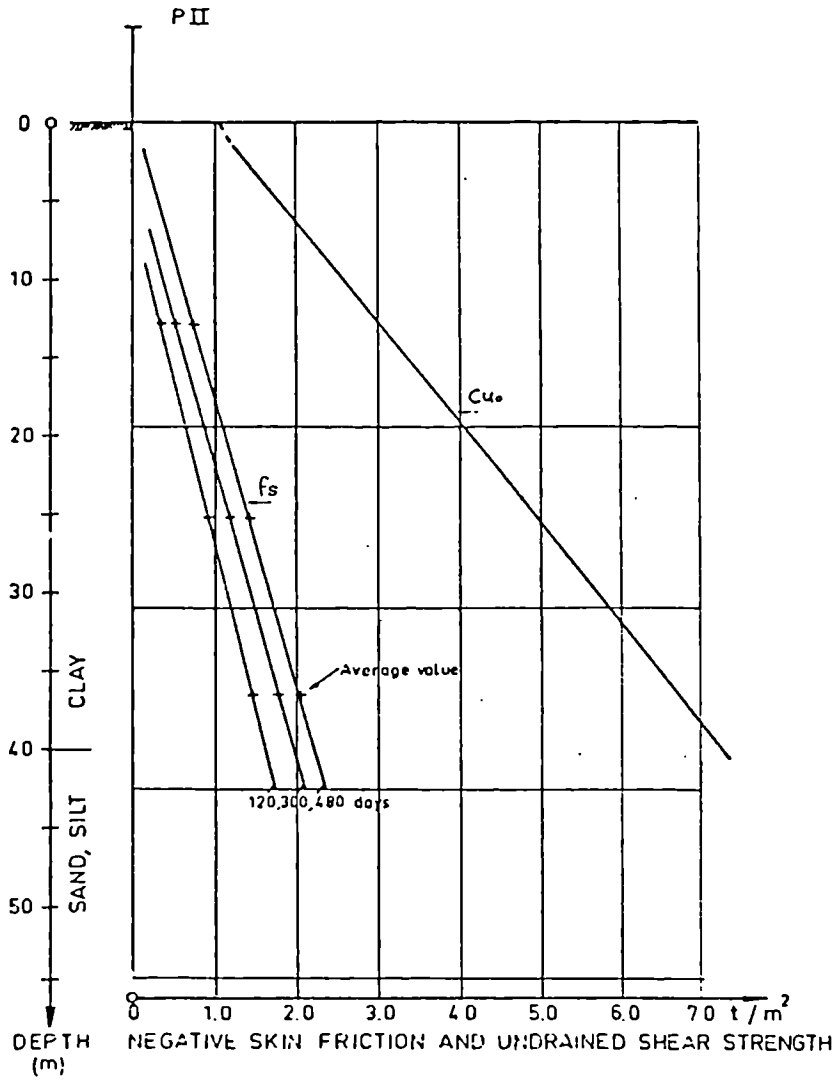

FIG. 2.3 NEGATIVE SKIN FRICTION OF A PILE COMPARED TO THE ORIGINAL UNDRAINED SHEAR STRENGTH OF CLAY (After FELLENIUS, 1972)

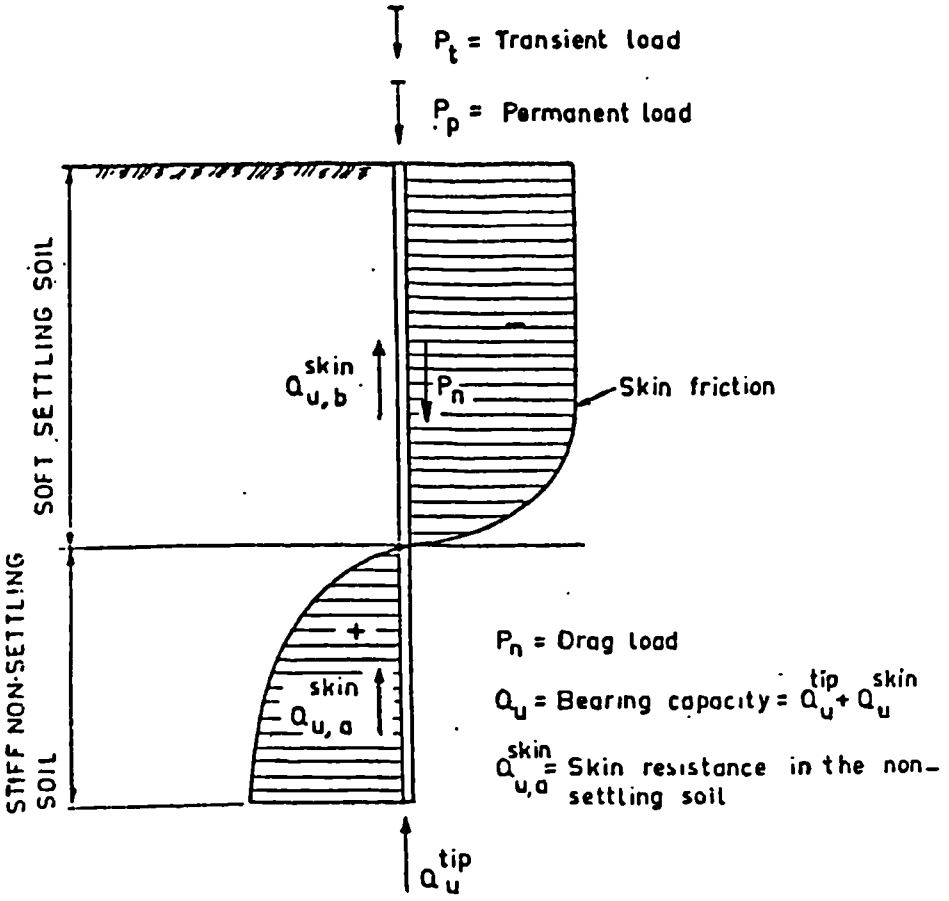

FIG. 2.4 UNIT SKIN FRICTION DISTRIBUTION ALONG A PILE IN AN UPPER LAYER OF SOFT SETTLING SOIL AND A LOWER LAYER OF NON SETTLING SOIL (After FELLENIUS, 1972)

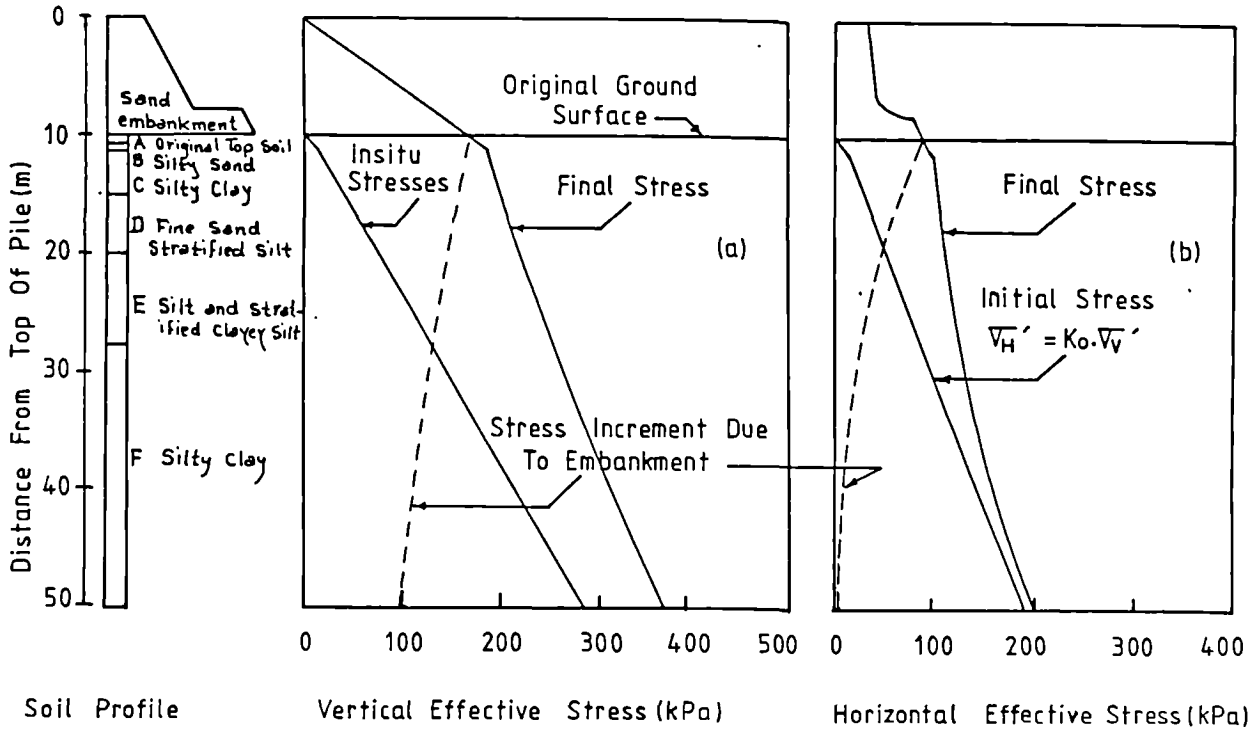

FIG. 2.5 DISTRIBUTION OF VERTICAL AND HORIZONTAL EFFECTIVE STRESSES UNDER CENTRELINE OF EMBANKMENT (After BOZOZUK, 1972)

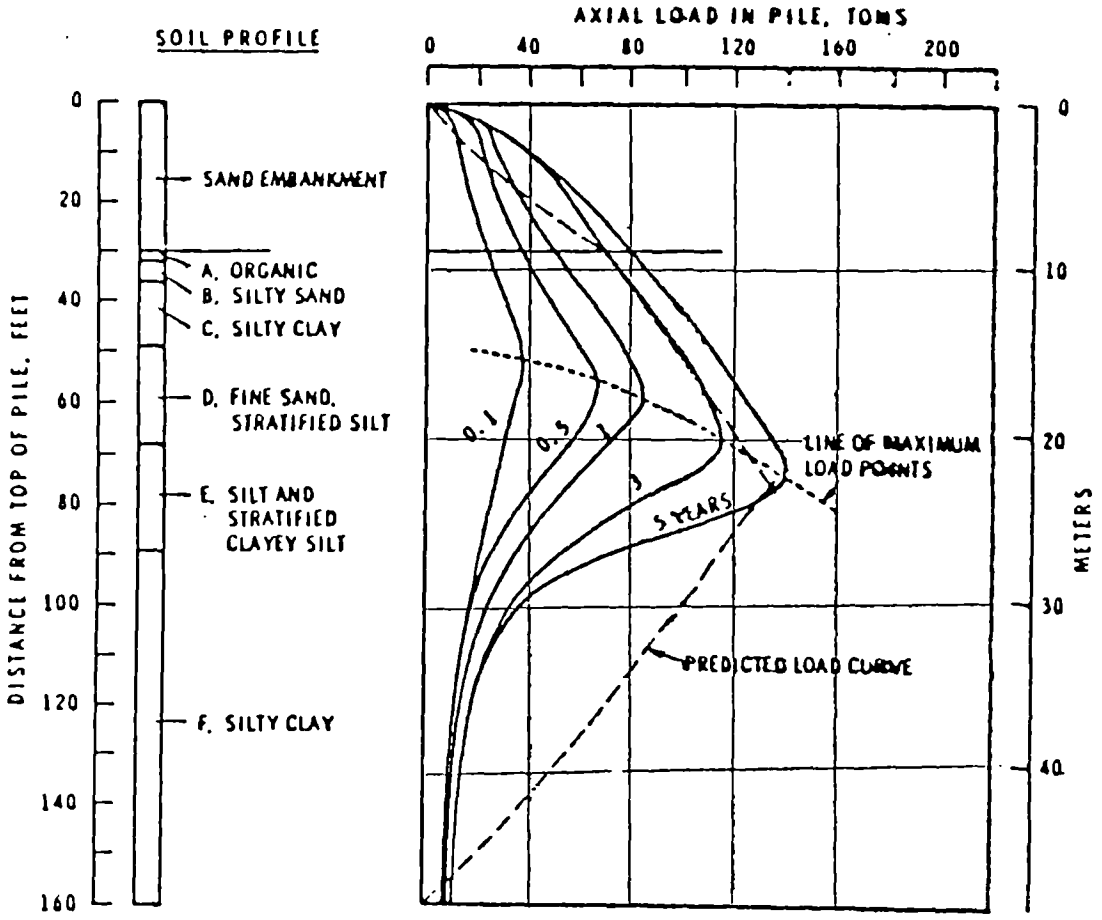

FIG. 2.6 VARIATION OF SKIN FRICTION LOAD IN 300 MM DIA. STEEL PIPE PILE WITH TIME (After BOZOZUK, 1972)

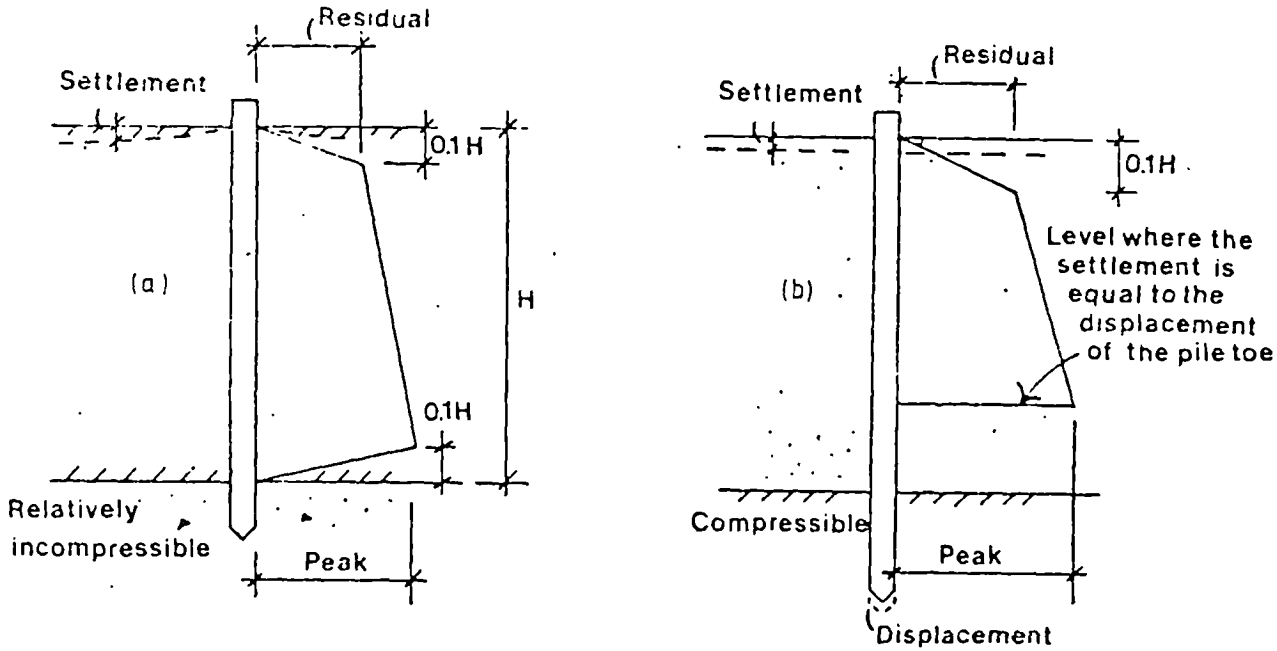

FIG. 2.7 NEGATIVE SKIN FRICTION ON SINGLE PILES

(After TOMLINSON, 1975)

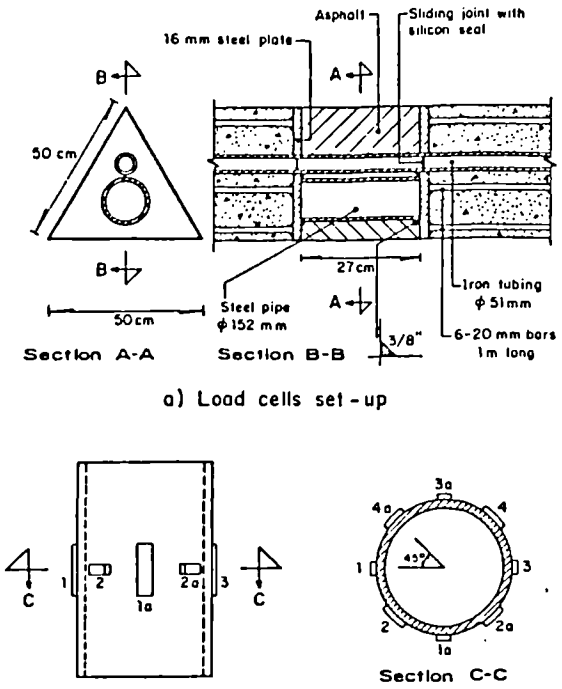

FIG. 2.8 LOAD CELLS (After AUVINET And HANELL, 1981)

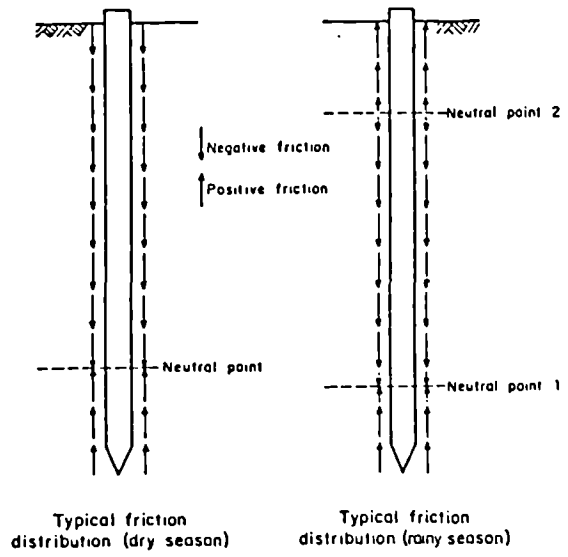

FIG. 2.9 SKIN FRICTION DISTRIBUTION

(After AUVINET And HANELL, 1981)

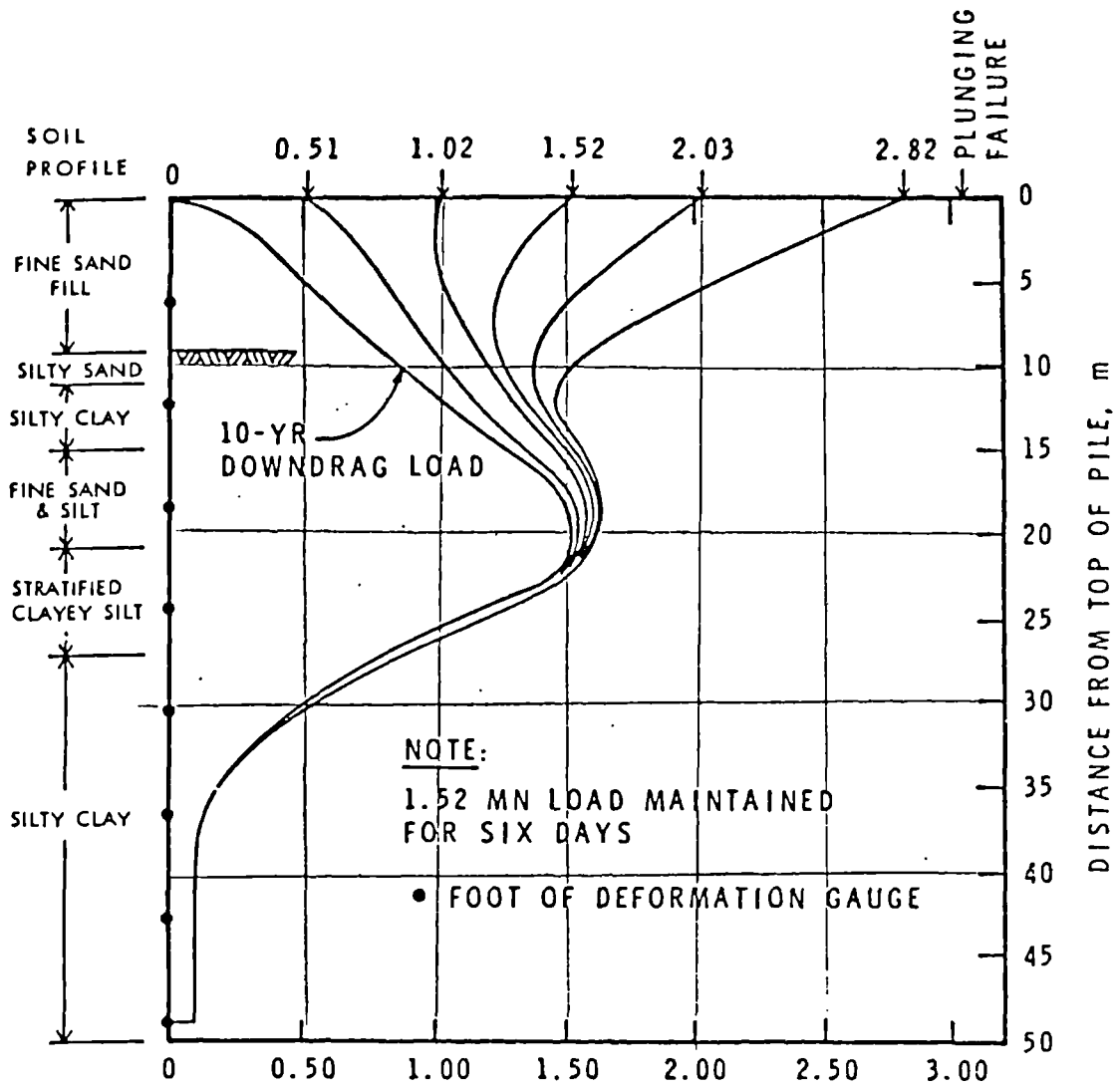

FIG. 2.10 LOAD DISTRIBUTION IN TEST PILE

(After BOZOZUK, 1981)

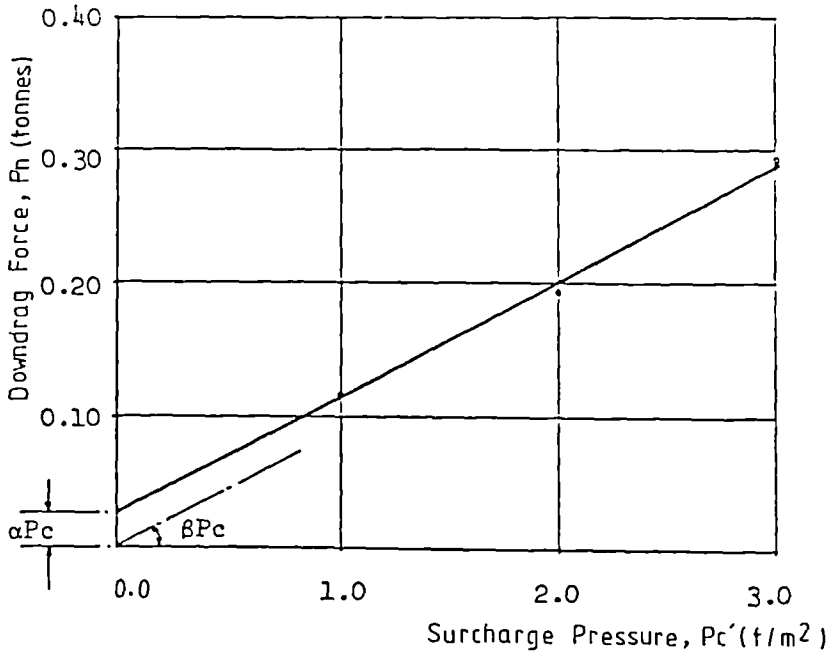

(a) Relationship between Fn and Pc

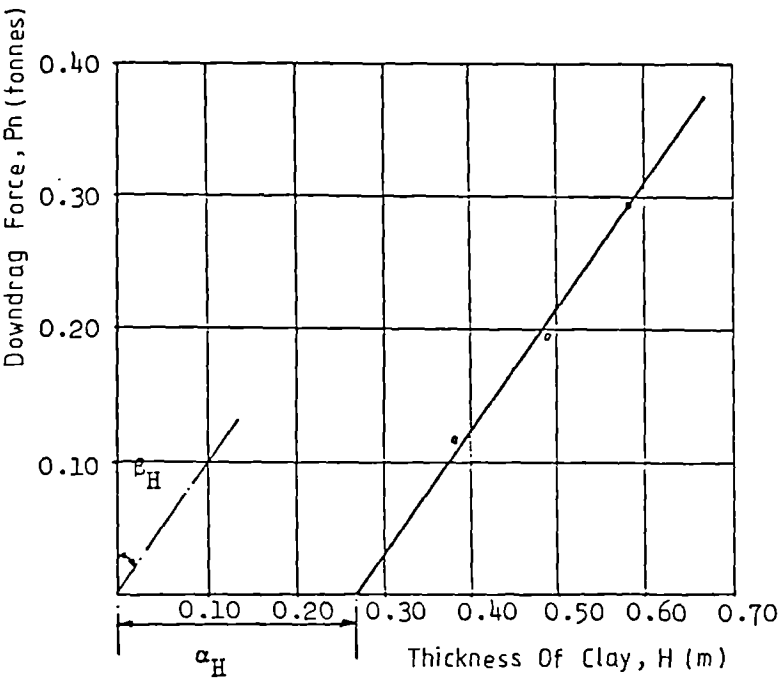

(b) Relationship between Fn and H

FIG. 2.11 EMPIRICAL RESULTS OBTAINED BY ELMASRY, 1963

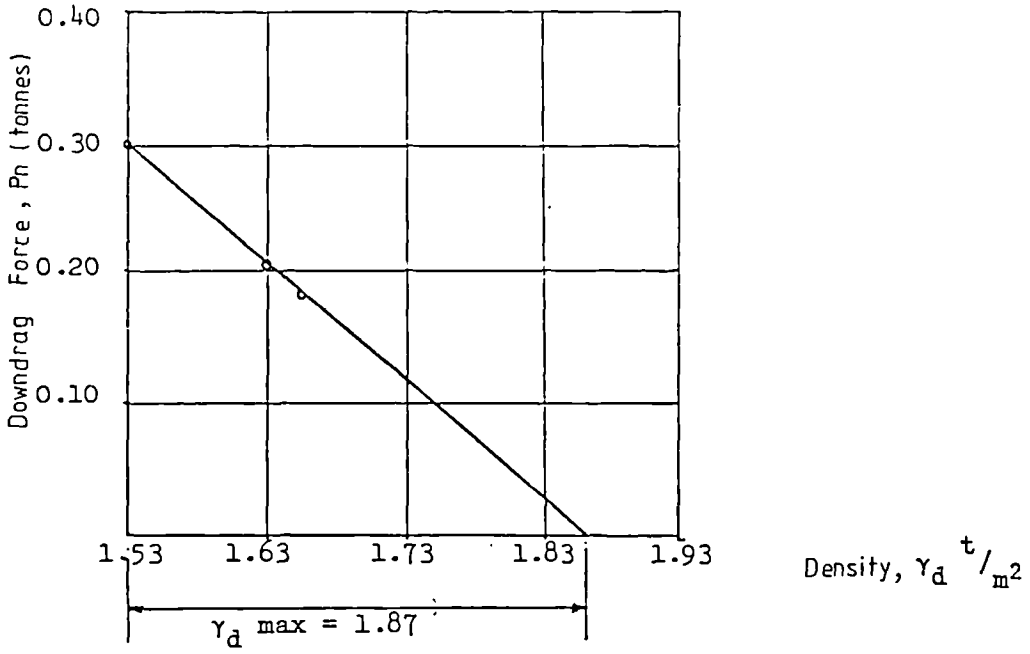

(c) Relationship between Fn and γ_d

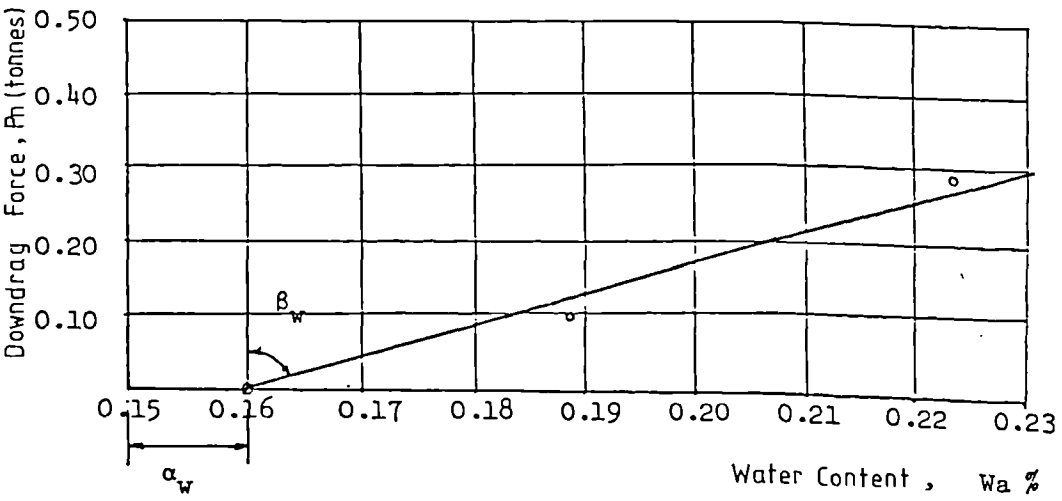

(d) Relationship between Pn and Wa

FIG. 2.11 EMPIRICAL RESULTS OBTAINED BY ELMASRY, 1963

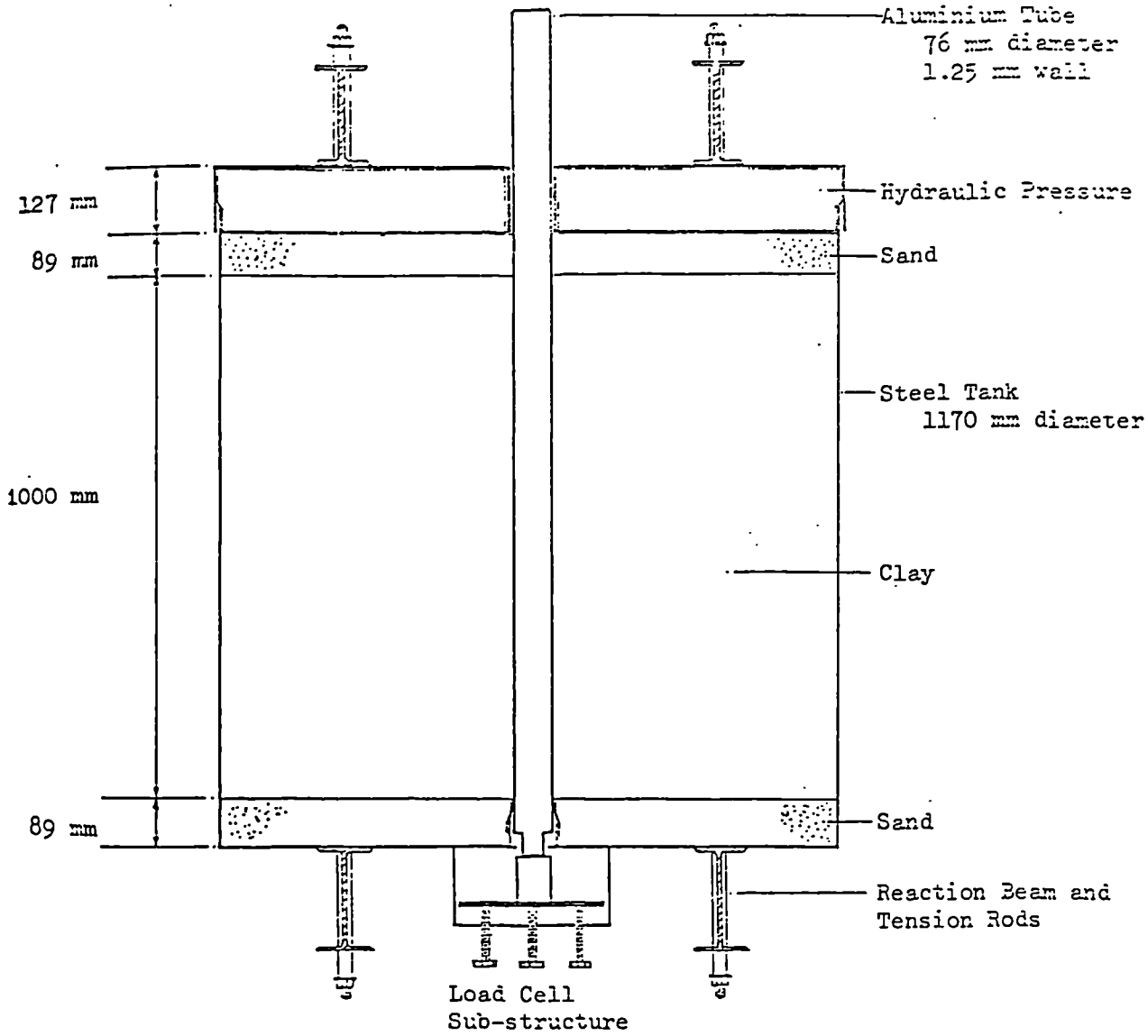

FIG. 2.12 MODEL TEST SET-UP, SILVA (1966)

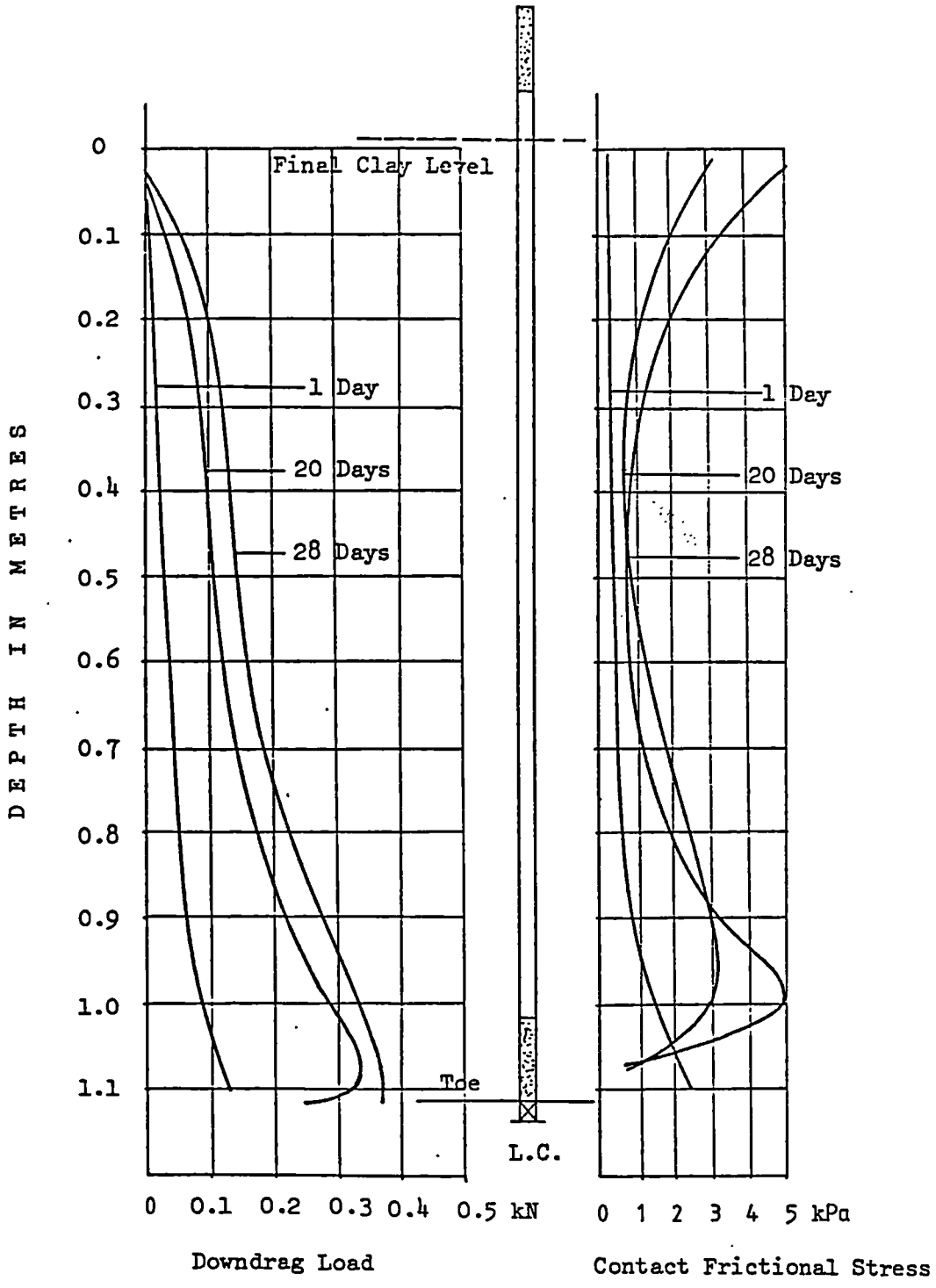

FIG. 2.13a AXIAL LOAD AND STRESS WITH 17.3 kPa SURCHARGE (After SILVA, 1966)

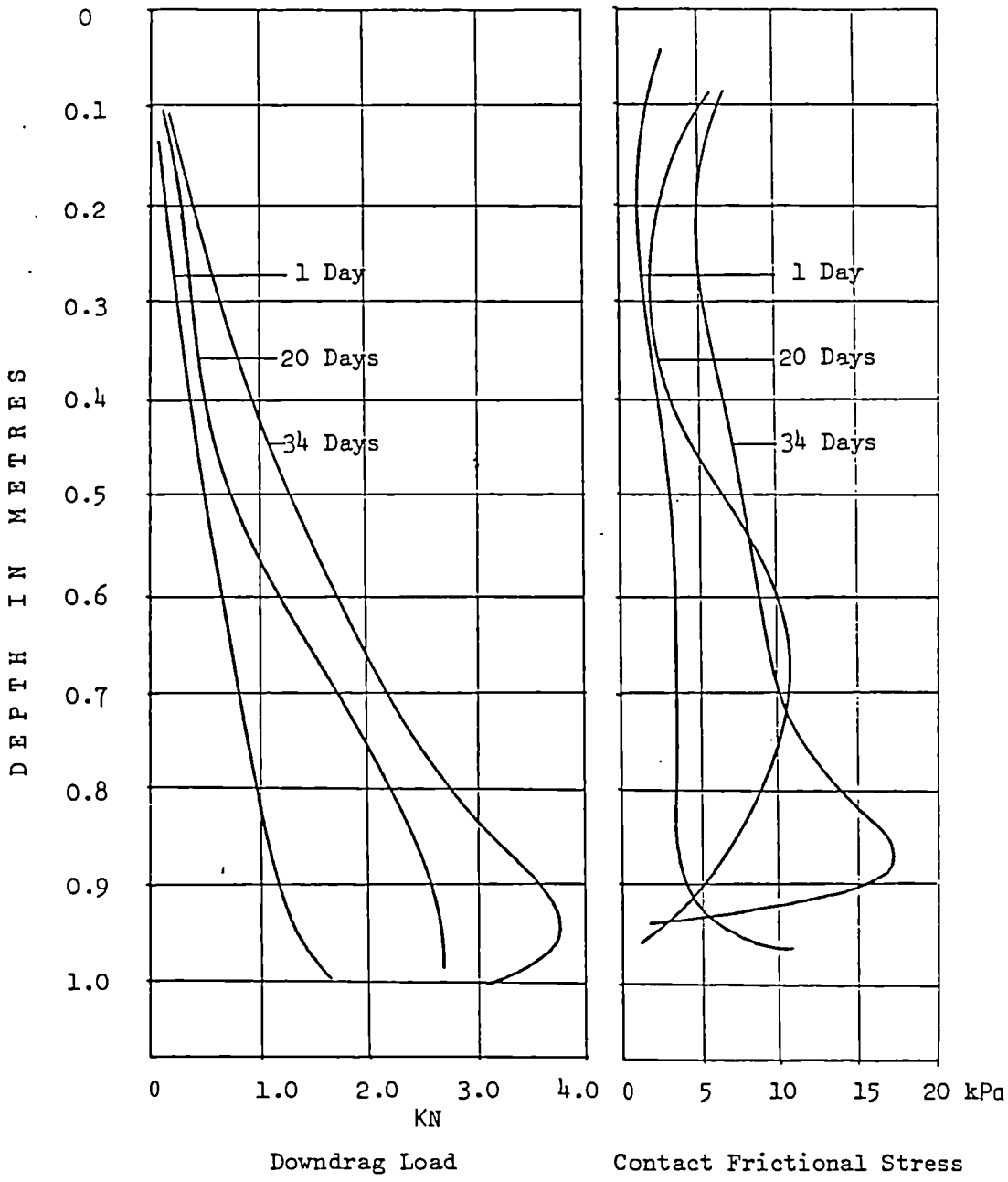

FIG. 2.13b AXIAL LOAD AND STRESS WITH 55.3 kPa SURCHARGE (After SILVA, 1966)

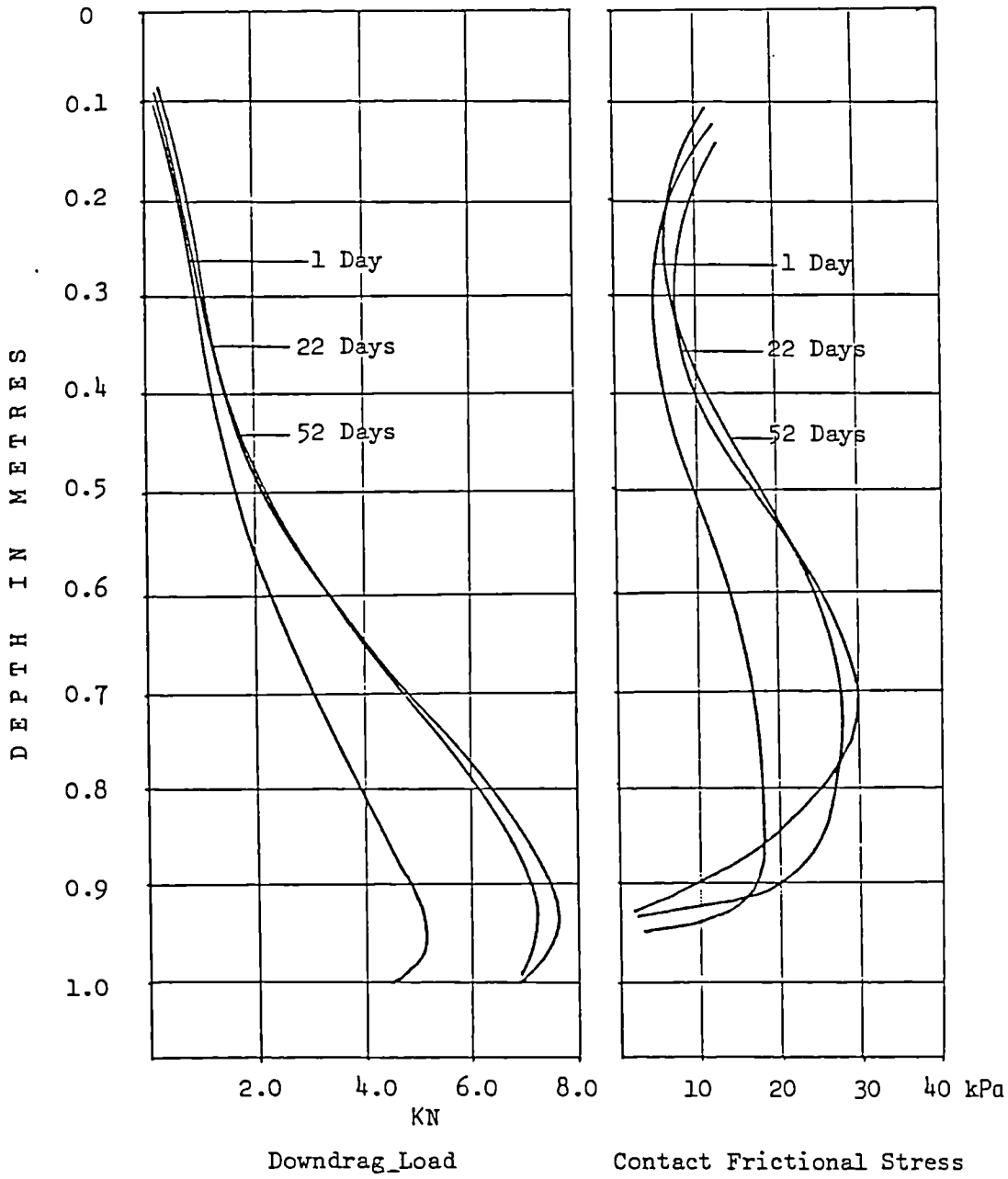

FIG. 2.13c AXIAL LOAD AND STRESS WITH 124.4 kPa SURCHARGE (After SILVA, 1966)

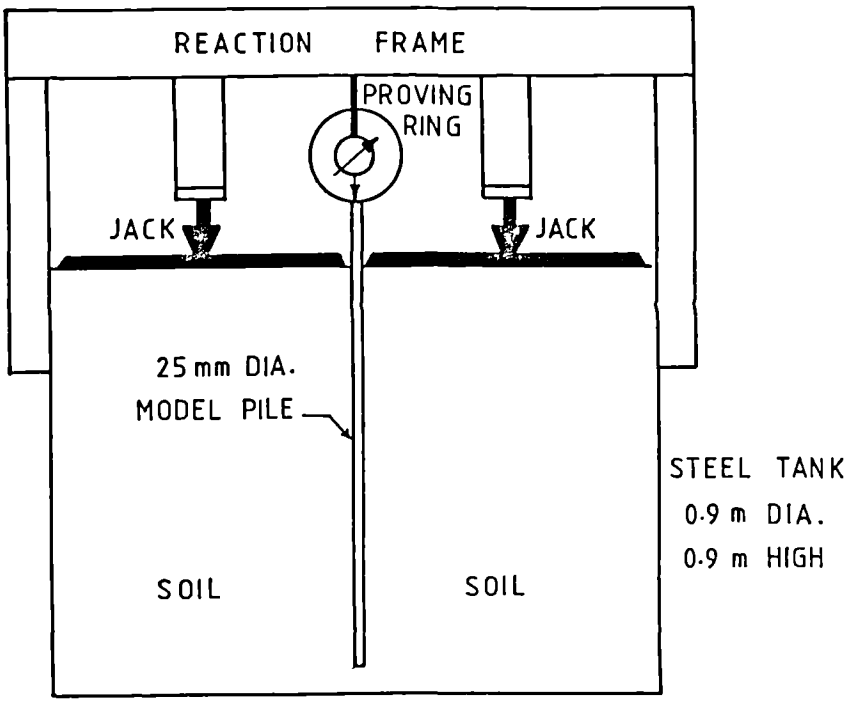

FIG. 2.14 EXPERIMENTAL SET-UP (After KOERNER And MUKHOPADHYAY, 1970)

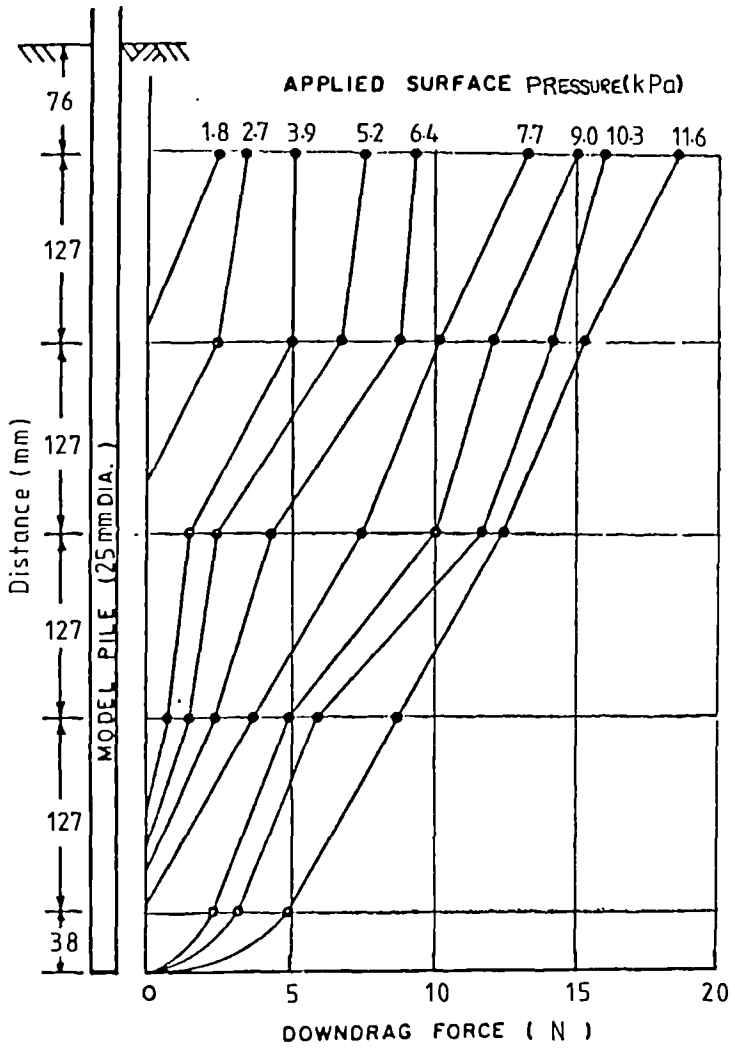

FIG. 2.15 DISTRIBUTION OF DOWNDRAG FORCE

(After KOERNER And MUKHOPADHYAY, 1970)

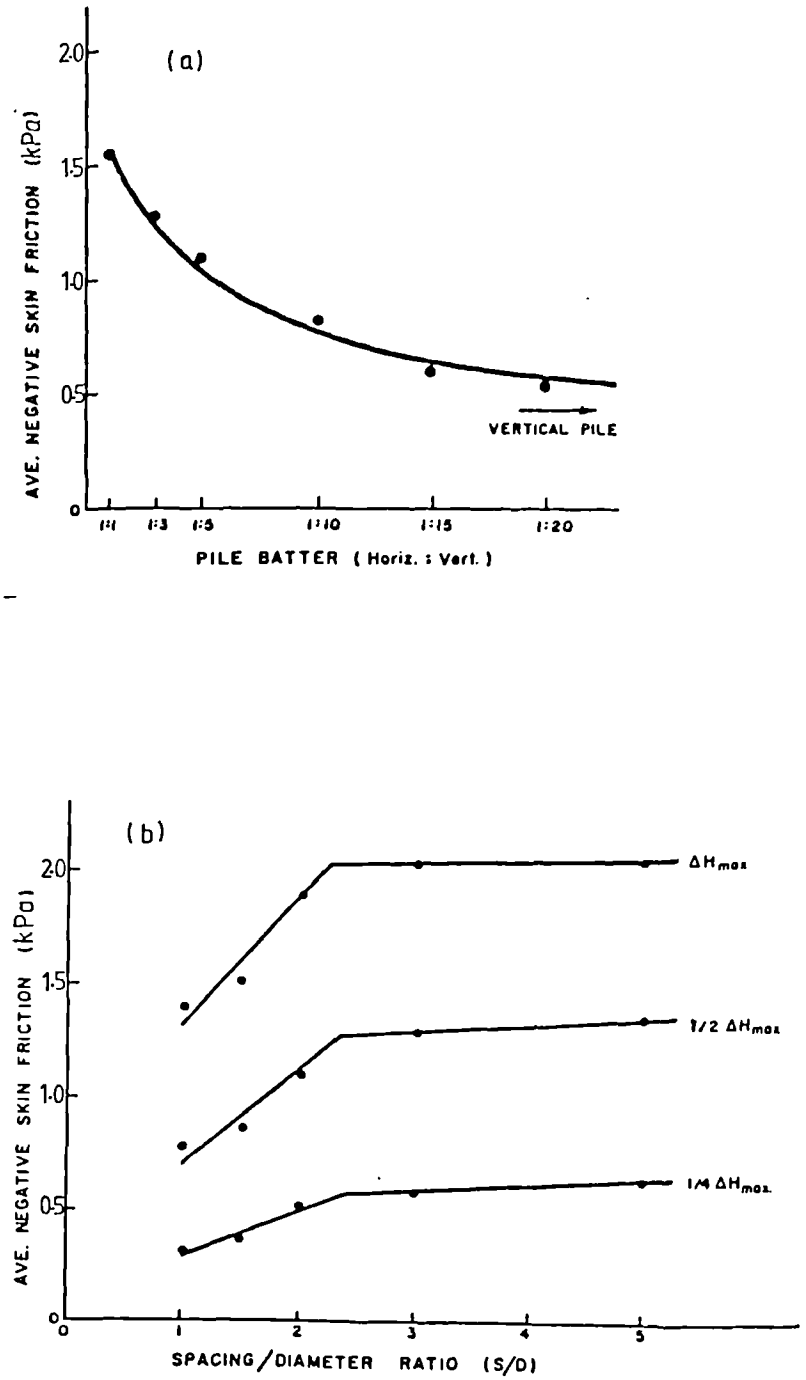

FIG. 2.16 EFFECT OF PILE BATTER AND PILE GROUP SPACING ON NEGATIVE SKIN FRICTION (After KOERNER And MUKHOPADHYAY, 1970)

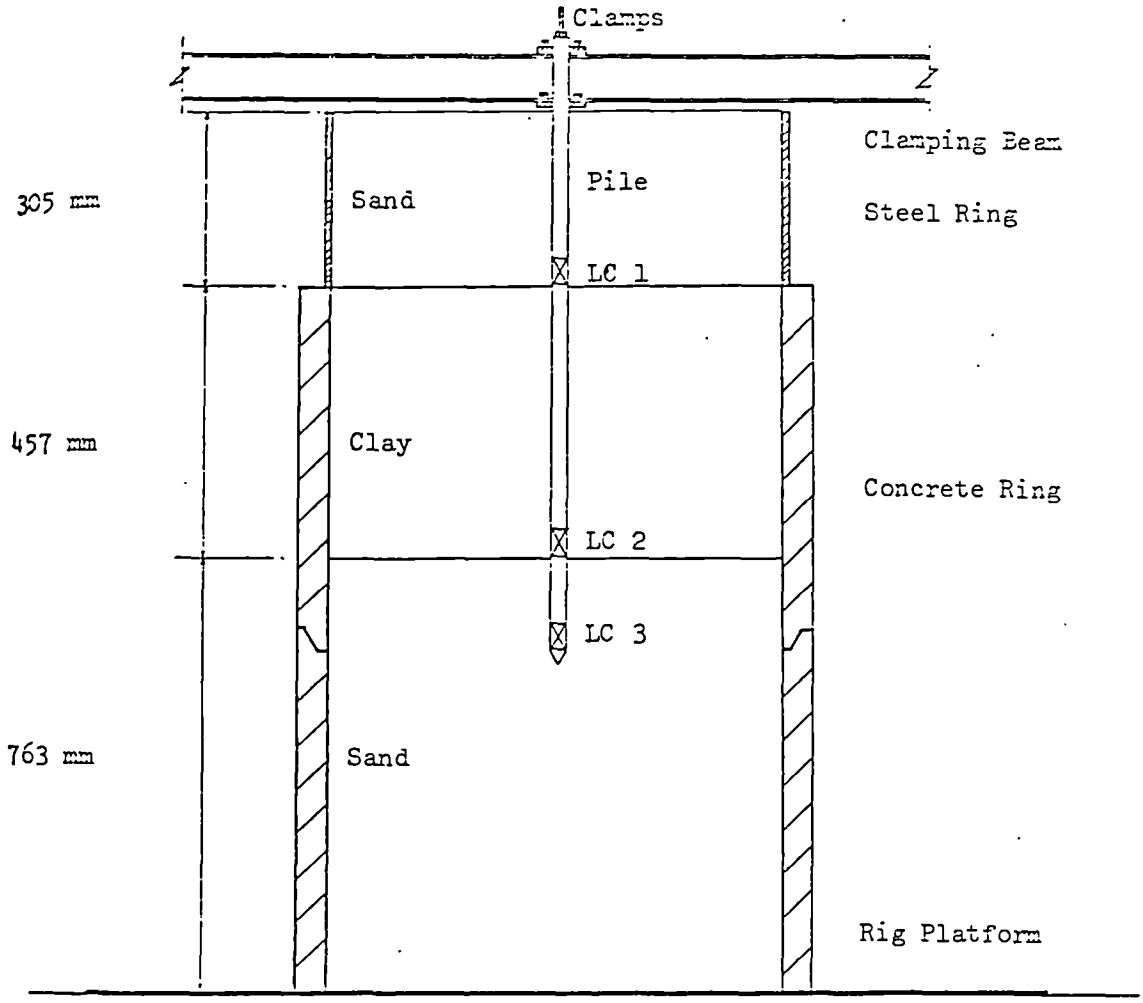

FIG. 2.17 TYPICAL PILE WITHIN TEST MEDIA

(After NICHOLLS, 1973)

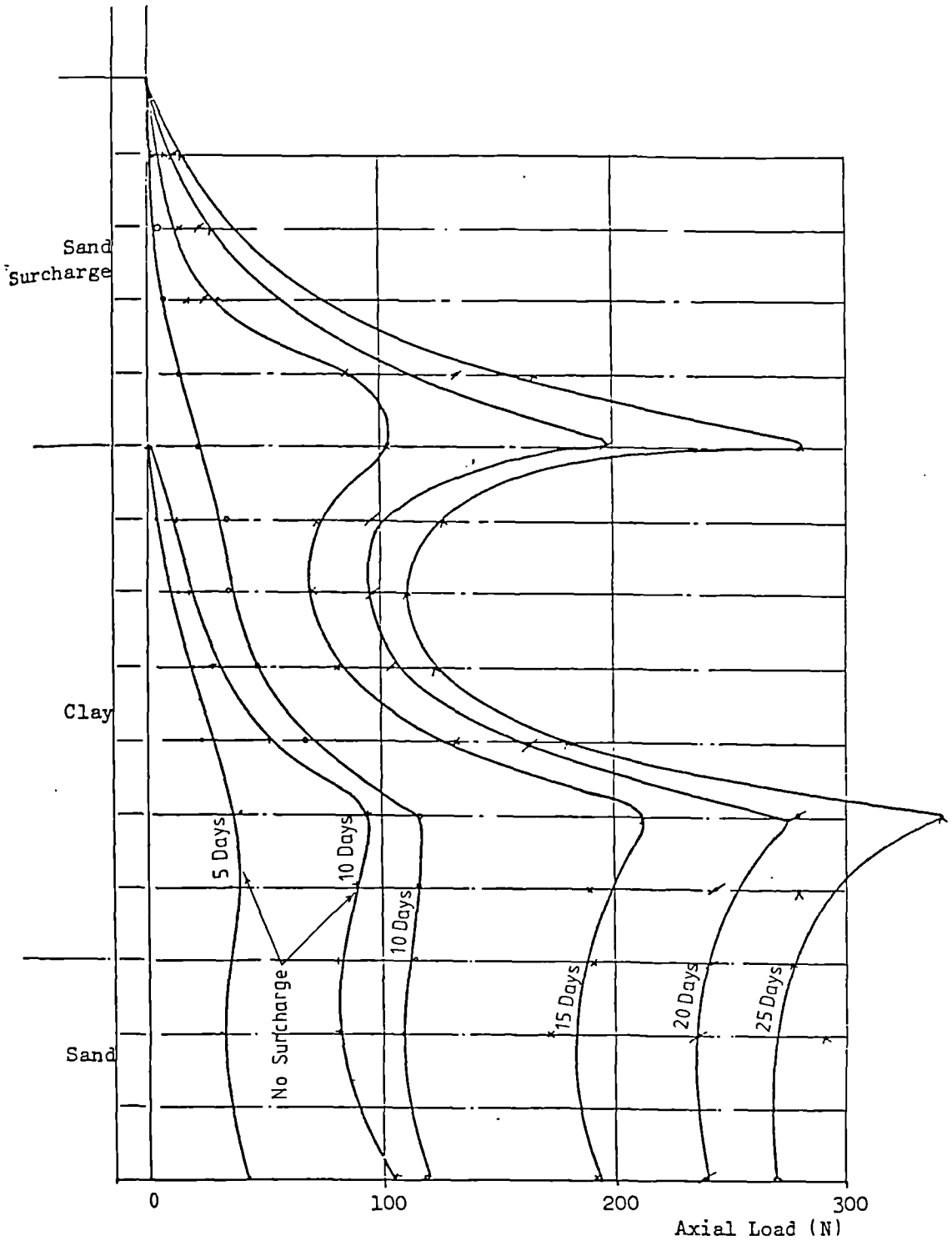

FIG. 2.18 LOAD DISTRIBUTION WITH DEPTH FOR 38mm DIAMETER COMPOUND PILE (After NICHOLLS, 1973)

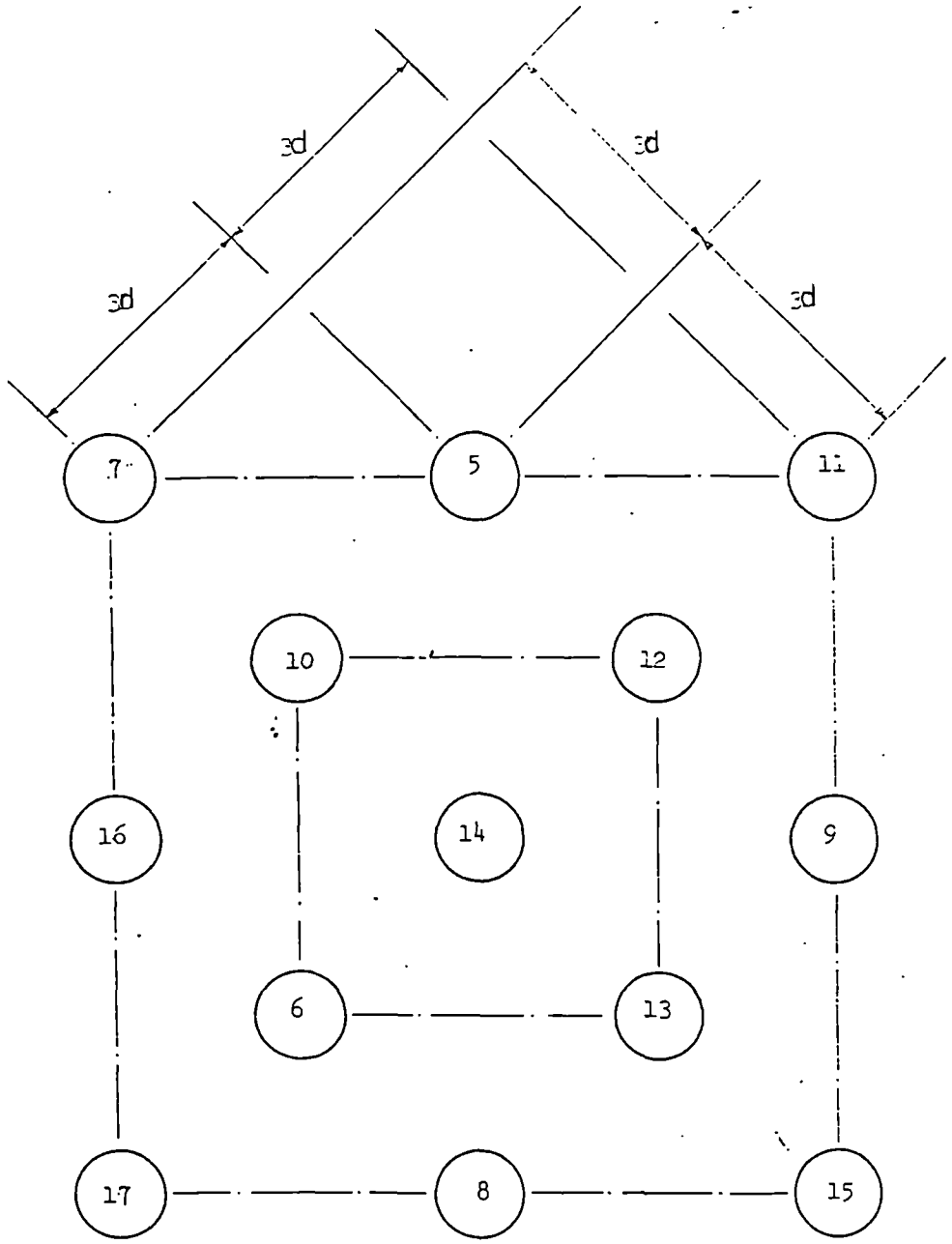

All piles 31.8mm diameter;
Spacing at 3d along diagonals.

FIG. 2.19 CONFIGURATION OF PILES IN GROUP TEST

(After NICHOLLS, 1973)

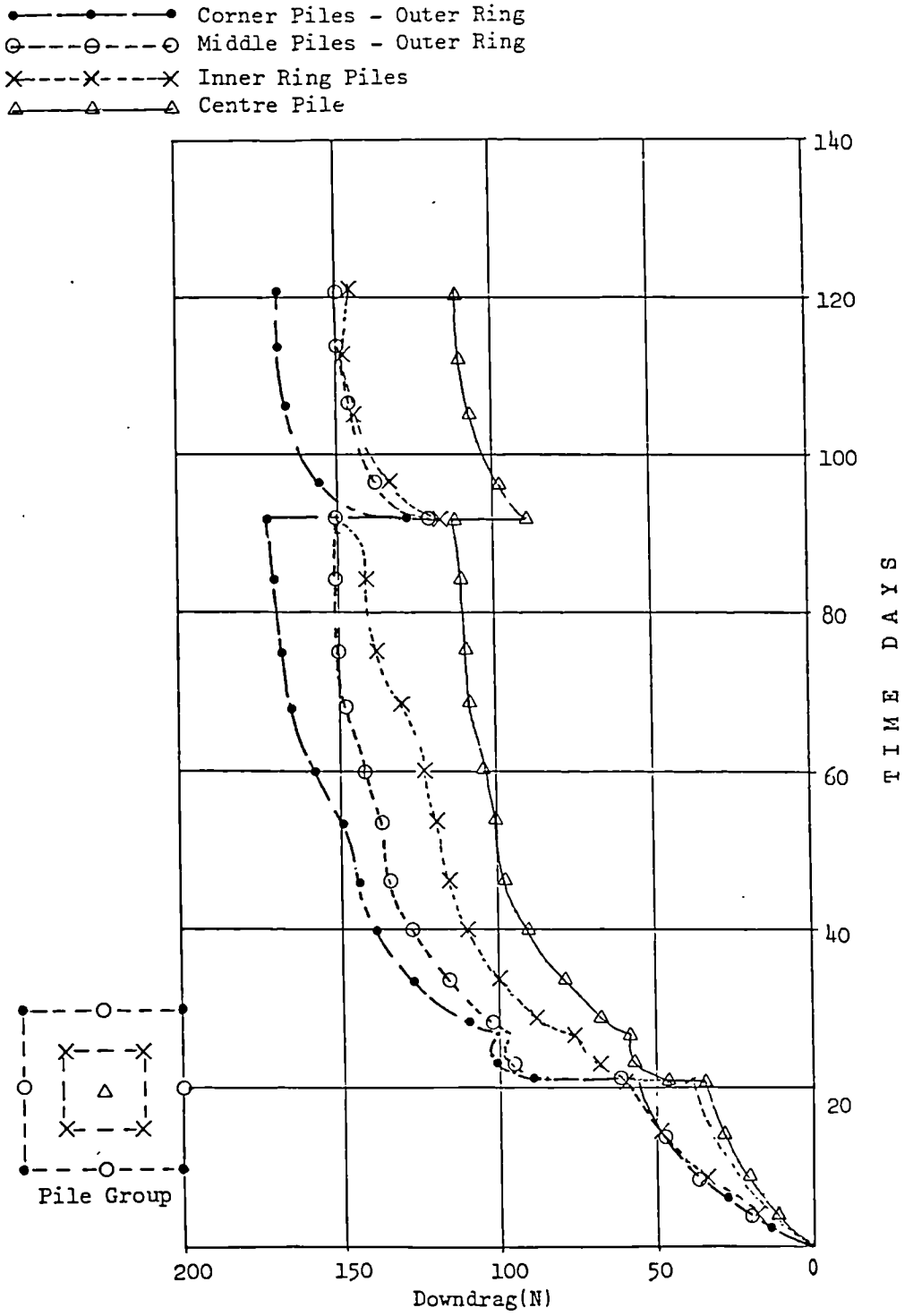

FIG. 2.20 DISTRIBUTION OF TOTAL DOWNDRAG WITHIN PILE GROUP (After NICHOLLS, 1973)

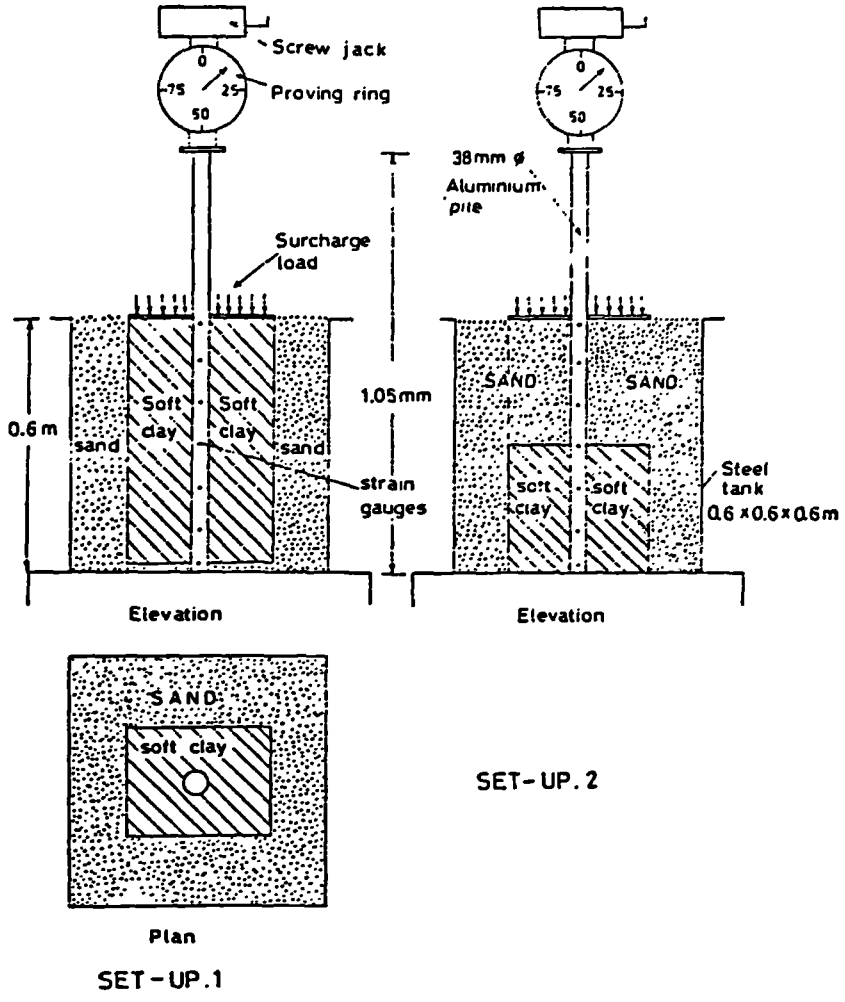

FIG. 2.21 EXPERIMENTAL SET-UP (After NARASIMHA And KRISHNAMURTHY, 1982)

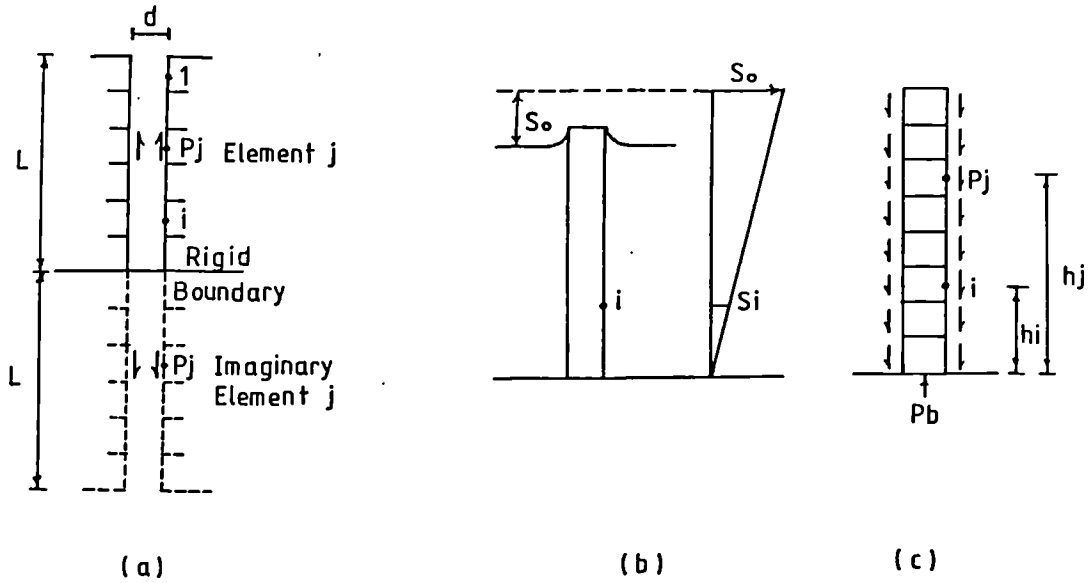

FIG. 2.22 STRESSES AND DISPLACEMENTS IN SOIL-PILE SYSTEM (After POULOS And MATTES, 1969)

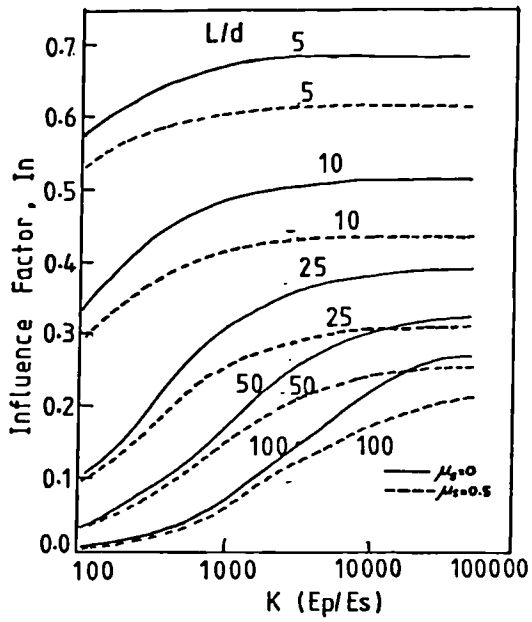

FIG. 2.23 INFLUENCE FACTORS FOR DOWNDRAG AT TOE OF PILE (After POULOS And MATTES, 1969)

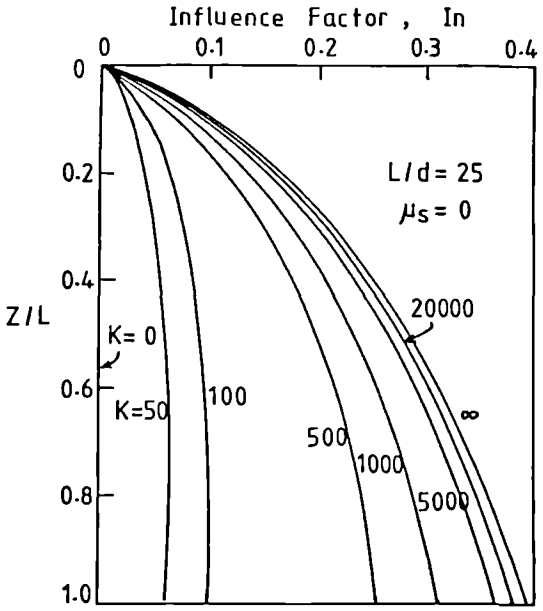

FIG. 2.24 ELASTIC DISTRIBUTION OF DOWNDRAG FORCE ALONG PILE (After POULOS And MATTES, 1969)

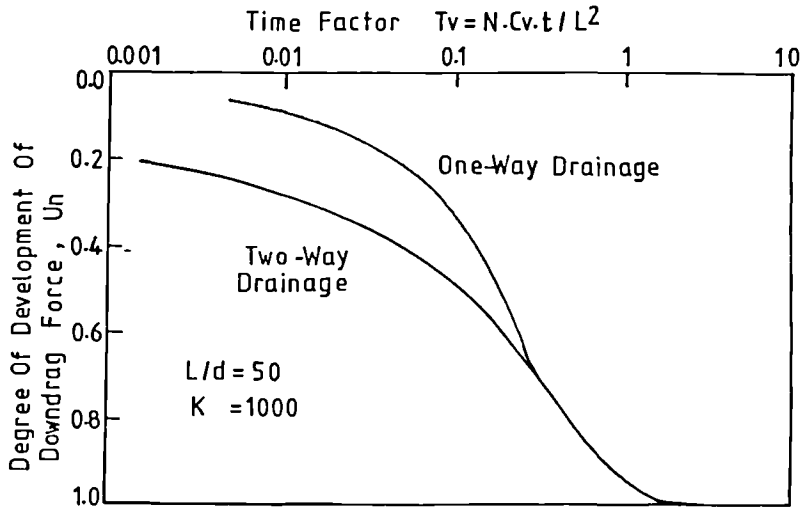

FIG. 2.25 RATE OF DEVELOPMENT OF DOWNDRAG FORCE (After POULOS And DAVIS, 1975)

Prediction	D'Appolonia	Davis	Esrig	Focht	Garlanger	Peres-Guerra	"Measured"
Load at top of pile, kN	268	357	401	535	250	357	780
β or K$\tan\phi_d$ for Fill	0.58	0.30	0.15		0.33	0.20	0.3-0.4
β or K$\tan\phi_d$ for Sand	0.58	0.30	0.15		0.33	0.20	0.3-0.4
β or K$\tan\phi_d$ for O.C. Clay	0.33	0.30	0.25		0.20	0.25	0.2-0.25
β or K$\tan\phi_d$ for N.C. Clay	0.23	0.30	0.21		0.20	0.12	0.2-0.25
Downdrag due to Sand & Fill, kN	980	327	254	598	375	272	312-446
Load in Pile at Bottom of Sand, kN	1250	682	624	1128	624	629	
Elev.of Neutral Point, m	-13.7	-14.0	-14.0	-14.2	-13.7	-14.1	
Downdrag due to Clay, kN	1160	954	1012	482	580	615	580-713
Load in pile at Neutral Point, kN	2408	1636	1668	1605	1204	1244	
Load at Pile Tip, kN	0	31	245	459	624	660	
Load in Pile @A before cutting, kN	268	433	468	535	392	446	1017

TABLE 2.1 SUMMARY OF PREDICTED AND MEASURED LOADS, CUTLER CIRCLE BRIDGE

Prediction	D'Appolonia	Davis	Esrig	Focht	Garlanger	Peres-Guerra	"Measured"
Strain @ A after cutting, μ "/"	100	150	160	190	140	155	365
Movement of Pile after cutting, mm	1.52	2.95	4.39	4.90	3.66	3.94	
Rebound of Till after cutting, mm	0	0.08	0	14.27	0	0	
Movement of A after cutting, mm	1.52	3.02	4.39	19.18	3.66	3.94	10.18
Movement of Pile after excavating Sand, mm	6.10	1.63	1.57	4.11	1.22	2.39	
Rebound of Till after excavating Sand, mm	0	0.05	0	0	0	0	
Movement of A after excavating Sand, mm	6.10	1.67	1.57	4.11	1.22	2.39	2.46
Movement of Pile after electro-osmosis, mm	4.57	3.30	3.43	2.03	2.97	2.34	
Rebound of Till after electro-osmosis, mm	0	0.25	0	0	0	0	
Total movement of Pile, mm	12.19	8.26	9.40	25.15	7.85	8.66	16.64

TABLE 2.2 SUMMARY OF PREDICTED AND MEASURED MOVEMENTS, CUTLER CIRCLE BRIDGE

Test No.*	Final And (Maximum) Downdrag Loads-N			
	Piles mm Diameters 25.4	31.8	38.0	50.8
1 (1)	100 (147.7)	125.9(131.7)	216.3(243.5)	
(2)	162.9	151.9	210.6	
2 (1)			Figure	16.7
			2.18 refers	5.2 (67.0)
3 (1)	62.1	53.6	19.3	
	117.2	75.7	84.6	
5 (1)		33.1 (34.9)	65.3	64.5 (65.0)

* (1) refers to the 1st consolidation pressure
(2) " " " 2nd " "

TABLE 2.3 DOWNDRAG LOADS CAUSED BY SAND SURCHARGE (AFTER NICHOLLS, 1973)

Test No.*	Final And (Maximum) Downdrag Loads-N			
	Piles mm Diameters 25.4	31.8	38.0	50.8
1 (1)	148 (187.1)	275 (286.0)	273.6 (284)	
(2)	227	322.6	305.2	
2 (1)			Figure	130.0
			2.18 refers	97.3 (214.5)
3 (1)	73.8	380.8	130	
	130.0	607.9	214.1	
5 (1)		132.6	179.9	224

* (1) refers to the 1st consolidation pressure
(2) " " " 2nd " "

TABLE 2.4 DOWNDRAG LOADS CAUSED BY CLAY AND SAND SURCHARGE (AFTER NICHOLLS, 1973)

CHAPTER (3)

EXPERIMENTAL APPARATUS AND TESTING PROGRAMME

The object of the research was to investigate the behaviour of negative skin friction through a laboratory experiment and in order to obtain both accuracy and reliability, all the elements included in the experiments described herein were thoroughly checked and tested before starting the testing programmes. Below is a detailed description of the apparatus design and experimental procedures.

3.1 Main Apparatus

The main apparatus was designed and constructed in order to confirm changes of negative skin friction during the process of consolidation. Fig. 3.1a shows a schematic drawing of the apparatus. Its basic components are as follows:

(1) Steel Circular Tank : This served as a consolidation container of dimensions 0.8m by 1.0m in diameter and height.

(2) Main Frame : This consisted of two box columns confining the steel tank and joined together from the top by an overhead horizontal steel beam with a hole in its centre. This served to keep the pile centrally in position. The two columns extended down to the bottom of the tank where they were welded to a base plate to give rigidity to the tank.

(3) An upper circular rigid steel plate acted as the tank lid. It was fixed at the top of the tank in such a way that it could be adjusted to move up and down by means of four long screw/tie bolts.

(4) Model Pile : This comprised a thin-walled brass pipe of 50mm outer diameter and 1.0mm wall thickness. It consisted of six sections of different lengths (600mm, 300mm, 200mm, 200mm, 200mm and 50 mm from top to bottom respectively). Five of these were instrumented with electrical resistance strain gauges on their inside surfaces.

(5) Loading System : A consolidation pressure was applied by means of a special cylindrical rubber bag (800mm diameter by 150mm deep) resting on the upper sand layer and bearing against the lid of the consolidation tank.

(6) Soil : A remoulded soft to firm intact greyish brown silty clay, from Stirling (see chapter 4), was the soil used as the consolidating medium. Drainage was provided

at the top and bottom as well as radially. Two sand layers (top and bottom) provided vertical drainage. A 2.0mm filter fabric (Terram 2000 Geotextile) was mounted on the inner surface of tank and provided the radial drainage.

(7) Other Measuring Devices : Twelve pore water pressure piezometers were embedded at four different levels and four settlement plates at two different levels in order to measure both pore pressure and settlement during the consolidation process.

3.2 Equipment Description And Adjustment Procedure

A detailed description of all elements included in the experimental work is given below; Fig. 3.1b shows a completed set up of the experimental apparatus.

3.2.1 Testing Tank

The tank was fabricated from mild steel with a wall thickness of 5.0mm and a bottom plate thickness of 25mm. The inside diameter of the tank was 800mm and inside height 1.0m, Fig. 3.1a.

Below the bottom plate the tank was extended to rest on a base plate leaving a 300mm high by 500mm wide opening mainly to provide a space for piezometer lines to pass through and settlement readings to be obtained. A 55mm

diameter steel ring plate, on which the pile shoe sat, was provided at the centre of the bottom plate. The ring plate was adjusted to move up and down by means of a 30mm diameter threaded bolt and a nut. Fig. 3.1a also shows six drainage valves three of which were at the top and the other three of which were positioned at the bottom of the tank. These drain valves were fixed on the tank by boring holes which were then tapped with 1/4" BSP threads. The bottom drains were equidistant from each other along the periphery of the tank while the top drains were positioned in a vertical line with 100mm centres to ensure drainage from the upper sand layer at all stages of the consolidation process.

3.2.2 Main Frame

The portal frame was erected to give sufficient restraint to the tank as well as to provide a guide for the pile through the overhead beam. The two columns were of box type, 100mm by 50mm in cross section and 5mm plate thickness. These columns were welded to the tank at three positions and extended down to the base plate. The overhead beam had dimensions 76mm by 50mm in cross section and was strengthened with another (43mm by 30mm) steel beam welded on top. A hole (51mm dia.) was made at its centre to guide the pile downwards. The beam was connected to the portal frame by four bolts (12.5mm dia.), two at each end.

3.2.3 Top Plate

The top plate which served as a reaction lid, was 780mm in diameter and 25mm thick. Its diameter was slightly smaller than the tank's inside diameter. A 60mm diameter hole was provided at its centre through which a 54mm inner diameter plastic tube (sleeve) was able to slide vertically so as to prevent the rubber bag from expanding against the pile. The sleeve was 400mm long with a 150mm diameter flange at its bottom resting on top of the clay bed. A portion (120mm) of the sleeve's length was above the top plate which was used as an indication of the top clay settlement. The reaction from the pressurised rubber bag was taken by four threaded compression rods (230mm long and 18mm in diameter). By means of those rods and four brackets the top plate was fixed in position in such a way that it could be adjusted to move up and down during the consolidation process, Figs. 3.2a and 3.2b.

3.2.4 Model Pile

The model pile was made from brass tubing with 50mm outside diameter and 1.0mm wall thickness. The total length of tube was 1.6m including a 40mm shoe which was made of the same material.

It was decided after some preliminary studies to cut

the brass tubing into six sections which could then be joined together by a specially made push-fit joints precisely machined for that purpose. Various alternative methods of measuring load used by a number of authors were considered but this method of splitting the tube proved to be the most practical and most efficient way for gaining access to the inside surface. The method used by Silva (1966) for example, required that the pile be split longitudinally throughout its length. That method was considered but rejected because of the possibility of the split joint opening and releasing locked-in manufacturing stresses. Moreover the true shape of a thin pipe can never be regained once it has been opened out. Another method which was considered was to fit the strain gauges on to the outside surface of the pile, located in circular grooves milled for that purpose, the groove being afterwards covered with a protective cement material following the installation of the gauges. That method also proved to be unsatisfactory, mainly because it would have required relatively thicker walls which would affect the sensitivity of the instrumentation under small loads.

3.2.5 Loading System

A specially-made pressurised rubber bag was used as a consolidation pressure source. It was fabricated to specification for the research project by Allied Rubber Products & Engineering Co. Ltd., Birmingham. The bag was

150mm high, 800mm in diameter, 3.0mm thick with the 65mm diameter hole at its centre to allow the pile to project down through, Fig. 3.3. As the main function of the bag was to furnish the consolidation pressure by expanding against the soil, its reaction was taken by the uprights on the tank sides as previously described in Section 3.2.3. A pressure regulator was used to maintain a constant pressure throughout the consolidation process. The operation of the system was based on the difference in pressure on each side of the pressure regulating valve, Figs. 3.4 and 3.5. Whenever a pressure drop occured (mainly due to soil settlement) air could be pumped into the bladder which in turn compressed the water in the cylinder to maintain the predetermined pressure. The surcharge pressure set by the rubber bag could always be inspected by the pressure gauge.

3.2.6 Pore Pressure Piezometers

The piezometer tips used in the investigation were designed by the Civil Engineering Department and manufactured in the department's workshop. Twelve piezometers were installed at selected positions in the soil surrounding the pile to monitor water pressures. In designing the piezometers it was kept in mind that stability, rapid response and a high degree of accuracy were important factors to be considered.

Preliminary tests on two sizes of piezometer tips were

carried out in a 300mm steel cubic box filled with soil to assess their reliability. The finally-adopted single piezometer tip consisted of a minute brass shell with two holes at its solid base, hypodermic tubes and a porous PVC disc. The piezometer shell had dimensions 15mm by 12mm in length and outer diameter respectively with 1.0mm wall thickness. Two ,10mm long by 1.0mm diameter, hypodermic tubes were fixed at the solid base. The piezometers were completed by glueing 2.0mm thick by 10mm dia. porous discs (porous plastic liners usually used in Rowe cells) at their ends, Fig. 3.6.

Water pressure on each piezometer tip was read via a digital strain meter through two pressure manifolds. Each manifold served six piezometers. Two additional manifolds were needed for deairing purposes. Figs. 3.7a and 3.7b show details of a typical manifold. The plastic tubes which connected the piezometer tips to the manifolds were 1.5mm in diameter. A complete network for connections is shown in Fig. 3.4.

3.2.7 Settlement Plates

Four settlement plates or discs were used at two different levels. The settlement plates consisted of 30mm diameter by 2.0mm thick steel discs attached to 1.5mm diameter steel rods. In order to allow a free movement and also to eliminate friction with the soil, the four rods were each sleeved with a 2.0mm inner diameter plastic

tube along their lengths. These plastic tubes penetrated the bottom of the tank through holes sealed afterwards to prevent water leakage. Six millimetre inner diameter brass tubes sleeved the plastic tubes so as to keep the rods in a vertical position, Fig. 3.8.

3.2.8 Pile Instrumentation

Nine positions were selected to record axial load within the pile, these are indicated by stations 1,2,...etc in Fig. 3.9. A full bridge load cell technique was adopted for this instrumentation. As previously mentioned, the pile was divided into six sections five of which were instrumented with electrical resistance strain gauges. The lengths of these shells were chosen such as to maintain equal distances between the various load cells. A large diameter as possible was selected for the model so as not to present practical problems with respect to instrumentation, whilst at the same time paying regard to pile length/diameter considerations.

Foil type, two directional strain gauges were applied on the inner surface of the pile at locations indicated in Fig. 3.9. The specification of these gauges is as follows:

Type : SHOWA, N21-FA-5 Two Directional

Gauge length (mm) : 5.0

Resistance (ohm) : 119.8 ± 0.3

Gauge Factor : 2.1

3.2.9 Strain Gauges Mounting Technique

Before mounting the strain gauges, they were examined to check their resistance and reliability. The area to be gauged was thoroughly cleaned and dried. Positioning marks were accurately scribed along the longitudinal axis of each section of the pile for locating the gauges. A sufficient amount of strain gauge cement (Loctite 15490, Cyanoacrylate adhesive) was applied on the prepared area and each strain gauge was then mounted carefully on its position. Pressure was applied by using the thumb in order to squeeze out the air and excess cement and hence to ensure proper adhesion. When the network was completed, the continuity was checked before the gauge coating was applied. Silicone rubber coating (RTV 3145) was used to cover all the gauges and terminals to ensure a fully water proof network.

Each load cell comprised eight strain gauges, four active and four dummy gauges connected to form a full bridge circuit, Fig. 3.10. The use of four active longitudinal gauges would minimise the effects of any bending within the load cell while the use of dummy lateral gauges, ensured that the effects of apparent strain (due for example, to temperature variations) would also be minimised. The lead wires and gauge leads were then soldered to the terminals, bundled into cables and cemented to the inside surface of the pile. The principle of strain-gauges technique along with the derivation of

the full bridge circuit can be found in Elmasry (1963), p:26.

Fig. 3.11 shows four strain gauges mounted on the outer surface of a pile specimen for demonstration purposes.

3.2.10 Digital Strain Indicator

The bridge circuits for the load cells were completed and balanced by connecting them to a digital strain indicator, Fig. 3.1b. The system was manually operated and had the following properties :

Type : SGA 1100 with basic amplifier unit
Bridge Supply Current : 60mA
Current Output : 20mA at a max. voltage of 6 volts
Gain in Voltage : up to 10000 times
No. of Channels : 13

The input bridge volts were adjusted through the front panel and maintained at 2 volts for each channel. The out-of-balance voltage across the full bridge circuit was read out directly through a digital screen. The signal output was magnified 2000 times which was sufficient to ensure the required precision.

3.3 Calibration Programme

An extensive calibration programme was carried out before starting the experimental procedure. This included load cells calibration, piezometer calibration and manifold calibration. The following sections provide a discussion of the above categories.

3.3.1 Calibration of Load Cells

After completion of the gauge mounting stage each section of the pile was placed in a calibration rig, essentially a triaxial compression rig. The load was cycled many times to seat the load cells and to examine any hysteresis tendency within the adhesive layer.

The preliminary calibration consisted of increasing the load in increments of 100N up to a maximum of 600N. At each increment the millivolt output was recorded by the digital strain indicator. The sensitivity of the load cells was determined from a plot of load versus output voltage. Each load cell was individually calibrated in this way.

At the end of the preliminary stage, the pile was assembled and then load tested for gauge response with the pile submerged in water for two days. The main calibration of the load cells (stations) started when the assembled pile was placed in the tank for load testing. Wires leading from every station were connected to the

strain indicator in separate channels. After setting each channel, readings were taken for every load increment the pile was subjected to. The sensitivity of this instrumentation was of the order of 0.90 ± 0.02 micro-strain per N. Fig. 3.12 represents a calibration chart for every station along the pile. All stations recorded a linear response above 30N. This behaviour (of a non-linear response) of the readings is believed to be a common feature of most of the load measuring devices based on strain gauge instrumentation.

3.3.2 Strain Gauges and Temperature

In order to maintain a constant temperature environment throughout the test programme, a thermostatically controlled air conditioning system was used. Although every effort was made to keep the room temperature stable, there were inevitable temperature variations, particularly during the summer period, and it is felt this may have affected slightly some of the test results. (This is dealt with in more detail in Chapter 5).

3.3.3 Piezometer Calibration

An ordinary oedometer ring was used in the calibration of the piezometer tips. The calibration was accomplished simply by replacing the top cap of the ring by a specially

made steel disc with a diameter of 76mm and thickness of 25mm. A hole, with a diameter slightly larger than the piezometer diameter, was made off centre of the disc to project the piezometer through.

The consolidation ring was set up by preparing the soil and placing the disc on top. After connecting the tubes of the piezometer to the manifold, which in turn was connected to the strain meter, the piezometer tip was pushed through the hole into the soil. Silicon rubber was used as a sealent. Air bubbles were flushed out of the system before any measurements were taken. The calibration started when the soil sample was loaded incrementally and pressure readings were taken for each load increment applied. The response time of the piezometer tip was monitored during both loading and unloading and was found to range between 2-4 seconds within each manifold.

Fig. 3.13 presents results of the piezometer calibration for the two manifolds.

3.3.4 Manifold Calibration

The piezometer transducers within each manifold were calibrated using a triaxial test chamber. This was achieved by connecting each manifold to a triaxial cell and a digital voltmeter. Water pressure was applied to the manifold via the triaxial chamber and read by a pressure gauge. Readings of the voltmeter were taken for each increment of pressure applied. So as to provide a check

on the pressure applied, a pre-calibrated digital voltmeter was also connected to the triaxial chamber. Fig. 3.14 shows the results obtained for each manifold.

It should be noted that the piezometer calibration discussed in the previous section is also a manifold calibration with the pressure transmitted through the piezometers to the manifolds. This was considered an important step in assessing the reliability of the piezometers prior to starting the testing programme. However, an examination of the results obtained by both calibrations, indicated that the calibration constant determined using the oedometer, Fig. 3.13, was less than that obtained from the triaxial cell, Fig. 3.14. The difference was of the order of 0.4 millivolt per 10 kPa or 0.6 kPa for every 10 kPa pressure applied. This is believed to be attributable to the natural decay of the water pressure due to dissipation through drainage, as is usual with the oedometer.

3.3.5 Manifolds and Temperature

After the completion of the calibration stage, the two manifolds were tested against temperature variation. A 40 day period was allowed to obtain a wide variation of temperature. As the water pressure in the manifolds was maintained unchanged (30 kPa), the output readings from the voltmeter were registered for any change in the ambient temperature. Fig. 3.15 presents data obtained

regarding the effect of temperature variation on the two manifolds. The voltmeter readings were zeroed at the start of the test.

By combining the results of Fig. 3.14 with Fig. 3.15, an example is given below to illustrate the effect of 1°C change of temperature on the measured pore water pressure:

- from Fig. 3.15, 1°C of the temperature change increases or decreases the voltmeter readings by an average value of 0.45 millivolts.
- from Fig. 3.14 with an average calibration constant for both manifolds of 7.2 millivolts per 10 kPa, this will result in an apparent change of 0.63 kPa in water pressure.

It should be noted herein that graphs showing the dissipation of pore water pressure at all stages have not been modified to take into account the ambient temperature variations present throughout the duration of testing programme.

3.4 Experimental Procedure

The following is a step-by-step summary of the procedures used in setting up the experiment and preparing the apparatus for the test programme :

1) The piezometer lines and the settlement rods were fixed in position by passing them through previously made threaded holes in the tank base. Hexagonal nipples, 1/4 BSP(6mm), sealed with 8mm rubber grommets, were screwed into the holes to give a completely water tight fitting. A total of 28 holes were made; two holes served each piezometer and one for each settlement rod. The position of all piezometers tips together with the settlement plates are shown in Fig. 3.8.

2) Radial drainage was provided by covering the inside surface of the tank with a 2mm thick filter fabric sheet.

3) The bottom sand layer, consisting of fairly uniform sand passing the No.16 (1.18mm) sieve and retained on the No.100 (150μm) sieve, was placed by hand and saturated with deaired water. All the drains were deaired and covered with filter paper before placing the sand layer.

4) At this stage, and before filling the tank with clay, the twelve piezometers were connected to the strain indicator via the two manifolds and all lines were filled with deaired water.

5) A remoulded soft silty clay obtained from Stirling was used as the consolidating medium. Chapter 4 offers a description of the area together with the geotechnical properties of the soil.
Originally in fairly large lumps supplied in 20kg plastic

bags, it was stored in the laboratory for one day before the filling operation began. The clay was thoroughly mixed by using a large bowl mixer. Each batch was mixed for approximately three minutes. No water was added during the mixing operation as the natural water content (54.5%) was found sufficient to give good workability both during the mixing and the filling stages. The clay was placed by hand and care was taken to prevent air pockets from being trapped in the clay. Each batch provided enough clay for approximately 20mm thickness of soil in the tank. After laying every 4 or 5 layers, the soil was compacted using a wooden rammer which proved to be an efficient way for compaction and removing as much air as possible. The filling operation took about 5 hours without any intermission until the clay bed reached its final level. No target density was sought during the clay placement, but it should be noted that the measured density of the clay at the time of filling operation was 17.4 kN/m^3 while that of undisturbed natural state sample was 17.8 kN/m^3.

6) Nine samples of the clay were taken for moisture content determination at three different levels of the clay bed during the filling operation. Samples for shear strength determination and consolidation tests were taken at mid-depth and were tested in three series of tests in order to minimise any inherent errors caused by sample preparation. Chapter (4) describes the testings carried out on the soil.

7) The plastic sleeve with the flange at the bottom was placed and positioned to be in line with the top hole of the overhead beam. The main purpose of the sleeve was to prevent the rubber bag from expanding against the pile. As a portion of the sleeve was above the top plate, it was also possible to record the top clay settlement.

8) An 80mm sand drainage layer was provided on top of the clay and saturated with water.

9) To allow stabilisation of pore water pressure and to permit the clay to consolidate under its own weight, a time period of 40 days, after clay placement, was found adequate for the pore water pressure to come into equilibrium. Pore pressure readings were taken during that time. Water content distribution along the clay bed was also believed to have been achieved during the 40 days.

10) After obtaining stable state readings of pore water pressure, both the rubber bag and the top steel plate were carefully placed in position. The pile was then pushed down through the hole in the overhead beam and projected vertically to sit on the ring plate. A 200 N dead weight was sufficient to push the pile downwards through the clay bed to its final position. Unfortunately no measurements concerning the rate of penetration of the pile with load was made. The pile was marked in order to ensure the required penetration for its final position on the ring

plate. Readings of pore water pressure, settlement as well as pile axial loads were started immediately after pile driving. The time period between driving the pile and commencement of the testing programme was six days. This time, as will be shown in Chapter 5, was required for the decay of excess pore water pressure due to pile driving.

3.5 Testing Programme

The testing programme comprised furnishing surcharge pressures of different magnitudes on the soil layer by means of the pressurised rubber bag. As a failure in the loading system occurred prior to accomplishing the testing programme, it was decided to conduct a "2nd" testing programme on the same soil. (The term "2nd" used to differentiate between the loading stages involved in the "1st" testing programme which was performed before the failure, and the following loading stages after the failure). Results obtained for both programmes are presented in chapter (5). Below is a detailed description of the two testing programmes.

3.5.1 1st Testing Programme

This testing programme comprised increasing the surcharged pressure in three successive stages, i.e., 0-30 kPa, 30-60 kPa and 60-90 kPa.

The first stage commenced at the end of the six day period required for pore water pressure equalisation. Readings were taken in short regular intervals (every 3 hours) and as the test progressed, these time intervals were lengthened. Since all the piezometers were connected to two manifolds, it was considered advisable to allow some time after valve switching to permit the pressure in the line to level off. A time period of half an hour, between the switchings and readings, was found adequate for this purpose. The 30 kPa pressure increment was maintained for a period of 35 days. The top plate was then lowered down approximately 40mm by adjusting the four bolts. The surcharge pressure was then increased to 60 kPa and was maintained for an additional 36 days. Once again, the top plate was lowered by about 30mm.

At the end of the 60 kPa stage, and after increasing the pressure to 90 kPa for the 3rd stage, the rubber bag burst on the second day following the pressure increase. Firstly, the pile was lifted and the top plate removed in order to remove the bag for repairing. After releasing the bag the top plate was lowered down again into position to rest on the sand layer. Two hydraulic jacks were then used to prevent swelling of the soil.

Despite these setbacks to the testing programme the third loading stage was carried out after repairing the rubber bag. The results of that stage (Chapter 5) showed no continuity with those of the previous stages. However, because of the discontinuity in the results, it was decided to conduct a similar testing programme on the same

soil with the same properties in order to make good any deficiency due to the last loading stage in the previous programme. The only difference between the two testing programmes was the magnitude of the loading stages involved; the 1st testing programme contained three loading stages while the 2nd testing programme contained four loading stages.

The time required to complete the 1st testing programme was about seven months. Comprehensive soil tests were then carried out in order to compare soil properties before and after consolidation.

3.5.2 2nd Testing Programme

The second testing programme started with the use of a new rubber bag. All the soil was removed from the tank and remoulded again to a predetermined water content, such that the same shear properties of the soil as those of the first testing programme could be maintained. That was achieved by shearing samples at different water contents until the required shear strength was determined. After filling the tank and setting out all measuring systems, a second testing programme started with pressure increments of 0-15 kPa, 15-30 kPa, 30-45 kPa and 45-90 kPa.

The duration of this second testing programme was six months.

3.6 Summary

The main apparatus described in this chapter was designed and constructed in the civil Engineering Department's workshops. All the elements included in the experimental work were checked and tested to obtain both accuracy and reliability.

Before starting the testing programme, an extensive calibration procedure was conducted on the measuring devices (load cells, pore pressure piezometers and pressure manifolds). It was realised that temperature variation, particularly during the summer period, had an inevitable effect on the pressure manifolds. A change of 1°C of the temperature resulted in an apparent change of 0.63 kPa in water pressure.

After preparing all the instrumentation and setting out the apparatus, the testing programme commenced by applying different load increments on the soil surface. Readings of downdrag loads, pore water pressure and settlement started soon after load application.

The use of a rubber bag as a pressure source together with a pressure regulator (to maintain a constant pressure) proved to be a successful system in furnishing surcharge pressures to model tests where consolidation problems are involved. The main advantage of this loading system over other systems, circular rigid plates with hydraulic jacks, (as in the case of Elmasry, 1963 and others) is believed to be its flexibility, i.e., it

provides a uniformly distributed load on the surface of the soil in which it simulates the application of a surcharge pressure (by fill) in field problems.

It is unfortunate that the pressurised bag broke down during the first testing programme, however it is believed that by carefully replicating all the previous testing conditions, the continuity of the main programme of work did not suffer.

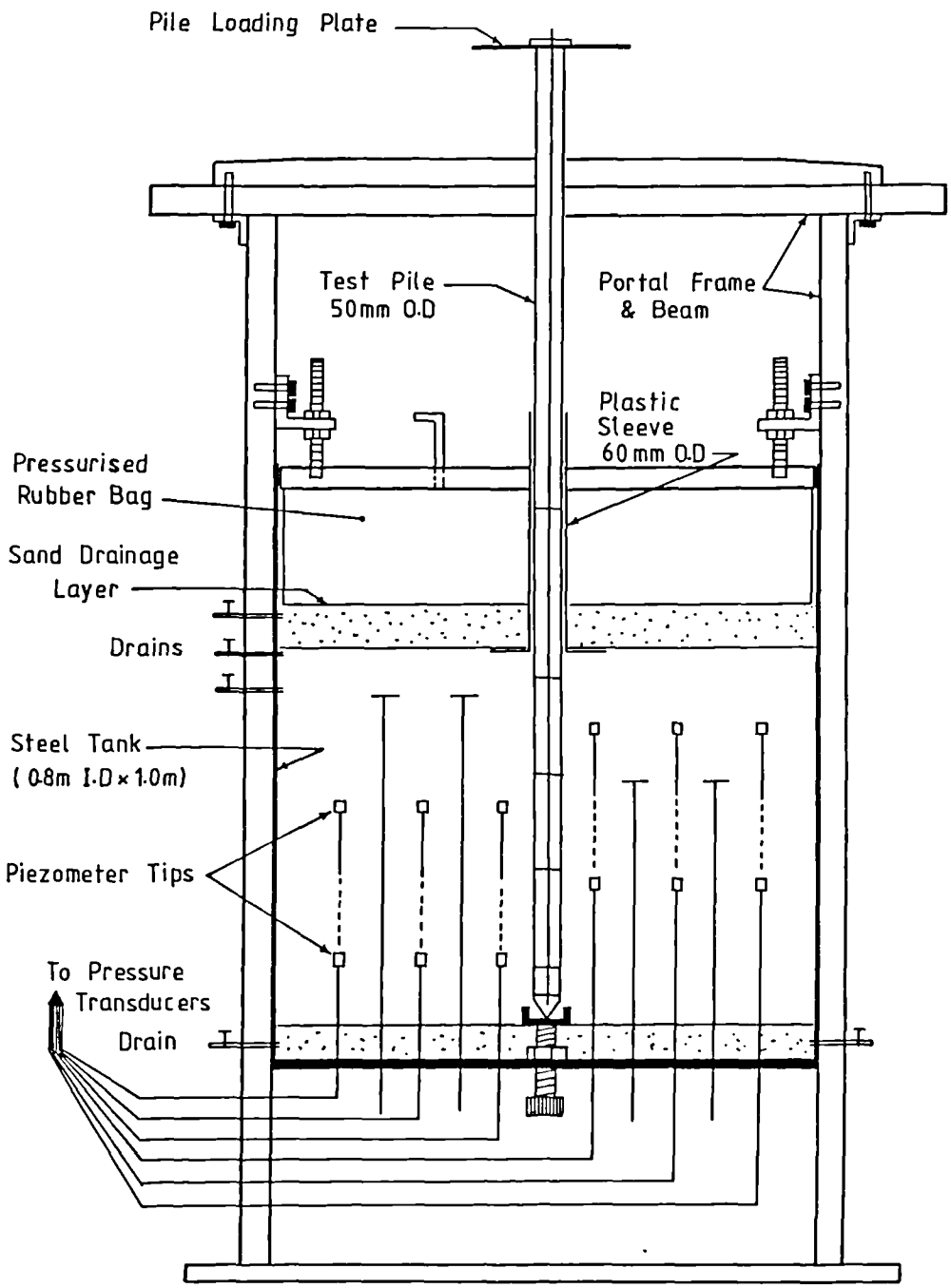

FIG. 3.1a EXPERIMENTAL SET-UP

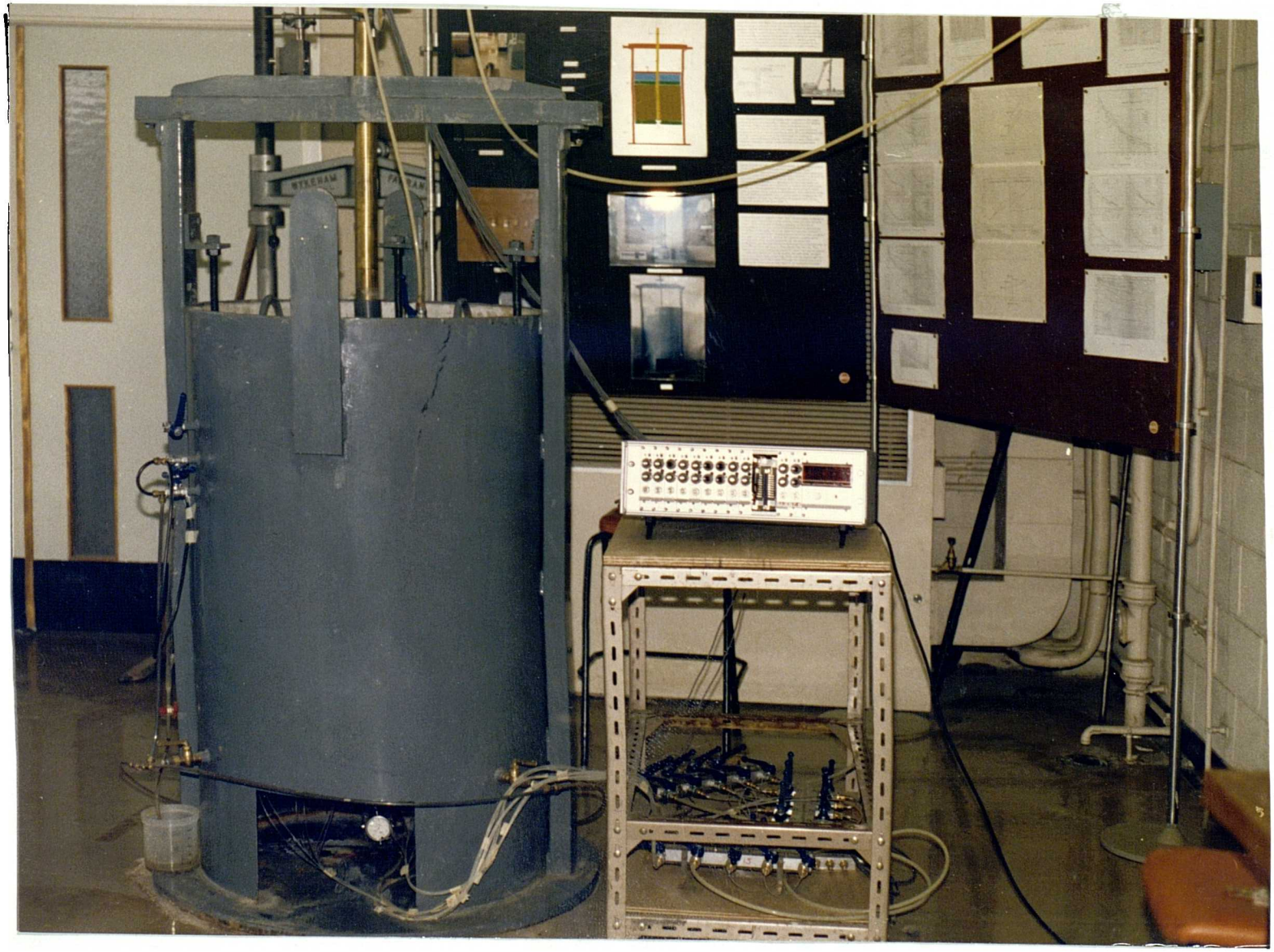

FIG. 3.1b EXPERIMENTAL SET-UP OF MAIN APPARATUS

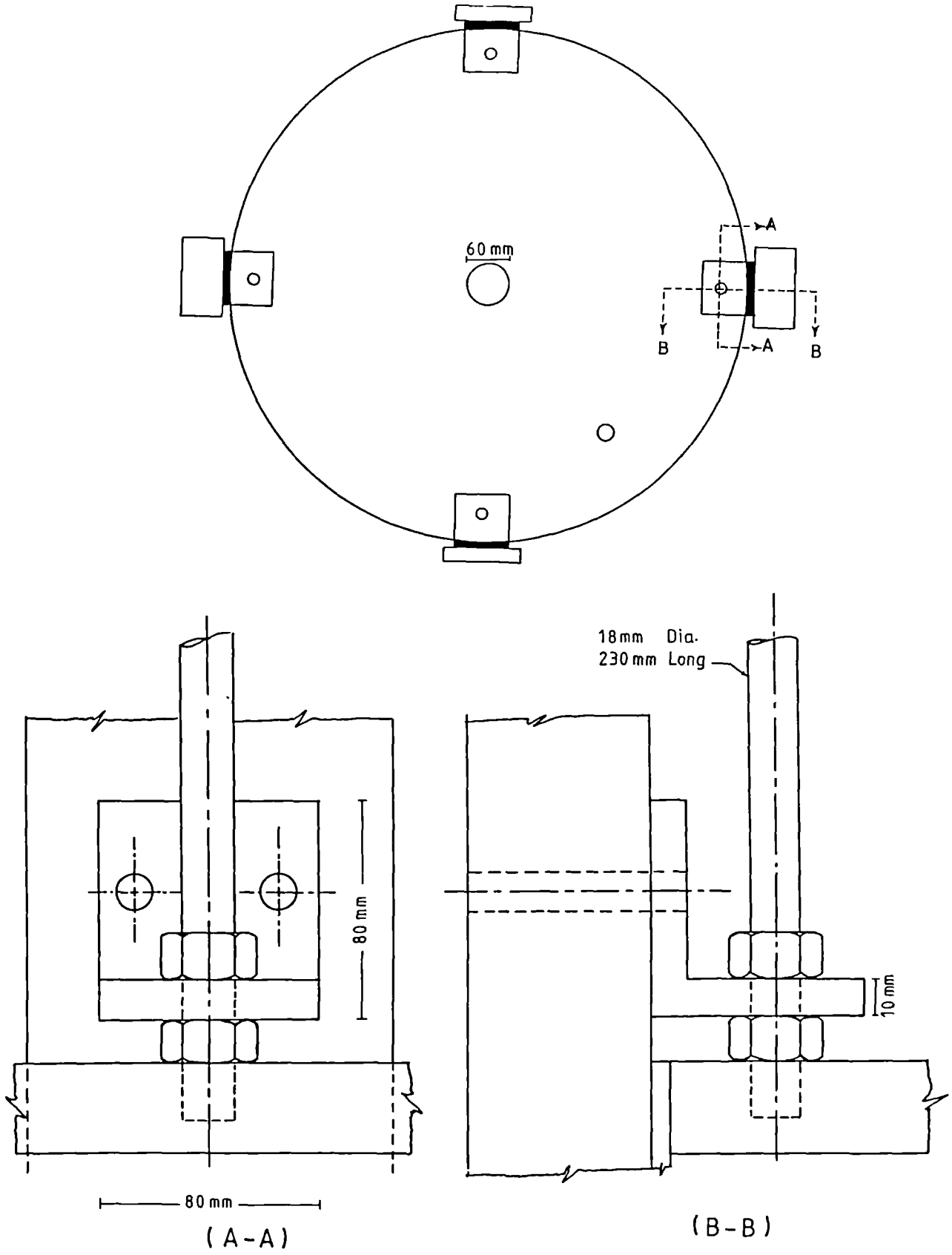

FIG. 3.2a TOP PLATE AND BRACKETS

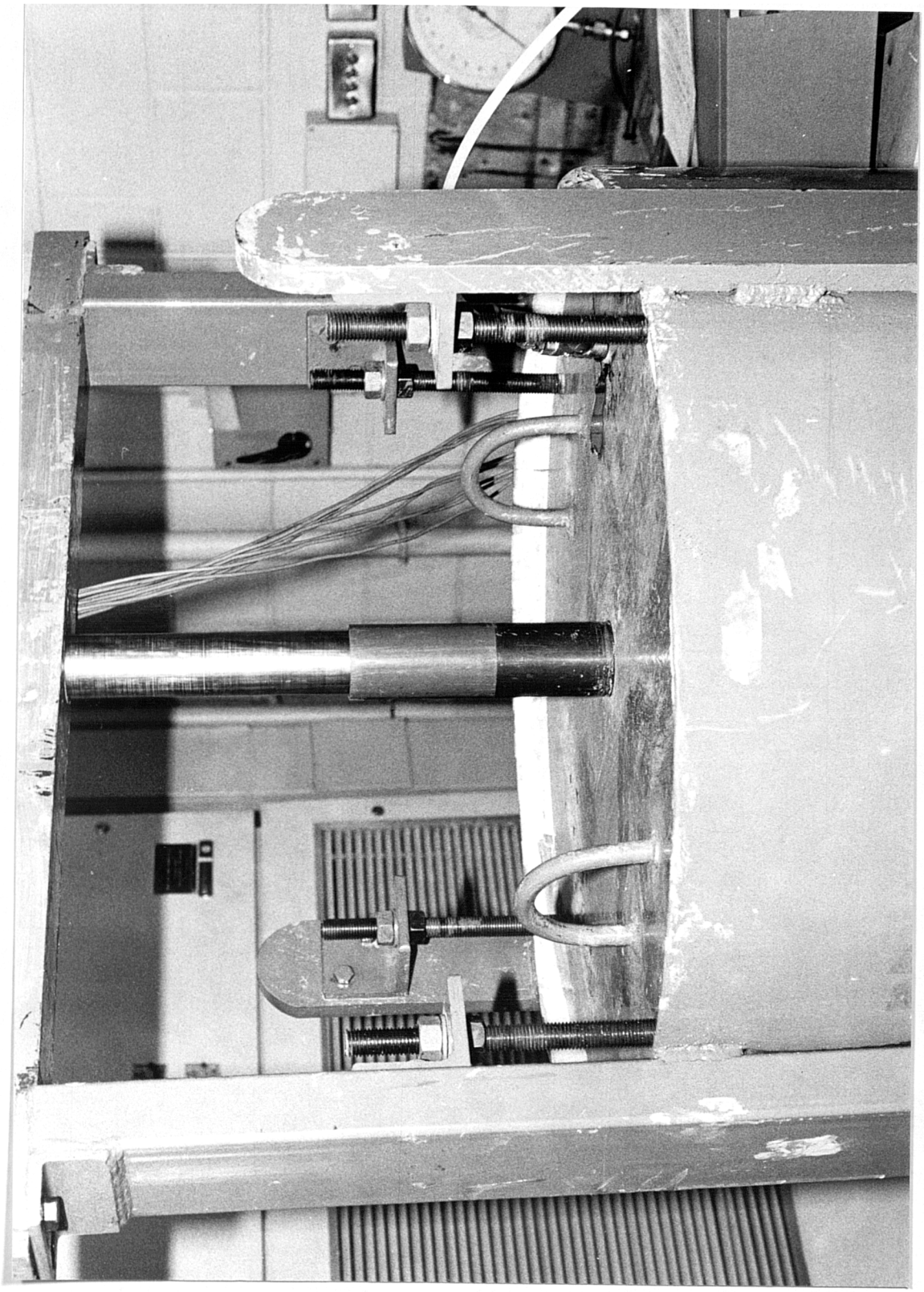

FIG. 3.2b TOP PLATE AND TIE BOLTS

FIG. 3.3 PRESSURISED RUBBER BAG (deflected)

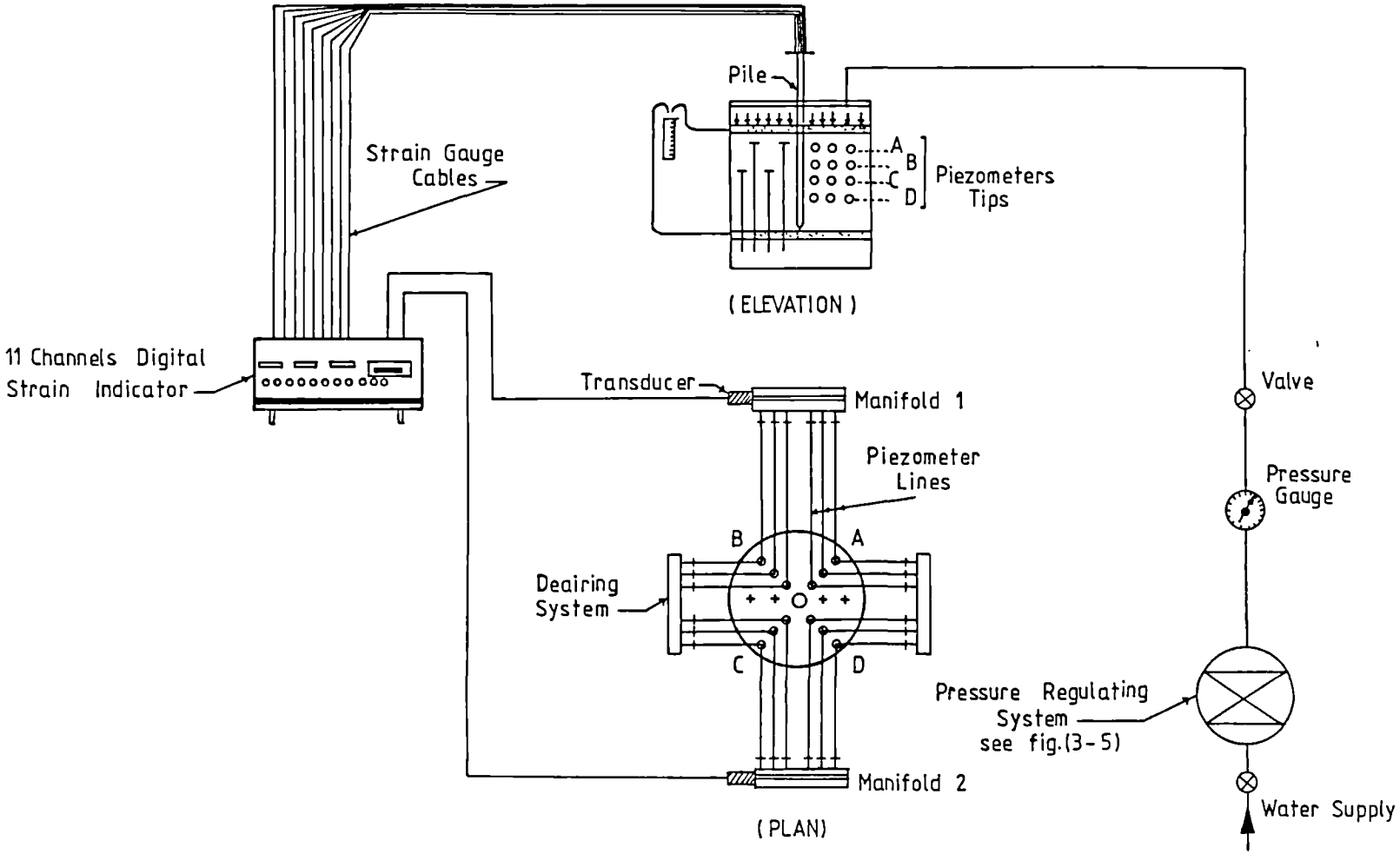

FIG. 3.4 SCHEMATIC DIAGRAM OF MEASURING SYSTEMS AND CONNECTIONS

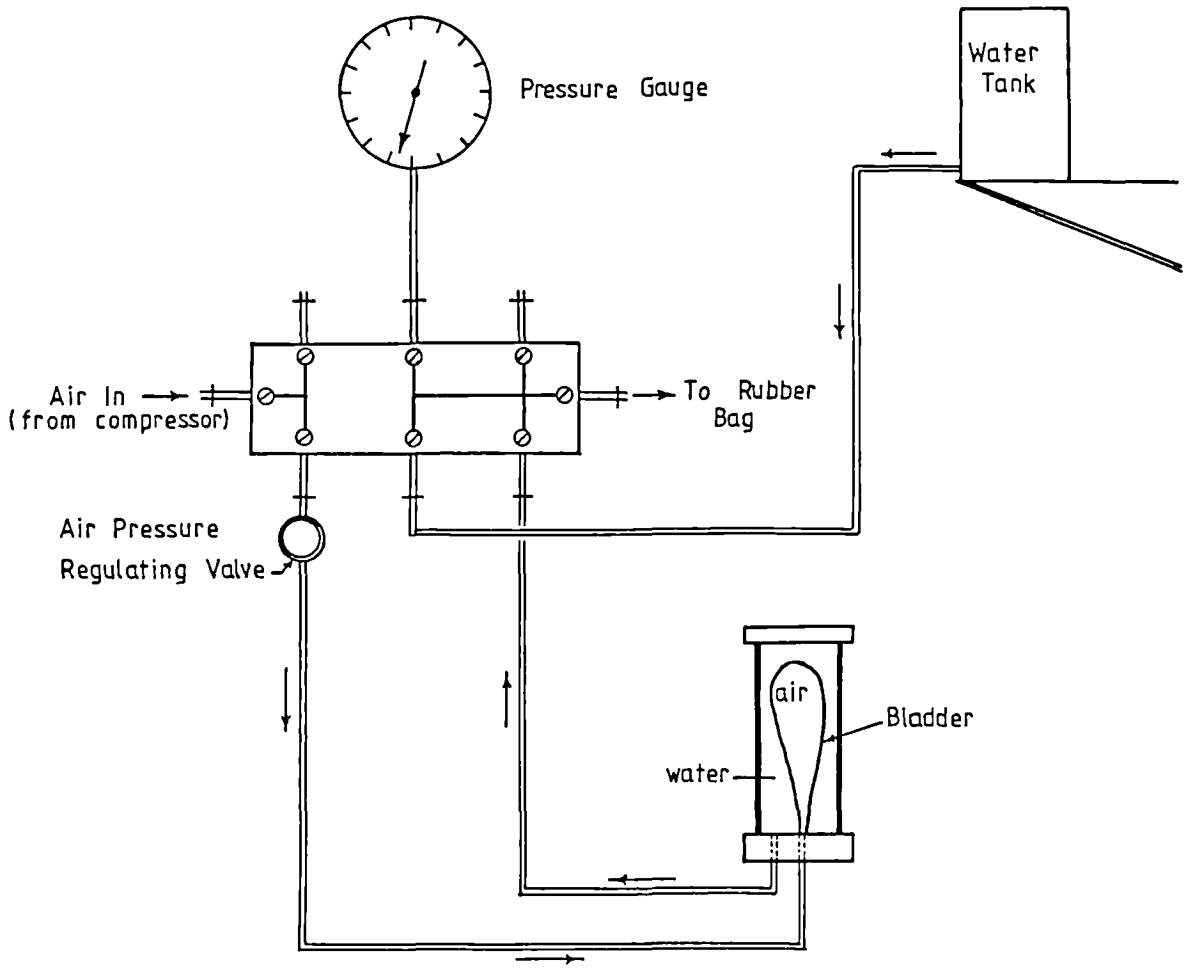

FIG. 3.5 PRESSURE SUPPLY SYSTEM

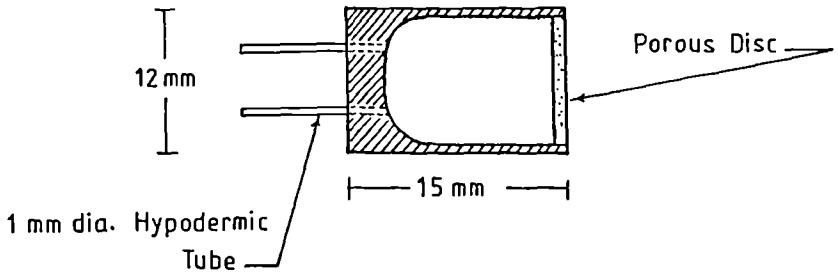

FIG. 3.6 PIEZOMETER TIP

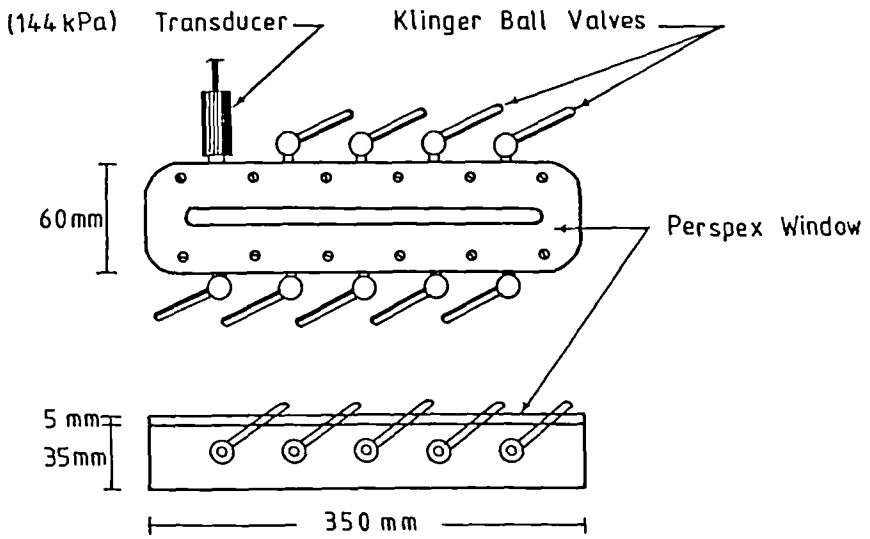

FIG. 3.7a MANIFOLD

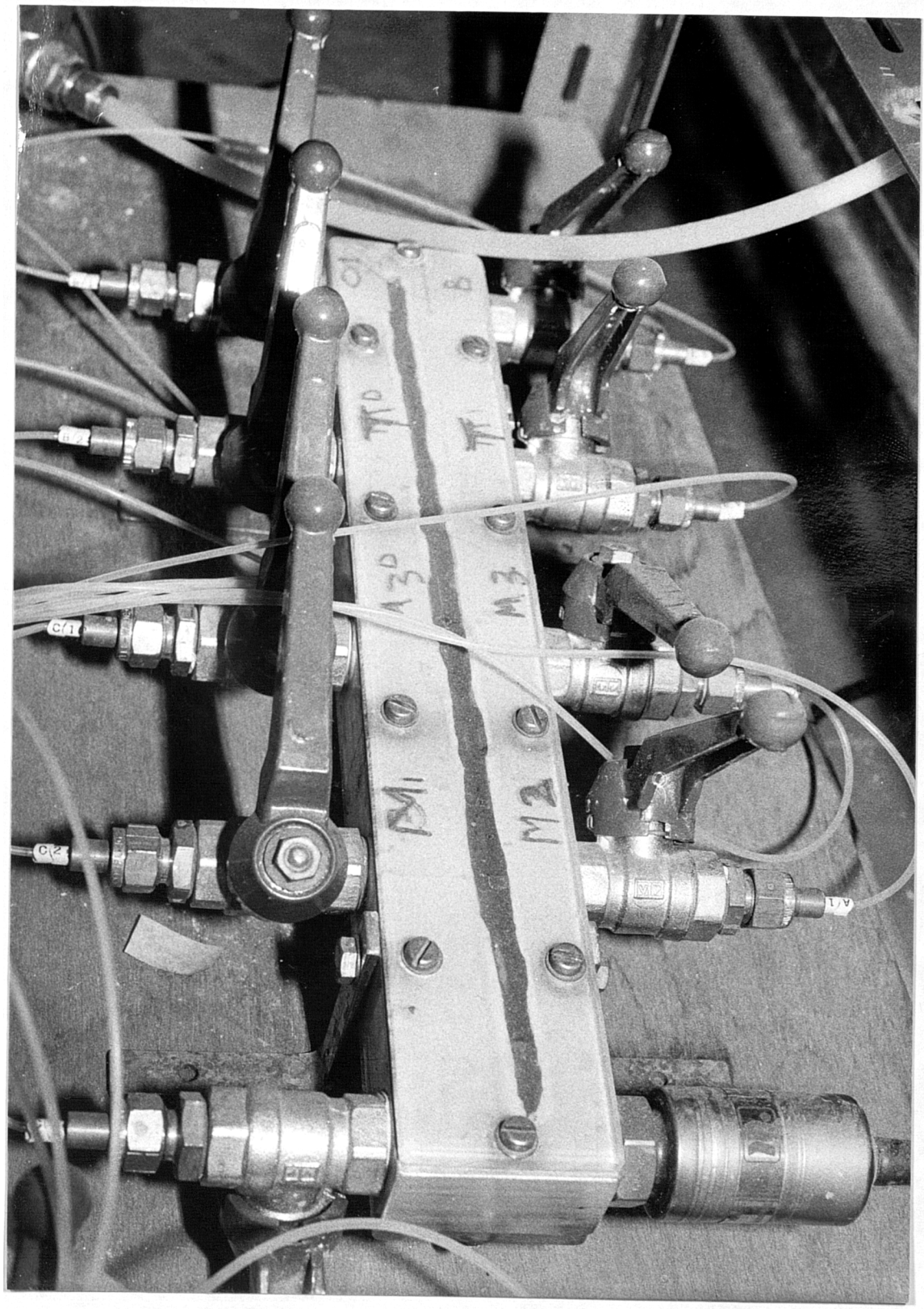

FIGURE 3.7b SINGLE MANIFOLD COMPLETE

WITH CONNECTIONS

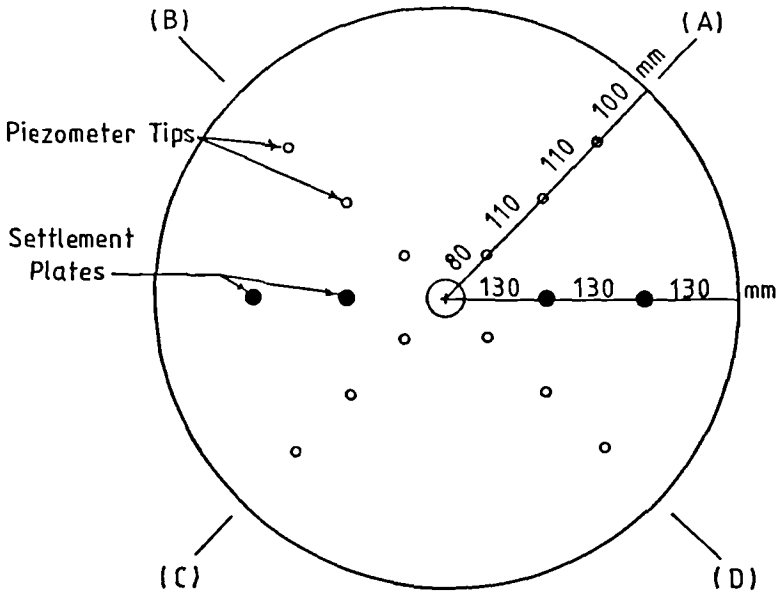

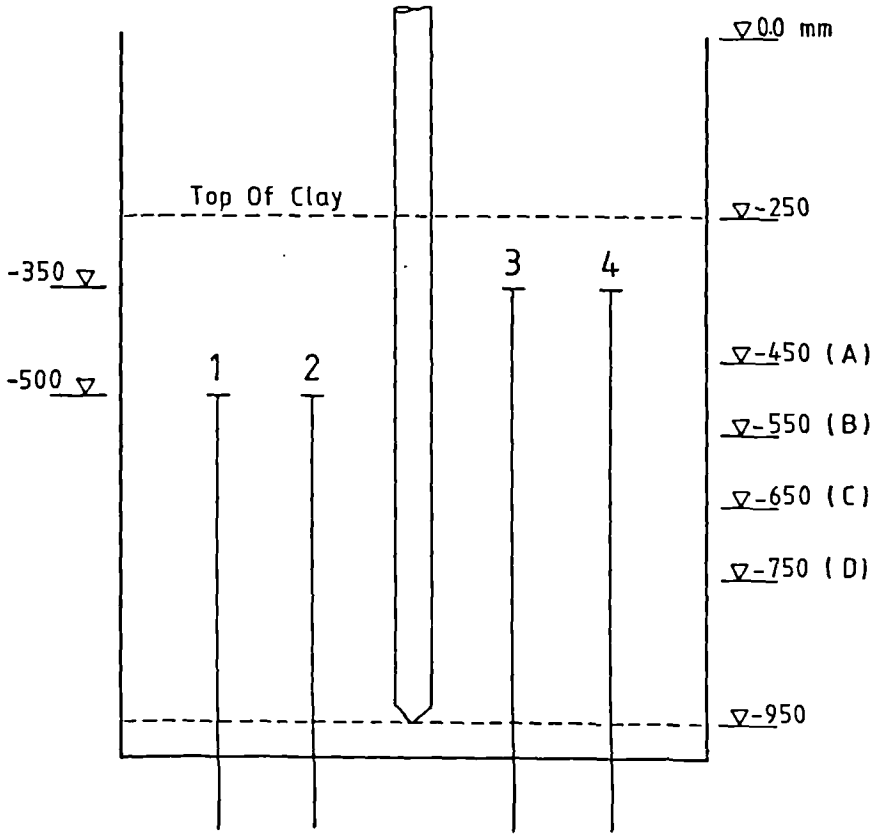

FIG. 3.8 INSTRUMENTATION ARRANGEMENT

A, B, C, D = Piezometers Locations
1, 2, 3, 4 = Settlement Plates

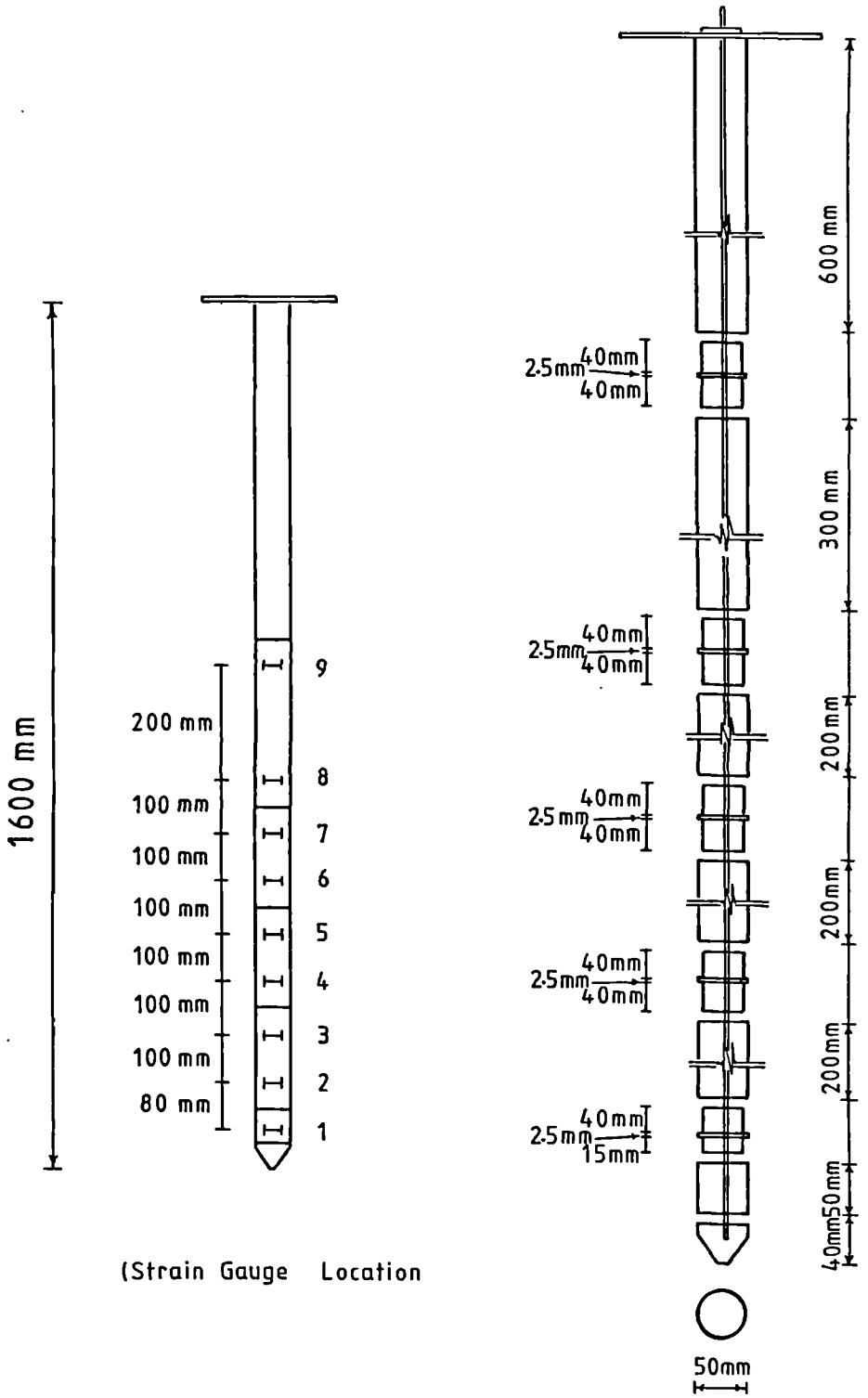

FIG. 3.9 THE MODEL PILE

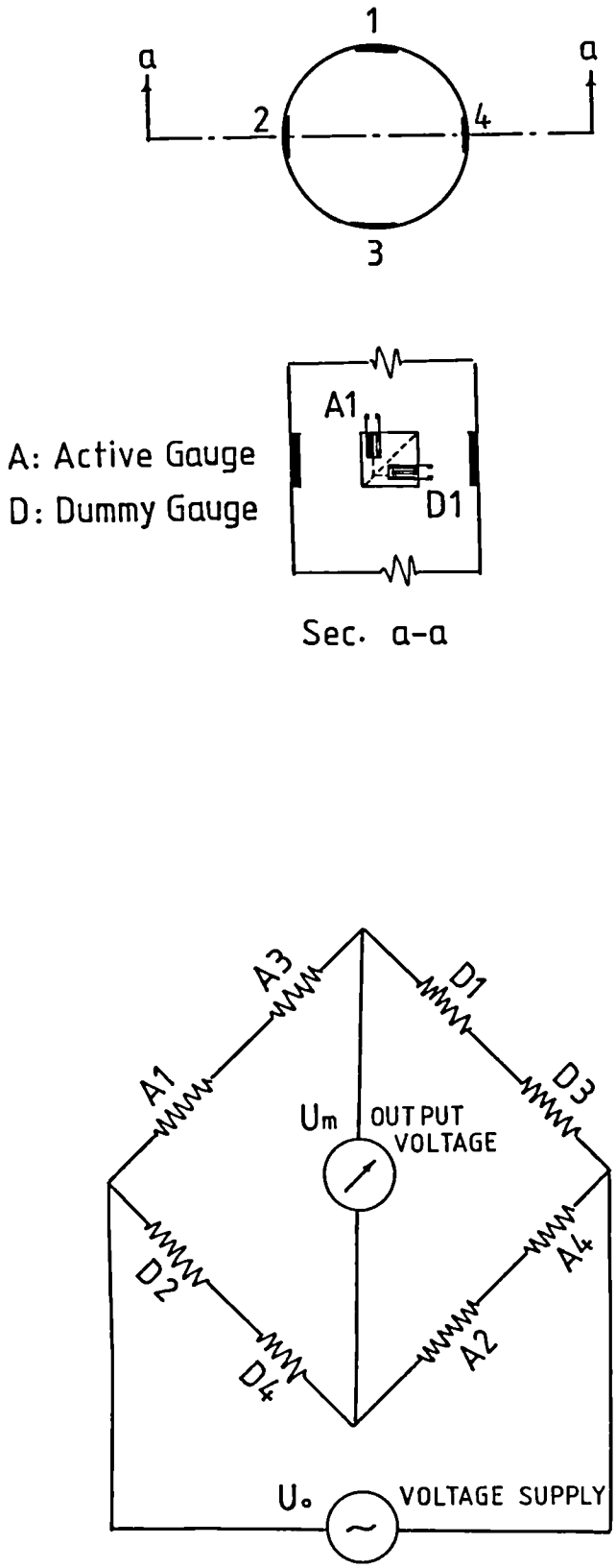

FIG. 3.10 FULL BRIDGE CIRCUIT CONFIGURATION

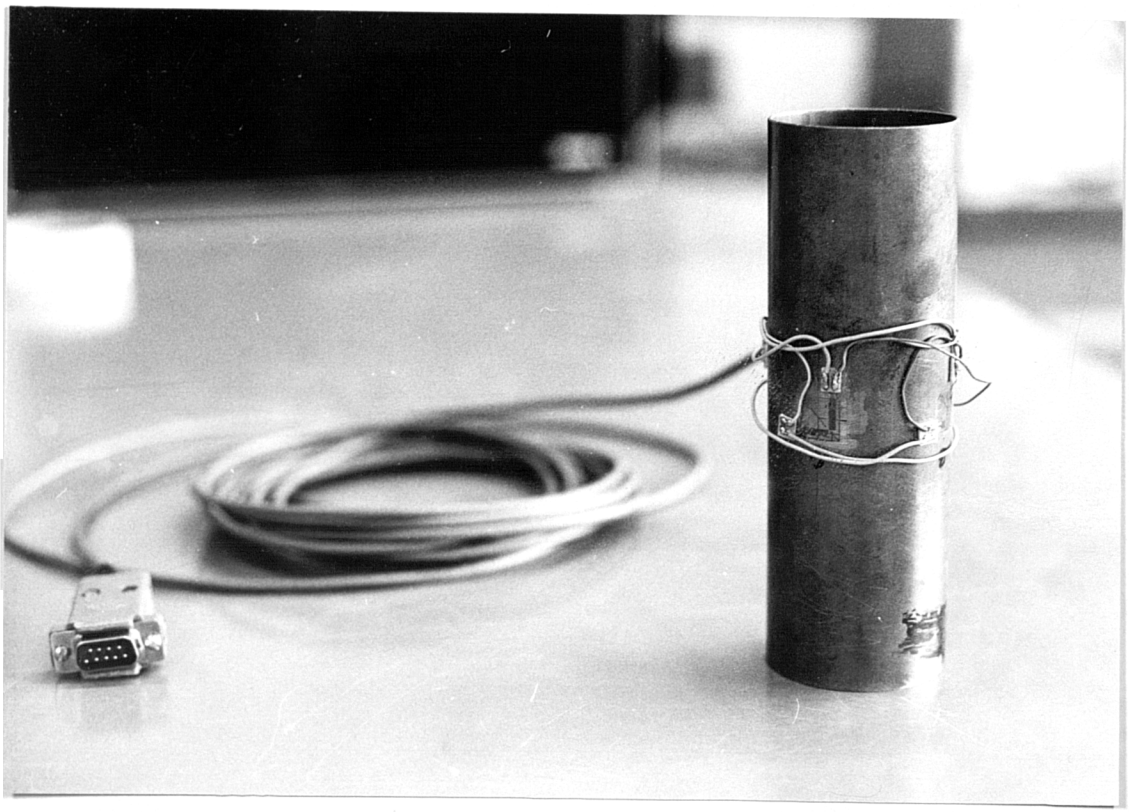

FIGURE 3.11 PILE SPECIMEN SHOWING TWO DIRECTIONAL STRAIN GAUGES ON ITS OUTSIDE SURFACE

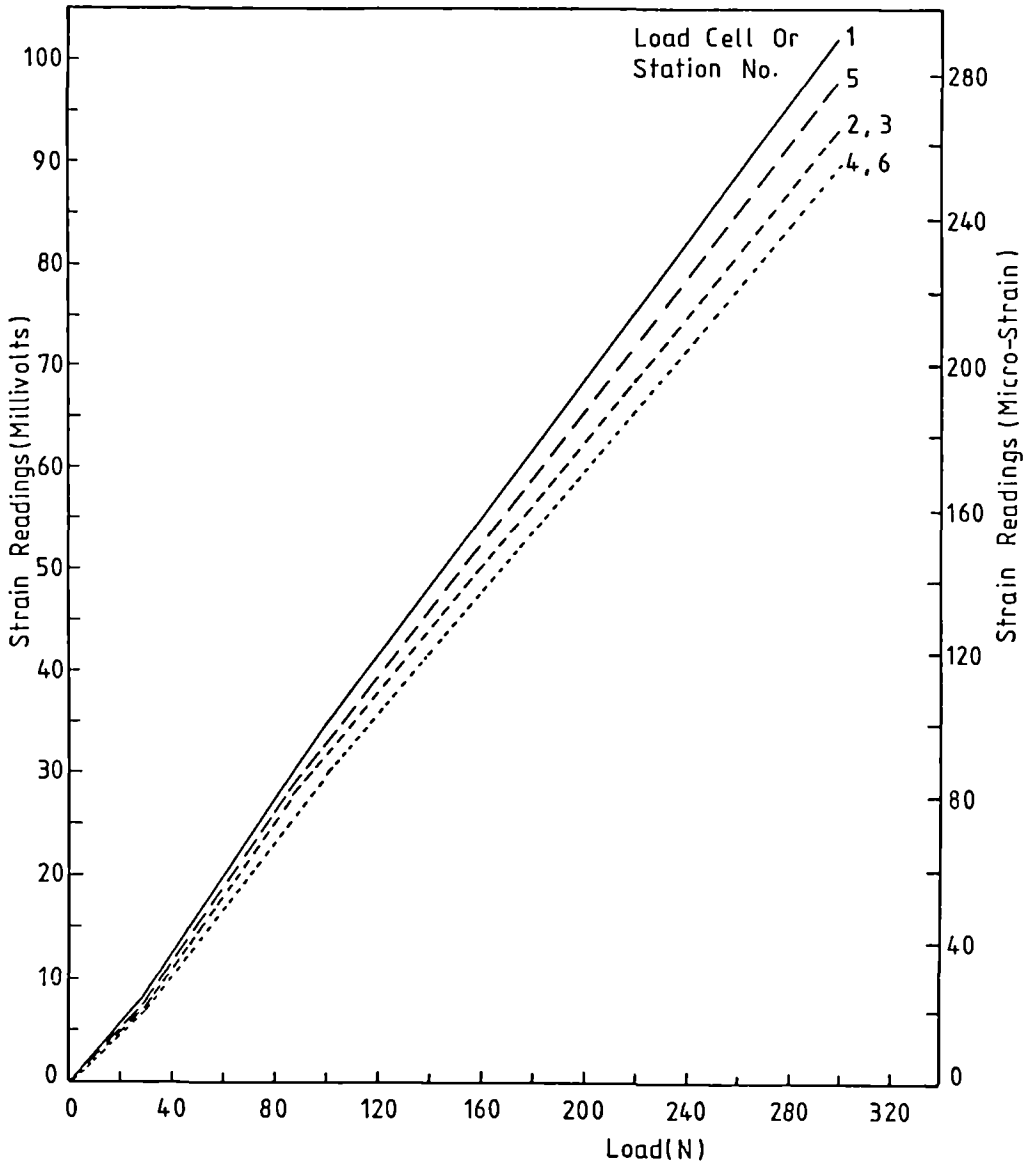

FIG. 3.12 LOAD CELLS CALIBRATION CHART

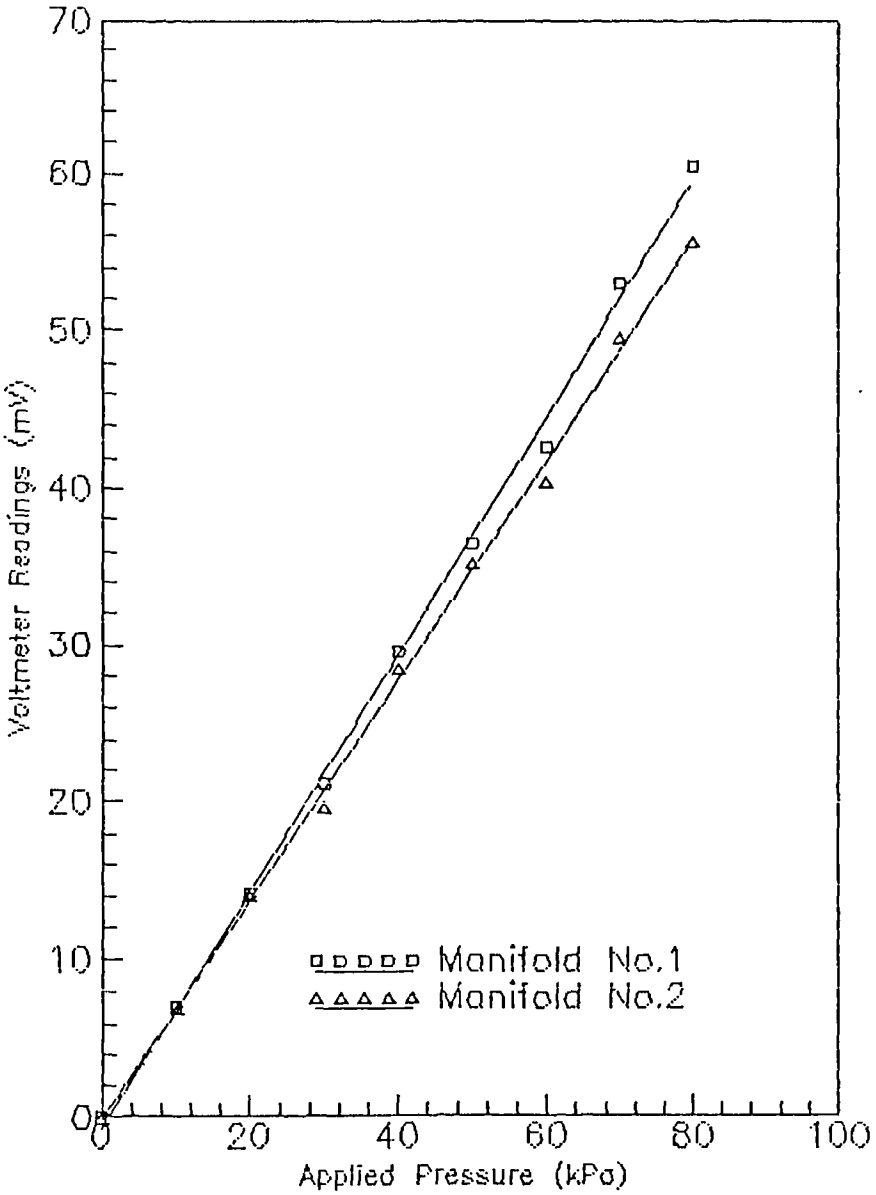

FIG. 3.13 CALIBRATION RESULTS FOR THE MANIFOLDS USING MINI PIEZOMETER AND OEDOMETER RING

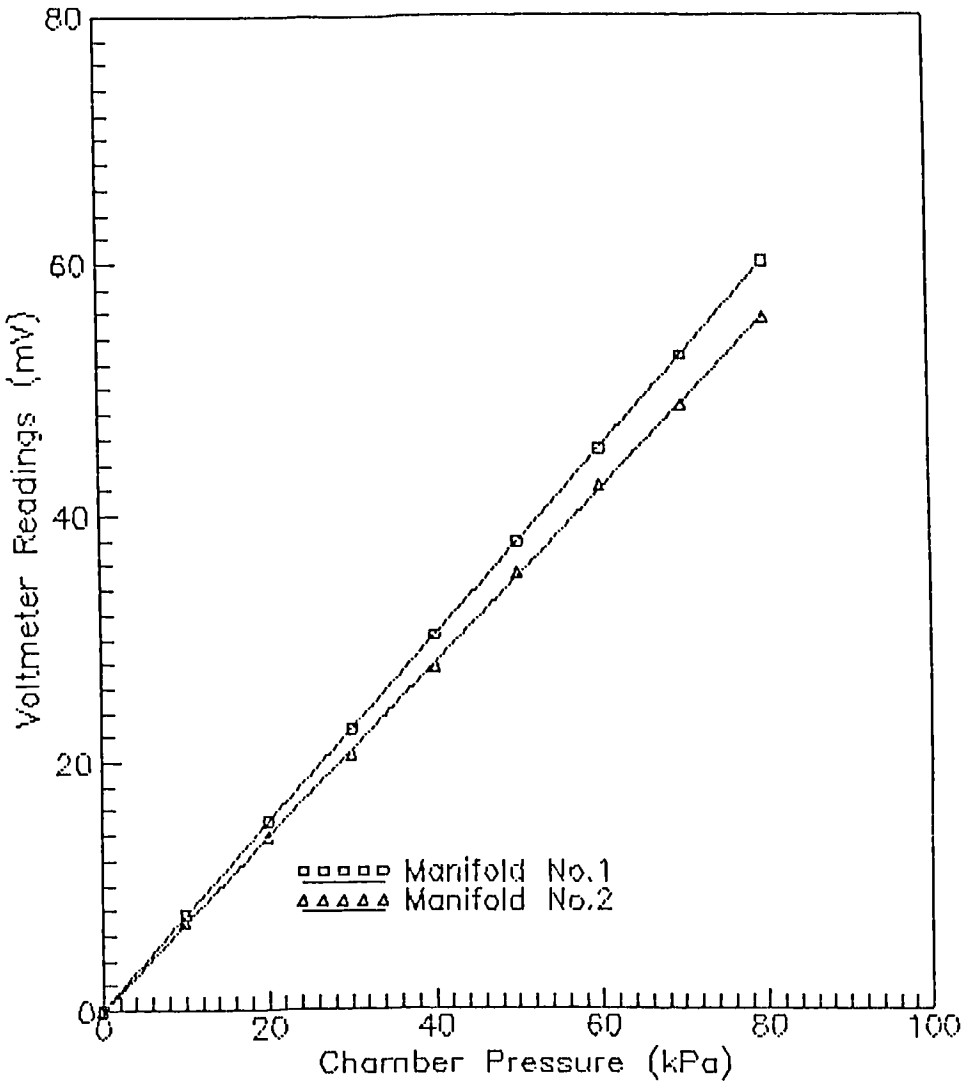

FIG. 3.14 CALIBRATION CHART FOR PRESSURE MANIFOLDS USING TRIAXIAL CHAMBER

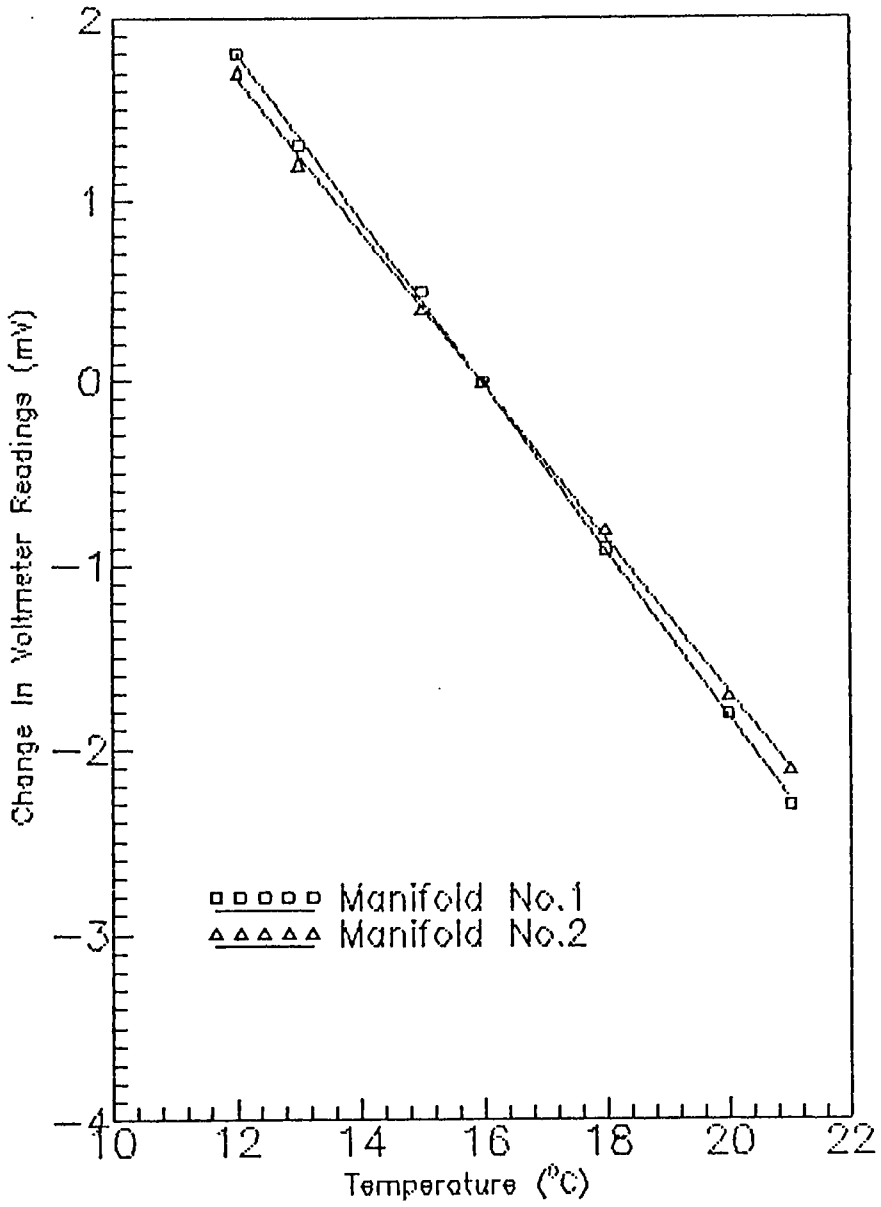

FIG. 3.15 EFFECT OF TEMPERATURE ON PRESSURE MANIFOLDS

CHAPTER (4)

SOIL DESCRIPTION AND TESTING RESULTS

The soil used in this study was obtained from the upper Forth Estuary in Scotland where a considerable thickness of glaciomarine sediments are present. A sufficient quantity of soil was sampled from a landsite at Bannockburn which is located 2 miles south of Stirling, see Fig. 4.1.

In the first part of this chapter (Section 4.1), the geology of the site and the geotechnical properties of the soil will be discussed, while Sections 4.2 and 4.3, present the sampling procedure and the laboratory test results, respectively.

4.1 Site Description And Soil Conditions

The Forth Estuary is regarded as an area of concern to the geotechnical engineer due to the presence of thick deposits of soft, normally consolidated clays and silts. Gostelow and Browne (1981) reported that the post-glacial Esturine and marine sediments, which vary in thickness between 50-60 m, consist of grey very fine sands and silts

overlain by clayey silts and silty clays which are known as the "carse".

The presence of soft carse clay deposits result in very difficult foundation conditions particularly in areas where large heavy structures exist. For example, all structures associated with the petroleom refining industry in Grangemouth are piled either to gravel or to till underlying the clay.

When problems concerning foundations and their design are involved in such areas, negative skin friction therfore becomes an important factor to be considered in such cases.

4.1.1 Geological Setting Of The Forth Estuary

The solid geology of the area consists of faulted Carboniferous rocks which extend to depths of 1500 metres. They include sequences of sandstones, mudstones, ironstones and a number of important economic coal seams. Igneous intrusive and extrusive rocks of Permo-Carboniferous age are also present, but in lesser amounts. The rocks are covered by a series of Quaternary sediments consisting of stiff glacial boulder clay, dense sands and gravels and comparatively weak late-and post-glacial gravels, sands, silts, peats, clays and man-made fill.

The area immediately surrounding the Forth Estuary is essentially low-lying and consists of extensive raised estuarine or marine deposits. Most of the sediments are of

low surface gradient (usually less than 1°), although in places post-and late-glacial marine erosion has produced steeper cliffs of between 8° and 16°.

4.1.2 Geotechnical Profiles

Seven basic sequences or profiles were encountered in site investigation boreholes as described by Gostelow and Browne (1981). A tentative distribution of the profile types is shown in Fig. 4.2. The geotechnical data of each of the profile types were given in the original report.

Profile type (3), which includes the site considered in BannockBurn, occurs within the boundaries of the post-glacial deposits, Fig. 4.2 and covers an extensive area to the north-west of Kincardine Bridge. The profiles are distinguished by the absence of late-glacial sediments. post-glacial carse clays and organic soils rest on sands, and gravels which overlie either glacial deposits or rock. The carse clays vary in thickness from one or two metres at the shoreline to over 12 metres in the centre of the Forth. They also thicken towards the west beneath the main post- glacial raised beach.

4.1.3 Geotechnical Properties

Typical geotechnical properties of the soil obtained

from the site are summarised below:

- A firm to stiff weathered crust 1-2 metres thick overlies soft to very soft silts and clays with undrained strengths of between 10 kPa and 20 kPa.

- Moisture contents are at or above the liquid limit and the sediments are highly compressible with coefficients of volume compressibility of 0.2-0.3 m^2/MN in the weathered zone increasing to 0.4-1.2 m^2/MN at depth.

- Bulk densities lie between 16.0 kN/m^3 and 17.0 kN/m^3.

- The silty clays are of intermediate to high plasticity, i.e., CI to CH on the Casagrandi's plasticity chart.

- A series of consolidated undrained triaxial tests on specimens from piston samples were carried out by Soil Mechanics Ltd.for the M876 Motorway site investigation. Results of the tests are shown in Table 4.1.

4.2 Soil Sampling

The soil, which was sampled 2-4 metres beneath ground level from the BannockBurn area, consisted of a greyish brown silty clay. A JCB shovel was utilised for the sampling operation which took approximately 2 hours. The

soil was originally obtained in fairly large lumps which were then cut into smaller lumps so that the soil could be supplied in 20 kg capacity plastic bags. The bags were sealed to prevent the soil from drying out and were transferred to the department's laboratory as soon as the sampling operation was completed. An extensive testing programme on the remoulded soil started on the next day as the filling operation began, see Chapter 3, Section 3.5.

4.3 Laboratory Testing Results

The soil was thoroughly mixed before being placed in the tank for the experiment. All soil properties presented herein are, therefore, for the remoulded state except those used for sensitivity calculations. Fig. 4.3 shows the grain size distribution determined in the laboratory according to BS 1377 Section 2.7.1. Table 4.2 presents the results of soil classification tests conducted on samples during the filling operation.

Below is a summary of all the laboratory tests.

4.3.1 Moisture Content: (BS 1377 Section 2.1.1)

A total of nine moisture content values at different depths were obtained during placement of the clay in the tank. Table 4.2 presents an average value determined from these tests. The variation of moisture content values

prior to and after completion of all loading stages are presented in Chapter 5.

4.3.2 Consolidation Tests:(BS 1377 Section 5.2)

Three series of fixed ring consolidation tests were conducted by the standard oedometer (76mm diameter). Samples during the filling operation were taken at mid-depth of the clay bed for both testing programmes. Compression versus square root of time results of these samples at three consolidation pressures are shown in Figs. 4.4, 4.5 and 4.6. Those figures were used to obtain coefficients of consolidation (C_v), coefficients of compressibility (m_v) and permeability coefficients (k_m) for the soil at different consolidation pressures, Table 4.3. Results obtained for the 2nd testing programme showed very similar trends.

4.3.3 Triaxial Shear Tests

Both consolidated undrained (CU) tests with pore pressure measurement and unconsolidated undrained (UU) tests were conducted on samples taken before and after completion of the experiment.

Figs. 4.7 and 4.8 represent the UU tests at the start of the 1st and 2nd testing programmes respectively while

Figs. 4.9 and 4.10 show the CU test results at the start of the test from which the effective stress parameters (c'and ø') were obtained (Fig. 4.9). These values were used, as will be discussed later in Chapter 6, for shear strength calculations at different stages throughout the consolidation process.

Sensitivity of the clay was determined by pushing three standard 38mm diameter tubes into one of the clay lumps prior to the filling operation and then performing a UU tests on those samples. Fig. 4.11 presents UU tests on undisturbed samples conducted at the start of the experiment. A sensitivity of 2.2 was obtained.

4.3.4 Shear Box Tests

Drained shear tests along with adhesion tests were performed on remoulded samples of clay by using a standard 60 x 60 mm shear box apparatus which was modified by replacing the bottom half of the box by a brass block of the same material used for the pile. After adjusting the brass plate in place, the inside faces of the upper half of the box and the contact area between the two halves were smeared with silicon grease in order to eliminate any friction. The clay was carefully placed into the upper half of the box and a porous plate was then placed on top of the sample. The initial thickness of the clay specimen was 15mm. Consolidation commenced under gradually

increased loads in order to prevent extrusion of the sample. Readings of settlement against time were taken for the final load increment to ensure that complete consolidation had taken place before the shearing was commenced. All the tests were strain controlled with a strain rate of 0.02mm/hour. This rate of strain was used so as to ensure total dissipation of excess pore water pressure.

Fig. 4.12 shows shear box results for clay-clay tests, while adhesion test result are presented in Fig. 4.13.

4.3.5 Vane Shear Tests

Tests using laboratory shear vane equipment, with the dimensions of 20mm by 40mm, were carried out on the soil in place. Shear strength values obtained by the vane tests were used, as will be discussed in Chapter 5, to establish the increase in soil shear strength due to consolidation.

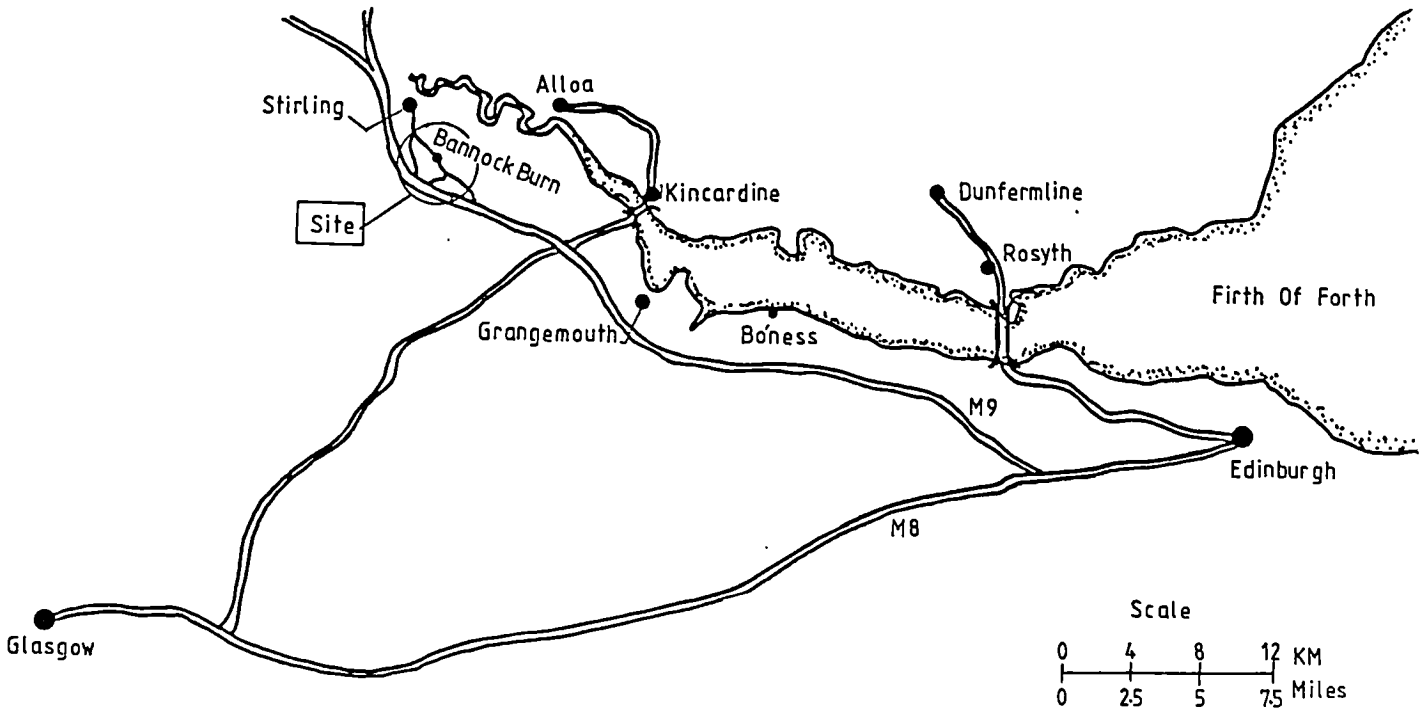

FIG. 4.1 LOCATION SITE

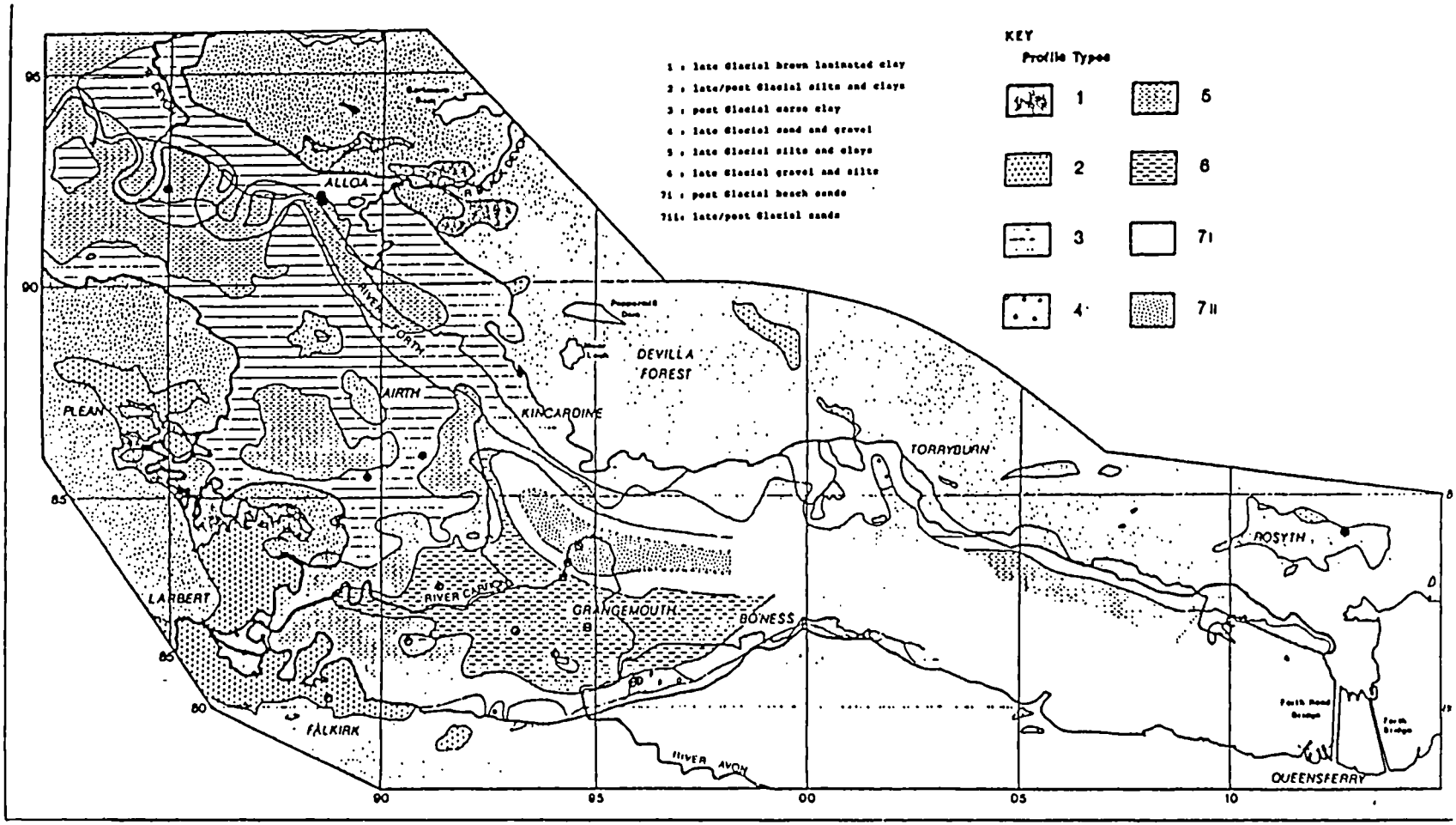

FIG. 4.2 GEOLOGICAL PROFILES OF THE UPPER FORTH ESTUARY
(After Gostelow and Browne, 1981)

ELE

PARTICLE SIZE DISTRIBUTION

Form No K4

LOCATION No..... BORE HOLE No..... SAMPLE No..... PRETREATMENT DETAILS.....

DATE OF TEST..... DESCRIPTION..... LOSS ON PRETREATMENT.....%

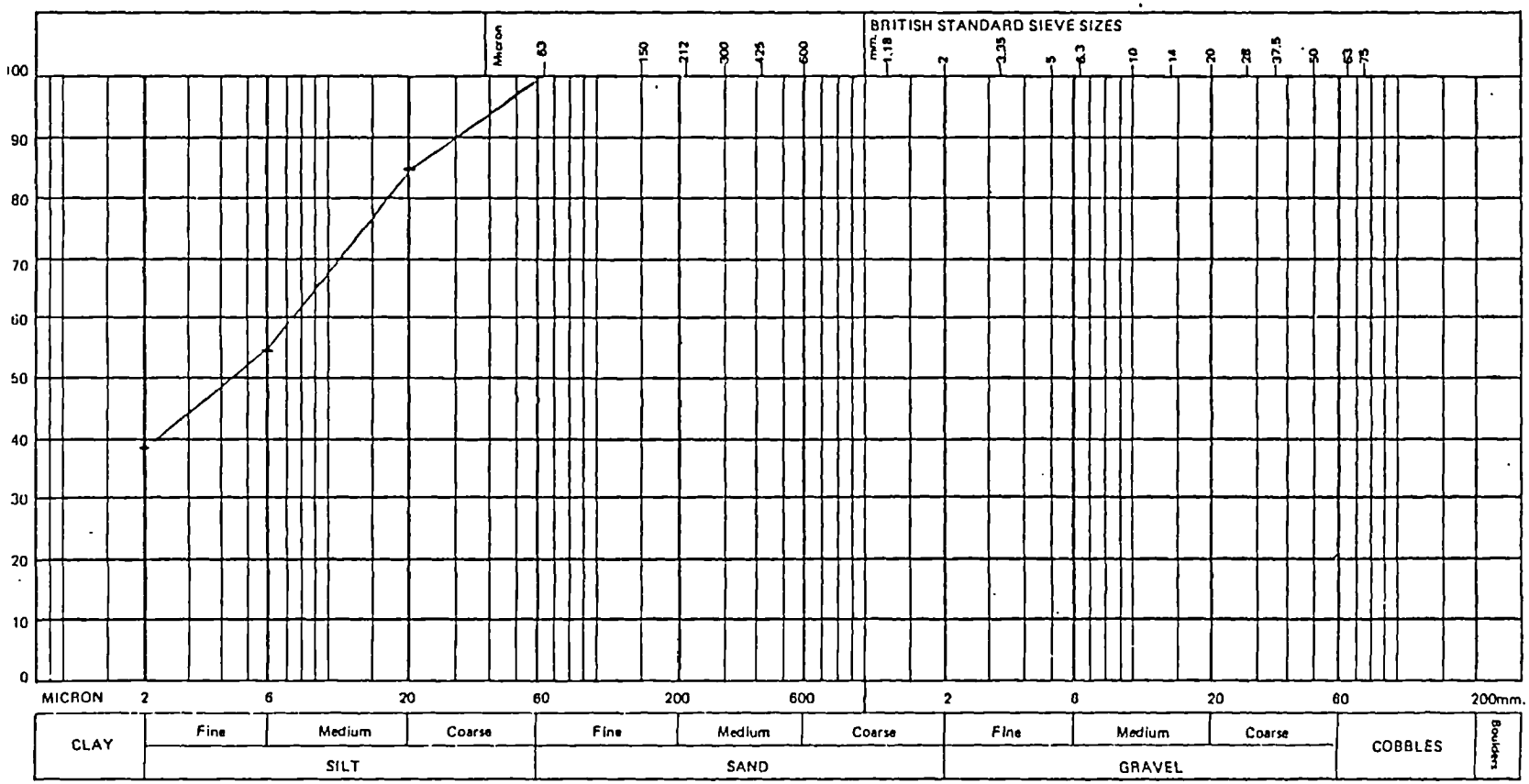

FIG. 4.3 GRAIN SIZE DISTRIBUTION CHART

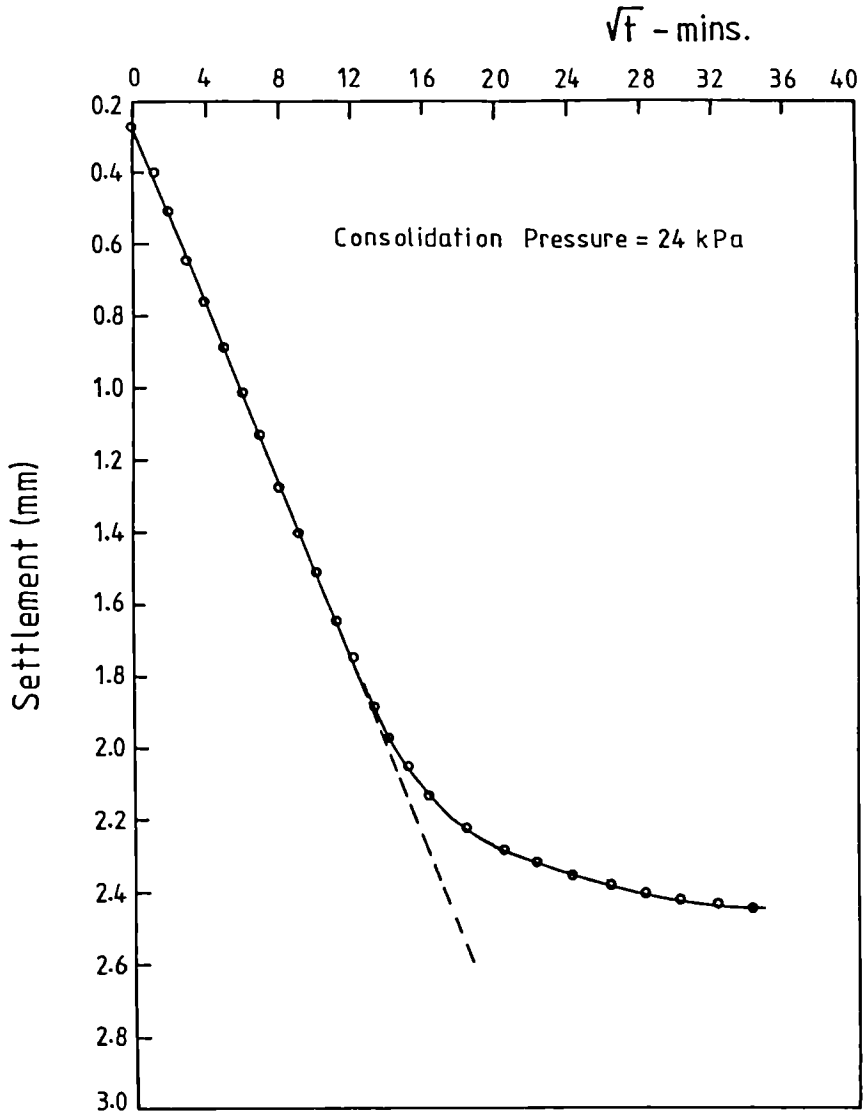

FIG. 4.4 TIME-SETTLEMENT CURVE, CONSOLIDATION PRESSURE= 24 kPa

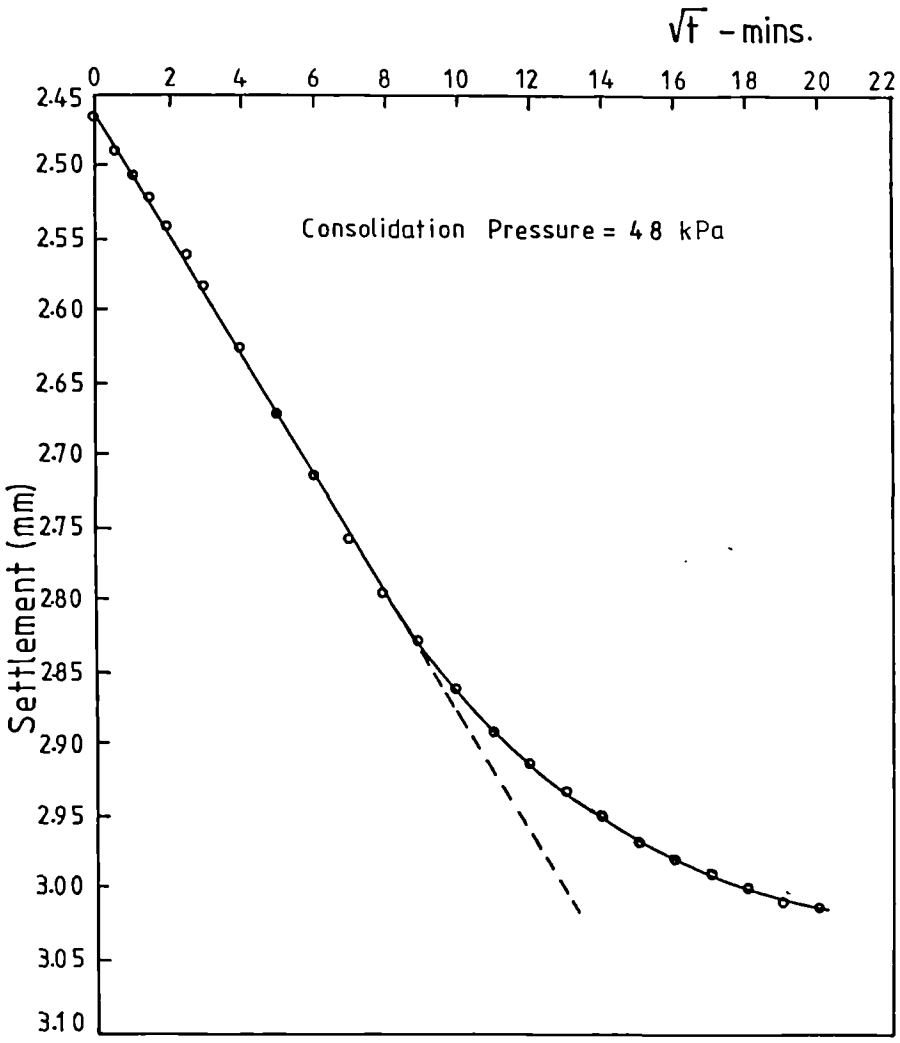

FIG. 4.5 TIME-SETTLEMENT CURVE, CONSOLIDATION PRESSURE= 48 kPa

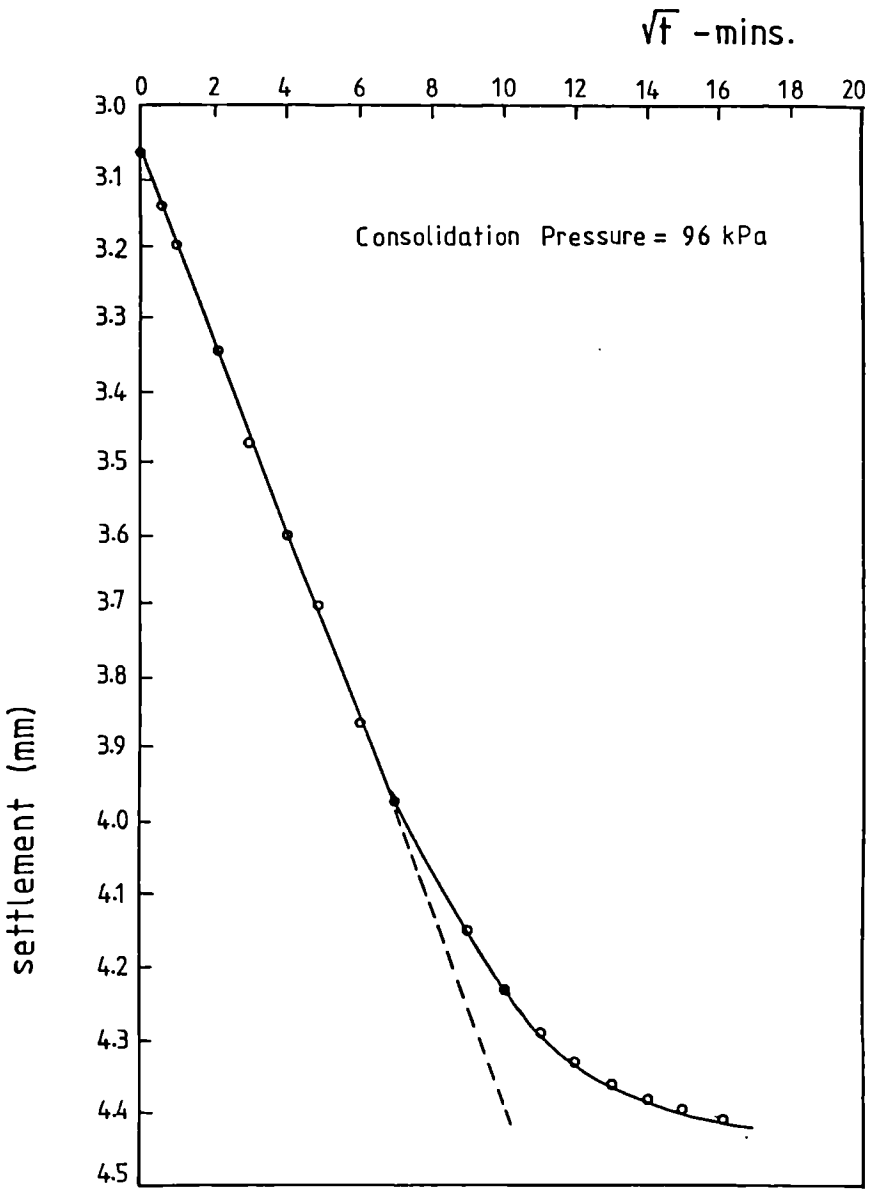

FIG. 4.6 TIME-SETTLEMENT CURVE, CONSOLIDATION PRESSURE= 96 kPa

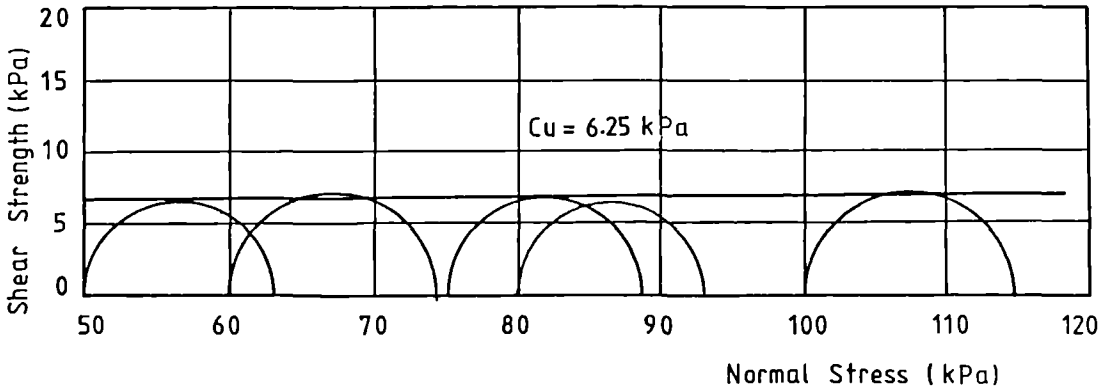

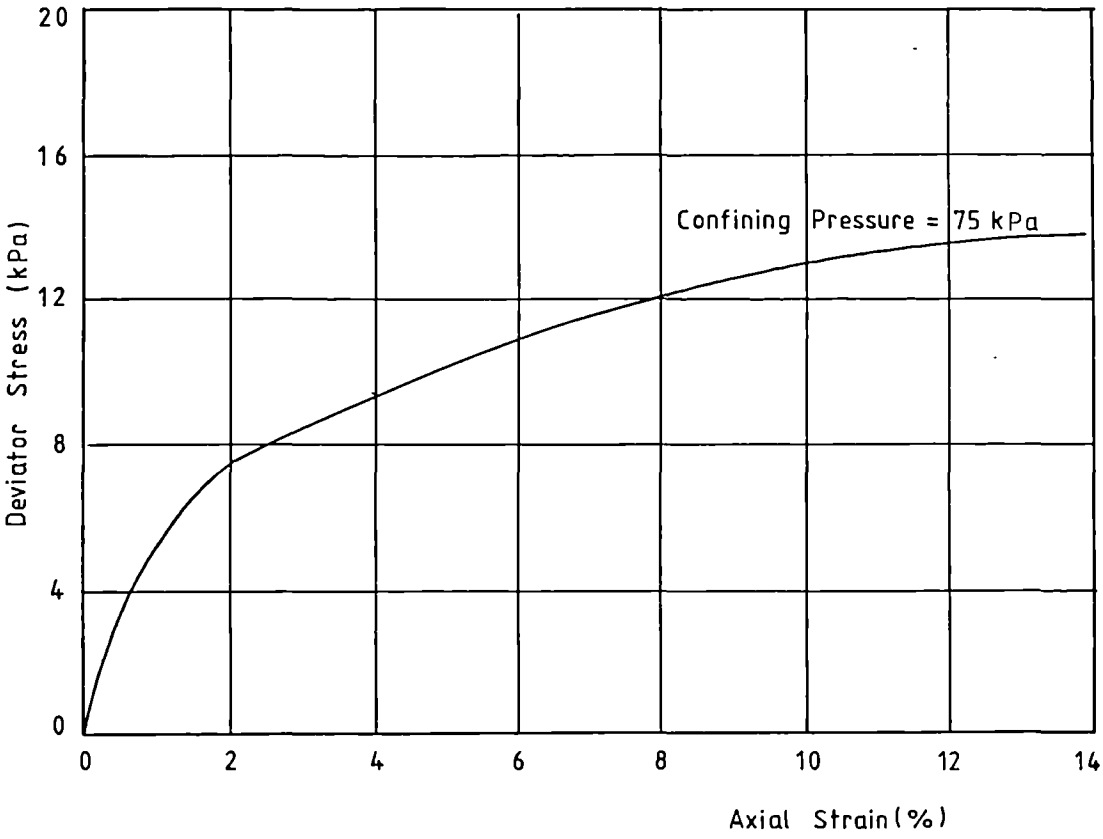

FIG. 4.7 UNDRAINED TRIAXIAL TEST RESULTS OF REMOULDED SAMPLES, AT START OF 1ST TESTING PROGRAMME

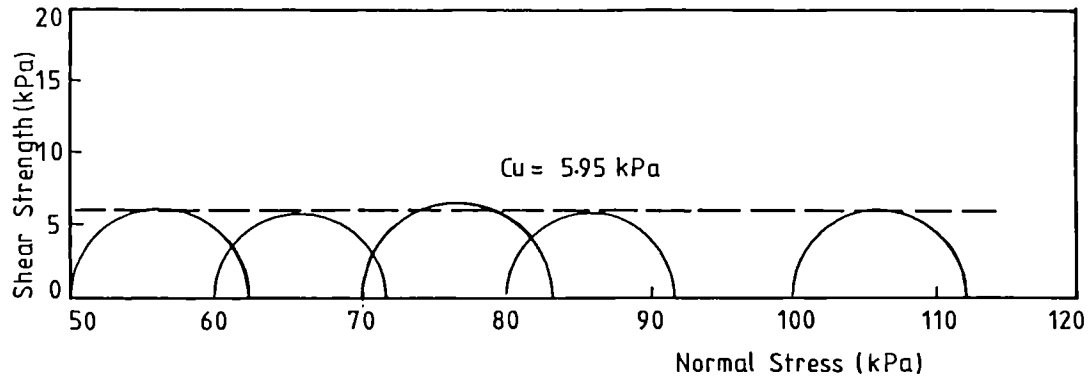

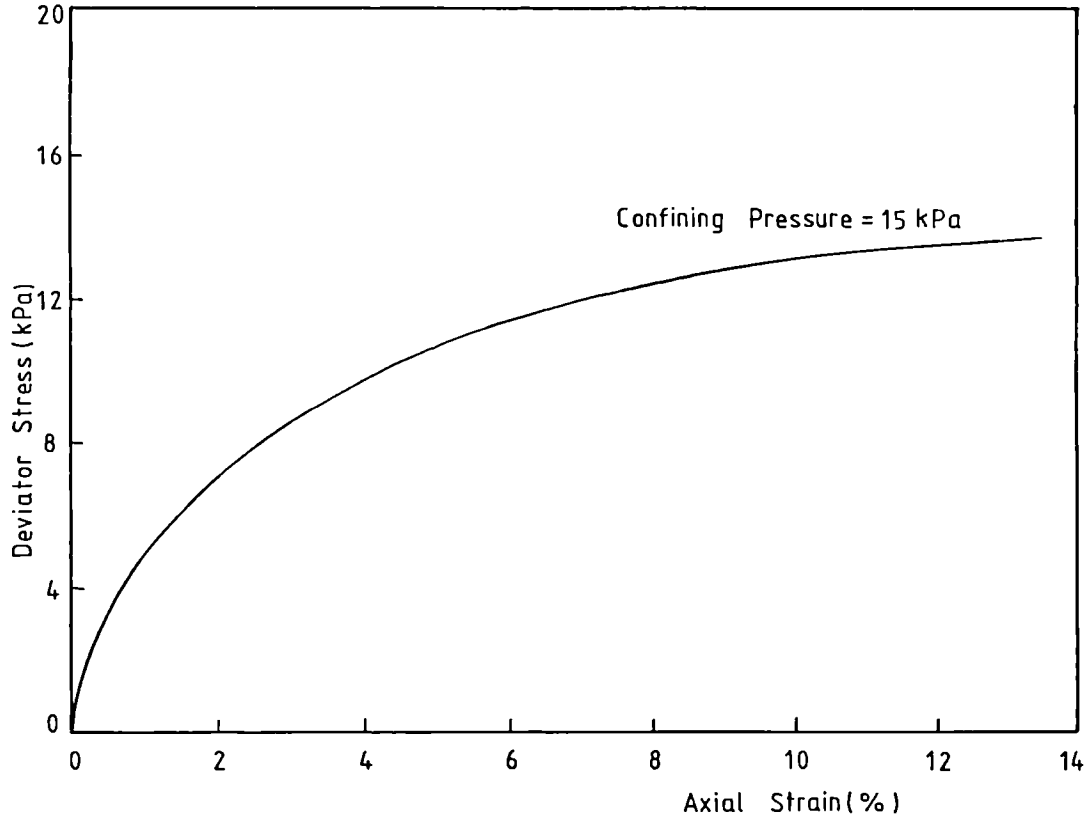

FIG. 4.8 UNDRAINED TRIAXIAL TEST RESULTS OF REMOULDED SAMPLES, AT START OF 2ND TESTING PROGRAMME

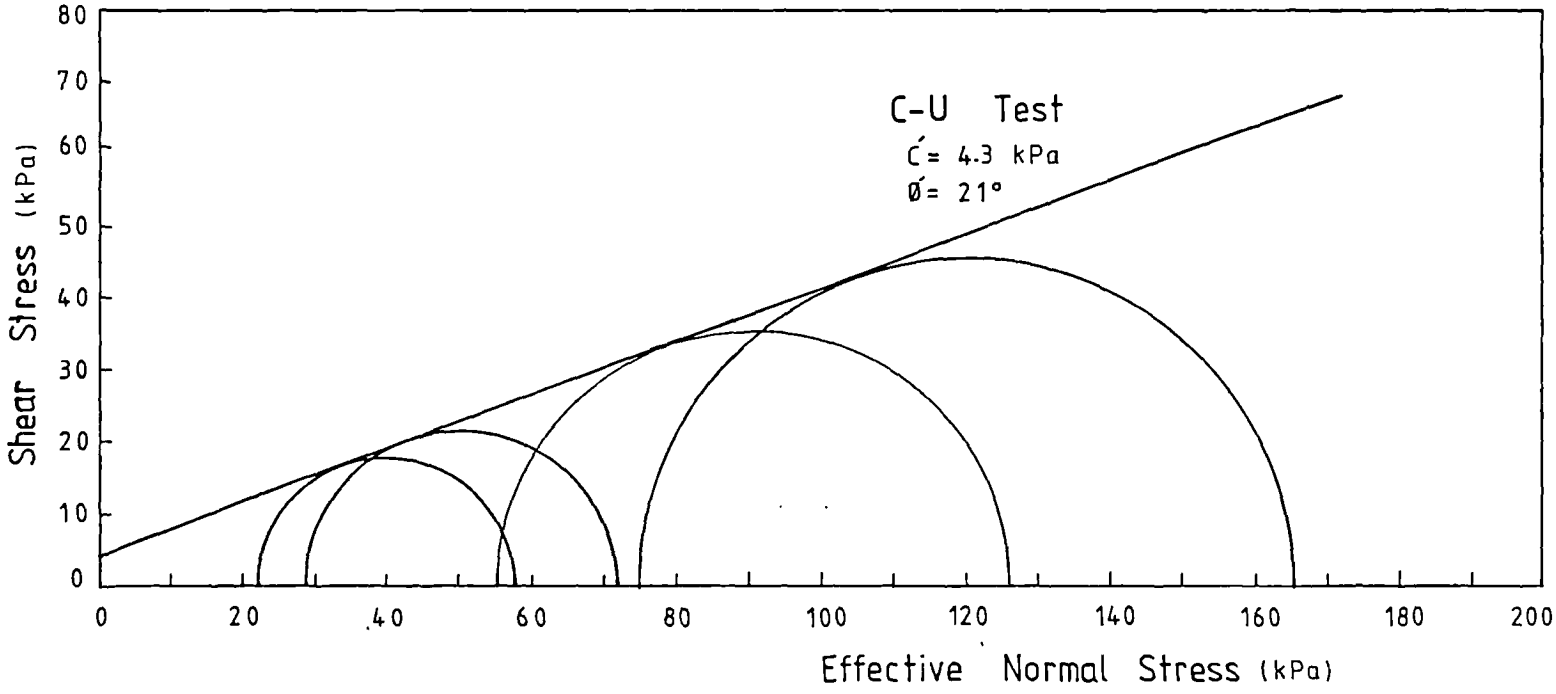

FIG. 4.9 EFFECTIVE STRESS MOHR CIRCLES AND FAILURE ENVELOPE: TRIAXIAL COMPRESSION TESTS (AT START OF TEST)

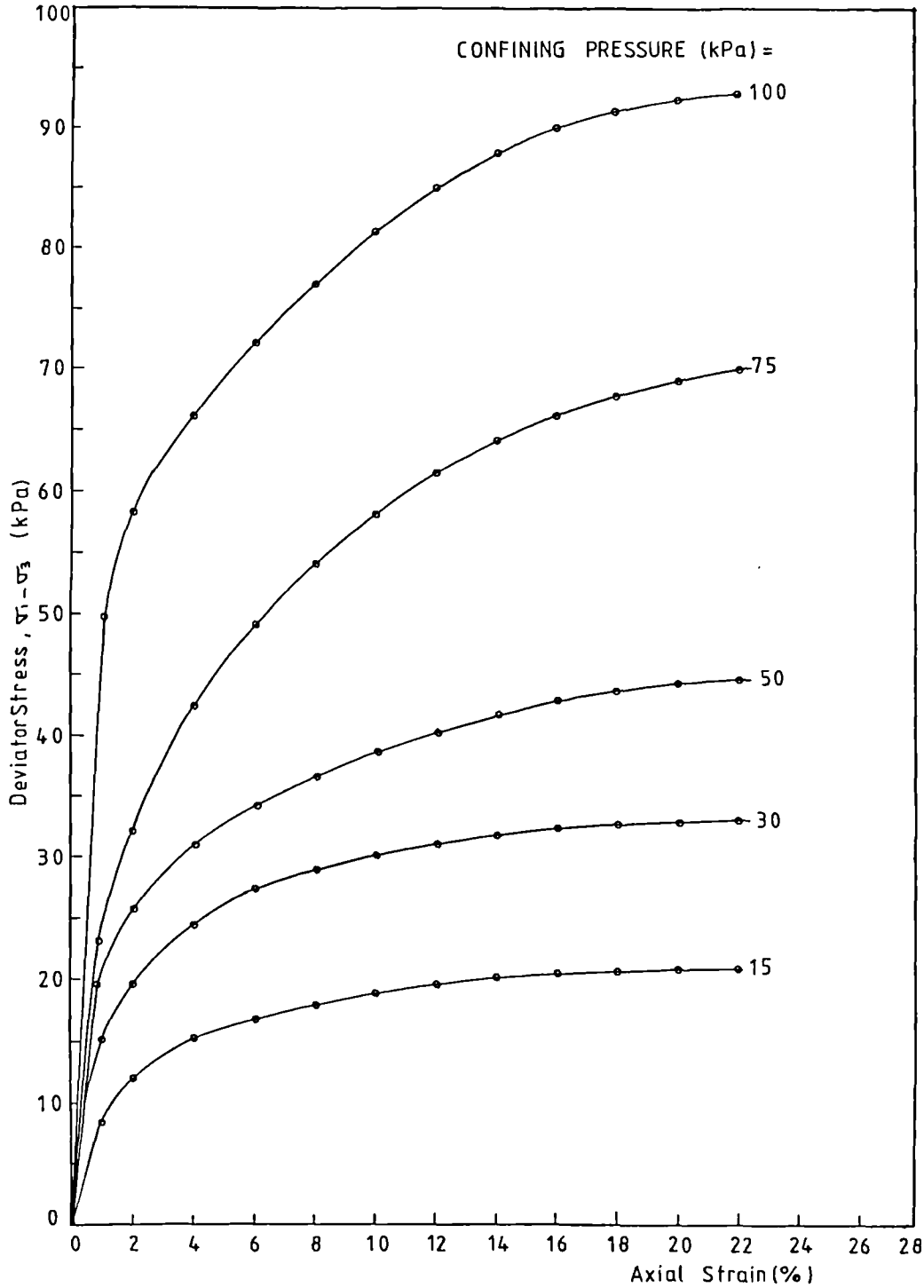

FIG. 4.10 STRESS-STRAIN RELATIONSHIP, TRIAXIAL TESTS

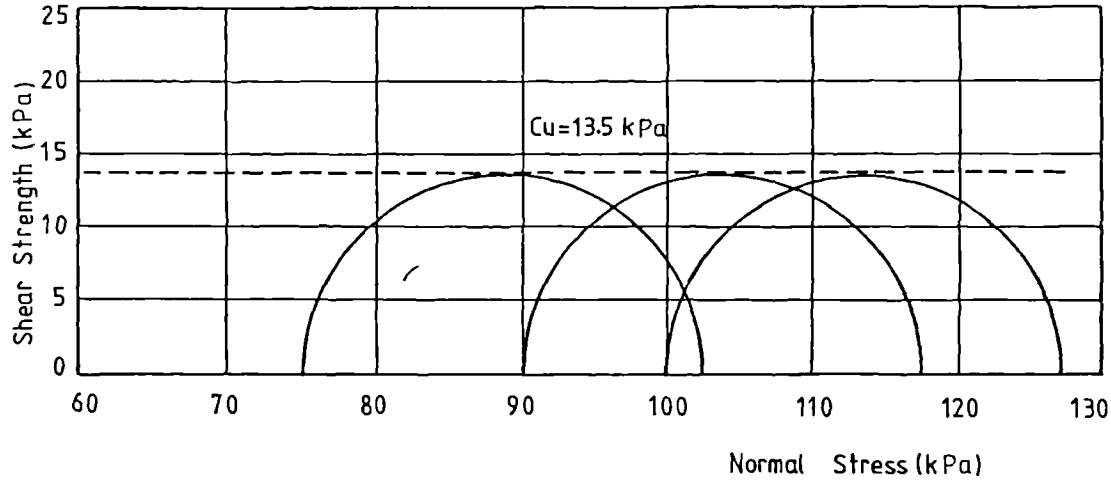

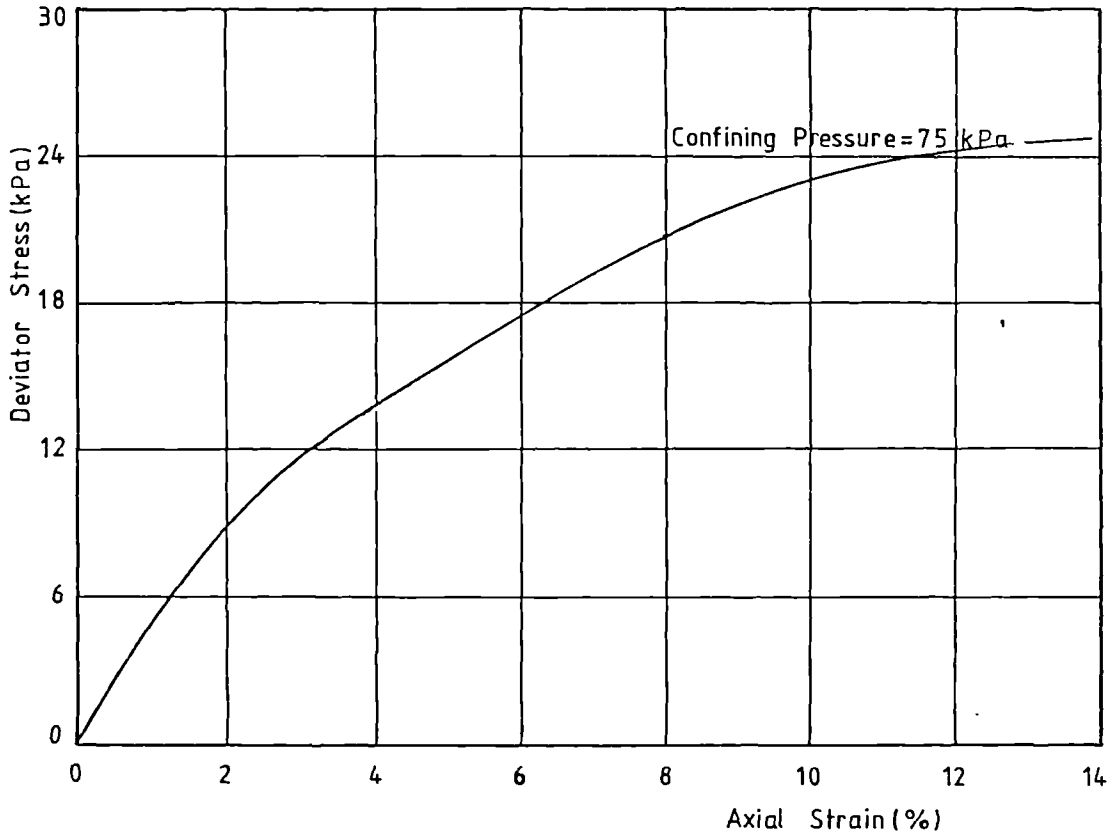

FIG. 4.11 UNDRAINED TRIAXIAL TEST RESULTS OF UNDISTURBED SAMPLES, AT START OF TEST

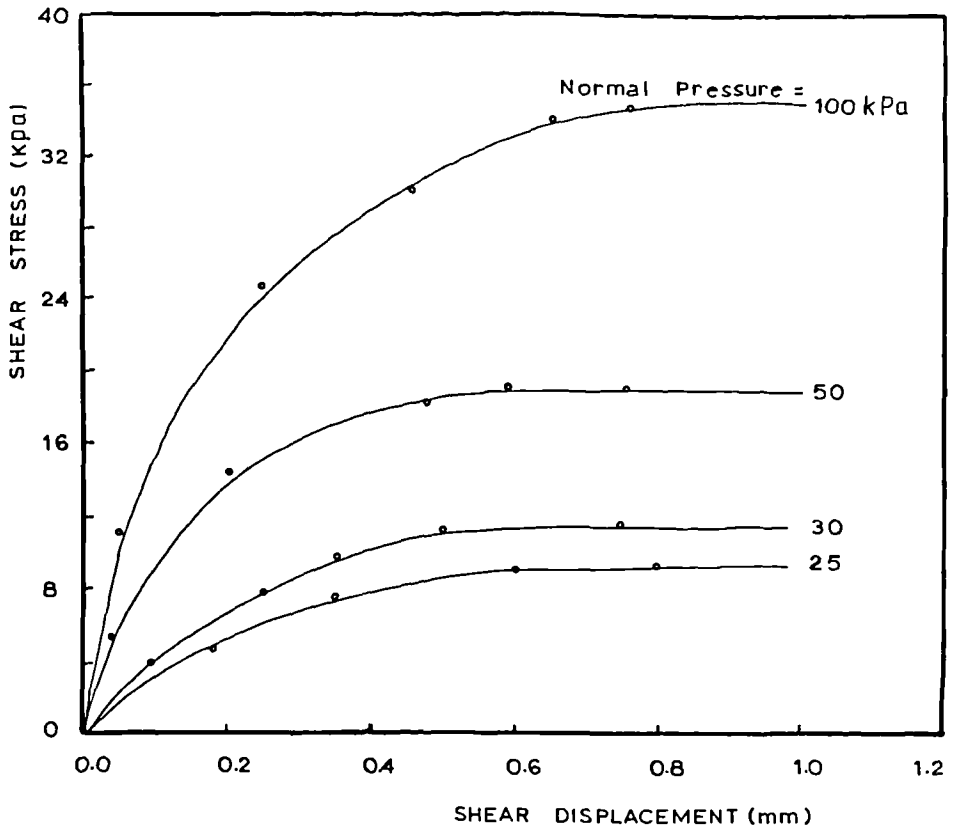

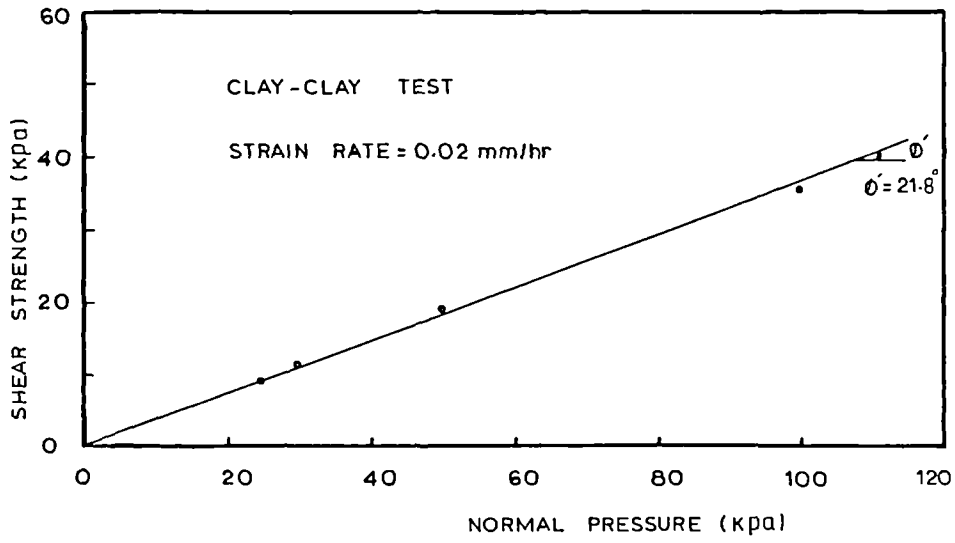

FIG. 4.12 DRAINED SHEAR BOX TEST RESULTS ON REMOULDED SAMPLES AT START OF TEST (CLAY-CLAY TESTS)

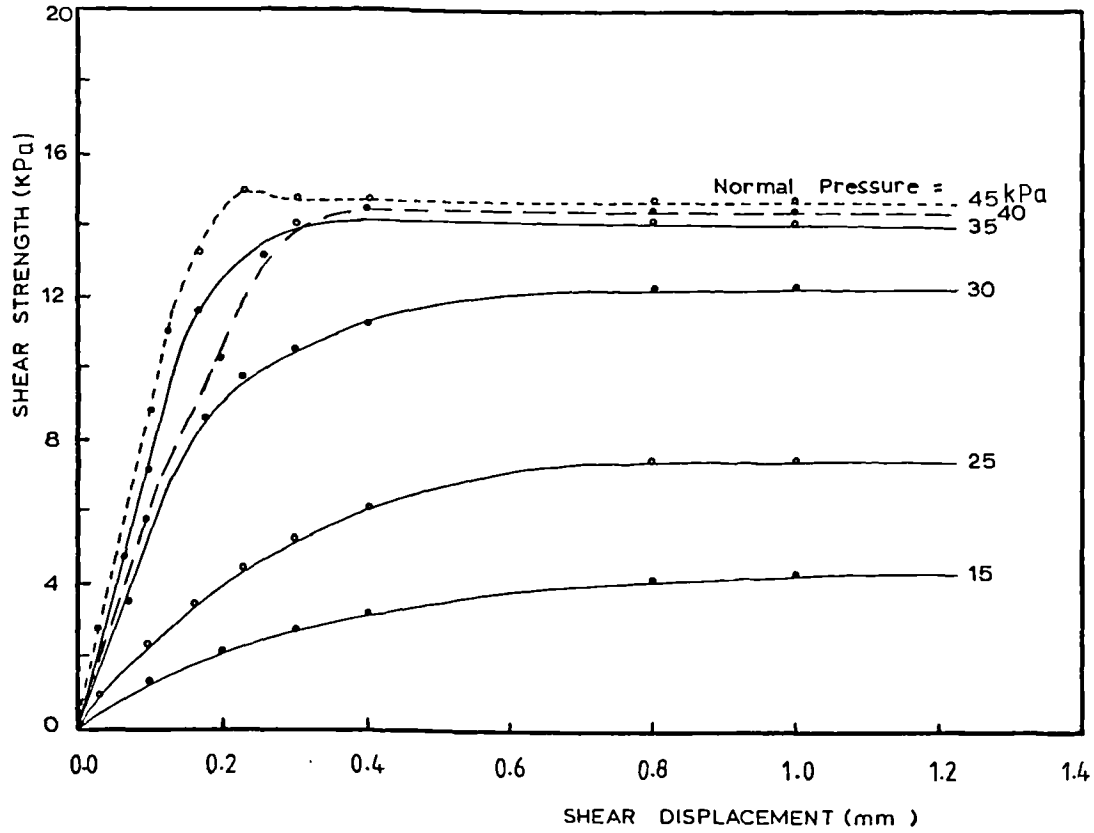

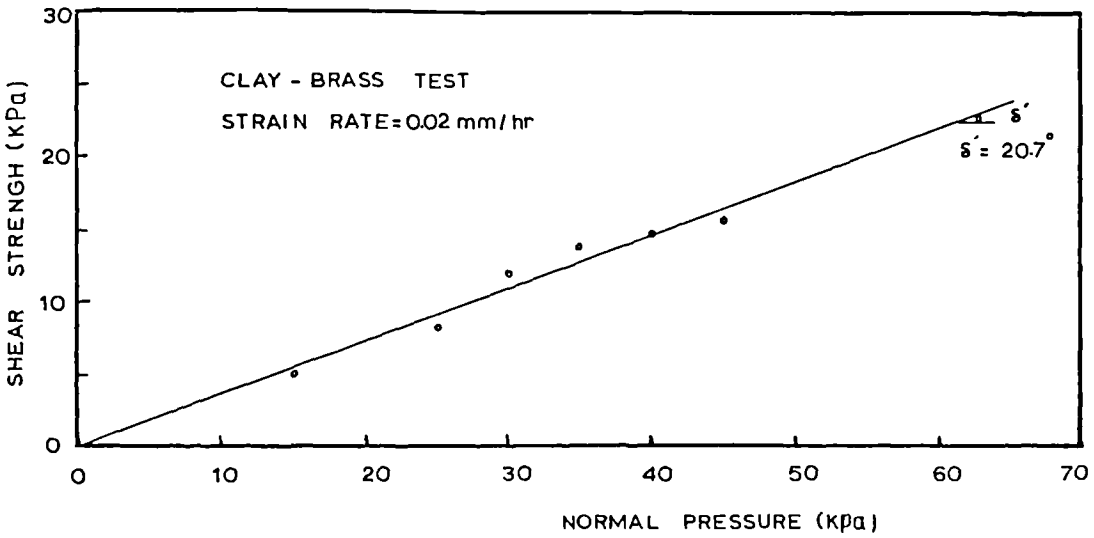

FIG. 4.13 DRAINED SHEAR BOX TEST RESULTS ON REMOULDED SAMPLES AT START OF TEST (CLAY-BRASS TESTS)

Sample depth (m)	Cohesion, c' (kPa)	Friction angle, ø' (°)
2.3	0.0	34.0
2.8	3.0	29.5
4.0	0.0	22.0
5.0	0.0	23.5
5.4	10.0	26.5

TABLE 4.1 CONSOLIDATED UNDRAINED TRIAXIAL TESTS FOR NORMALLY CONSOLIDATED POST-GLACIAL CARSE CLAYS (AFTER GOSTELOW AND BROWNE, 1981)

Atterberg Limits	Liquid Limit (Wl)=55% Plastic Limit (Wp)=30% Plasticity Index (IP)=25%
Average Moisture content	W = 54.5 %
Grain Size Analysis By Weight	Fine Sand (0.06-0.2)=0.5% Silt (0.002-0.06)=61.5% Clay (<0.002) =38.0%
Specific Gravity of Solids	Gs = 2.62
Wet Unit Weight Dry Unit Weight	γ_w = 17.4 KN/m³ γ_d = 11.3 KN/m³

TABLE 4.2 SOIL CLASSIFICATION

Consolidation Pressure, P_c' (kPa)	Coefficient of Consolidation, C_v (mm^2/min)	Coefficient of Compressibility m_v (kPa^{-1})	Coefficient of Permeability, k_m (mm/sec)
0-24	0.26	5.15×10^{-3}	2.23×10^{-7}
24-48	0.41	1.45×10^{-3}	1.00×10^{-7}
48-96	0.52	0.90×10^{-3}	0.78×10^{-7}

TABLE 4.3 COMPRESSION PROPERTIES AT START OF TEST

CHAPTER (5)

PRESENTATION OF EXPERIMENTAL TESTING RESULTS

5.1 Introduction:

In this chapter, soil tests conducted after completion of the loading stages are presented (Section 5.2) in order to determine the changes in soil properties and also to enable determining, as will be discussed in Chapter 6, the shear strength values of the clay at different stages throughout the various consolidation processes.

Plots of pore pressure readings for all surcharge loading stages are presented in Section 5.3 along with the variation of those pressures at lateral distance from the pile surface.

Regarding negative skin friction, the measuring stations (load cells) along the pile shaft recorded the load imposed upon the pile and have been referred to as a downdrag load. The difference in load between each measuring station represents the increased loading caused by the downward moving clay layer. These readings are reported in Section 5.4.

Settlement results of the clay layer obtained by means of the settlement plates, the plastic sleeve and the

drainage calculation (displaced water volume) are given for each loading stage in Section 5.5.

A time schedule for all loading stages within the tasting programmes is shown in Table 5.1.

5.2 Soil Testing Results

This section presents all soil test results conducted during and after completion of both testing programmes.

5.2.1 Moisture Content:(BS 1377 Section 2.1.1)

The moisture content of the clay was determined prior to and after completion of both loading stages. A specially made 10mm inner diameter by 1.0m long steel tube sampler with a piston was used to obtain samples at different depths. This was manufactured in the department's workshops.

In an attempt to monitor vertical and horizontal variation in moisture content, 18 samples were taken through the depth of the clay bed and radially. Fig. 5.1 shows moisture content variation after completion of the first testing programme, while Fig. 5.2 is for the second testing programme. Significantly high values of moisture content were observed at the bottom of the clay bed, i.e.,

at the end of testing programmes, values of moisture content at the bottom of the clay were higher than those near the surface by 8% and 5% for the 1st and 2nd testing programmes respectively. Regarding radial variation of moisture content, higher values were observed at points equidistant between the pile surface and the tank's wall. Table 5.2 lists moisture content values before and after completion of the loading stages at nine different locations. An average reduction in moisture content of 27% and 32%, compared to that at the start of the test, was observed at the end of 1st and 2nd testing programmes respectively.

5.2.2 Consolidation Tests:(BS 1377 Section 5.2)

Results regarding coefficients of compressibility, coefficients of consolidation and permeability coefficients obtained at the end of both testing programmes are presented in Table 5.3. Values determined before starting the test are also included in that table.

5.2.3 Triaxial Shear Tests

Triaxial test results were used (as will be discussed in Chapter 6) for shear strength calculations at different stages throughout the consolidation process. Shear

strength tests conducted after completion of both testing programmes are summarised below:

(i) Consolidated undrained (CU) test results for the 1st and 2nd testing programmes are shown in Figs. 5.3 and 5.4 respectively.

(ii) Unconsolidated undrained (UU) test results for both testing programmes are presented in Figs. 5.5 and 5.6.

(iii) At the end of 1st testing programme four series of triaxial unconsolidated undrained (UU) tests were conducted on remoulded samples with different moisture contents in order to achieve the same shear strength properties as those of the 1st testing programme. Results of these tests are presented in Figs. 5.7 and 5.8.

5.2.4 Shear Box Tests

Drained shear box results for clay-brass tests at the end of 1st testing programme are shown in Fig. 5.9, while those for the 2nd testing programme are presented in Fig. 5.10.

It is interesting here to note that when comparing shear box results for clay-brass tests (at start of test) with those of clay-clay tests, a steeper stress-displacement curves were observed for the clay-brass case. Moreover, a residual value was noticed at normal stress of 45 kPa while no residual values were registered for the

clay-clay tests, Figs. 4.12 and 4.13.

5.2.5 Vane Shear Tests

Three sets of readings were taken at three different levels. The first set was performed at the end of the second loading stage (60 kPa), while the other two sets were conducted after completion of both testing programmes. Shear strength values obtained by the vane tests were used together with the results of the unconsolidated undrained tests in order to establish the increase in strength due to consolidation. This will be discussed in Chapter 6.

Table 5.4 summarises vane shear results at mid-depth of the clay bed together with all strength properties before and after completion of both testing programmes. Unit weight and moisture content values are also included in that table.

5.3 Pore Water Pressure Results

Pore pressure readings obtained during both testing programmes are plotted and presented in Figs. 5.11 to 5.25. Locations of the piezometer tips are designated by the letters shown on each figure. Fig. 3.7, Chapter 3, refers to the level and detailed distances in (mm) from

the pile surface to the piezometer tips.

Although Klinger ball valves were used to minimise volume change due to valve switching, it was considered advisable to allow some time after switching to permit the pressure in the line to level off. As noted in Chapter 3, a time period of 30 minutes was considered adequate in this respect.

The time required for the pore water pressure to reach its maximum value was reasonably short, 24 hours, although the previously measured response time for the piezometers was appreciably quick (5-10 seconds).

The following sections present pore pressure values obtained during the consolidation process for both testing programmes.

5.3.1 Pore Water Pressure During 1st Testing Programme

The pore pressures at different depths along the clay bed induced by the pile driving are presented in Fig. 5.11.

Figs. 5.12, 5.14 and 5.16 show the decay of pore water pressure for each piezometer along the clay depth near the pile shaft, while Figs. 5.13, 5.15 and 5.17 show the decay of pore water pressures radially. The following comments apply to each loading stage:

a) **Pile installation, Fig. 5.11**

During pile installation only readings from those piezometers adjacent to the pile shaft were taken. As shown from Fig. 5.11, installation of the pile caused a relatively low excess pore water pressure, (3.2 kPa at the bottom piezometer reducing to 2.2 kPa at the top piezometer). At the end of the six days period which was needed for the excess pore pressure to dissipate, the four piezometers (A1 to D1 from top to bottom) registered readings of approximately the static hydraulic pressure heads at those positions. It was expected that the lower zone would be the one mostly affected by the pile driving since a displaced volume of soil would be encountered in this region.

b) **Surcharge Pressure of 30 kPa, Figs. 5.12 and 5.13**

Regarding the vertical variation of excess pore pressure along the pile shaft, a value of 25.7 kPa (86% of the applied surcharge pressure) was recorded at level B1. Excess pore pressure in the top half of the clay bed (piezometers A1 and B1) was higher than in the lower half (piezometers C1 and D1). As shown in Fig. 5.12 a steady rate of decay could not be obtained because of the temperature variation through that loading stage.

It is realised that quoting pore pressure values to 1/10th kPa may not be realistic when temperature effect is encountred, however, by considering an equal temperature effect on all piezometers, then these values when compared

together should represent the real difference in piezometer readings.

Considering the dissipation of pore water pressure in the lateral direction, Fig. 5.13, an average difference of only 2.0 kPa was recorded for the piezometers close to the pile shaft and those near the tank's wall.

c) Surcharge Pressure of 60 kPa, Figs. 5.14 and 5.15

A maximum value of 28 kPa excess pore pressure was registered by piezometer C1 at mid-depth of the clay bed on application of 60 kPa surcharge. The pore water pressure generated amounted to 93% of the applied surcharge pressure.

Lateral dissipation of pore water pressure indicated a larger difference in value when compared to the previous loading stage. A variation of 3.0 kPa, 3.5 kPa, 6.0 kPa, and 3.5 kPa for piezometers A, B, C, and D respectively was recorded between points close to the pile shaft and those near the tank's wall.

d) Surcharge Pressure of 90 kPa, Figs. 5.16 and 5.17

As a result of surcharge discontinuity involved at this loading stage, see Chapter 3, Section 3.5, the trend of pore pressure dissipation, unlike the previous stages, was slow. The generated pore water pressure was only 71% of the applied surcharge pressure. The maximum pore pressure values were measured at levels B and C which showed similar trends, Fig. 5.16.

5.3.2 Pore Water Pressure During 2nd Testing Programme

Results of pore water pressure dissipation during the 2nd testing programme are presented in Figs. 5.18 to 5.25. The following comments are applicable to each loading stage.

a) Surcharge Pressure of 15 kPa, Figs. 5.18 and 5.19

Readings of the four piezometers nearest the pile shaft (A1, B1, C1, D1) registered excess pore water pressures of 12.3 kPa, 13.4 kPa, 14.3 kPa and 11.5 kPa from top to bottom respectively due to the 15 kPa surcharge.

Regarding the lateral variation of excess pore water pressure, it may be seen that points near the pile shaft registered the highest values. The differance in values between two extreme points, specially at early stages of the consolidation process, was of the order of 4.0 kPa and 3.5 kPa at levels C and D while levels A and B registered a difference of only 1.6 kPa.

b) Surcharge Pressure of 30 kPa, Figs. 5.20 and 5.21

After application of the 30 kPa surcharge pressure, an excess pore pressure of 14.0 kPa was registered at level C, and a minimum value of 10.0 kPa at level D, corresponding to 93% and 67% of the surcharge pressure respectively. The time required for the initial excess

pore water pressure to decay was longer (38 days) at this loading stage than that of the previous stage (36 days).

Regarding radial variation of pore water pressure, level B showed a variation of approximately 3.0 kPa between points nearest to the pile shaft and those at the tank's wall, while the piezometer at level D registered the smallest variation (1.5 kPa).

c) Surcharge Pressure of 45 kPa, Figs. 5.22 and 5.23

Comparing this loading stage with the previous stages, it was noticed that : (i) the decay of pore water pressure for this loading stage appeared to be steady with higher values generated at level C. (ii) the time required, for the same percentage of pore water pressure dissipation was longer.

The four piezometers (A1 - D1 from top to bottom) registered readings of 14.0 kPa, 12.8 kPa, 11.4 kPa and 10.7 kPa respectively. Apparently, all the curves concerning radial drainage showed a difference in pore pressure of 1.7 kPa. This difference was maintained approximately constant throughout the consolidation process.

d) Surcharge Pressure of 90 kPa, Figs. 5.24 and 5.25

The piezometer at level C registered the maximum value of 41.2 kPa. This represented 91% of the applied surcharge pressure. A relatively slow and steady rate of pore water pressure dissipation was noticed at this

loading stage.

Maximum readings of the four piezometers were 33.0 kPa, 37.3 kPa, 41.2 kPa and 30.2 kPa from top to bottom respectively.

5.4 Downdrag Results

In the following sections, presentation of downdrag results is given with a specific comment on each stage of the two testing programmes.

5.4.1 Downdrag After Pile Driving

After pile driving, six days were allowed to pass before starting the first loading stage. During that period readings of negative skin friction were recorded in order to examine the build-up of downdrag under the self-weight of the soil.

In Fig. 5.26 the measured downdrag load is plotted at two different time intervals (1st and 6th day). The build-up of negative skin friction showed an increased rate with time reaching a maximum value of 1.3 kPa (0.2 Cu) at the bottom of the pile.

5.4.2 Downdrag - 1st Testing Programme

Results of downdrag loads during each consolidation stage are presented in Figs. 5.27, 5.29 and 5.31. These curves show the build-up of accumulated downdrag loads with time for each station. The following comments are offered on each figure :

Figure 5.27 : Surcharge Pressure = 30 kPa

In the first few days the rate of load increase was greater for stations 1, 2 and 3, which are located at the lower part of the pile, than of those at the top. Downdrag friction stresses were mobilised along the entire length of the pile surrounded by the clay. This is indicated by the fact that the load at the bottom was greater than anywhere else. There is a pronounced limiting value for most of the curves on the 18th day followed by peaking of the curves on the 26th day. This indicates that pile-soil slip might have occurred somewhere along the pile. The load dropped off over a period of 6 days and then increased steadily over the next two days.

Figure 5.29 : Surcharge Pressure = 60 kPa

Unlike the previous stage, a steady rate of downdrag increase was noticed although there was a tendency for the load at stations 4, 5, and 6 to level off at about 22 days. The load at the very bottom (station 1) of the pile

maintained the maximum value up to 12 days after which station 2 (100mm from bottom of pile) recorded the maximum value.

The fact that the point of maximum load gradually shifts upwards would indicate that upward friction stresses began to develop at the bottom where consolidation was very rapid.

Figure 5.31 : Surcharge Pressure = 90 kPa

The failure of the rubber bag at this loading stage and the time lag (77 days) induced by the bag repairing made it difficult to control the consolidation process. No continuation of the results could therefore be maintained with respect to the previous stages.

The fact that low downdrag load registered in this loading stage could be explained by the clay swelling during the replacement of the rubber bag and the resetting of the surcharge pressure. It should be noted that station No.3 has not been included in Fig. 5.31 due to unreliable fluctuating readings.

Using the results presented in Figs. 5.27, 5.29 and 5.31, a curve showing the variation in downdrag load along the pile length can be obtained for any intermediate time. Some typical curves on the 7th, 21st and 35th day are shown in Figs. 5.28, 5.30 and 5.32 for the three loading stages respectively. The following comments refer to the curves of downdrag load variation along the length of the

pile.

Figure 5.28 : Surcharge Pressure = 30 kPa

The vertical distribution of axial forces in the test pile is shown in Fig. 5.28a. Each point plotted in the figure represents the average value derived from four strain gauge readings. It can be seen that the drag load has increased continuously with depth along the pile shaft, the maximum value being at the pile tip. The rate of increase of downdrag load within the first 7 days was slower in comparison with readings of the 21st and 35th day. However, 61% of the maximum developed negative skin friction has occurred during the first 7 days. This high value of negative skin friction, developed at early stages, may be attributed to the high effective stresses generated during the 6 days consolidation period before the loading stage began and after pile driving.

Distribution of contact friction stresses along the pile length can be determined by differentiation of the curves showing the distribution of downdrag load. Therefore, the inverse of the slope of the downdrag load distribution curve divided by the perimeter of the pile will give the friction stress at the soil-pile interface. This was carried out for each curve by dividing the difference between downdrag loads in the given vertical interval by the corresponding perimeter area for that interval. The results of these calculations are given in Figs. 5.28b, 5.30b, and 5.32b in the form of curves

showing the distribution of contact friction stresses along the pile at various stages of the 1st testing programme.

In examining the curves of Fig. 5.28b, it can be seen that the contact friction developed at mid-depth of clay was less for the 7th day than for the 21st and 35th day. This could be the result of the high excess pore water pressure generated at early stages. Moreover, and because of the occurrence of slippage mentioned earlier in Section 5.4.2, a decline of the value of negative skin friction was recorded at the 35th day curve between stations 4 and 5. The amount of negative skin friction developed during the initial 7 days was 61% of the total negative skin friction measured at the end of this loading stage.

It should be noted that changes in the exact shape of the downdrag distribution curves could result in considerable alteration of frictional stress distribution curves. It is therefore more important to look at the indicated trends rather than at the exact magnitude of frictional stresses at any given time and location.

Figure 5.30 : Surcharge Pressure = 60 kPa

The 7th day readings showed a high downdrag load along the entire pile length thus indicating a continuation of negative skin friction building up from the previous stage, whereas the 21st and 35th day readings show a maximum downdrag force in the vicinity of station No.2. Therefore, in the early stages of the test, a downward

friction was being mobilised along the entire length and then an upward friction was gradually developed in the lower portion of the pile. The point of transition from downward to upward friction stresses on the pile corresponds to the point of maximum downdrag load. As mentioned earlier in Chapter 1, this point is called the neutral point and is indicated by the symbol NP on the graph.

Regarding the magnitude of downdrag, it can be seen that the 7th day readings indicated high downdrag loads compared to the 35th day readings, i.e, 70% of the maximum negative skin friction had been developed during the first week.

The high values of negative skin friction at the upper portion of the pile can be explained by the possibility of high confinement of the soil at that zone which is believed to be induced by the settling plastic sleeve. Moreover, the high effective stresses at that level also contribute to the high negative friction values registered due to rapid dissipation of pore water pressure.

Comparing the frictional stresses of this loading stage with the previous one (30 kPa), it can be seen that :

a) Both stages produced maximum negative skin friction values at about mid-depth of the clay bed.

b) For the 2nd loading stage (60 kPa) additional negative skin friction was building up at the lower region of the pile.

Figure 5.32 : Surcharge Pressure = 90 kPa

Comments on these curves will not be given as they do not represent the real values of the applied surcharge pressure, see comments regarding Fig. 5.31.

5.4.3 Downdrag - 2nd Testing Programme

As the second testing programme was carried out using the same soil with the same shear properties as those used in the first testing programme, it is not unrealistic to suppose that using the same surcharge pressures should provide similar results to the first testing programme.

This testing programme comprised four loading stages, 15 kPa, 30 kPa, 45 kPa and 90 kPa. The build-up of downdrag loads during each consolidation stage is shown in Figs. 5.33 to 5.40. With regard to these figures, the following comments apply :

Figure 5.33 : Surcharge Pressure = 15 kPa

Results of this loading stage indicated a relatively slow build-up of downdrag up to 16 days after which the rate started to increase particularly at the lower part of the pile. Limiting values were obtained on the 32nd day for all stations along the pile. A total load of 0.25 kN was recorded at the end of this loading stage.

Despite differences in surcharge pressure applied during this stage and the 30 kPa for the 1st testing

programme, the same trend of load increase was noticable for both stages with one exception : for full downdrag mobilisation a longer time was needed for the 15 kPa than had been for the 30 kPa surcharge.

Results from station No.4 were not continued at this stage as the load cell registered fluctuating readings.

Figure 5.35 : Surcharge Pressure = 30 kPa

A constant rate of downdrag increase was apparent throughout the consolidation period of this loading stage. A comparison of these results with those obtained from the 30 kPa surcharge of the 1st testing programme indicated the following :

a) A higher rate of downdrag build-up was noticed on the 1st testing programme particularly during the initial 16 days.

b) at the end of consolidation, the maximum accumulated downdrag loads were 0.38 kN and 0.42 kN for the 1st and the 2nd testing programmes respectively.

The higher amount of downdrag for this second loading stage is believed to be due to the residual effects of the previous loading stage of 15 kPa which acted as stored "energy" in terms of effective stresses before starting the 30 kPa stage, (see Fellenius, 1972).

Figure 5.37 : Surcharge Pressure = 45 kPa

At this loading stage a slight decrease of downdrag values, through all stations, was noticed at the 14th day.

Loads started to increase up to 28 days after which a constant rate was continued. Maximum downdrag of 0.55 kN was recorded at the lower part of the pile.

The decline of the readings at that period (14th day) is thought to be due to a slip between the pile and the clay, although this cannot be substantiated.

Figure 5.39 : Surcharge Pressure = 90 kPa

In examining the trend of downdrag build-up of this loading stage and because of the high load increment of this stage compared to previous stages, a depression of downdrag values was noticable soon after load application. This reduction of downdrag which occurred over a period of 5 days may be attributed to the high pore pressures developed on applying the surcharge pressure. However, a constant rate of downdrag increase was maintained at the lower part of the pile while a slight decrease was registered at stations 6 and 7. At the end of consolidation a maximum load of 1 kN was recorded at the bottom of the pile.

As for the 1st testing programme, curves showing variation in downdrag load along the pile length as well as the distribution of contact friction stresses are drawn and presented in Figs. 5.34, 5.36, 5.38 and 5.40 for each of the surcharge pressure within the 2nd testing programme.

Figure 5.34 : Surcharge Pressure = 15 kPa

A relatively constant rate of increase of downdrag loads along the pile was indicated by the first week measurements. An increase in downdrag was noticeable at station 1 during the 21st day.

Regarding negative skin friction distribution, it can be seen from Fig. 5.34b that a slight decrease of frictional stresses was recorded at the bottom of the pile at 35 days. This may be explained by the developement of a small amount of upward frictional stress in the lower zone of the pile.

Approximately 40% of the measured maximum negative skin friction had been mobilised during the first week of this loading stage. This compares with 61% for the 30 kPa surcharge of the 1st testing programme.

The measured average degree of consolidation at the end of the 35 days was approximately 90%.

Figure 5.36 : Surcharge Pressure = 30 kPa

The 7 day readings indicated a cosiderable amount of downdrag (0.32 kN) whereas the curves from 21 days and 35 days showed a reduction of downdrag values along the lower portion of the pile.

Frictional stress distribution for the 7th, 21st and 35th days remained at their maximum values at the approximate mid-depth of the clay bed.

At the end of this surcharge loading time, the measured average degree of consolidation was 86%.

Figure 5.38 : Surcharge Pressure = 45 kPa

Downdrag loads continued to build up over this loading stage reaching a value of 0.49 KN seven days after surcharge application. A maximum load of 0.55 kN was recorded at the end of 35 days.

Concerning the distribution of frictional stresses, it is interesting to note that negative skin friction was building up further down the pile than compared with the previous stage (30 kPa).

The measured average degree of consolidation was 86% .

Figure 5.40 : Surcharge Pressure = 90 kPa

This loading stage involved an incremental surcharge pressure of 45 kPa. Accordingly, negative skin friction increase was noticable. A maximum downdrag of 0.94 kN was recorded at the end of 35 days.

Fig. 5.40b shows a constant value of 12.7 kPa of negative skin friction along the entire length of the pile.

An average degree of consolidation of 71% was measured at the end of this loading stage.

5.5 Settlement Results

Results of the settlement readings are shown in Figs. 5.41 to 5.47 for each stage of surcharge corresponding to

the two testing programmes.

5.5.1 Settlement During 1st Testing Programme

A settlement of 76mm was registered by the sleeve and 44mm by the drainage calculation method during the 30 kPa surcharge of the first testing programme, Fig. 5.41.

During the 60 kPa stage, Fig. 5.42, the clay surface showed consistent settlements compared with the previous stage. The maximum settlement at the end of the period, registered by means of drainage , was 31mm and that by the sleeve was 38mm.

5.5.2 Settlement During 2nd Testing Programme

Settlements of magnitude 44mm and 27mm were indicated by the sleeve and the drainage calculation mathods respectively during the first stage of 15 kPa surcharge, while settlements of 31mm and 21mm were registerd for the second loading stage of 30 kPa, Fig. 5.45. It is interesting to note that the sum of the measured sleeve settlements for both the stages represents approximately the same magnitude of settlement recorded at the 30 kPa stage of the 1st testing programme.

Measured sleeve and calculated drainage settlement values decreased to 17mm and 10mm respectively for the 3rd

loading stage of 45 kPa, Fig. 5.46.

On application of the 90 kPa surcharge both the sleeve and the drainage settlements showed nearly the same magnitude, 38mm and 36mm respectively, Fig. 5.47. This behaviour suggests that the clay in the central zone around the pile was approaching its limit compression due to the large settlements it experienced during the earlier stages. The difference in settlement between this zone and that near the edges of the tank was therefore diminishing as the soil became stiffer.

Readings of the settlement plates are not included in the 2nd testing programme since accurate readings could not be obtained at the previous stages of the 1st testing programme. The following remarks should be mentioned regarding the behaviour of the settlement plates during the 1st testing programme :

i) In Fig. 5.41, plates No.1 and No.2 showed no sign of settlement.

ii) Fig. 5.42 shows that plate No.2 (250mm below clay surface) had settled twice the value of plate No.4 (100mm below clay surface).

iii) Plate No.4 registered no settlement during the last stage of 90 kPa surcharge, Fig. 5.43.

However, the volumes of drained water collected consequently upon surcharge application enabled calculation of settlement to be obtained by the simple expedient of dividing the measured volume of drained water by the cross sectional area of the tank (soil only).

All settlement figures mentioned earlier indicated that the sleeve settlement (which represents the settlement of the clay surface at the tank's centre) was the largest. A significant difference between the sleeve and the drainage settlement was registered during the early stages of the testing programme, i.e., a difference of 32mm between the sleeve settlement and the drainage settlement was recorded during the 30 kPa loading stage, Fig. 5.41. As the consolidation pressure increased, this difference reduced indicating that the volume change of the clay bed was initially larger (immediately after application of surcharge).

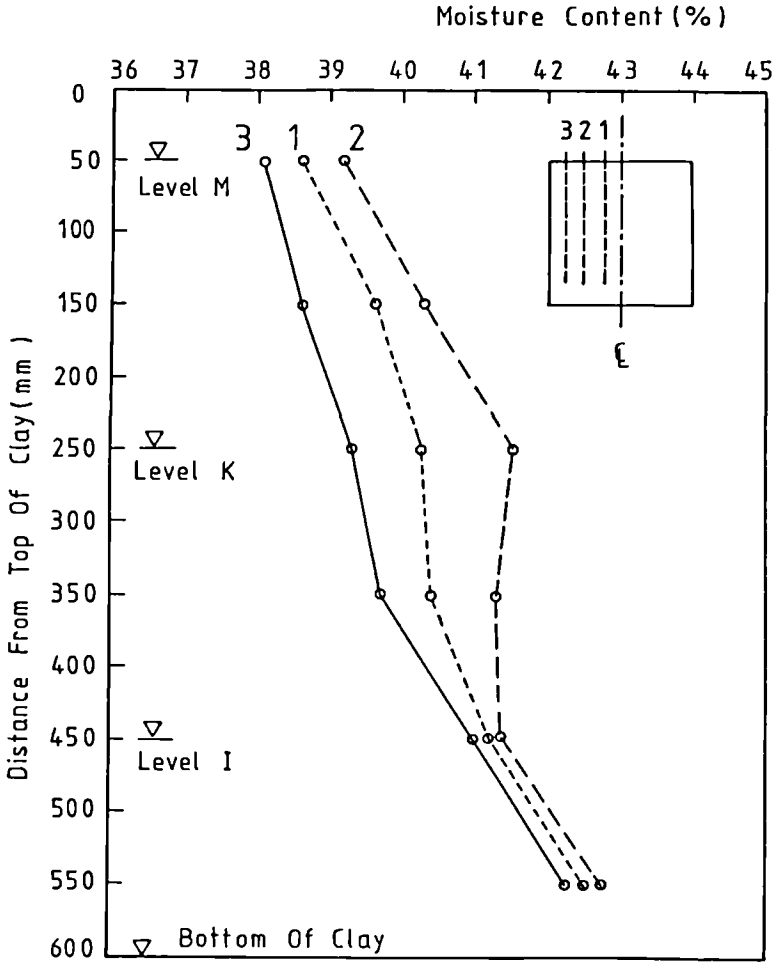

FIG. 5.1 MOISTURE CONTENT VARIATION AFTER COMPLETION OF THE FIRST TESTING PROGRAMME

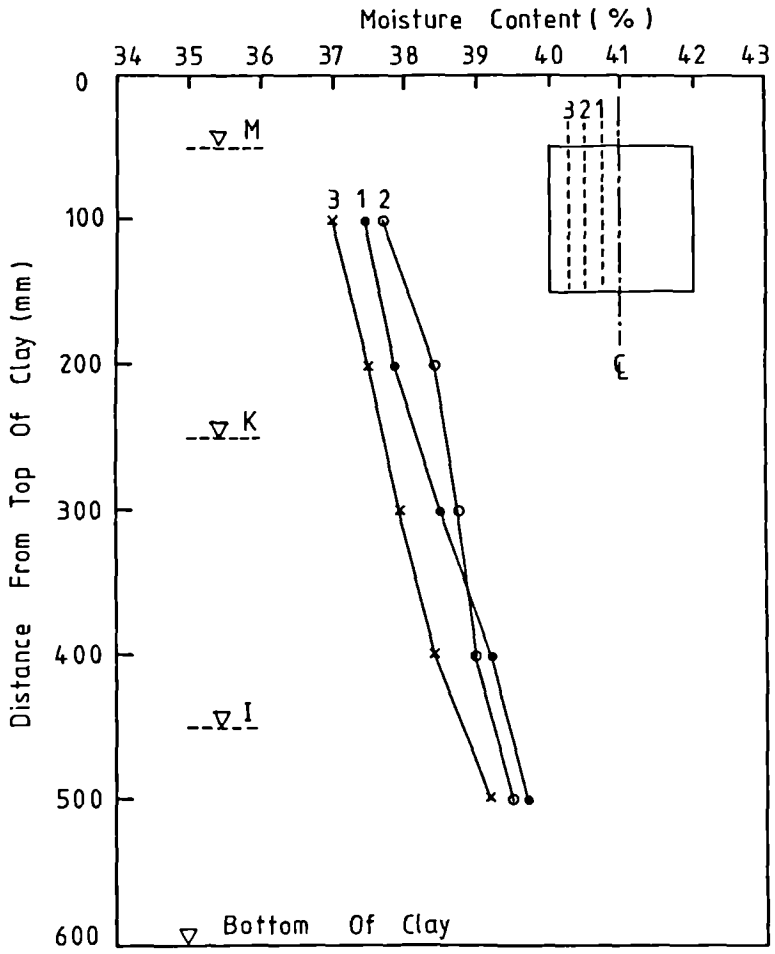

FIG. 5.2 MOISTURE CONTENT VARIATION AFTER COMPLETION OF THE SECOND TESTING PROGRAMME

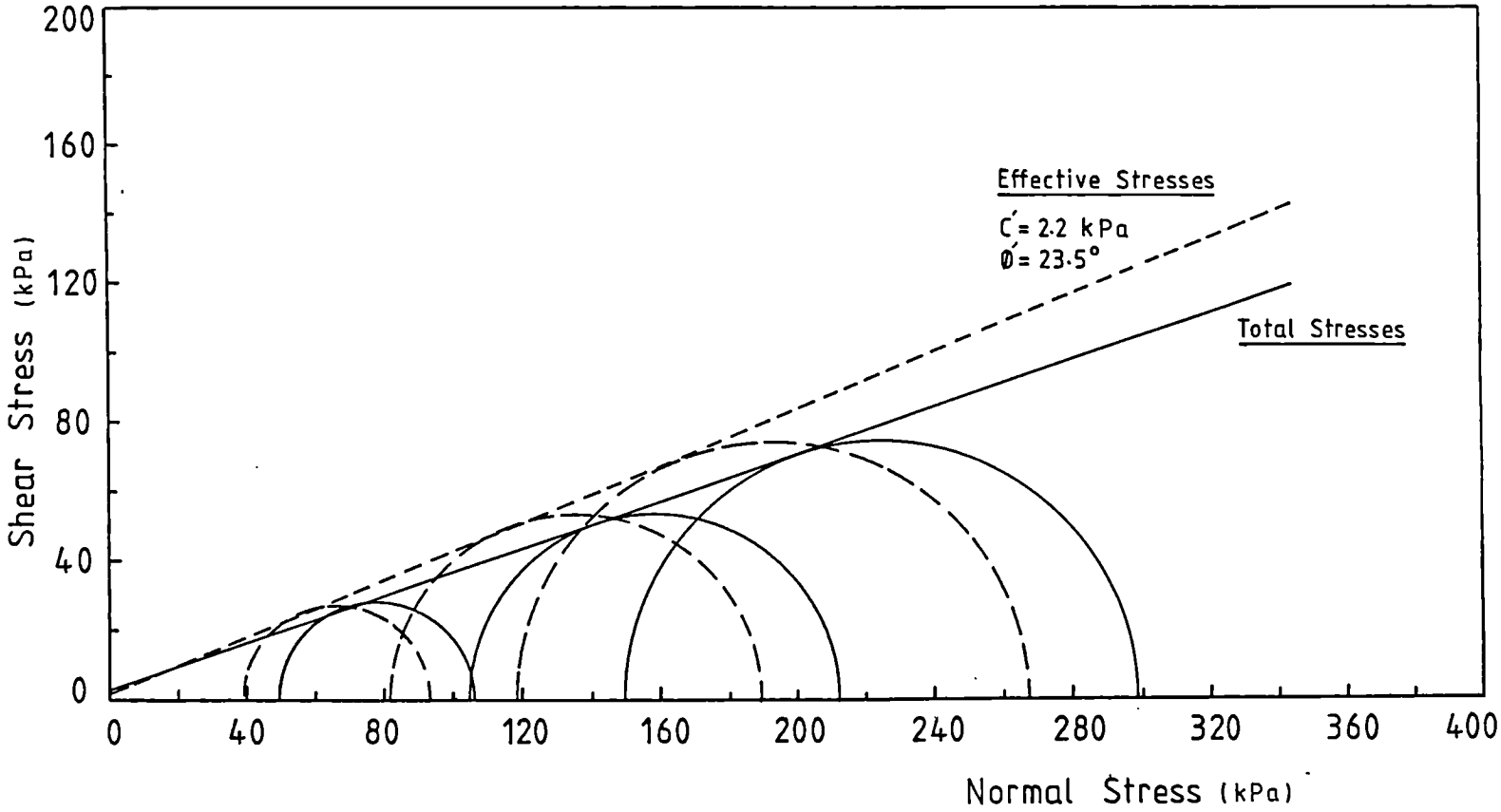

FIG. 5.3 TOTAL AND EFFECTIVE MOHR CIRCLES AND FAILURE ENVELOPES AT END OF FIRST TESTING PROGRAMME

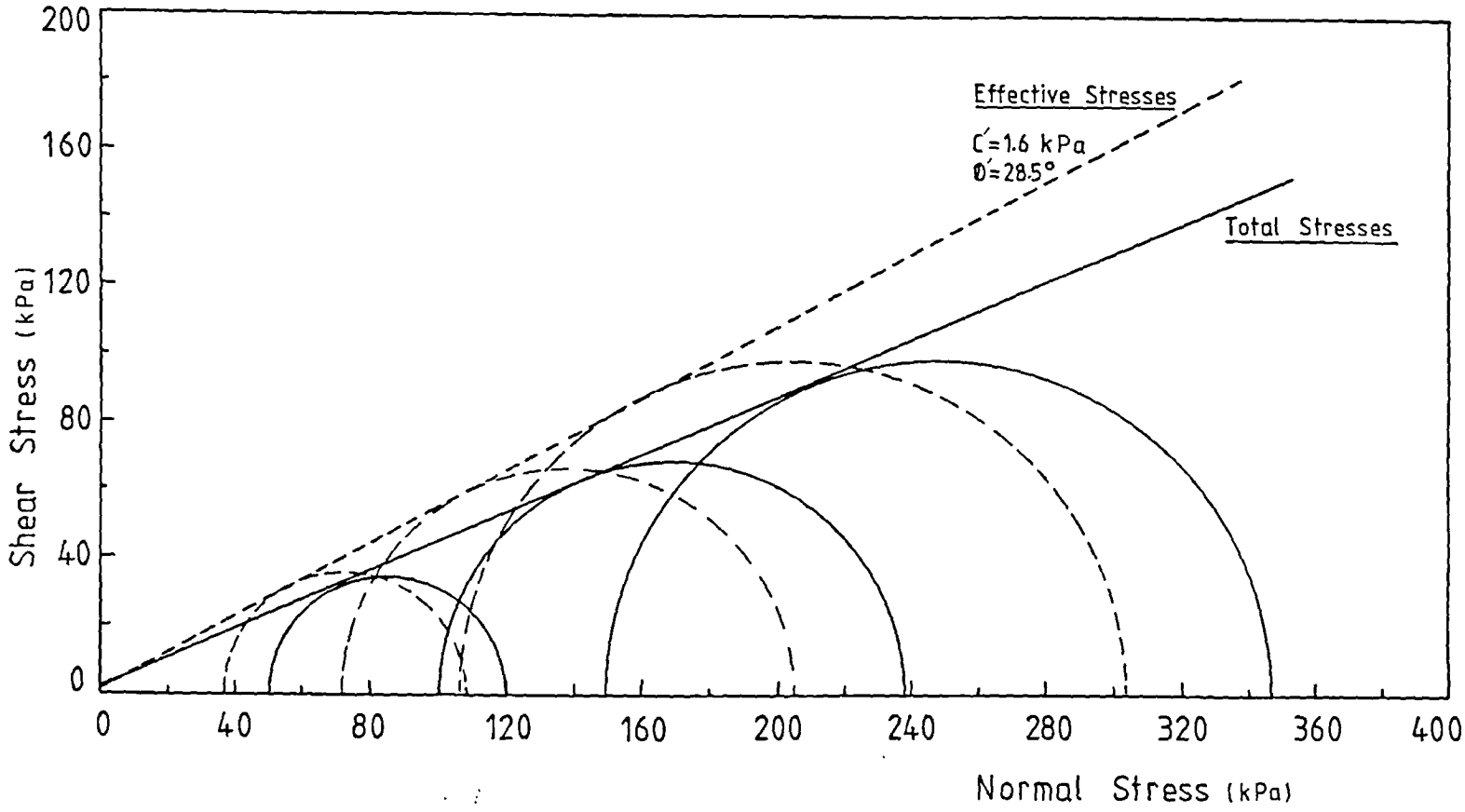

FIG. 5.4 TOTAL AND EFFECTIVE MOHR CIRCLES AND FAILURE ENVELOPE AT END OF SECOND TESTING PROGRAMME

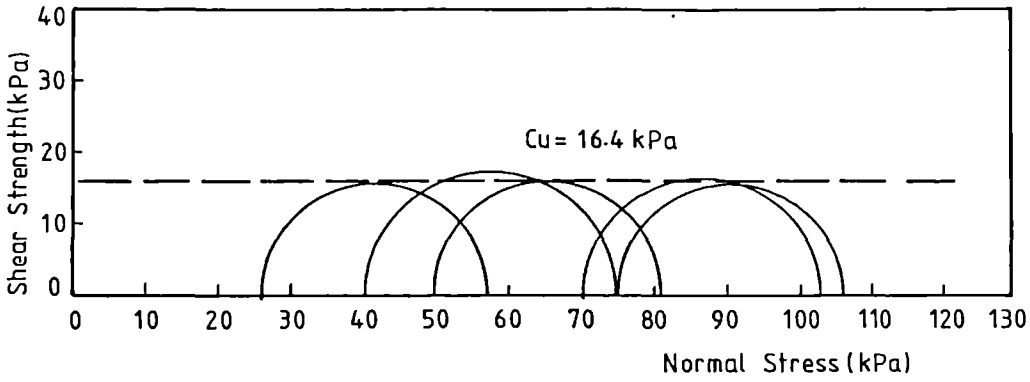

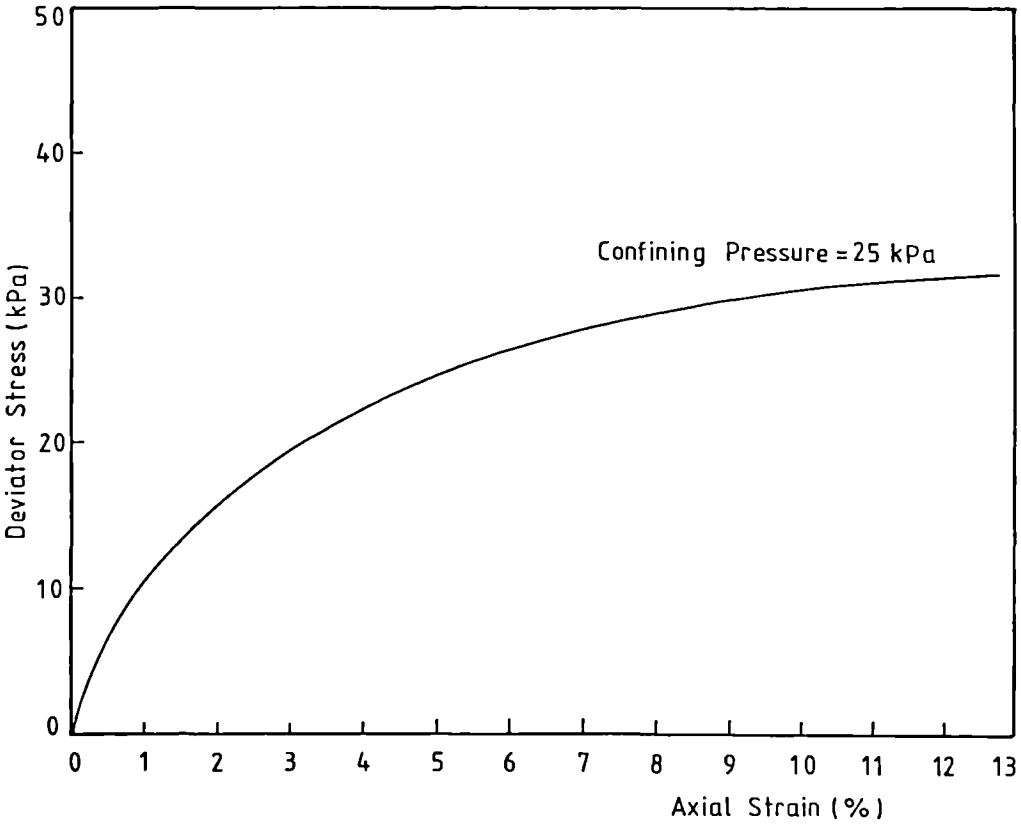

FIG. 5.5 UNDRAINED TRIAXIAL TEST RESULTS OF REMOULDED SAMPLES, AT END OF 1ST TESTING PROGRAMME

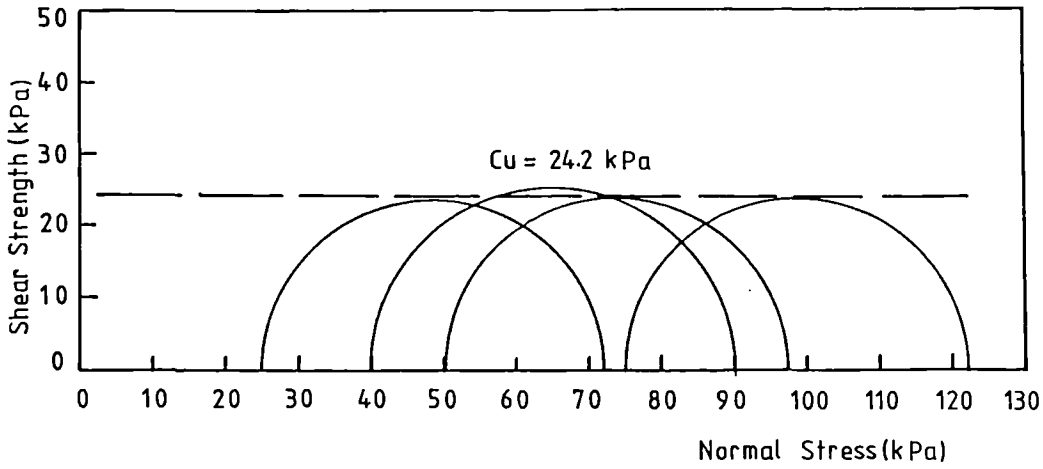

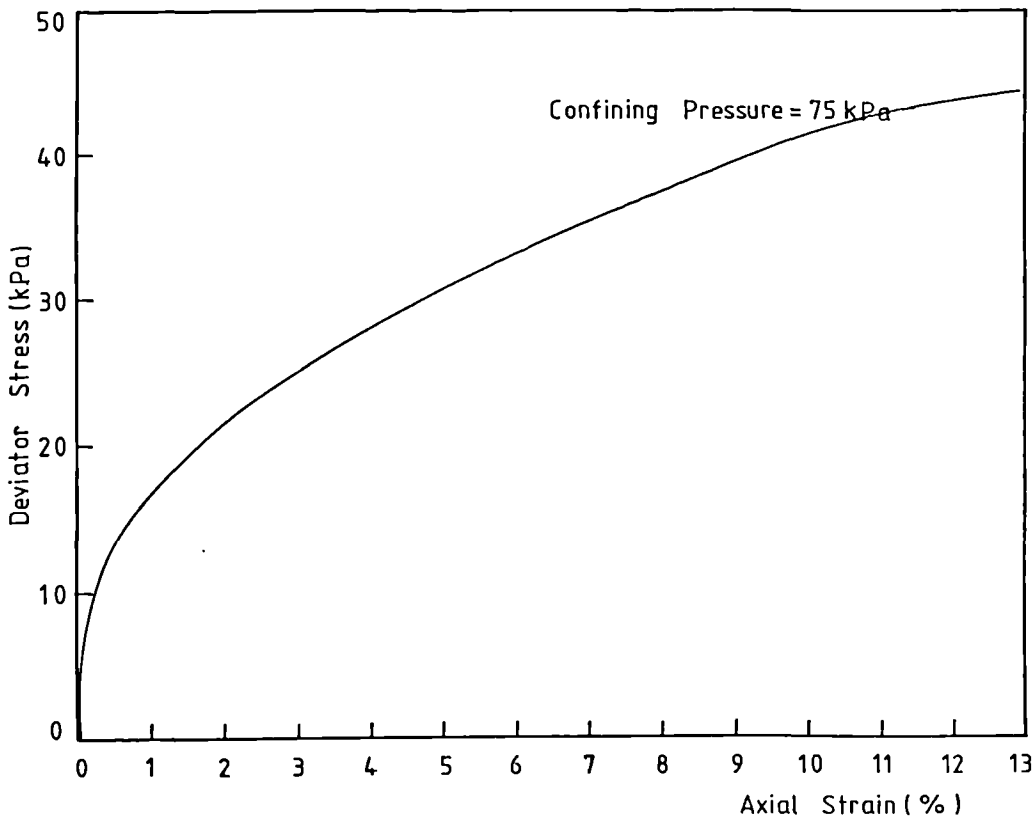

FIG. 5.6 UNDRAINED TRIAXIAL TEST RESULTS OF REMOULDED SAMPLES, AT END OF 2ND TESTING PROGRAMME

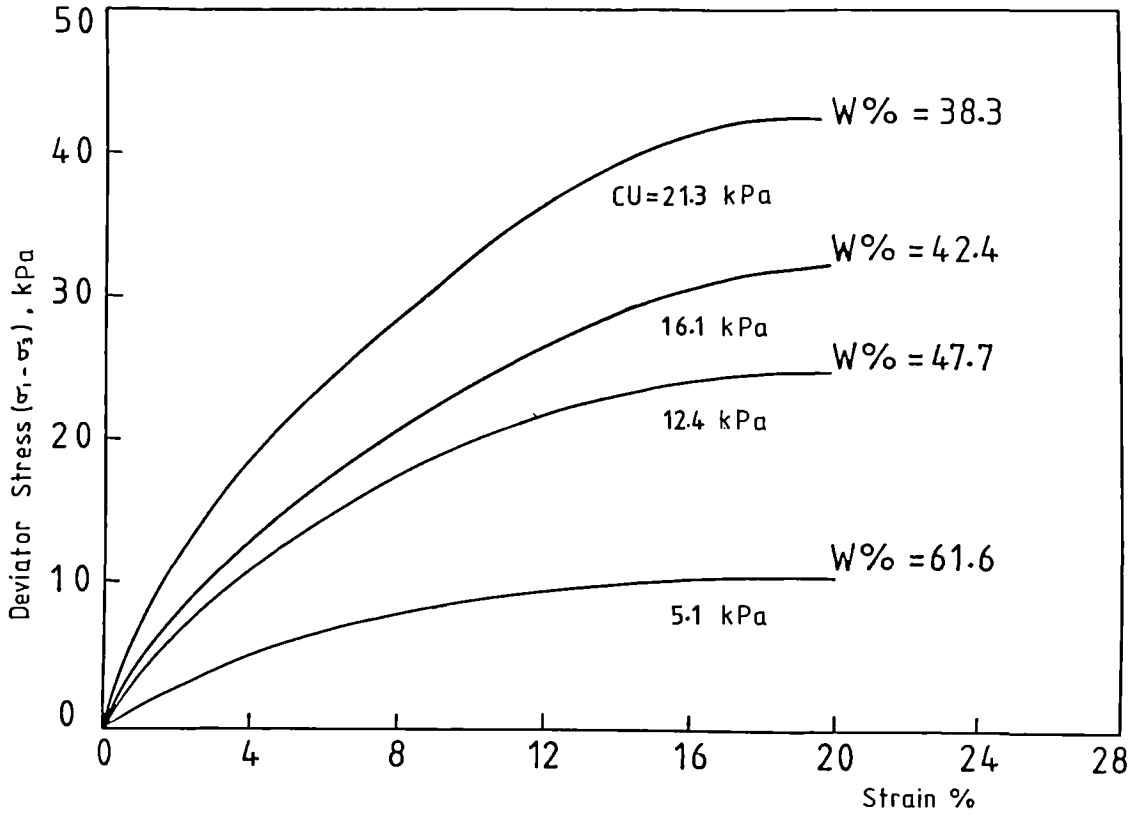

FIG. 5.7 STRESS-STRAIN RELATIONSHIPS OF SAMPLES WITH DIFFERENT MOISTURE CONTENTS

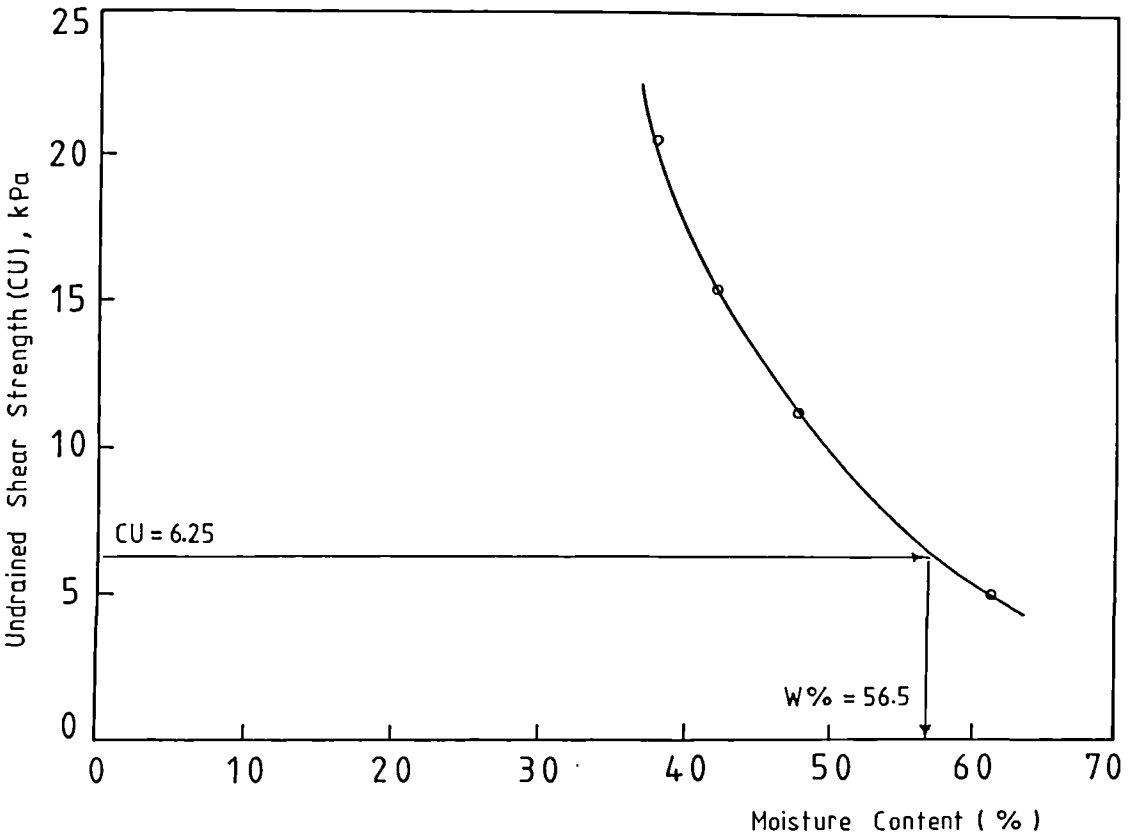

FIG. 5.8 UNDRAINED SHEAR STRENGTH Vs. MOISTURE CONTENTS

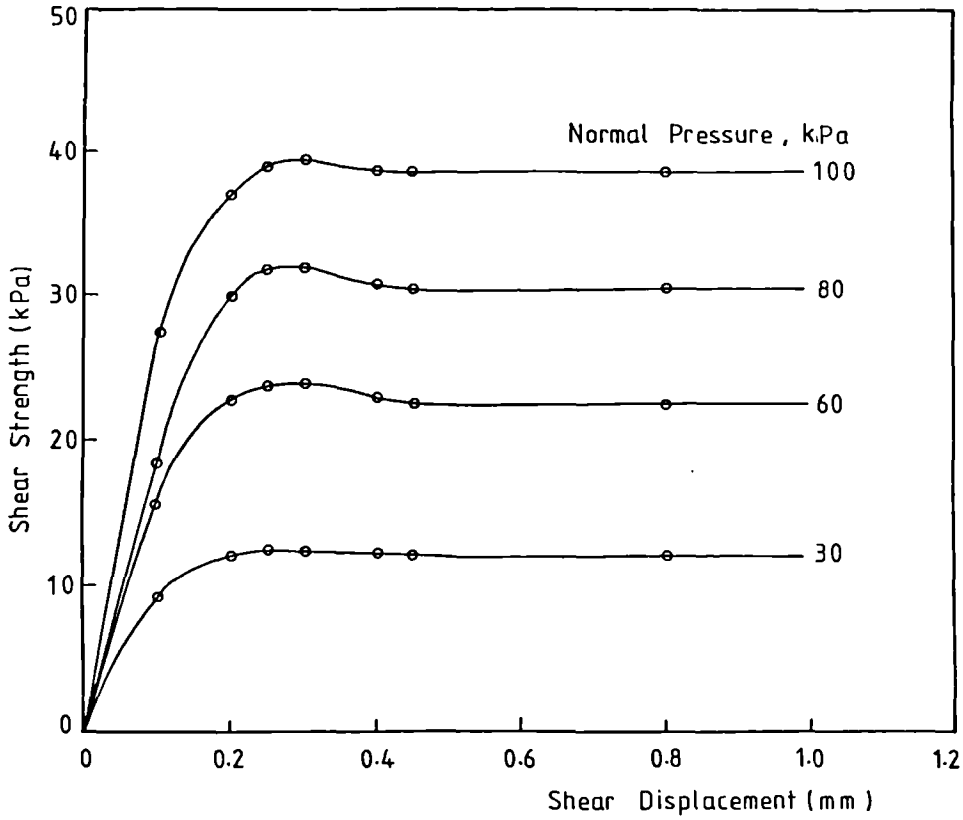

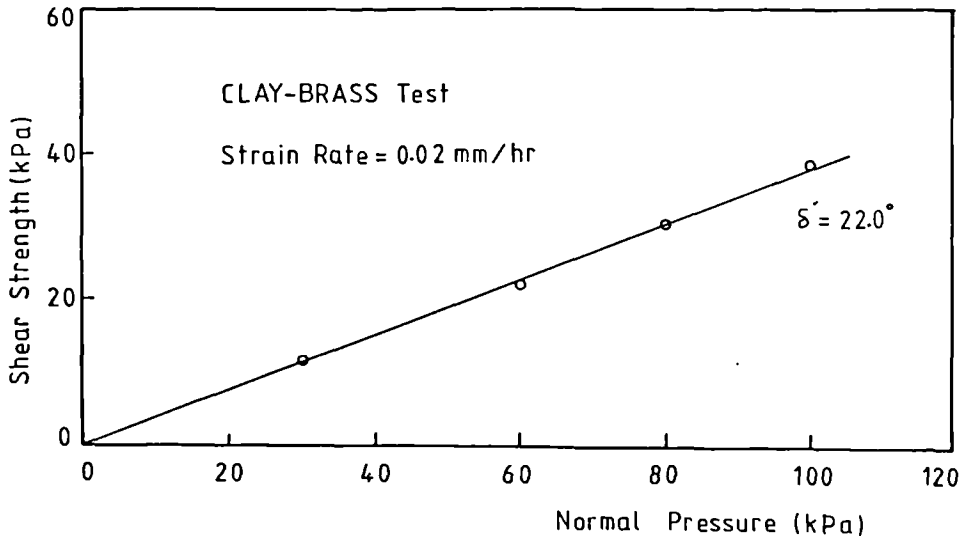

FIG. 5.9 DRAINED SHEAR BOX TEST RESULTS ON REMOULDED SAMPLES (CLAY-BRASS TESTS) AT END OF FIRST TESTING PROGRAMME

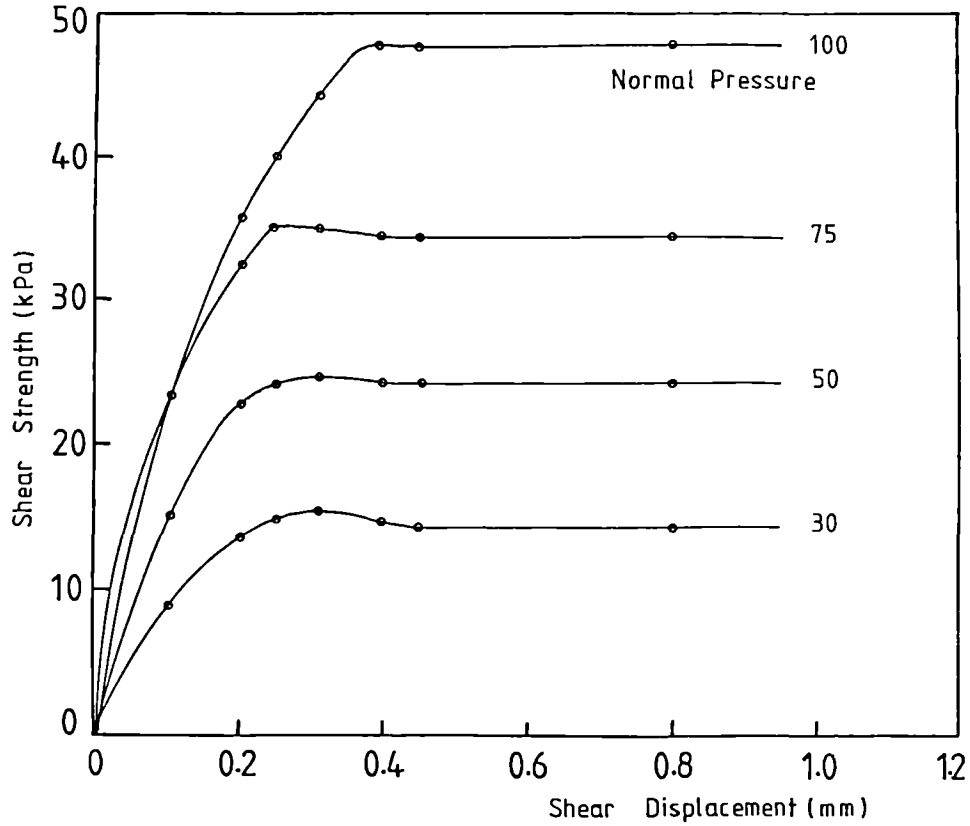

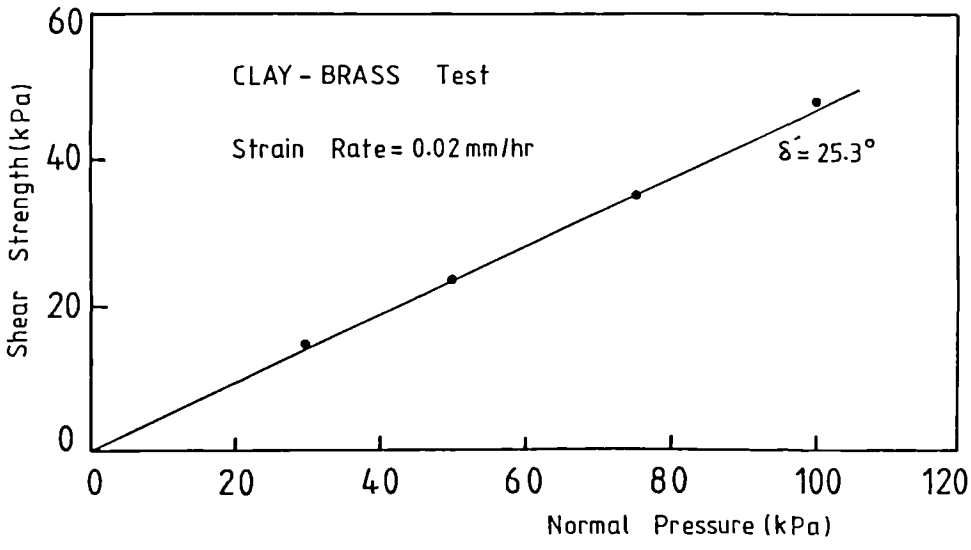

FIG. 5.10 DRAINED SHEAR BOX TEST RESULTS ON REMOULDED SAMPLES (CLAY-BRASS TESTS) AT END OF 2ND TESTING PROGRAMME

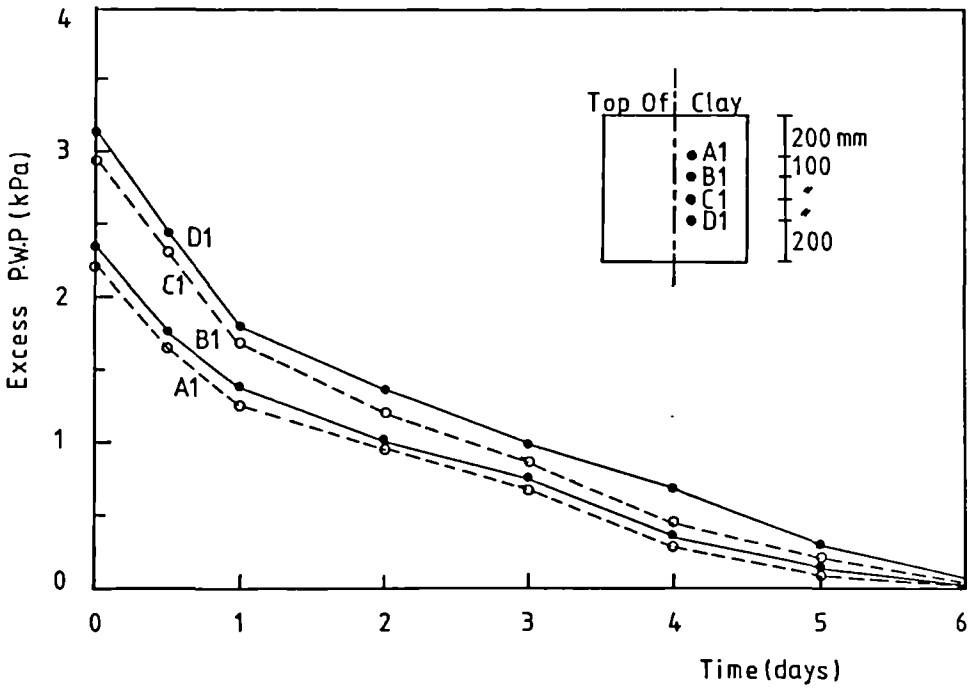

FIG. 5.11 PORE PRESSURE READINGS AFTER PILE DRIVING

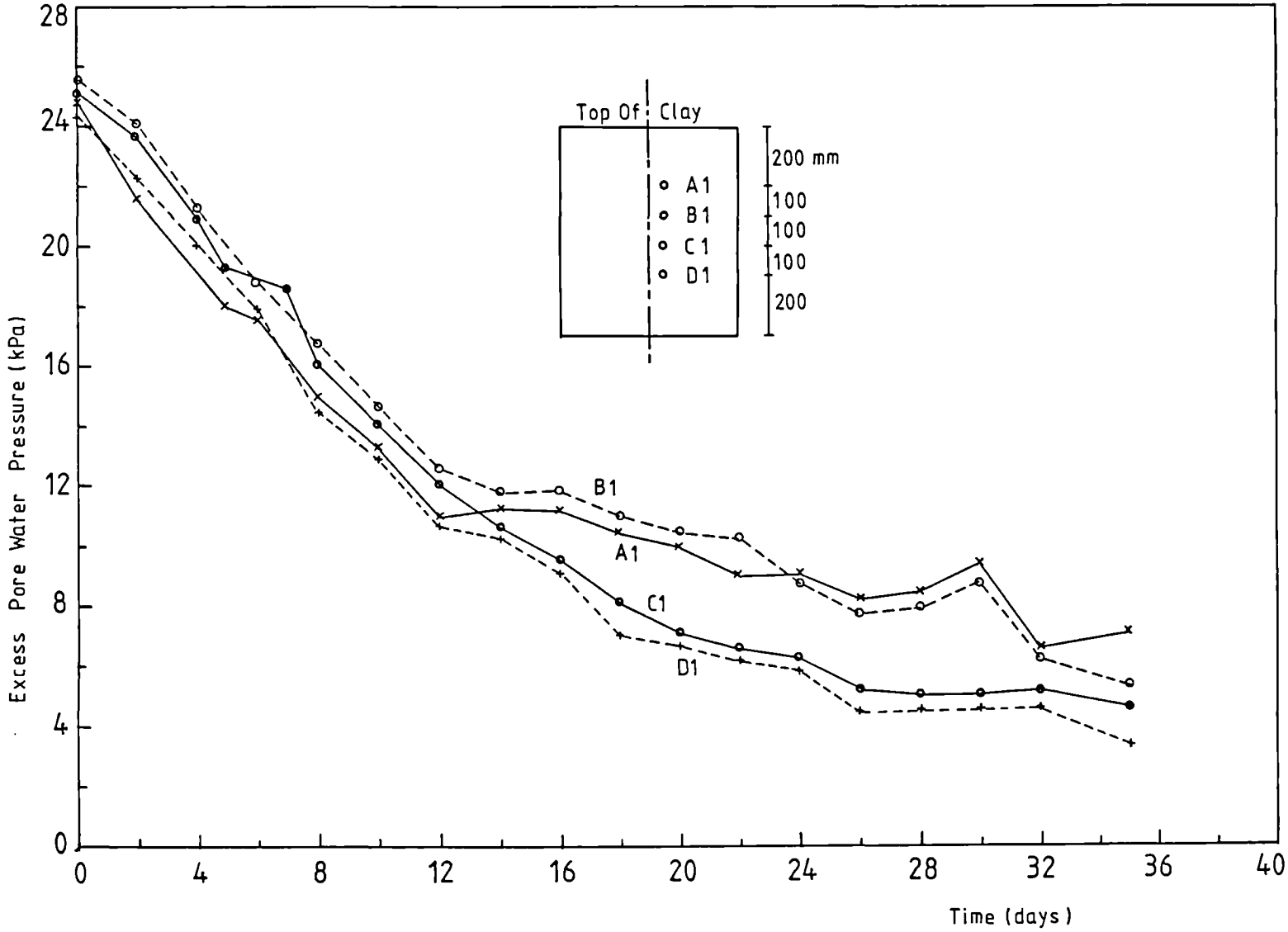

FIG. 5.12 PORE PRESSURE READINGS, 1ST TESTING PROGRAMME, SURCHARGE PRESSURE = 30 kPa

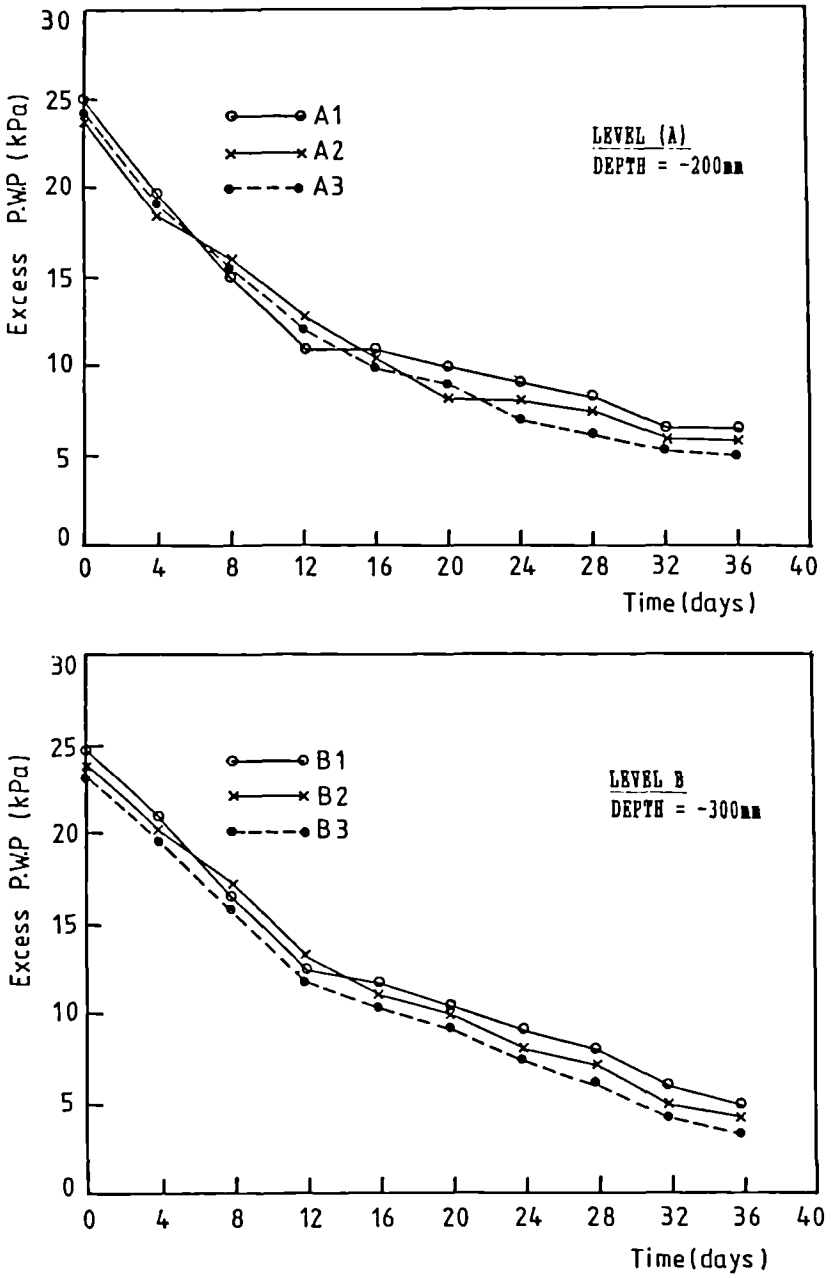

FIG. 5.13 PORE PRESSURE READINGS (RADIAL DIRECTION), 1ST TESTING PROGRAMME (SURCHARGE PRESSURE=30kPa)

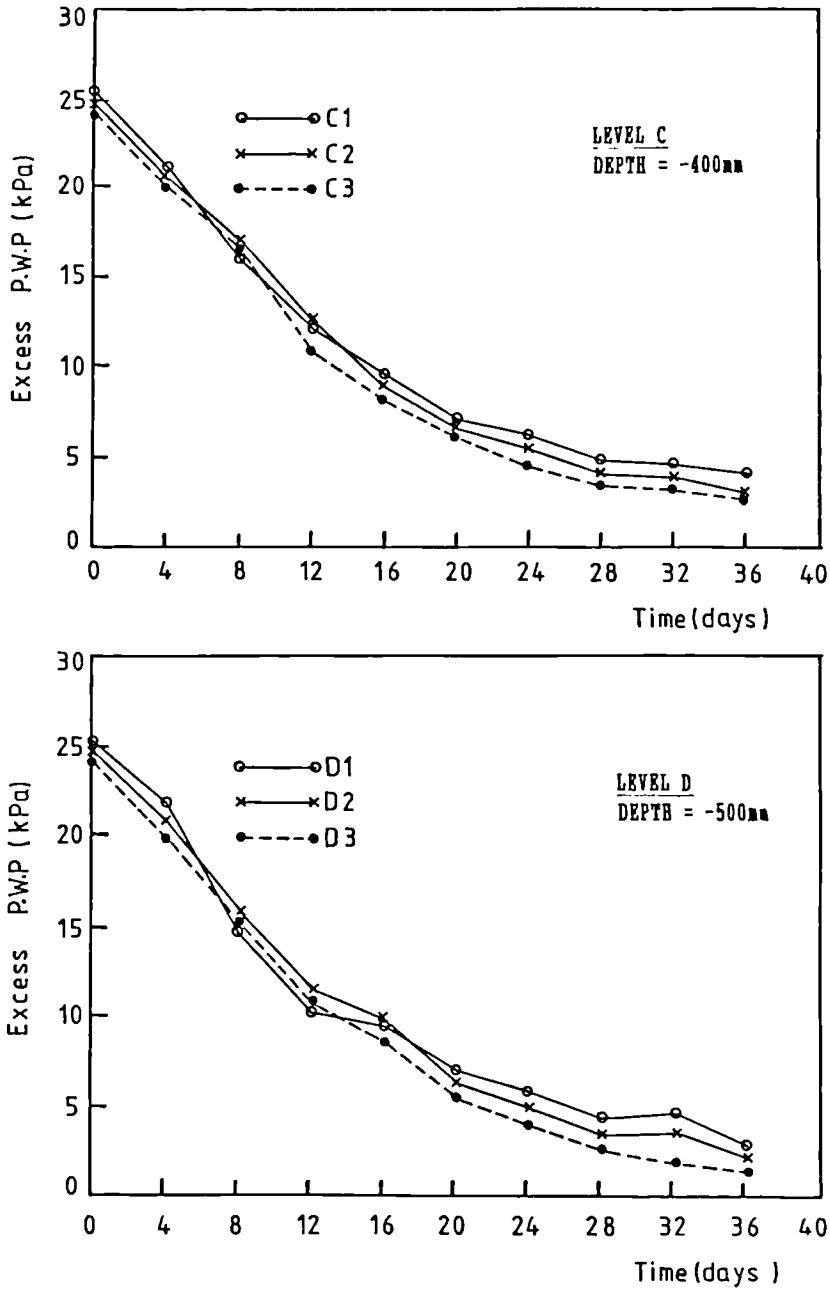

FIG. 5.13 PORE PRESSURE READINGS (RADIAL DIRECTION), 1ST TESTING PROGRAMME (SURCHARGE PRESSURE=30kPa)

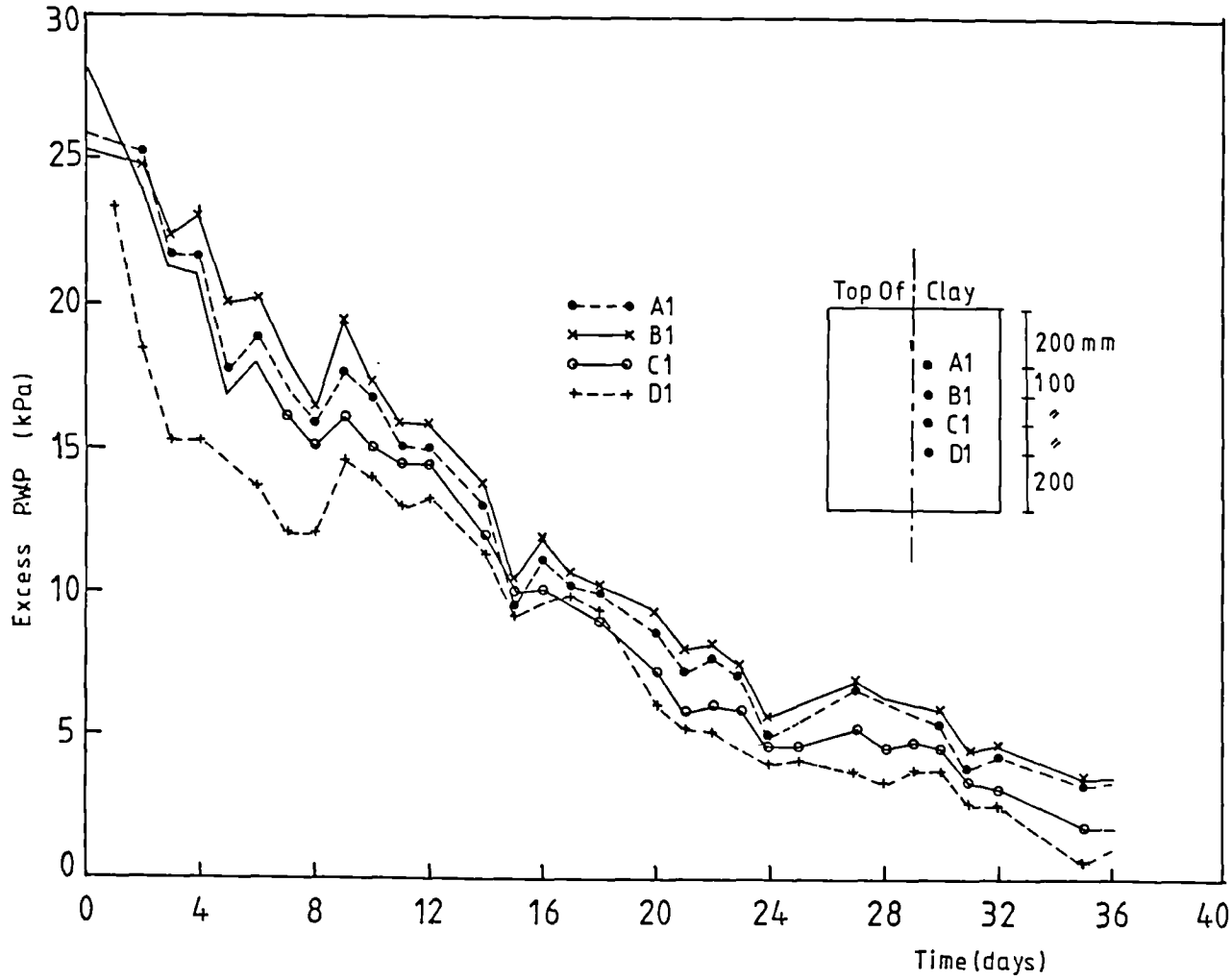

FIG. 5.14 PORE PRESSURE READINGS, 1ST TESTING PROGRAMME, SURCHARGE PRESSURE = 60 kPa

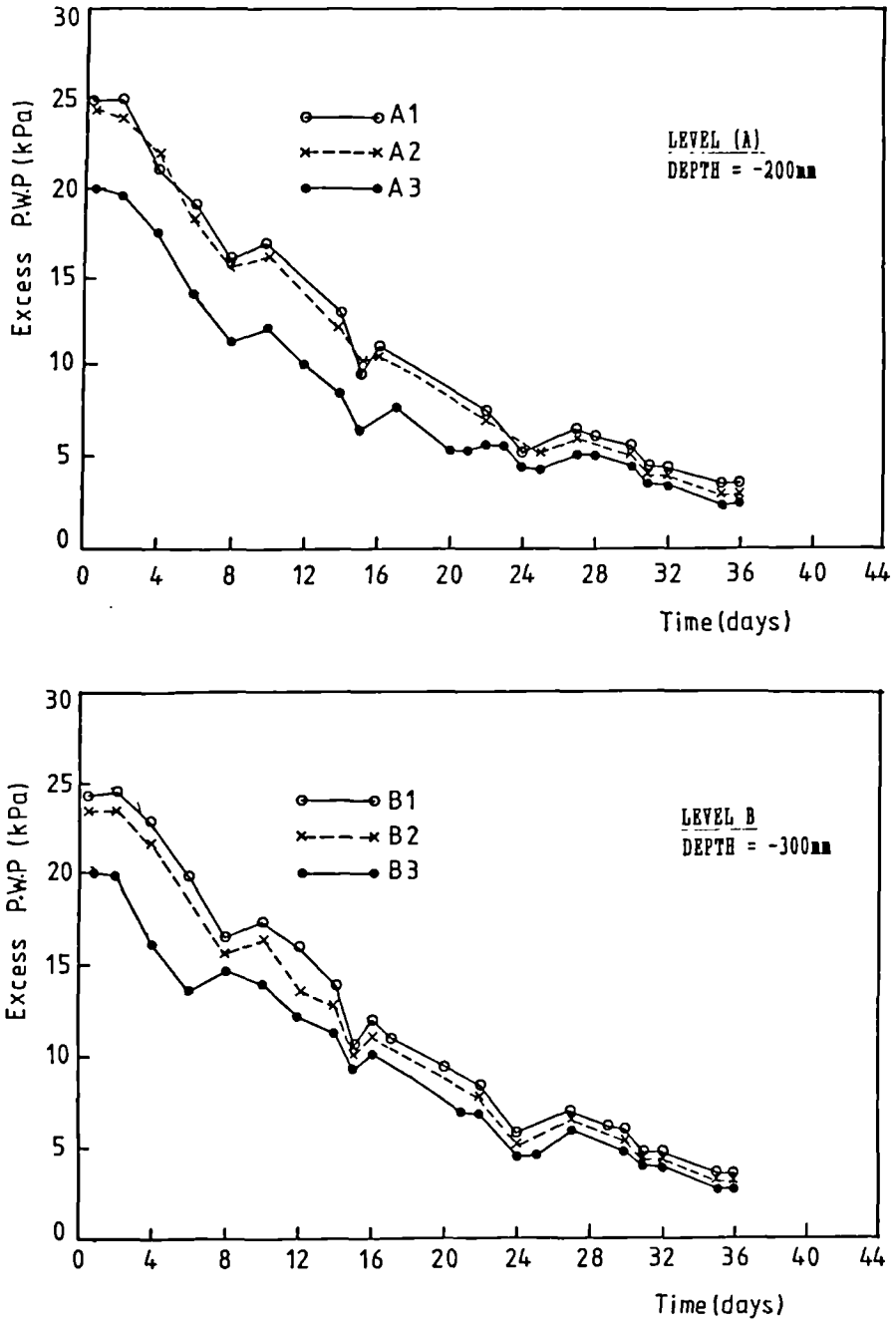

FIG. 5.15 PORE PRESSURE READINGS (RADIAL DIRECTION), 1ST TESTING PROGRAMME (SURCHARGE PRESSURE=60kPa)

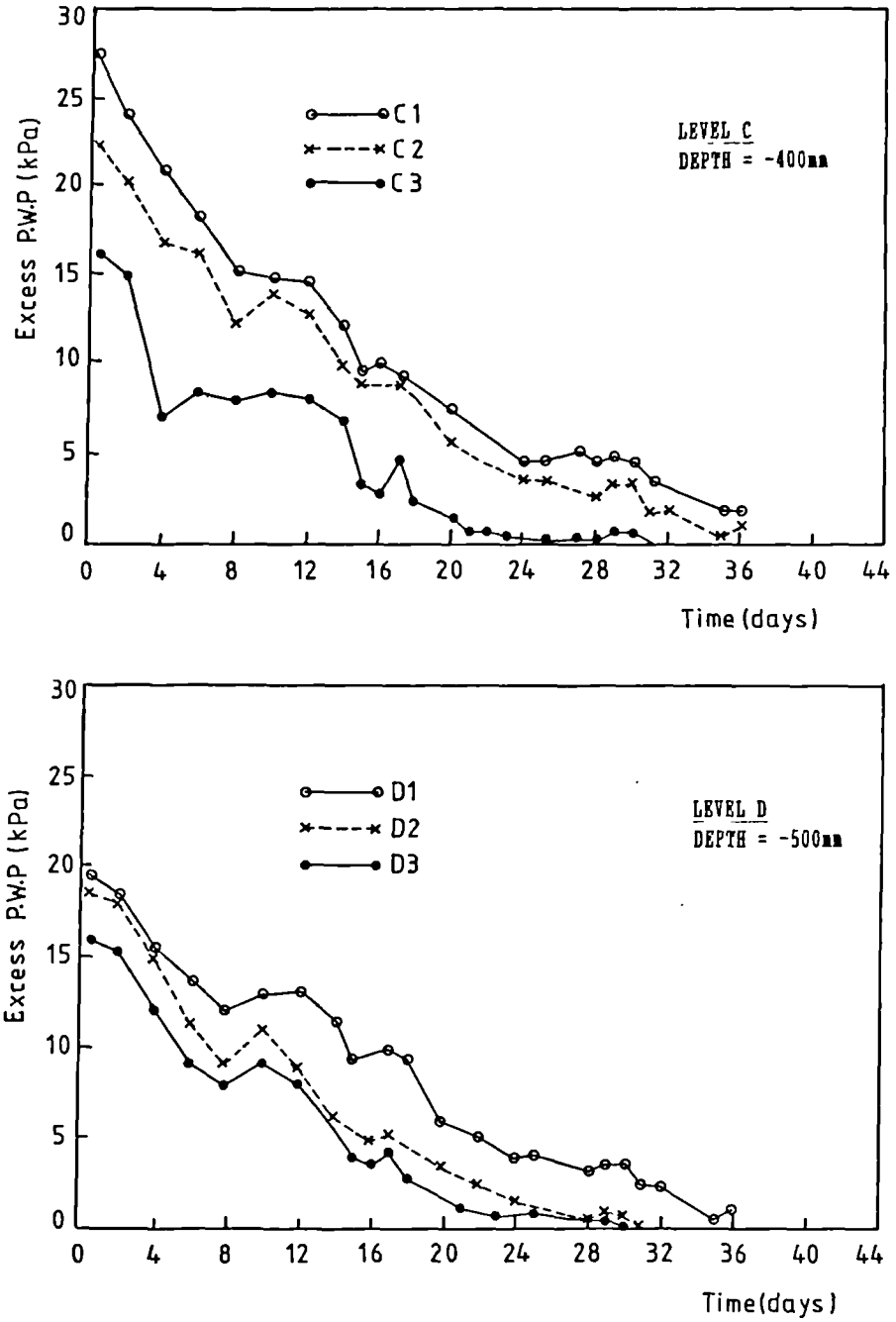

FIG. 5.15 PORE PRESSURE READINGS (RADIAL DIRECTION), 1ST TESTING PROGRAMME (SURCHARGE PRESSURE=60kPa)

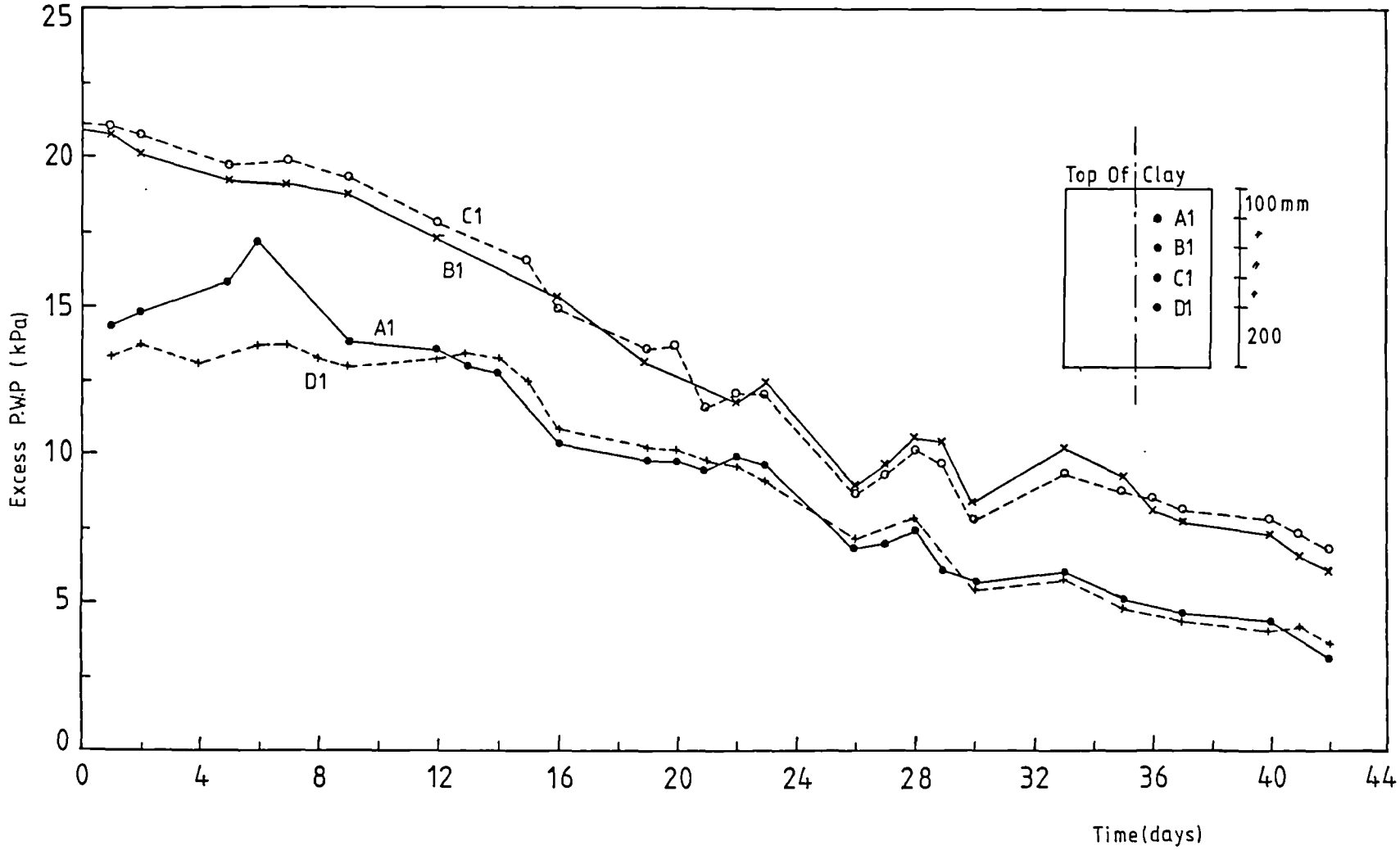

FIG. 5.16 PORE PRESSURE READINGS, 1ST TESTING PROGRAMME, SURCHARGE PRESSURE = 90 kPa

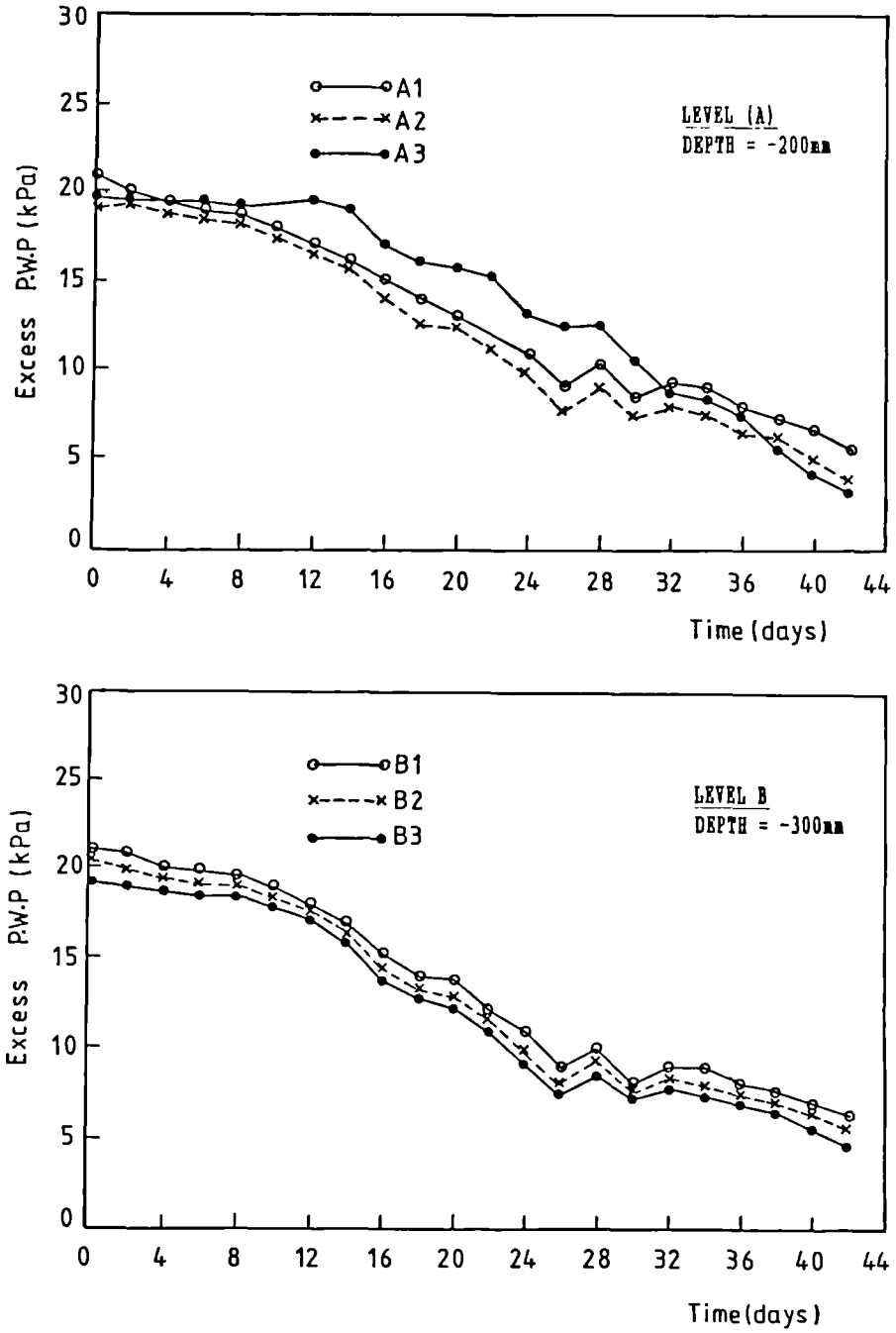

FIG. 5.17 PORE PRESSURE READINGS (RADIAL DIRECTION), 1ST TESTING PROGRAMME (SURCHARGE PRESSURE=90kPa)

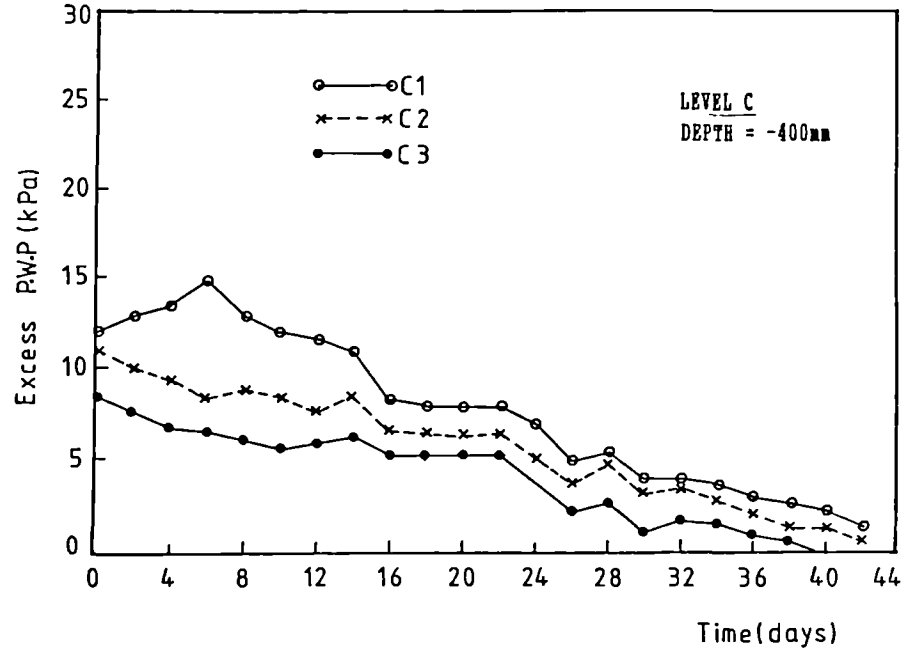

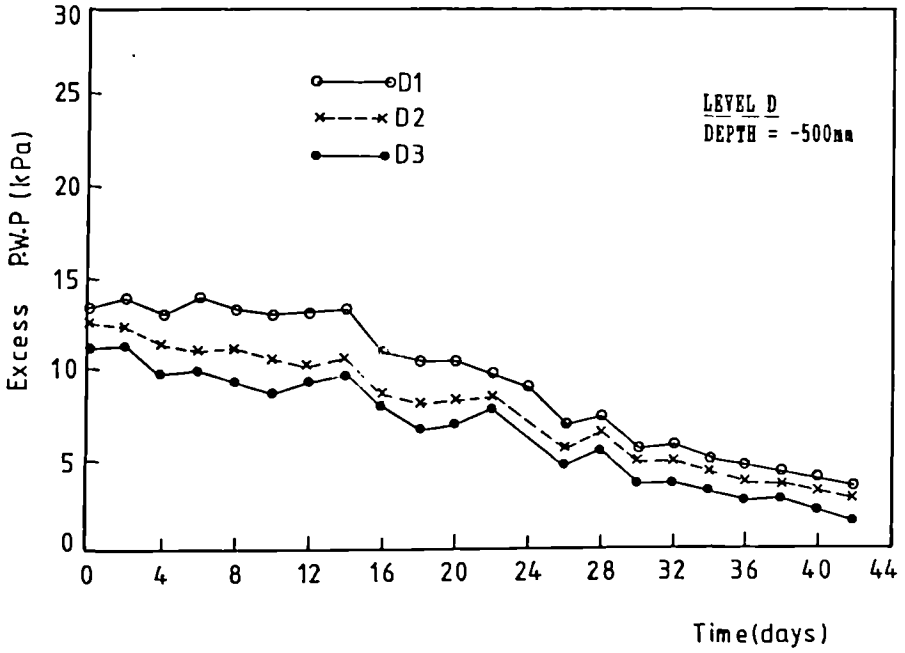

FIG. 5.17 PORE PRESSURE READINGS (RADIAL DIRECTION), 1ST TESTING PROGRAMME (SURCHARGE PRESSURE=90kPa)

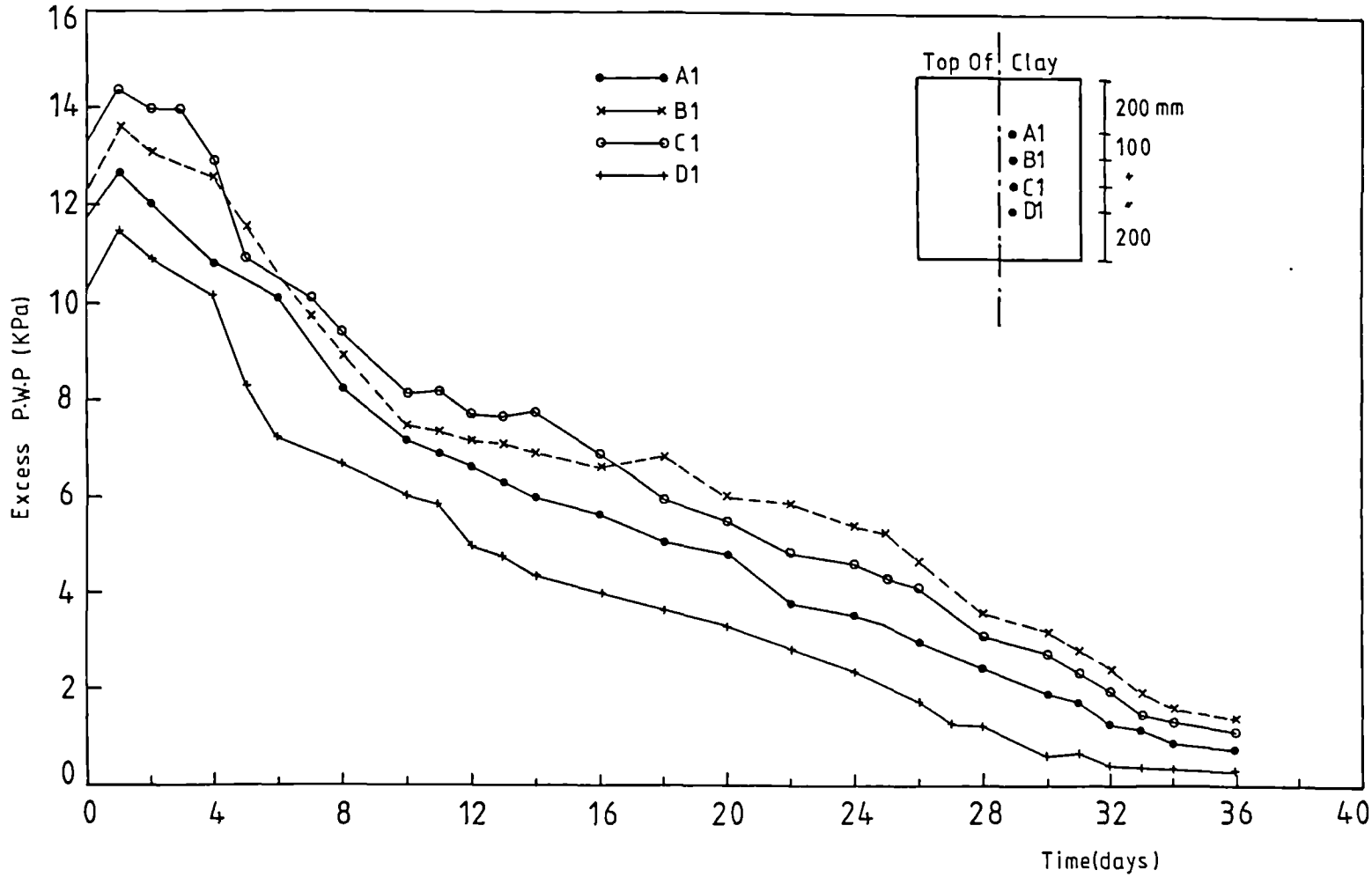

FIG. 5.18 PORE PRESSURE READINGS, 2ND TESTING PROGRAMME, SURCHARGE PRESSURE = 15 kPa

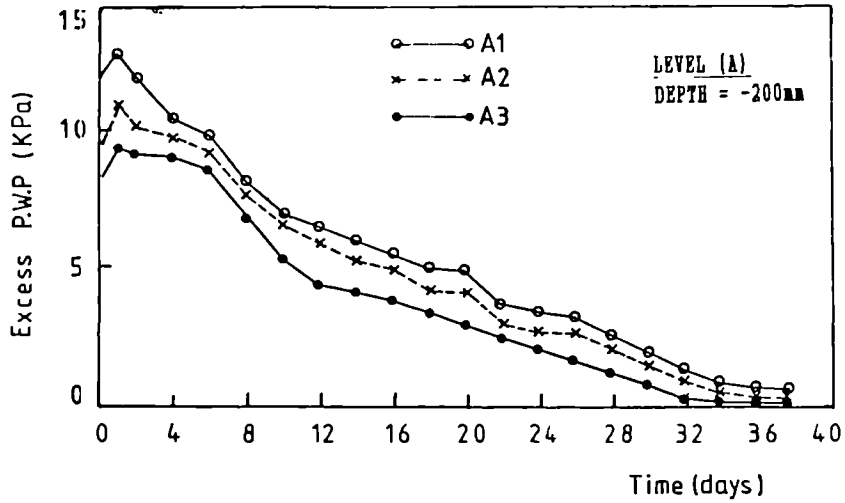

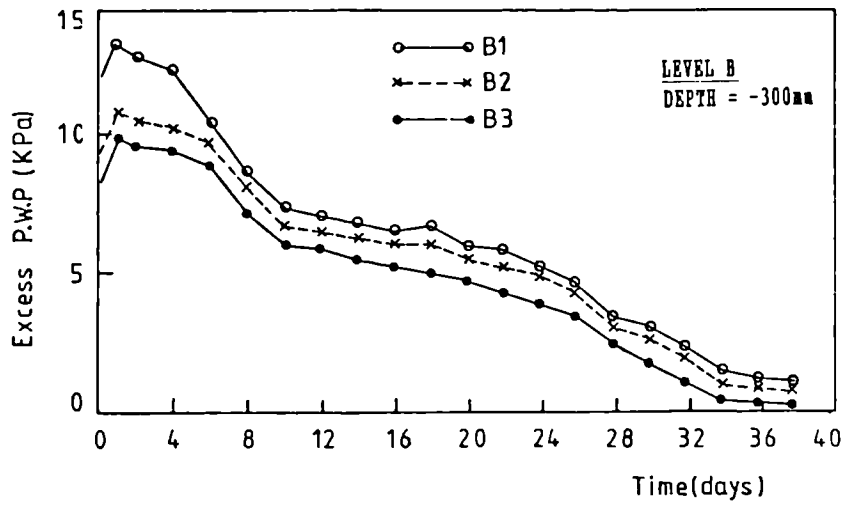

FIG. 5.19 PORE PRESSURE READINGS (RADIAL DIRECTION), 2ND TESTING PROGRAMME (SURCHARGE PRESSURE=15kPa)

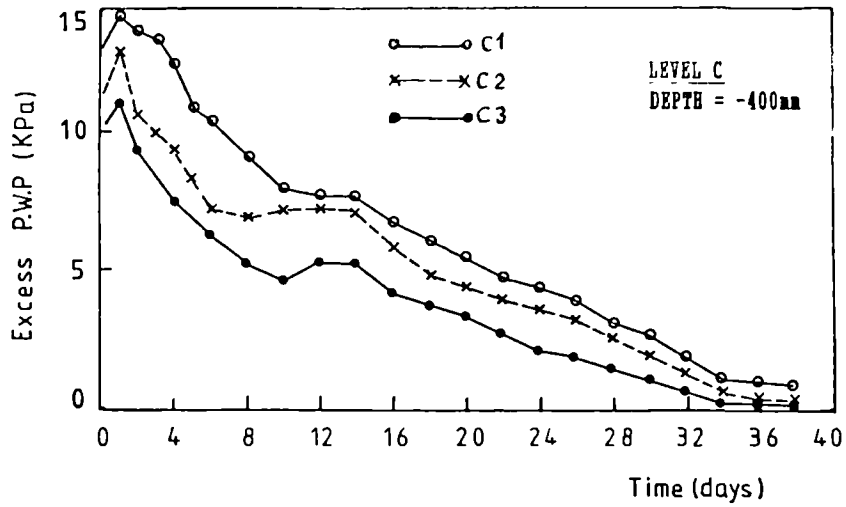

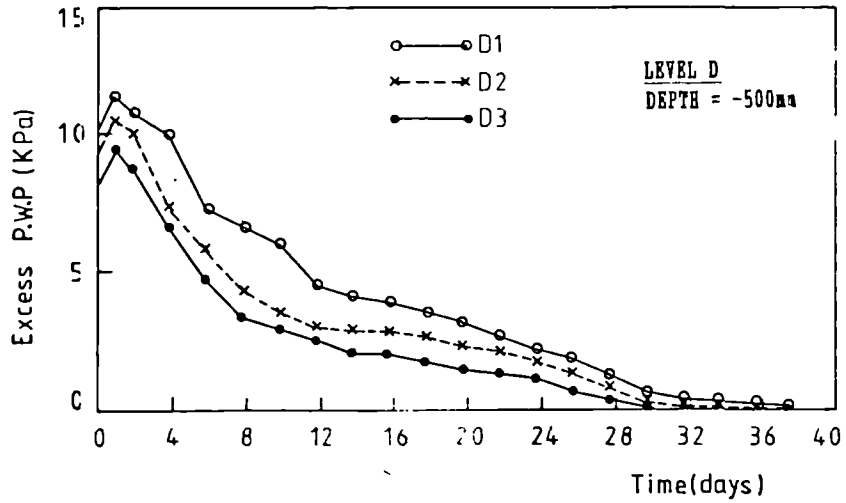

FIG. 5.19 PORE PRESSURE READINGS (RADIAL DIRECTION), 2ND TESTING PROGRAMME (SURCHARGE PRESSURE=15kPa)

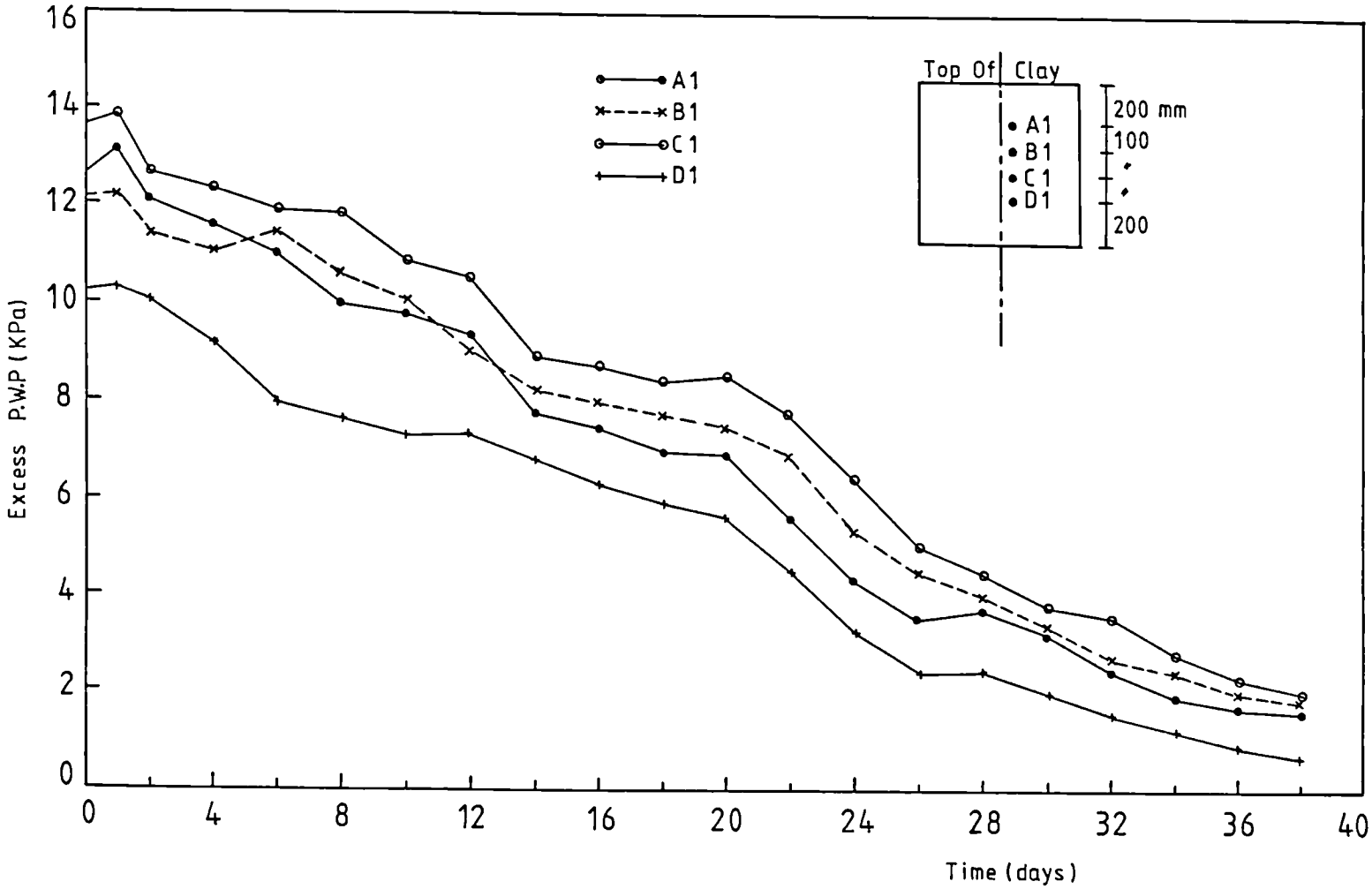

FIG. 5.20 PORE PRESSURE READINGS, 2ND TESTING PROGRAMME, SURCHARGE PRESSURE = 30 kPa

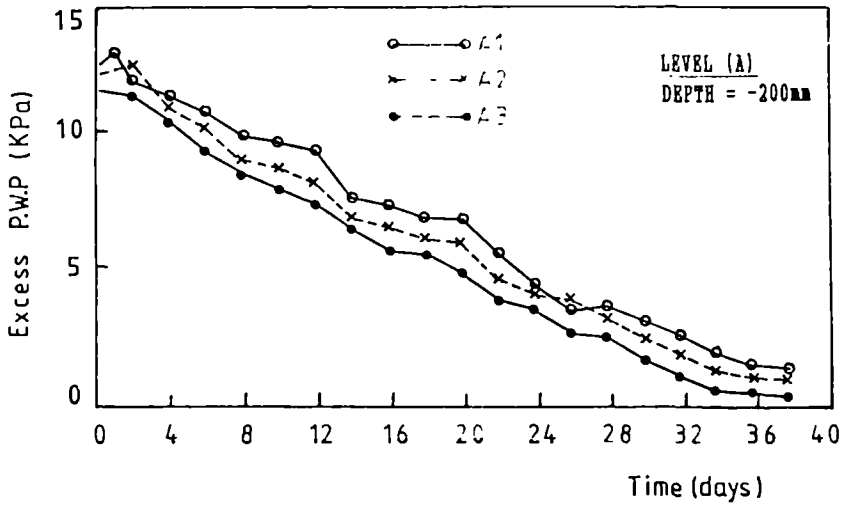

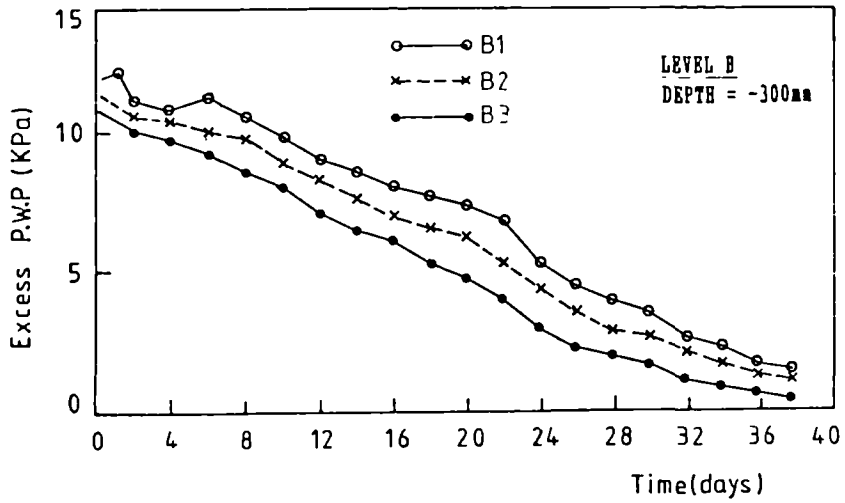

FIG. 5.21 PORE PRESSURE READINGS (RADIAL DIRECTION), 2ND TESTING PROGRAMME (SURCHARGE PRESSURE=30kPa)

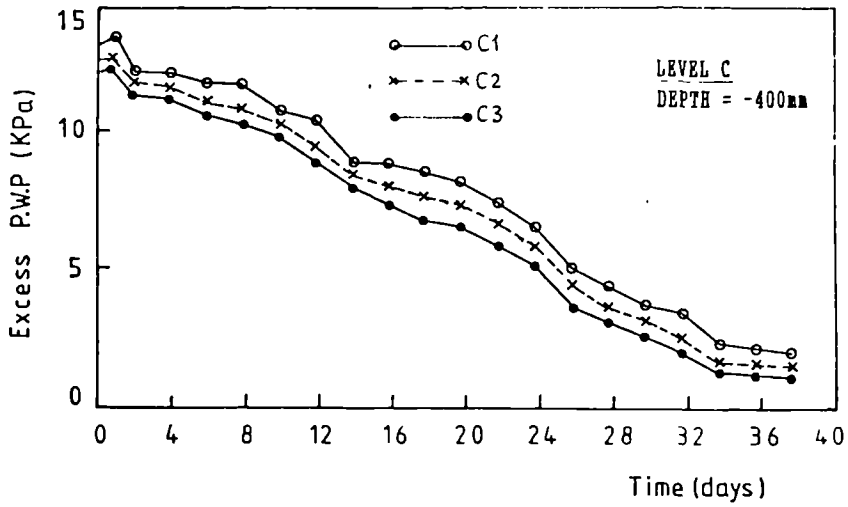

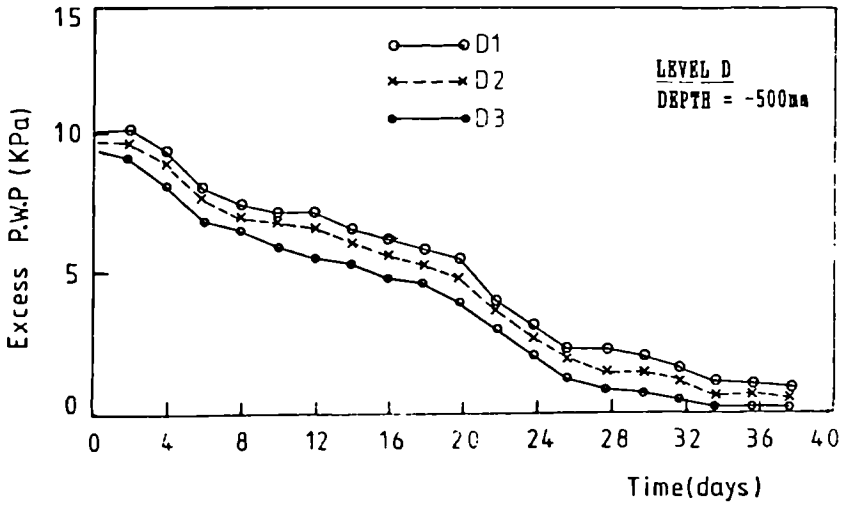

FIG. 5.21 PORE PRESSURE READINGS (RADIAL DIRECTION), 2ND TESTING PROGRAMME (SURCHARGE PRESSURE=30kPa)

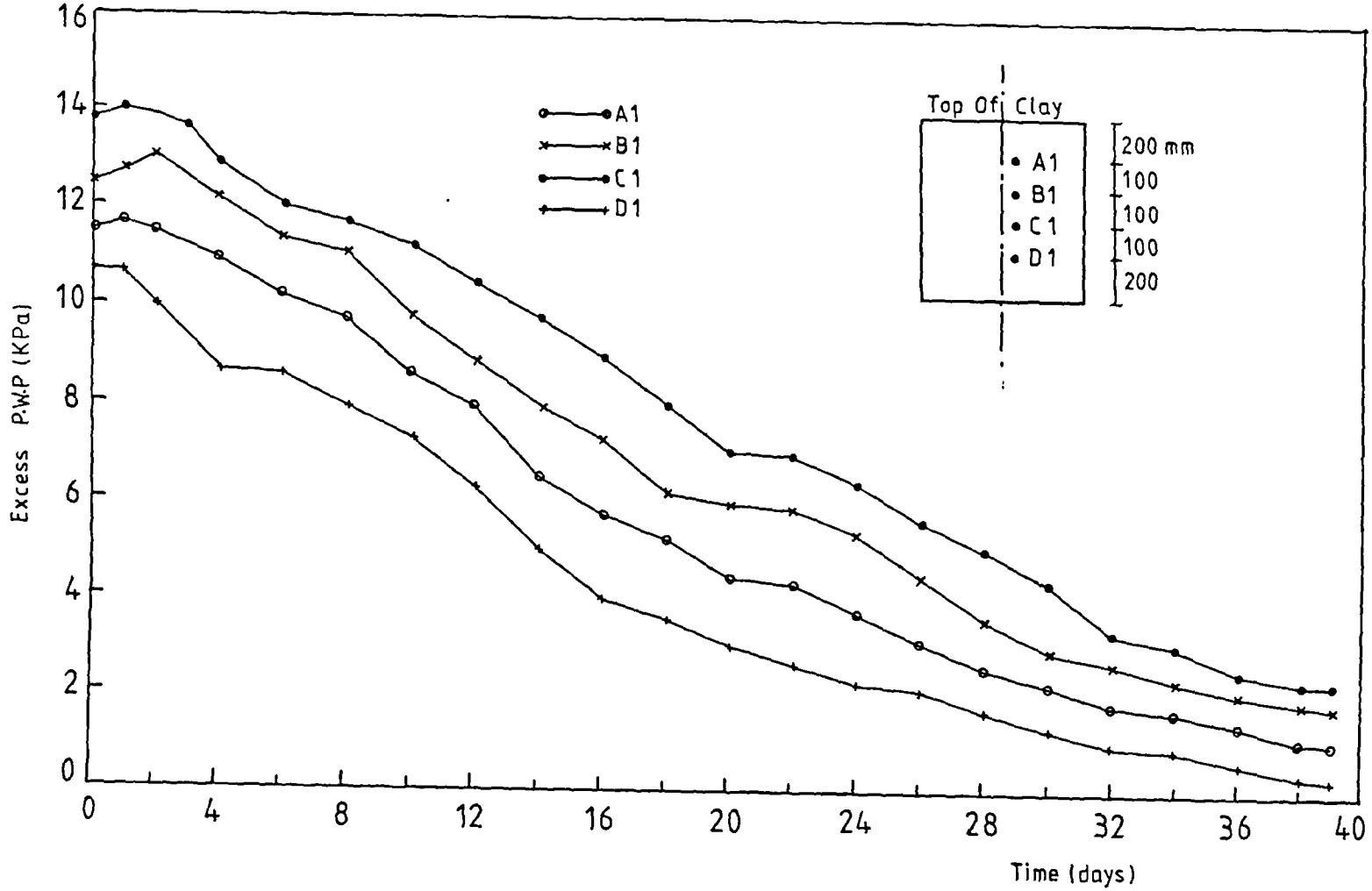

FIG. 5.22 PORE PRESSURE READINGS, 2ND TESTING PROGRAMME, SURCHARGE PRESSURE = 45 kPa

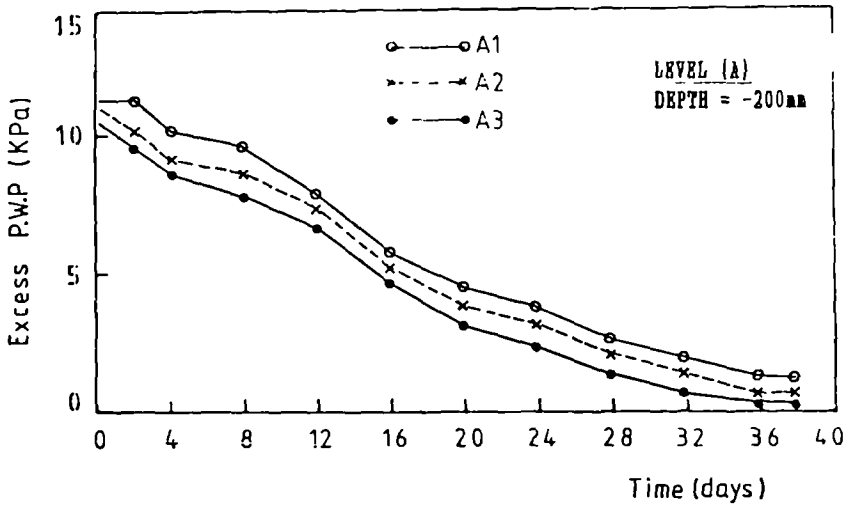

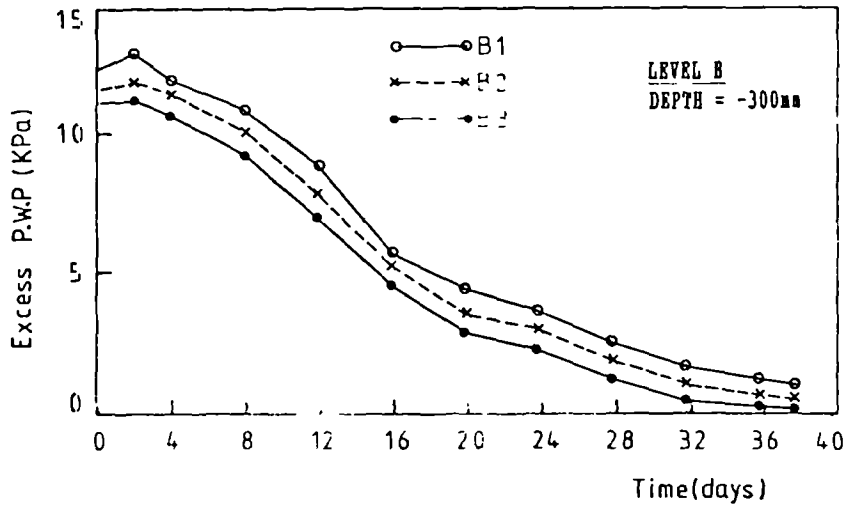

FIG. 5.23 PORE PRESSURE READINGS (RADIAL DIRECTION), 2ND TESTING PROGRAMME (SURCHARGE PRESSURE=45kPa)

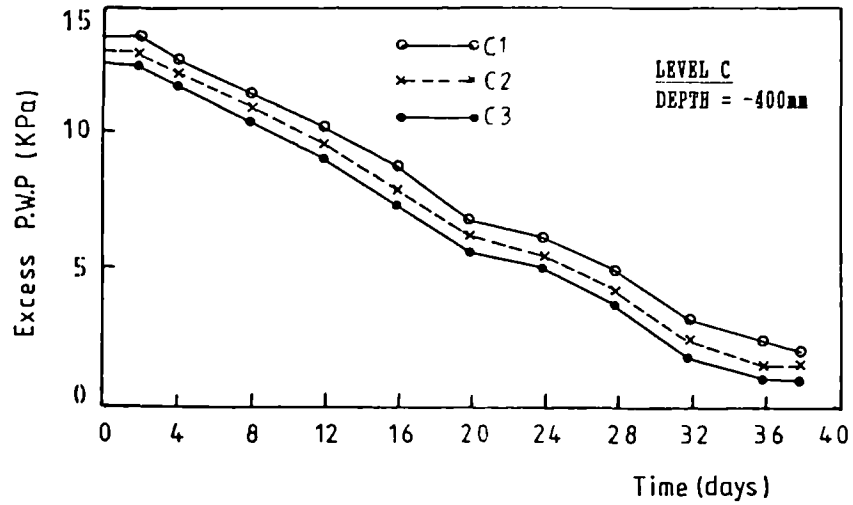

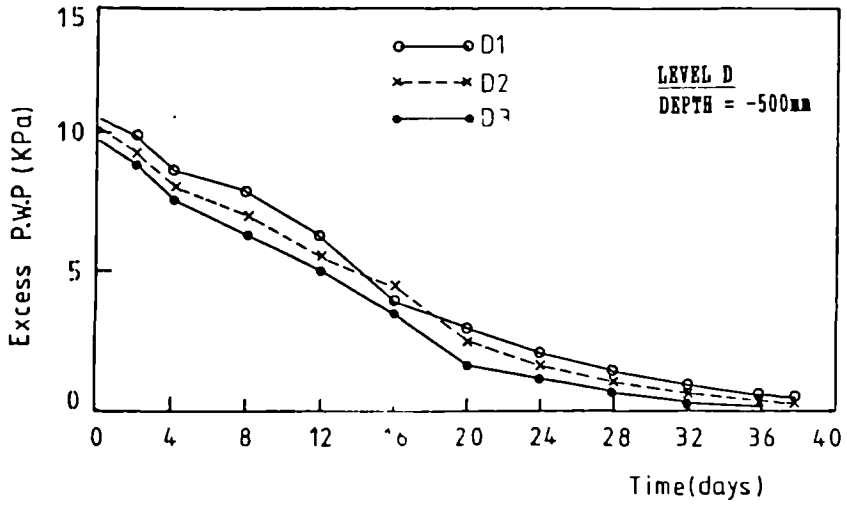

FIG. 5.23 PORE PRESSURE READINGS (RADIAL DIRECTION), 2ND TESTING PROGRAMME (SURCHARGE PRESSURE=45kPa)

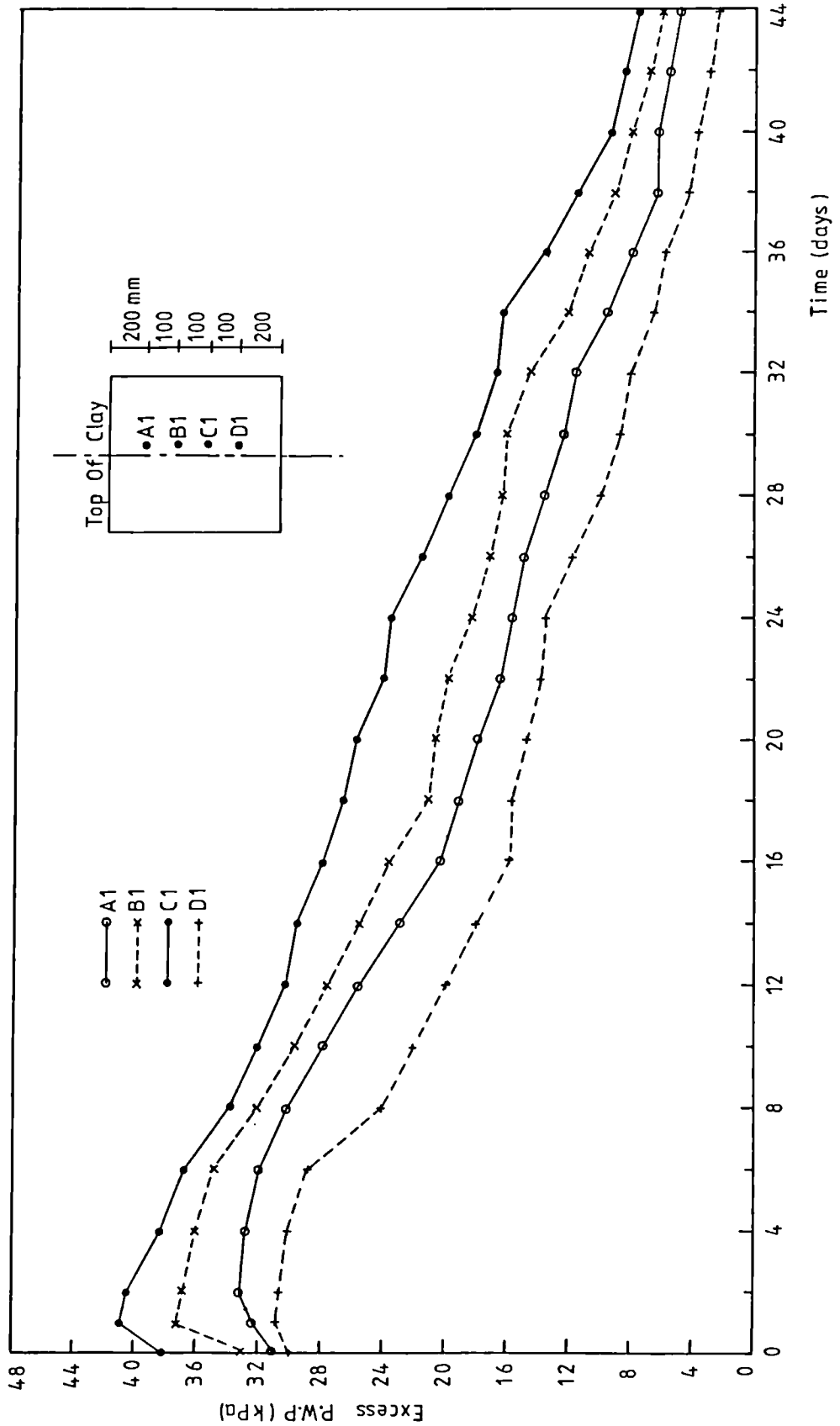

FIG. 5.24 PORE PRESSURE READINGS, 2ND TESTING PROGRAMME, SURCHARGE PRESSURE = 90 kPa

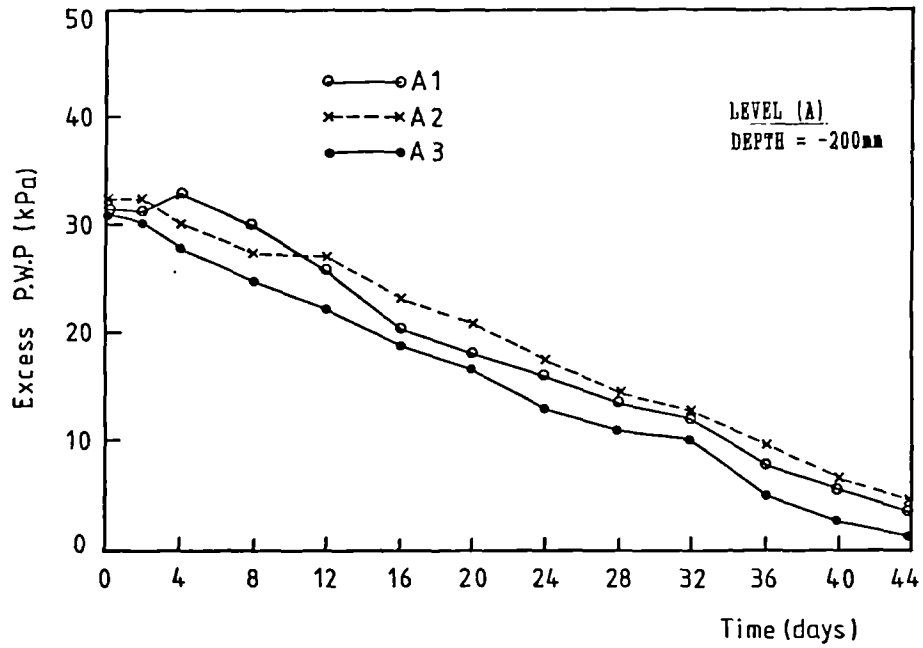

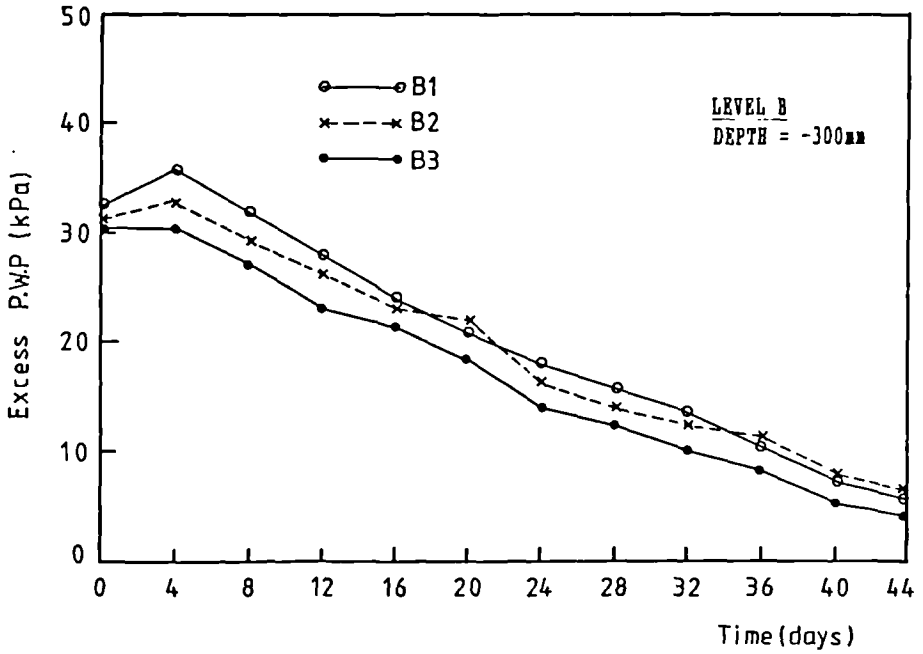

FIG. 5.25 PORE PRESSURE READINGS (RADIAL DIRECTION), 2ND TESTING PROGRAMME (SURCHARGE PRESSURE=90kPa)

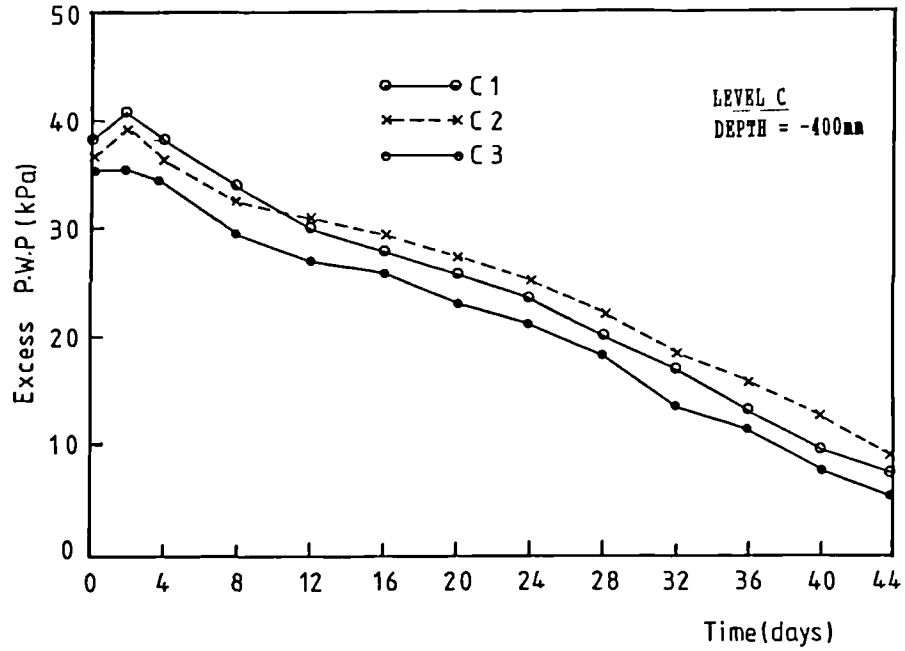

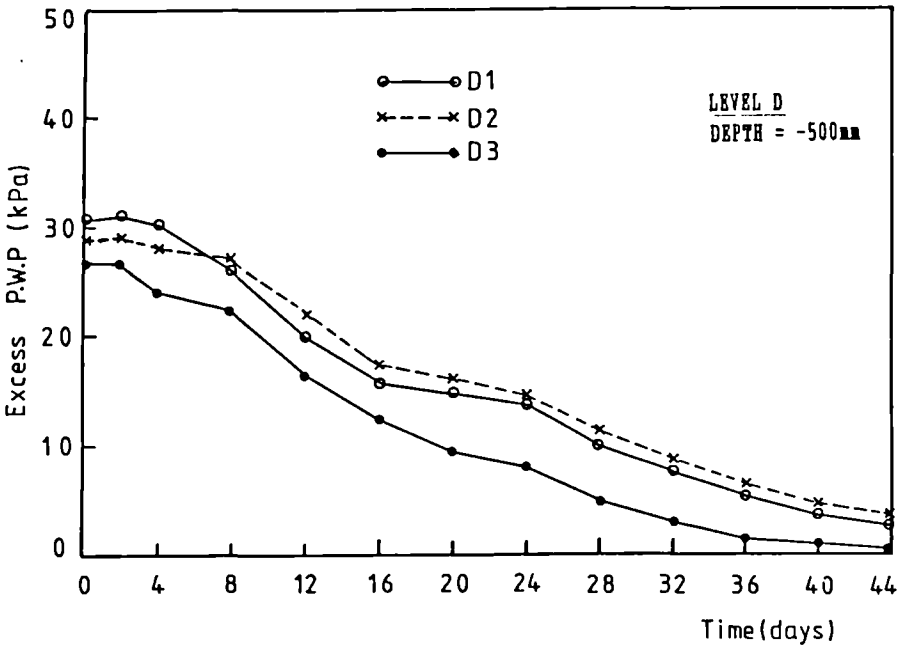

FIG. 5.25 PORE PRESSURE READINGS (RADIAL DIRECTION), 2ND TESTING PROGRAMME (SURCHARGE PRESSURE=90kPa)

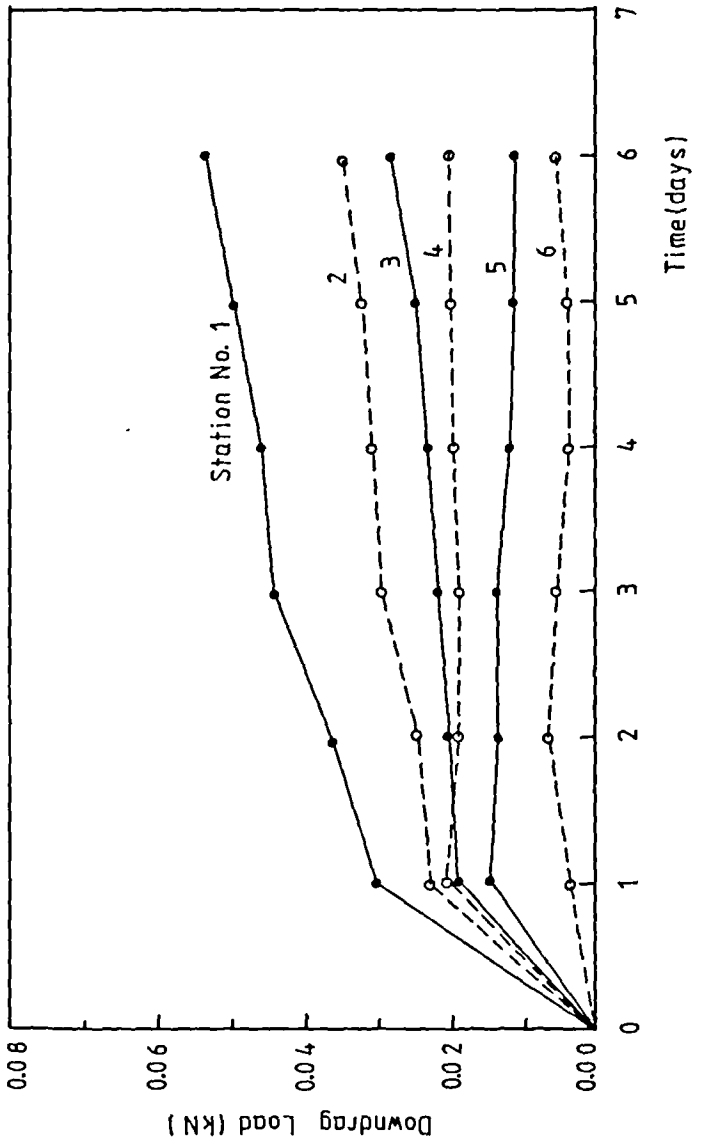

FIG. 5.26 DOWNDRAG BUILD-UP AFTER PILE DRIVING

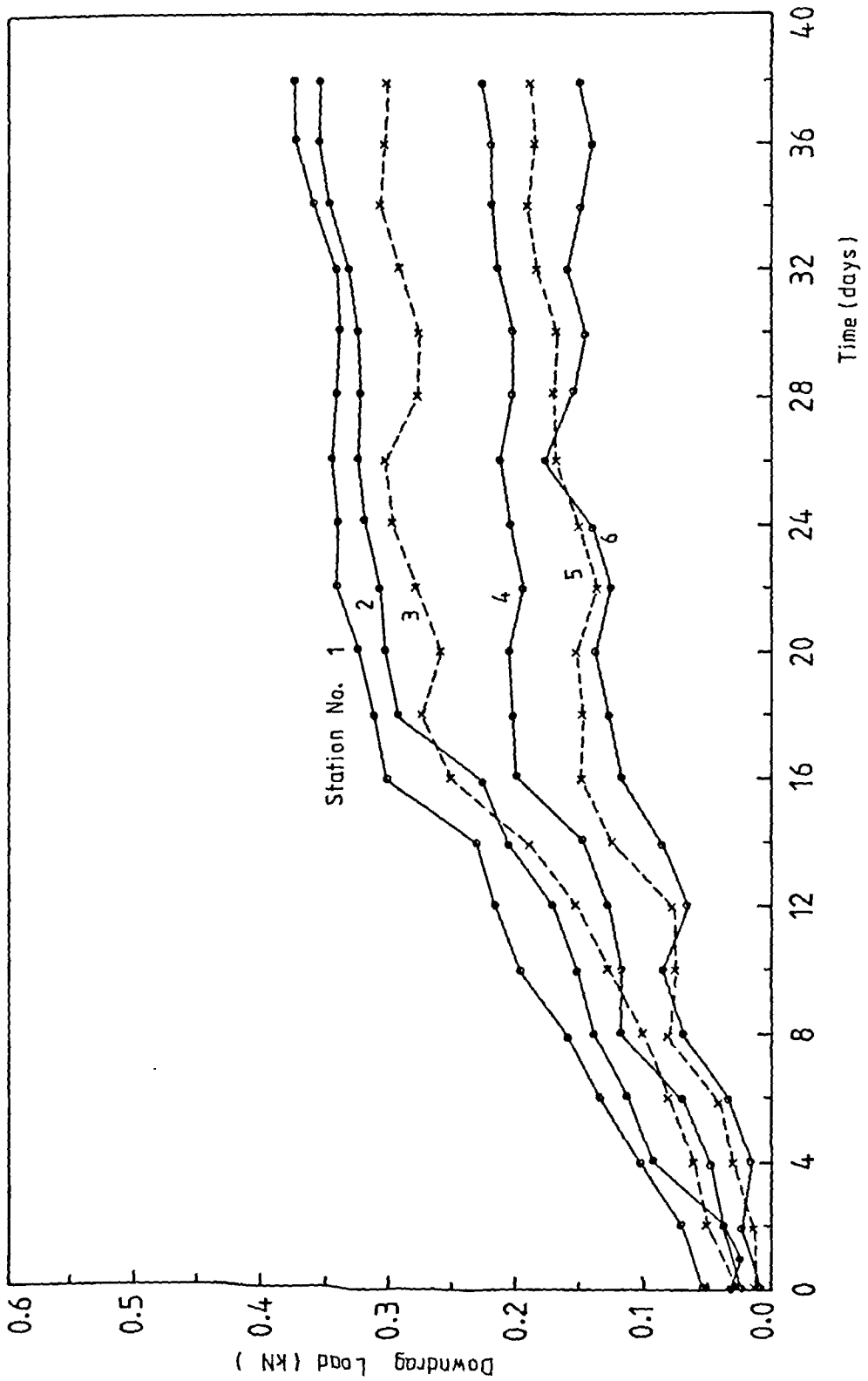

FIG. 5.27 TOTAL DOWNDRAG Vs.TIME, 1ST TESTING PROGRAMME, SURCHARGE PRESSURE = 30 kPa

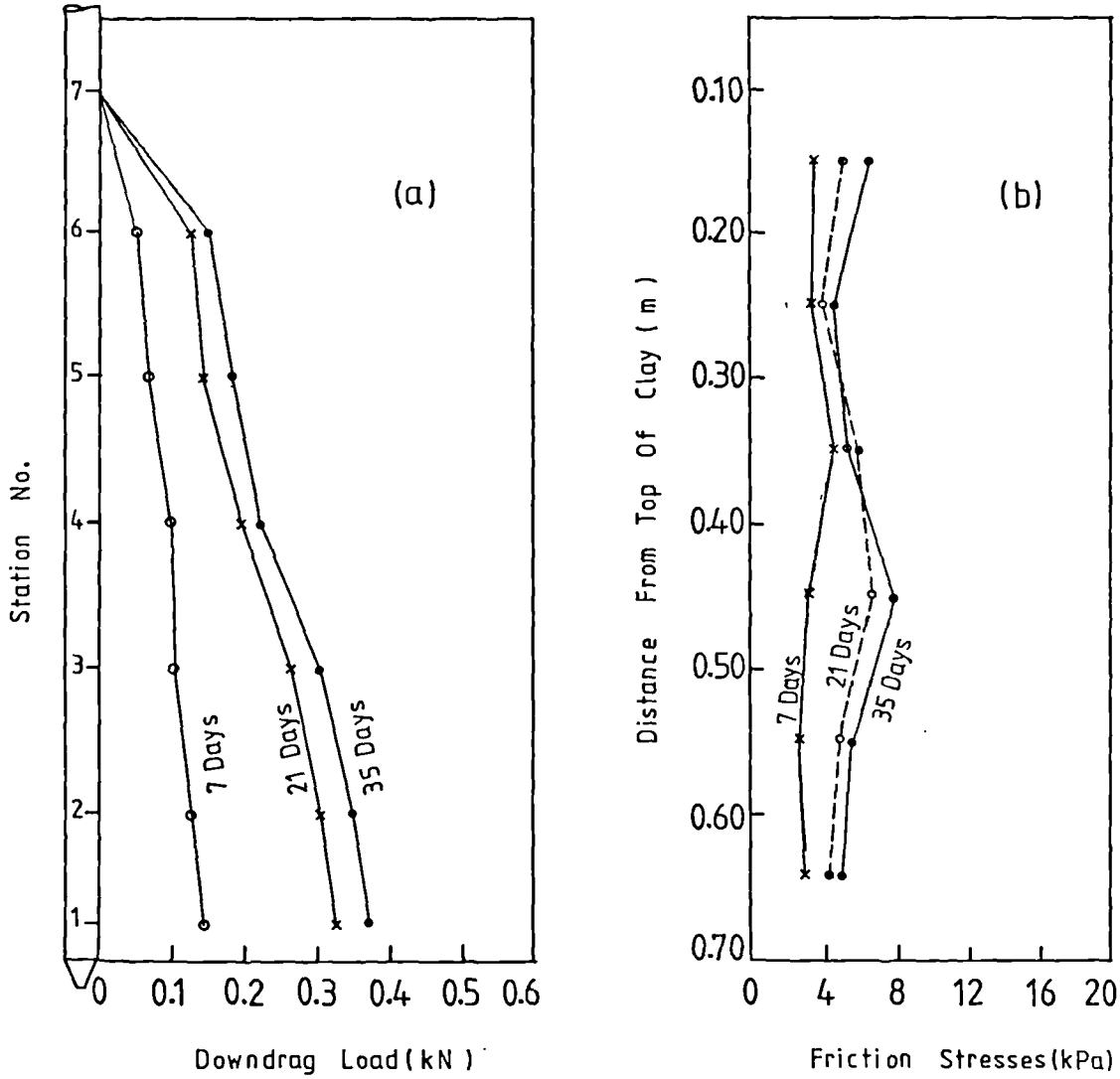

FIG. 5.28 DISTRIBUTION OF DOWNDRAG LOAD AND CONTACT FRICTION STRESS, 1ST TESTING PROGRAMME, SURCHARGE PRESSURE = 30kPa

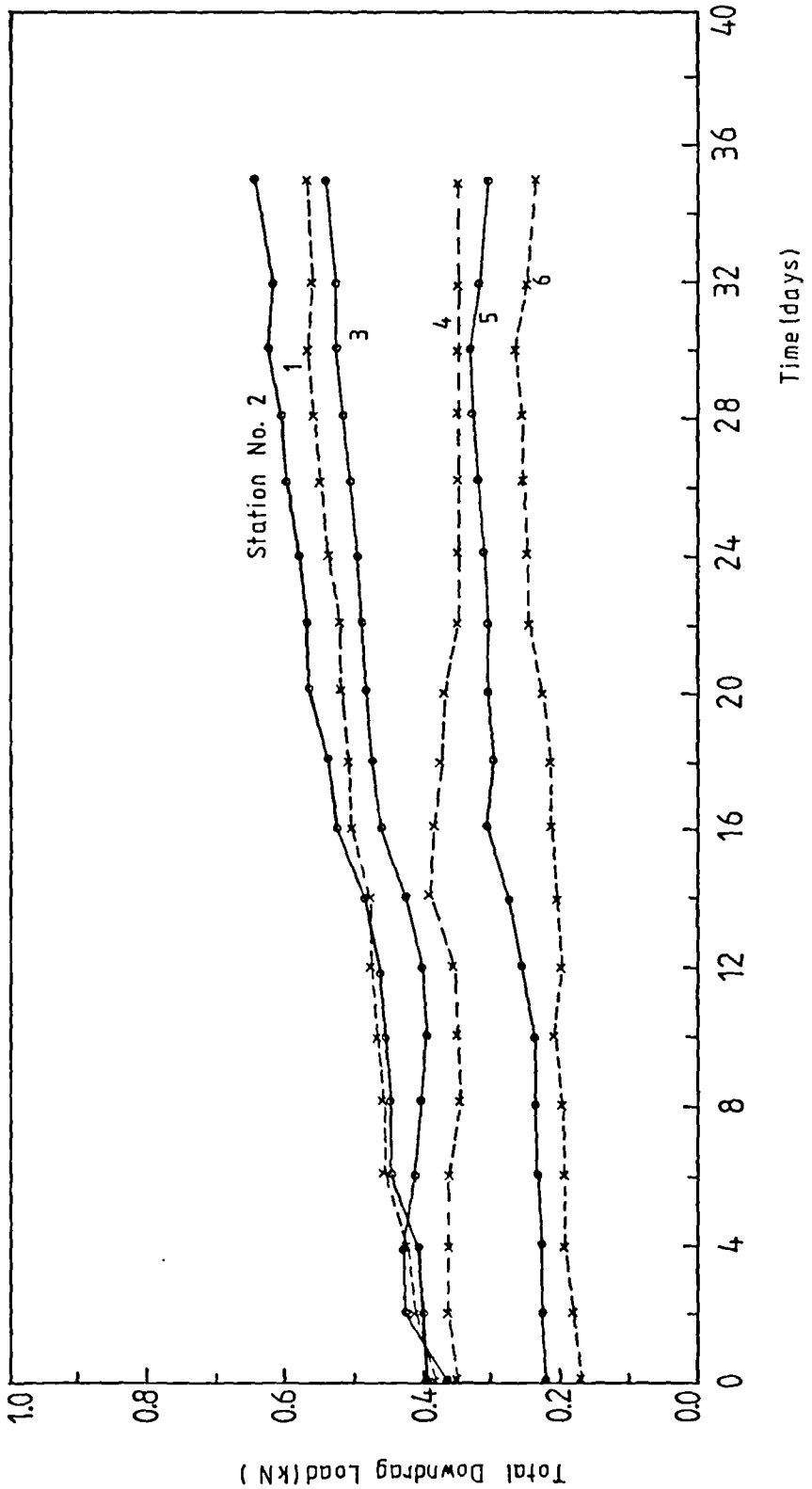

FIG. 5.29 TOTAL DOWNDRAG Vs.TIME, 1ST TESTING PROGRAMME, SURCHARGE PRESSURE = 60 kPa

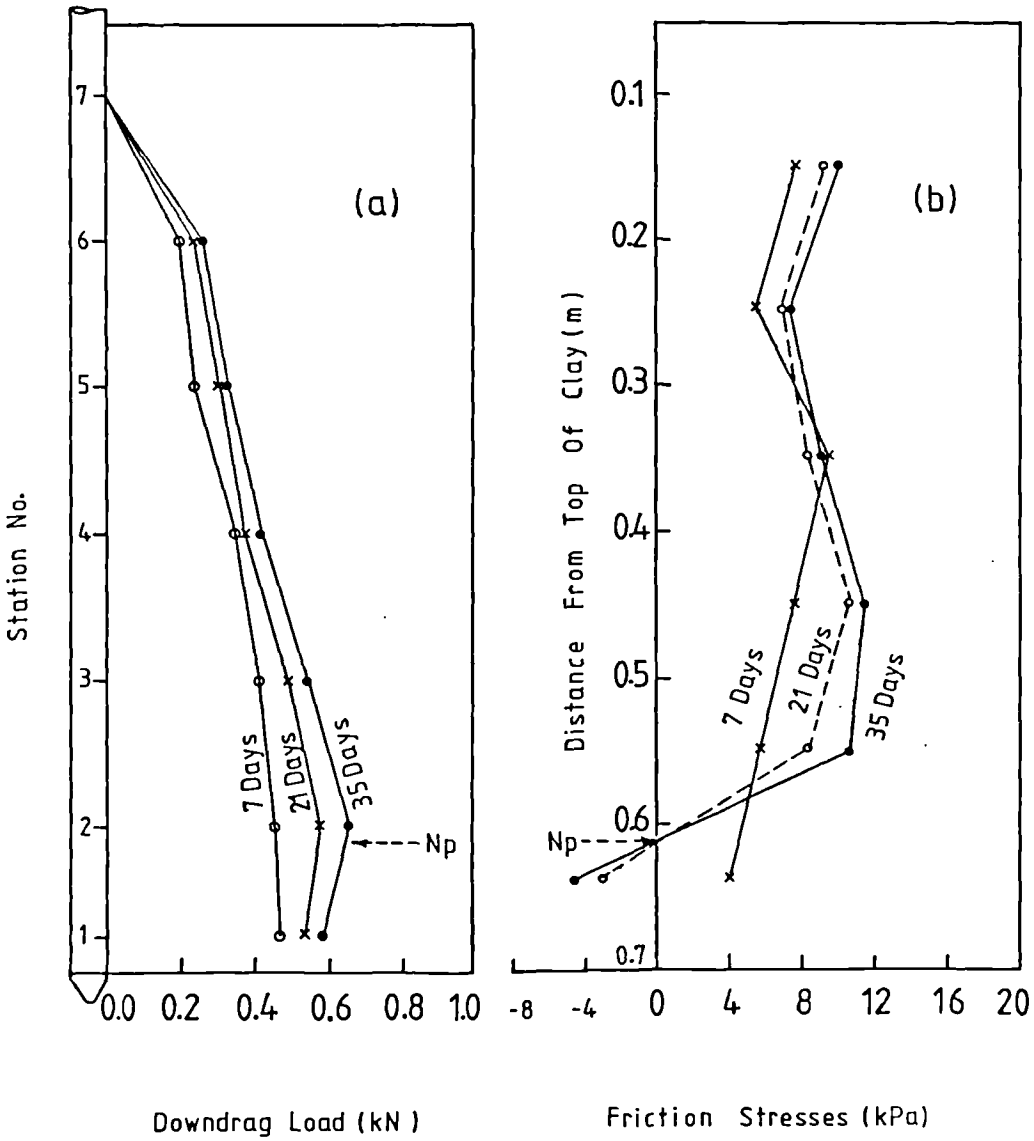

FIG. 5.30 DISTRIBUTION OF DOWNDRAG LOAD AND CONTACT FRICTION STRESS, 1ST TESTING PROGRAMME, SURCHARGE PRESSURE = 60kPa

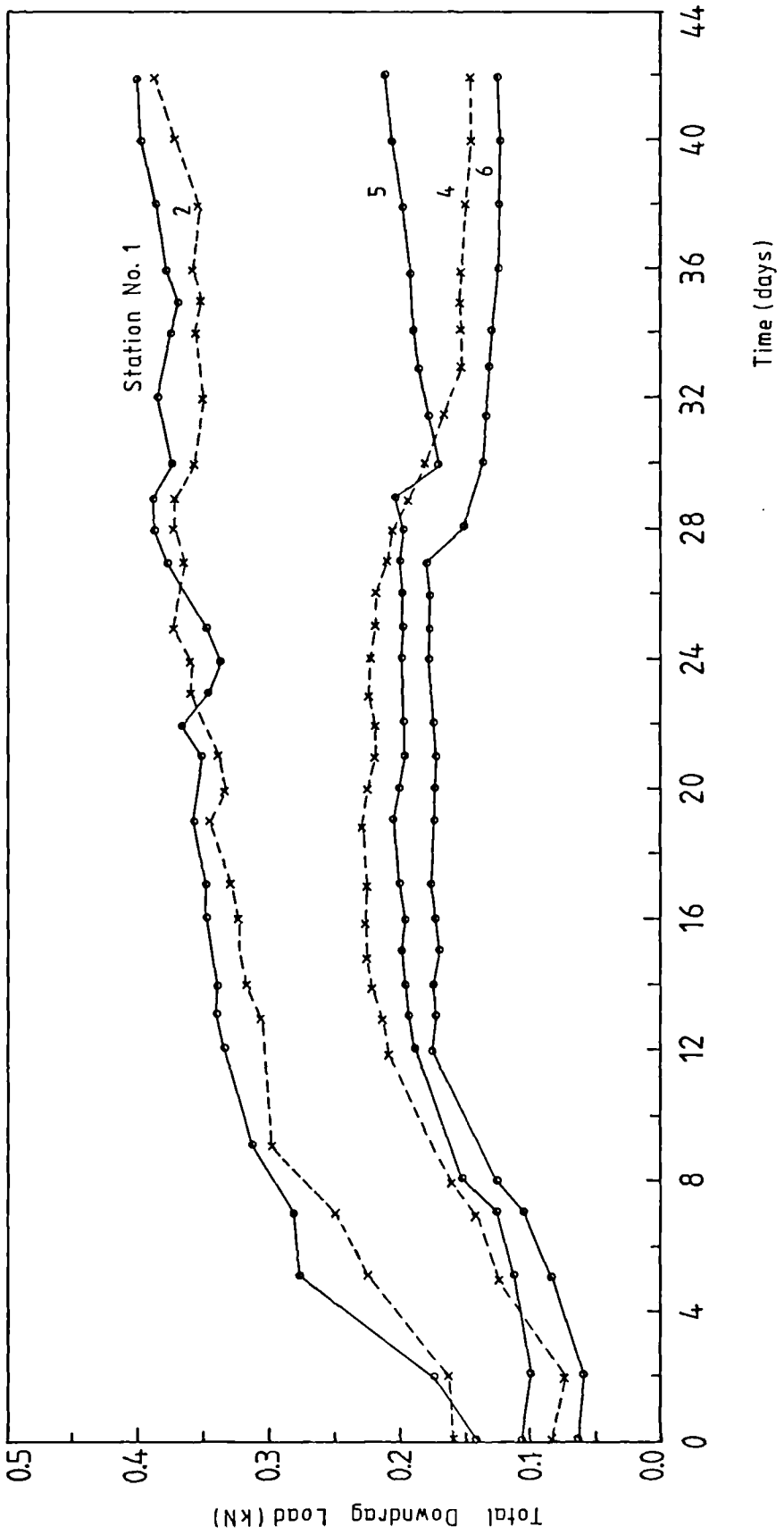

FIG. 5.31 TOTAL DOWNDRAG Vs.TIME, 1ST TESTING PROGRAMME, SURCHARGE PRESSURE = 90 kPa

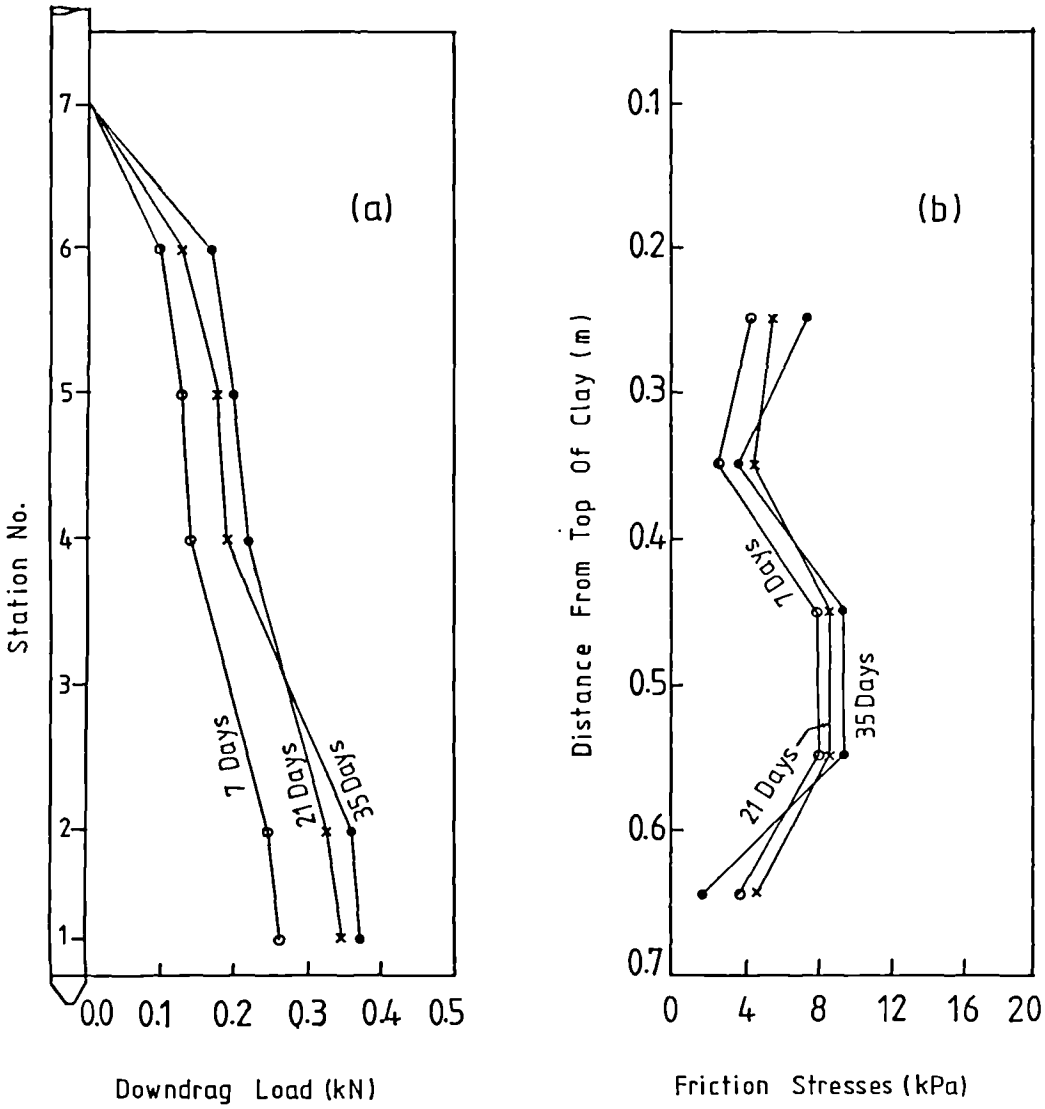

FIG. 5.32 DISTRIBUTION OF DOWNDRAG LOAD AND CONTACT FRICTION STRESS, 1ST TESTING PROGRAMME, SURCHARGE PRESSURE = 90kPa

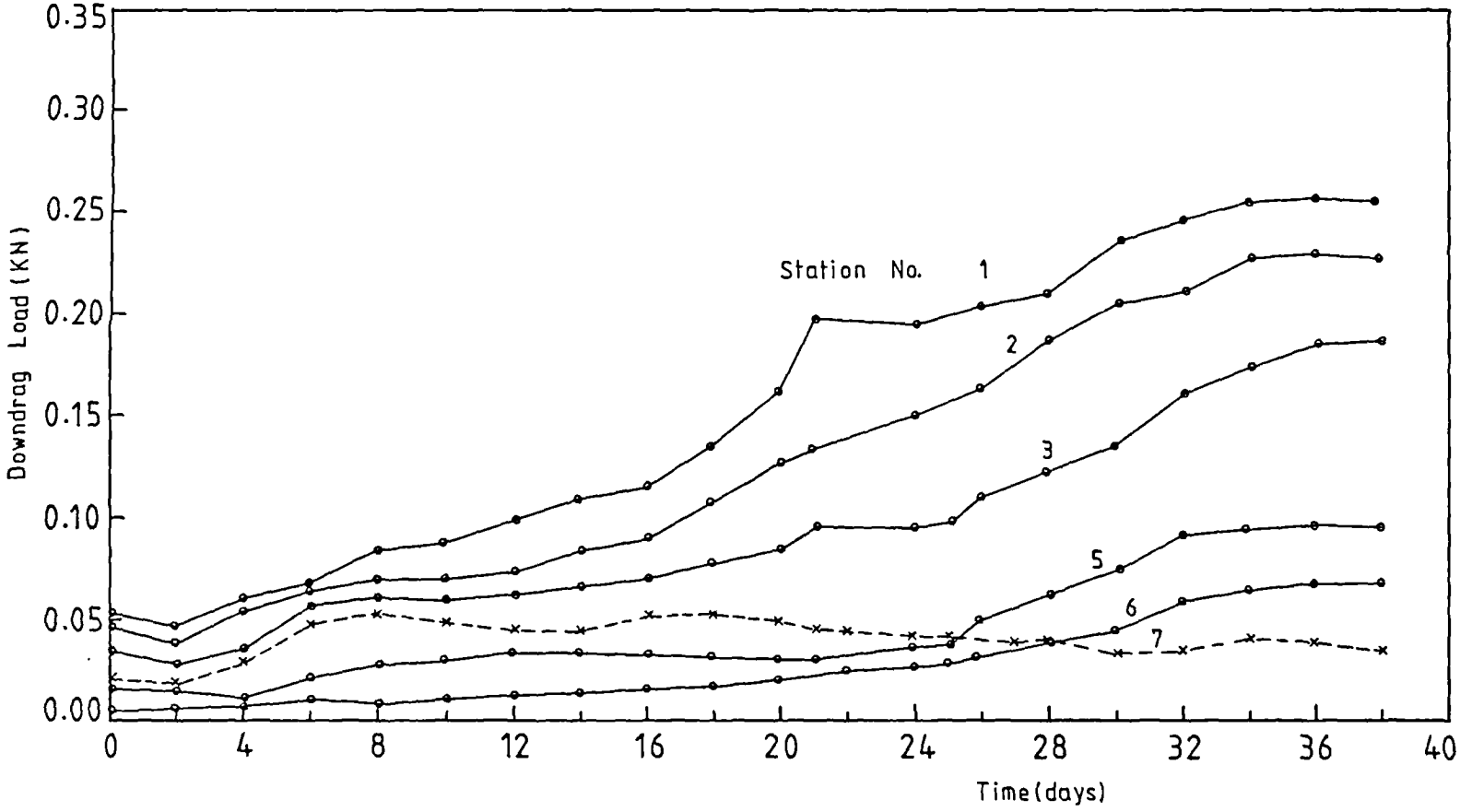

FIG. 5.33 TOTAL DOWNDRAG Vs.TIME, 2ND TESTING PROGRAMME, SURCHARGE PRESSURE = 15 kPa

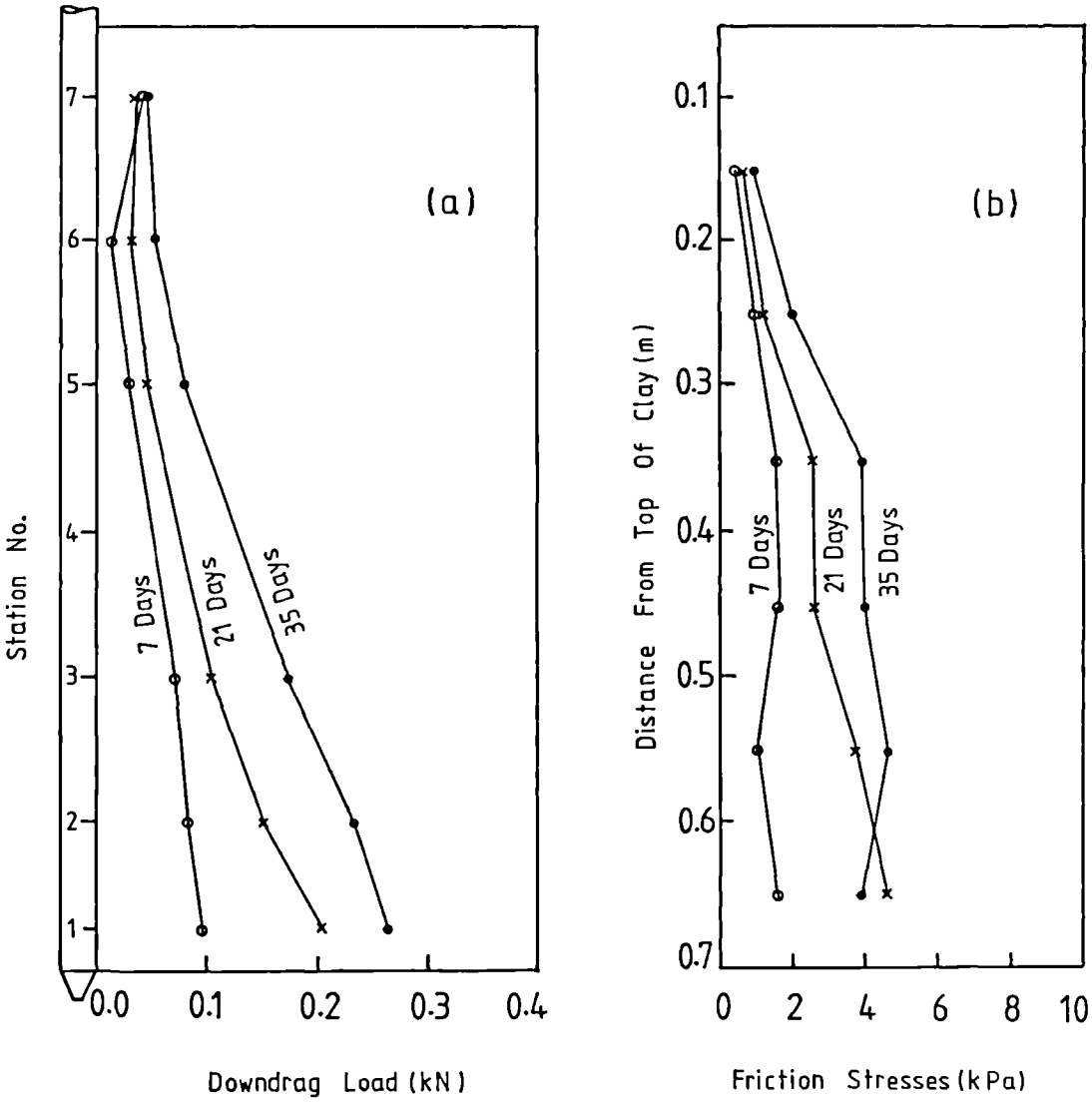

FIG. 5.34 DISTRIBUTION OF DOWNDRAG LOAD AND CONTACT FRICTION STRESS, 2ND TESTING PROGRAMME, SURCHARGE PRESSURE = 15kPa

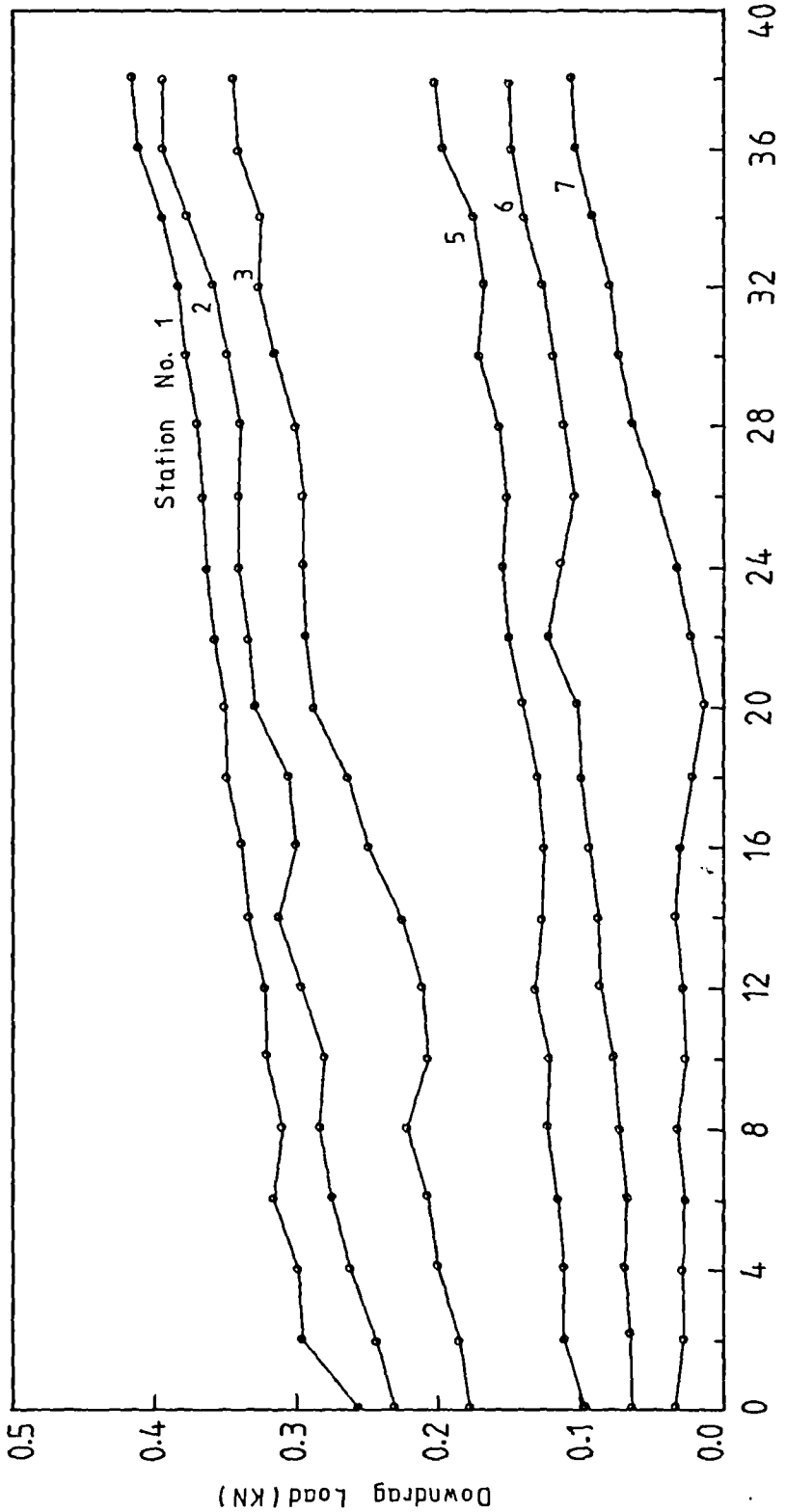

FIG. 5.35 TOTAL DOWNDRAG Vs. TIME, 2ND TESTING PROGRAMME, SURCHARGE PRESSURE = 30 kPa

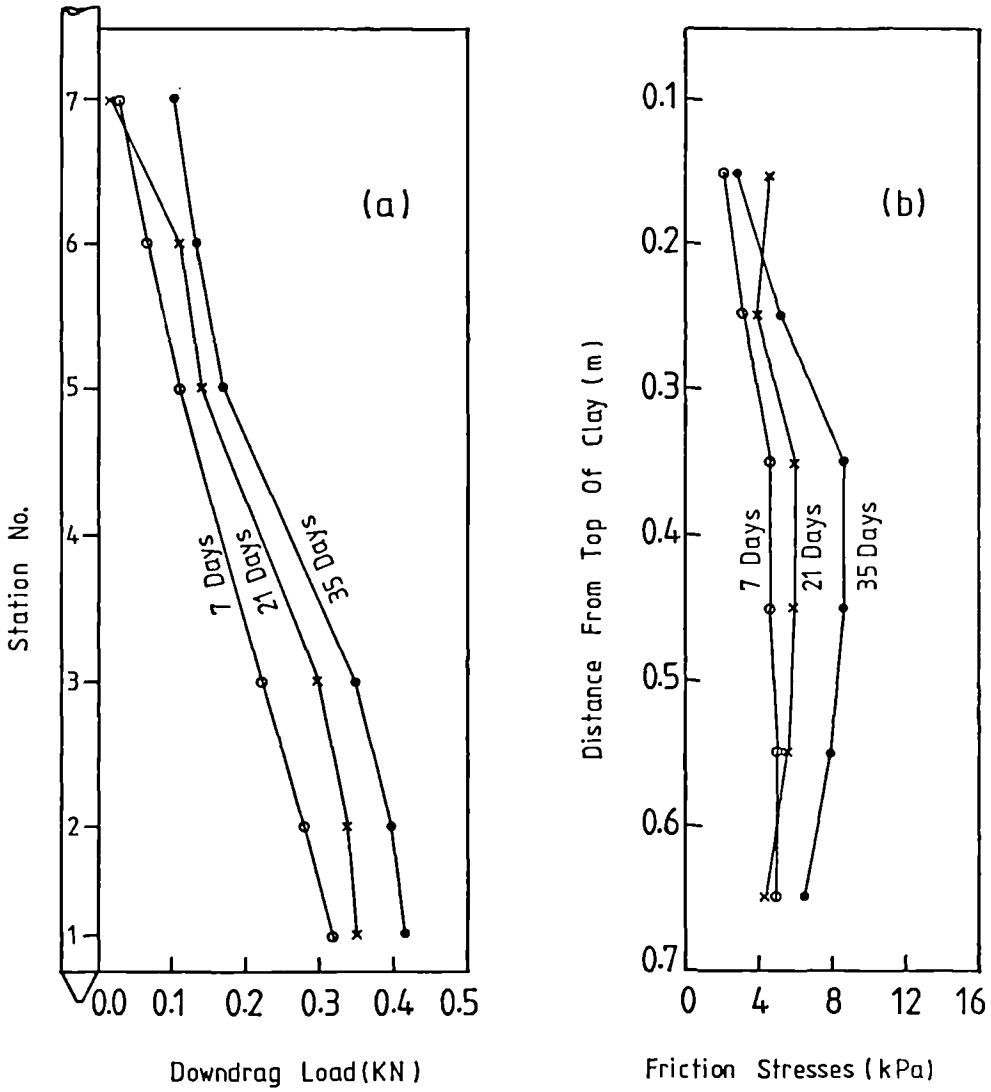

FIG. 5.36 DISTRIBUTION OF DOWNDRAG LOAD AND CONTACT FRICTION STRESS, 2ND TESTING PROGRAMME, SURCHARGE PRESSURE = 30kPa

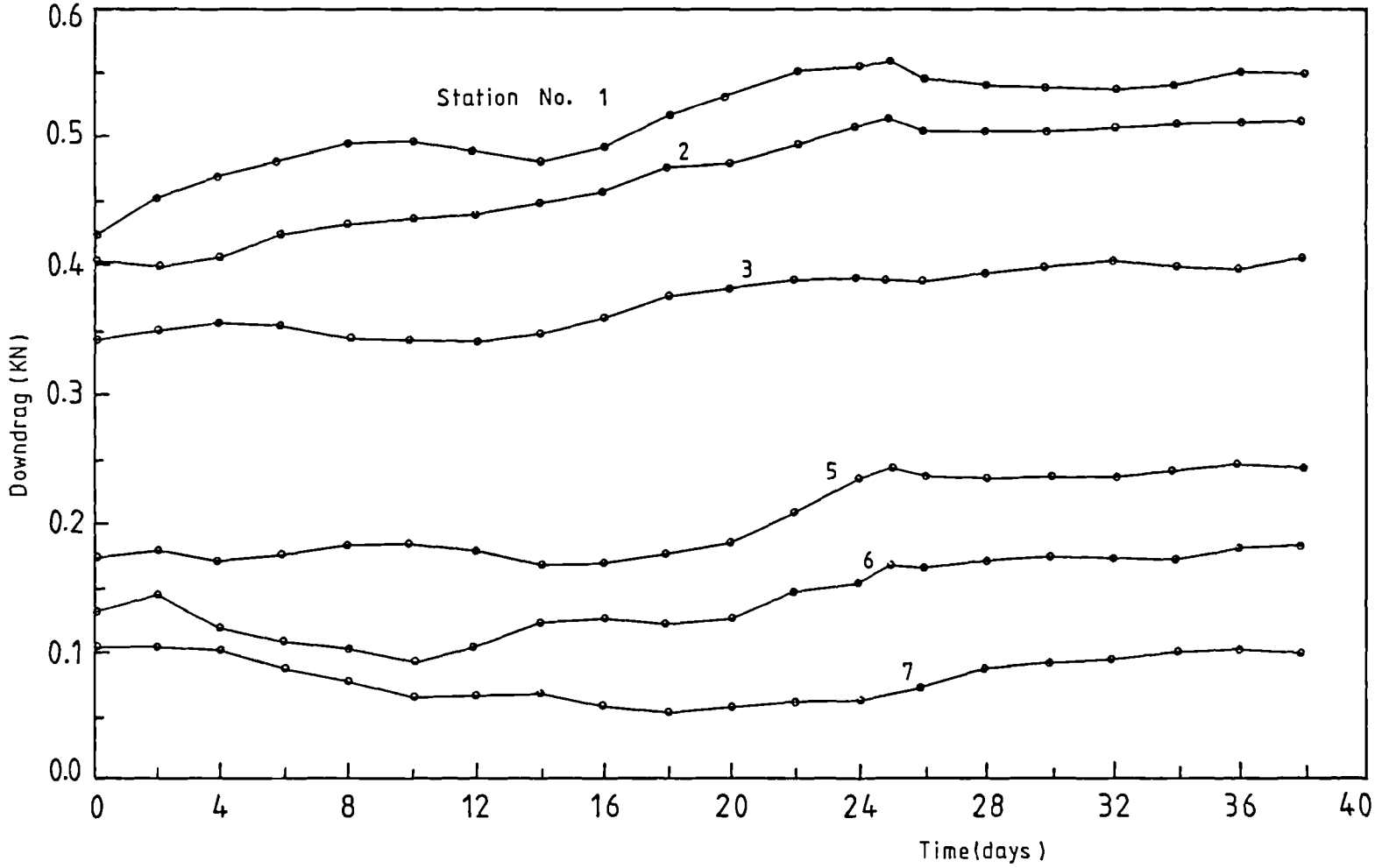

FIG. 5.37 TOTAL DOWNDRAG Vs.TIME, 2ND TESTING PROGRAMME, SURCHARGE PRESSURE = 45 kPa

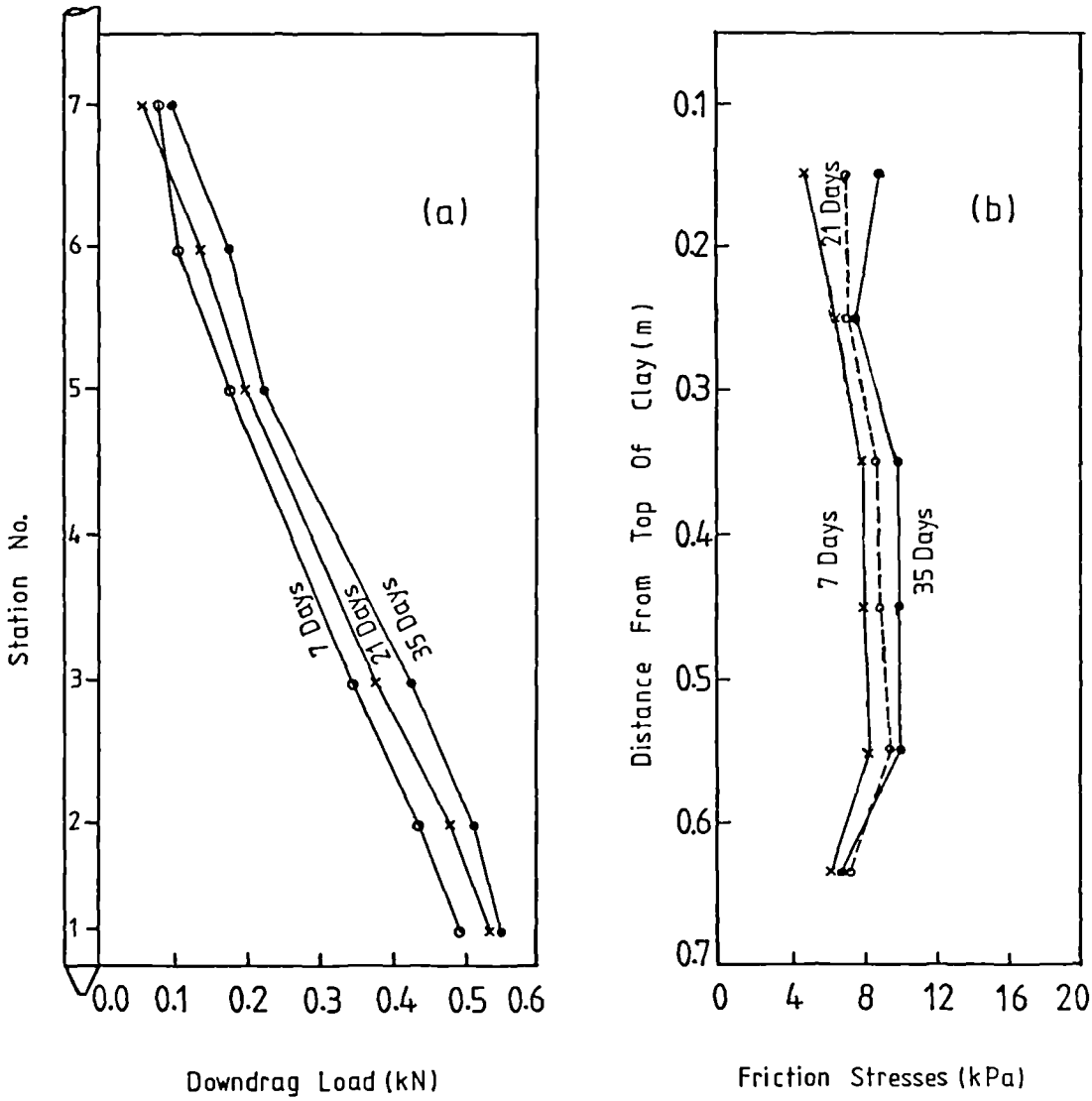

FIG. 5.38 DISTRIBUTION OF DOWNDRAG LOAD AND CONTACT FRICTION STRESS, 2ND TESTING PROGRAMME, SURCHARGE PRESSURE = 45kPa

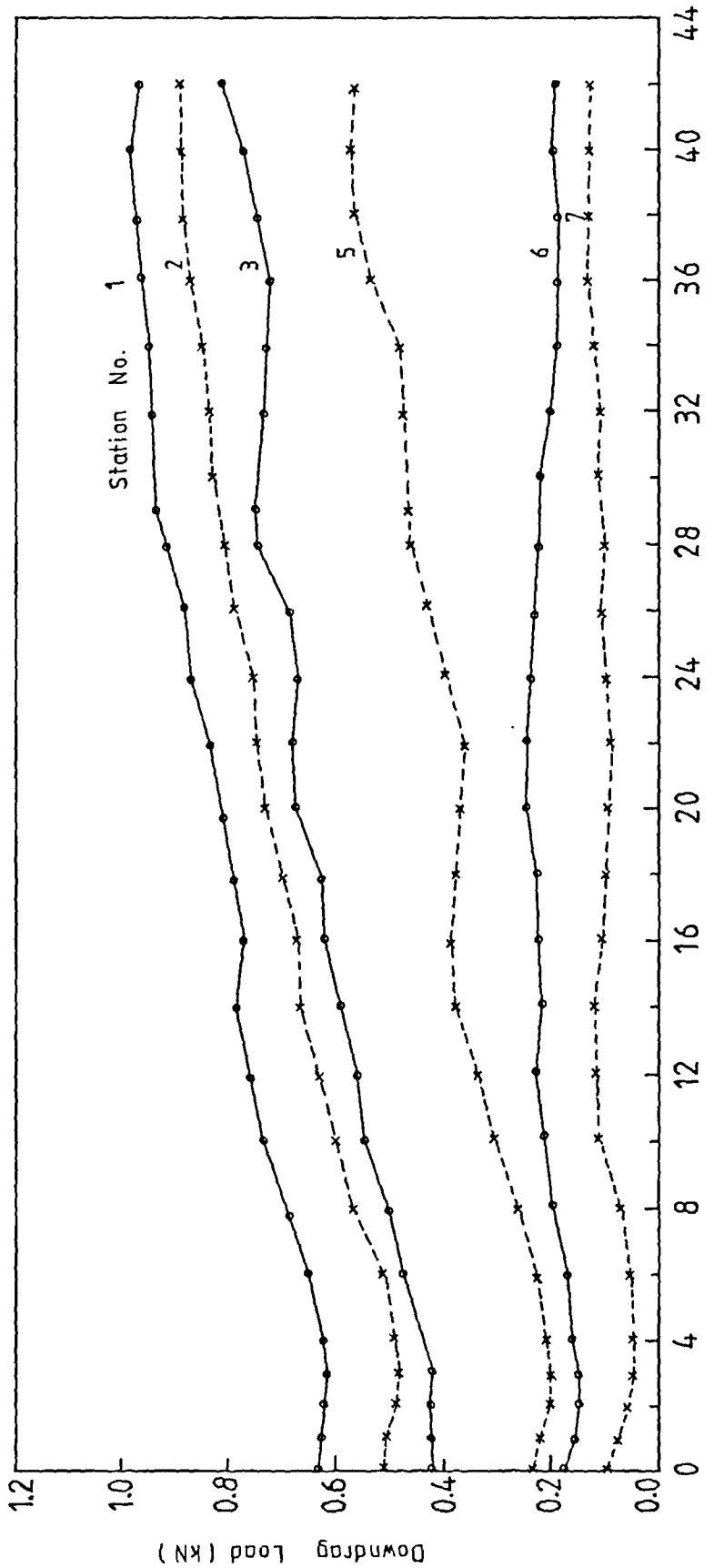

FIG. 5.39 TOTAL DOWNDRAG Vs. TIME, 2ND TESTING PROGRAMME, SURCHARGE PRESSURE = 90 kPa

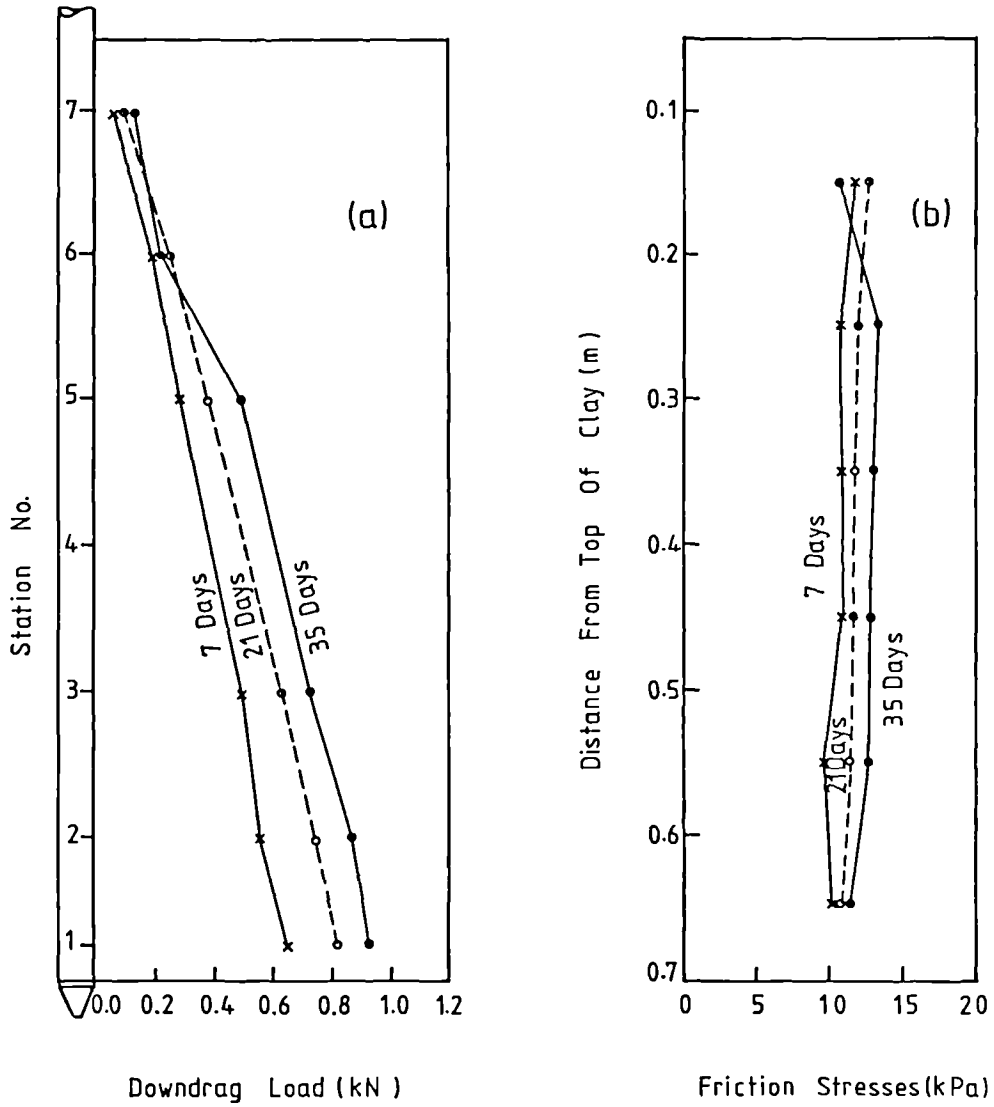

FIG. 5.40 DISTRIBUTION OF DOWNDRAG LOAD AND CONTACT FRICTION STRESS, 2ND TESTING PROGRAMME, SURCHARGE PRESSURE = 90kPa

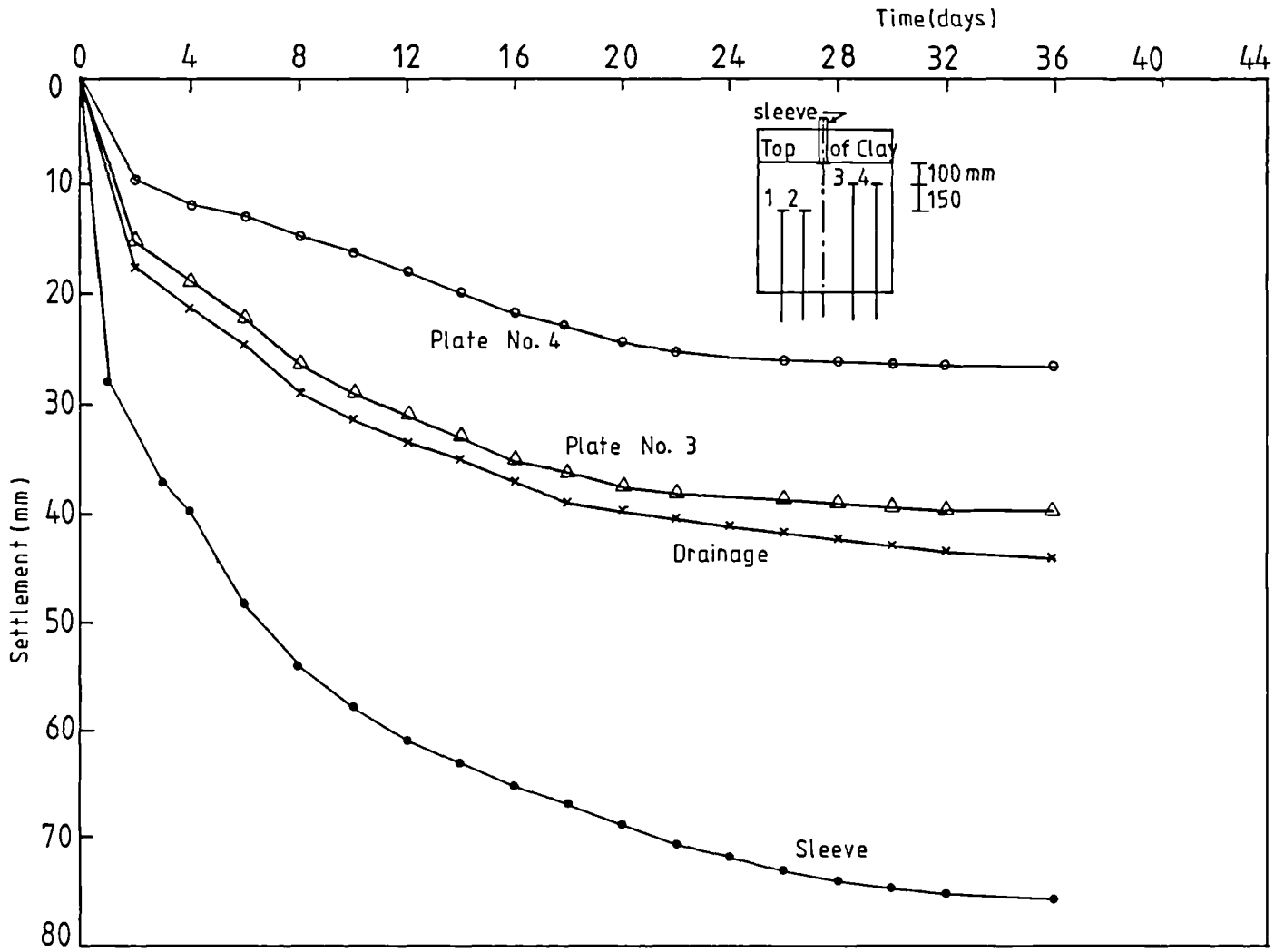

FIG. 5.41 SETTLEMENT READINGS, 1ST TESTING PROGRAMME, SURCHARGE PRESSURE = 30 kPa

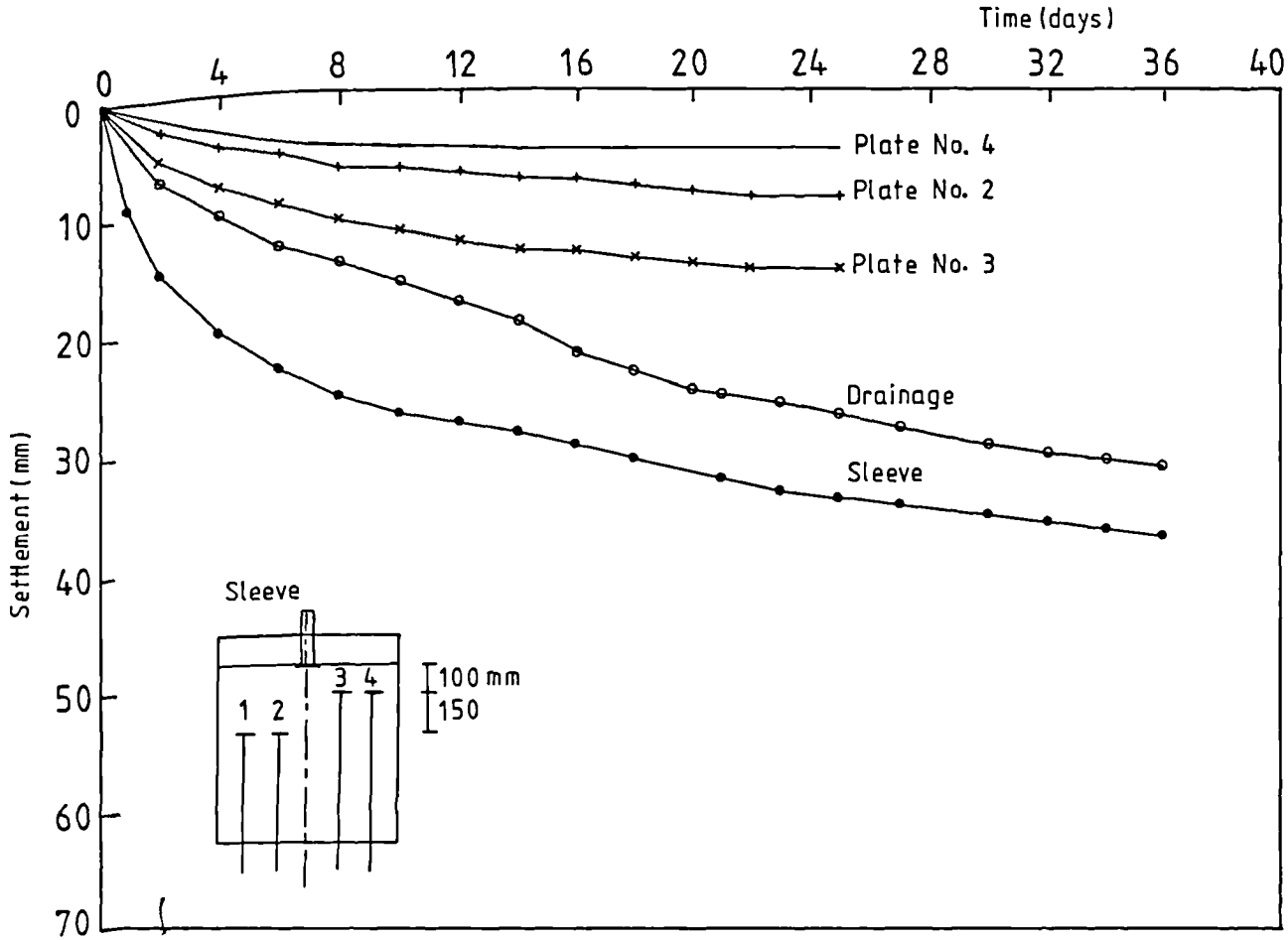

FIG. 5.42 SETTLEMENT READINGS, 1ST TESTING PROGRAMME, SURCHARGE PRESSURE = 60 kPa

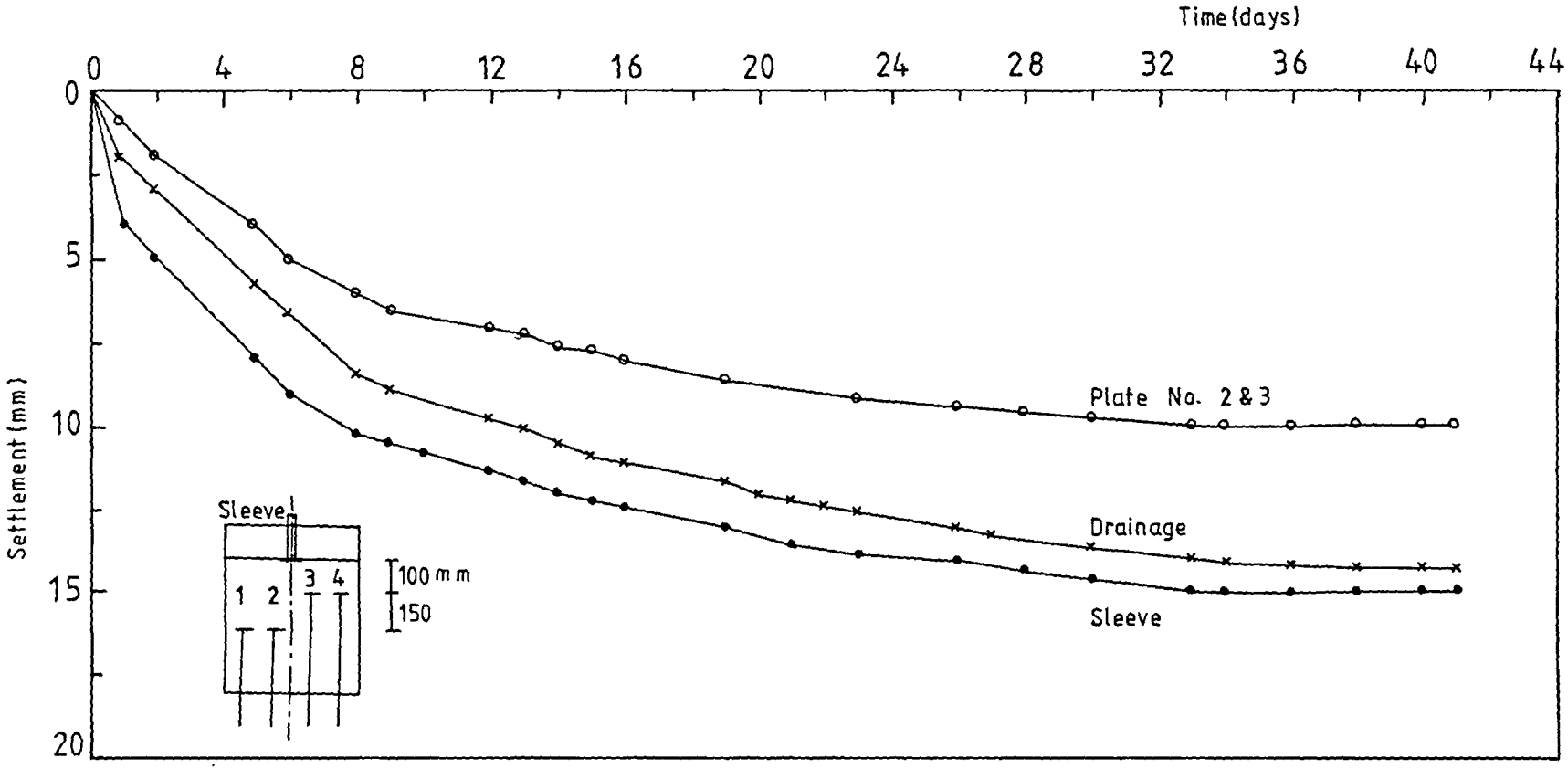

FIG. 5.43 SETTLEMENT READINGS, 1ST TESTING PROGRAMME, SURCHARGE PRESSURE = 90 kPa

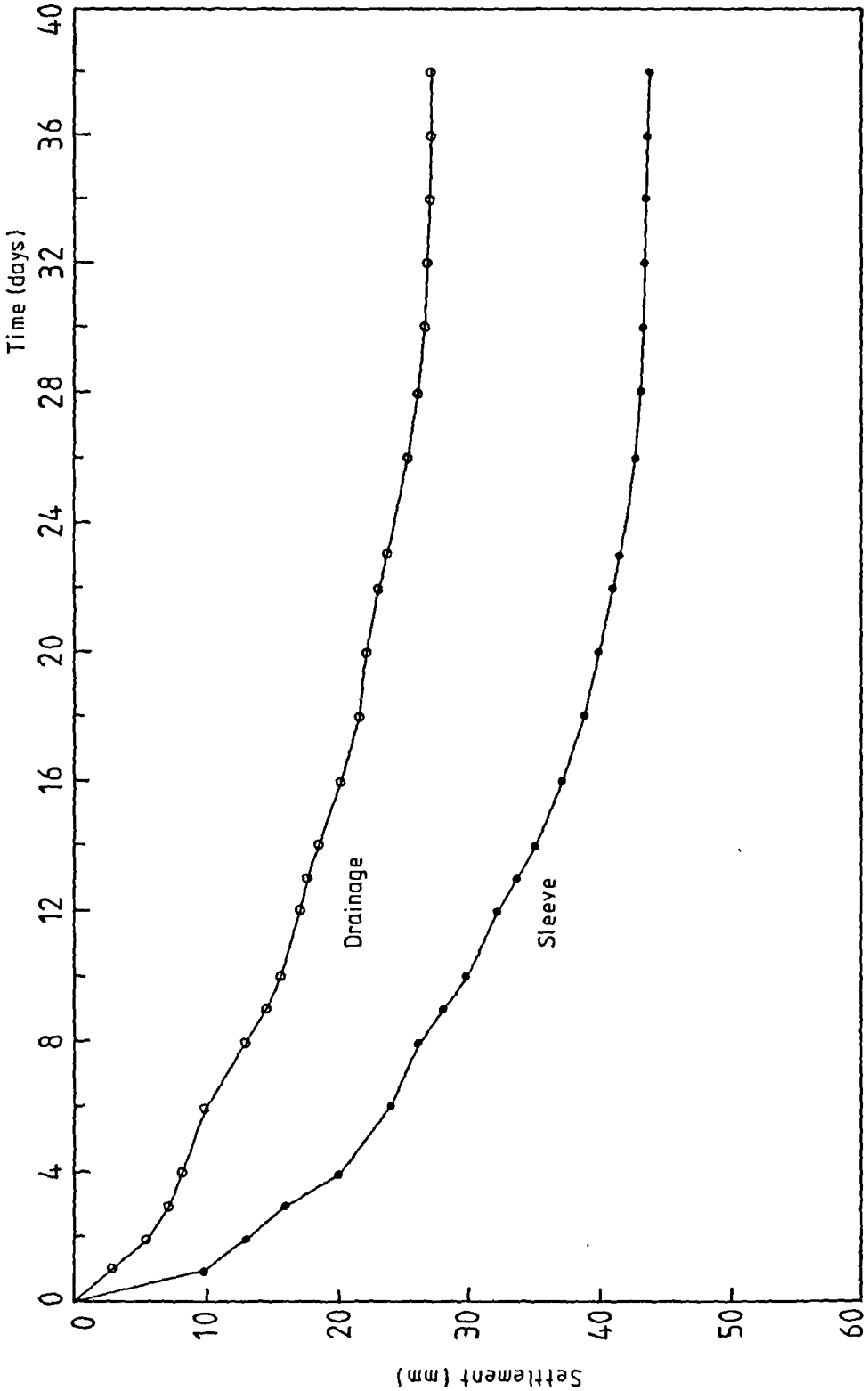

FIG. 5.44 SETTLEMENT READINGS, 2ND TESTING PROGRAMME, SURCHARGE PRESSURE = 15 kPa

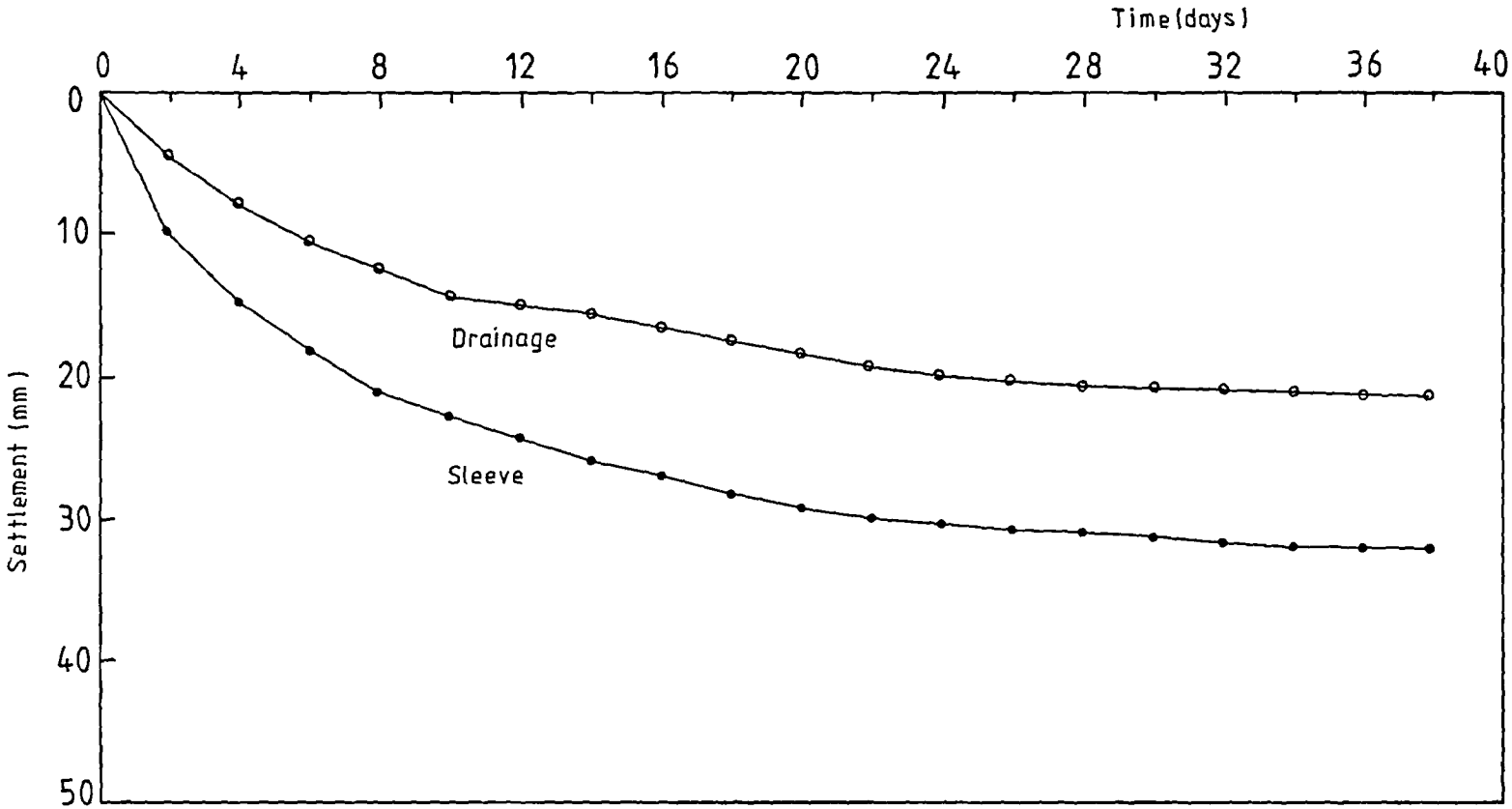

FIG. 5.45 SETTLEMENT READINGS, 2ND TESTING PROGRAMME, SURCHARGE PRESSURE = 30 kPa

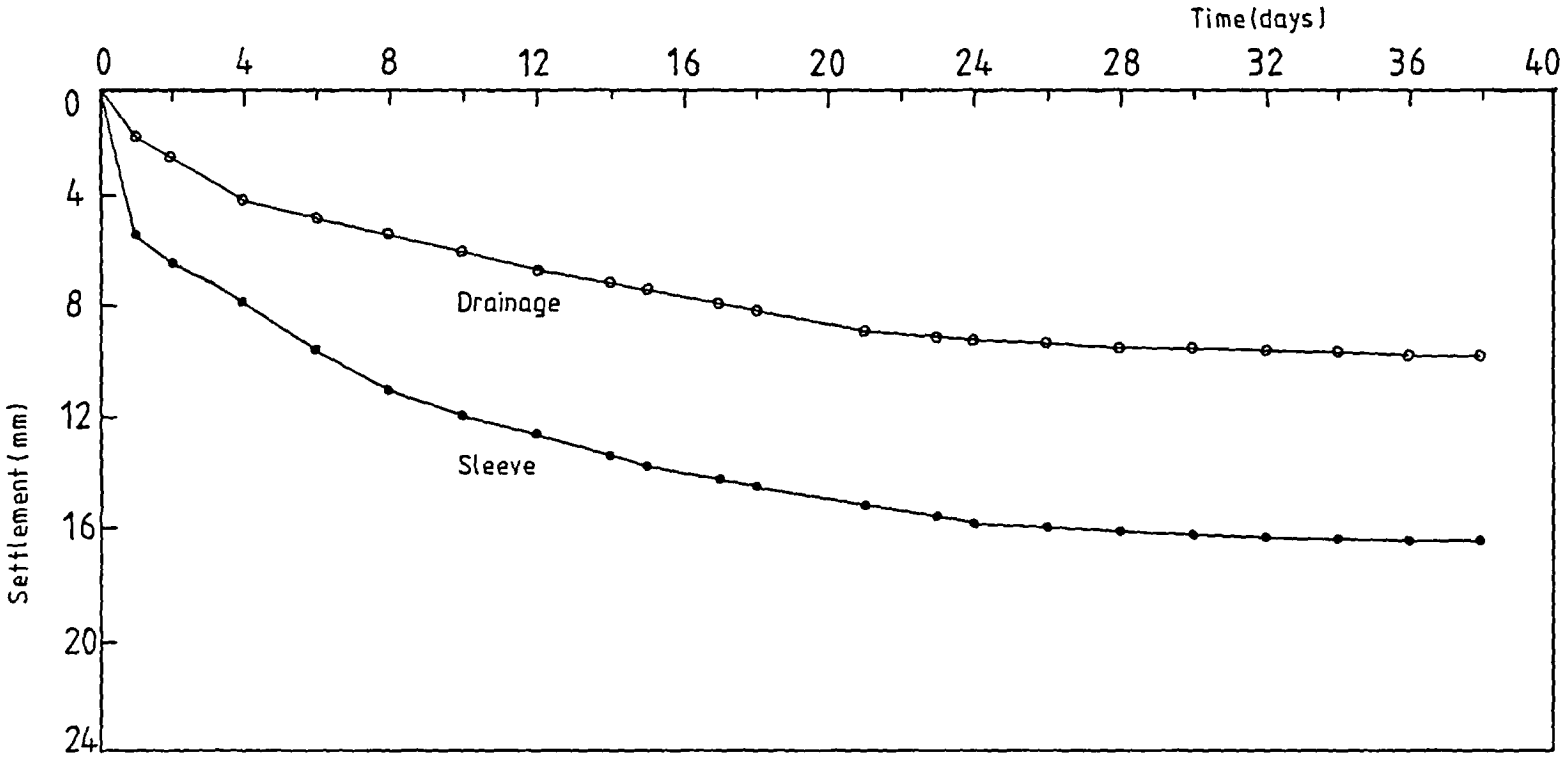

FIG. 5.46 SETTLEMENT READINGS, 2ND TESTING PROGRAMME, SURCHARGE PRESSURE = 45 kPa

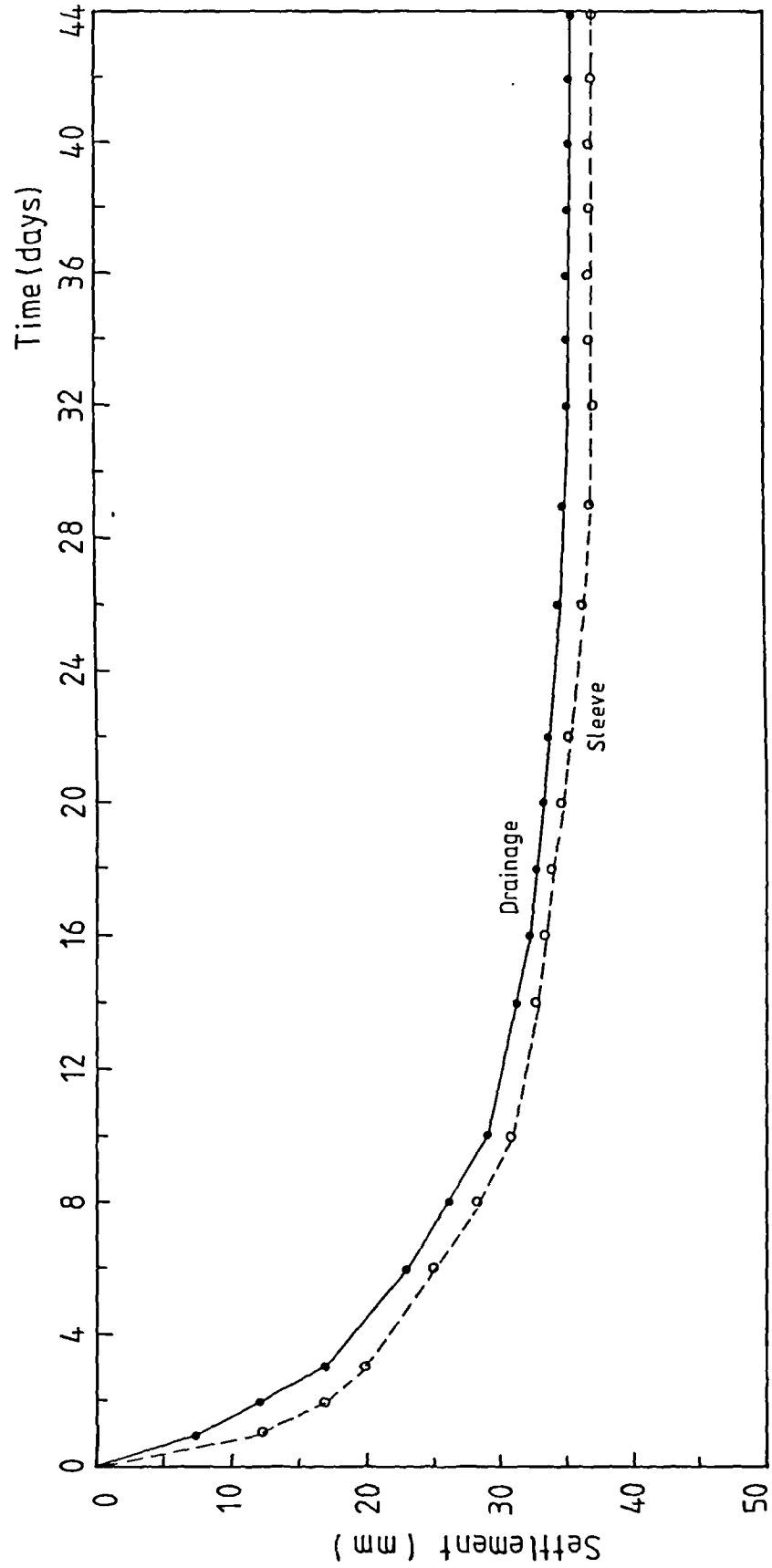

FIG. 5.47 SETTLEMENT READINGS, 2ND TESTING PROGRAMME, SURCHARGE PRESSURE = 90 kPa

Testing Programme	Event	Start of event	End of event	Duration (Days)
1st testing programme	Filling the tank with soil	12/3/87	21/4/87	40
	Pushing the pile in place	21/4/87	27/4/87	6
	Loading Stages			
	0-30 kPa	27/4/87	4/6/87	38
	30-60 kPa	4/6/87	9/7/87	45
	Intermission (Bag Repair)	9/7/87	24/9/87	77
	60-90 kPa	24/9/87	5/11/87	42
2nd testing programme	Filling the tank with soil	11/12/87	20/1/88	40
	Pushing the pile in place	20/1/88	26/1/88	6
	Loading Stages			
	0-15 kPa	26/1/88	3/3/88	36
	15-30 kPa	3/3/88	10/4/88	38
	30-45 kPa	10/4/88	19/5/88	39
	45-90 kPa	19/5/88	2/7/88	44

TABLE 5.1 TIME SCHEDULE FOR TESTING PROGRAMMES

Sample Position *	Moisture Content Values			
	At Start of Test	At End of 2nd Loading Stage (60 kPa)	After Completion of 1st testing progm.	After Completion of 2nd testing progm.
M1	54.6	40.7	38.6	37.4
M2	54.4	41.5	39.2	37.7
M3	54.5	39.8	38.1	37.0
K1	52.4	43.2	40.2	38.2
K2	53.3	42.3	41.5	38.6
K3	54.6	40.8	39.2	37.7
I1	55.6	43.0	41.2	39.5
I2	55.5	41.6	41.3	39.3
I3	55.7	41.2	41.0	38.8

(*) See Fig. 5.1 for sample position.

TABLE 5.2 MOISTURE CONTENT VARIATION BEFORE AND AFTER TEST

Consolidation Pressure. (kPa)	At Start of Test			At End of 1st Test Programme			At End of 2nd Test Programme		
	C_v mm^2/min	$m_v \times 10^3$ kPa^{-1}	$k_s \times 10^7$ mm/sec	C_v mm^2/min	$m_v \times 10^3$ kPa^{-1}	$k_s \times 10^7$ mm/sec	C_v mm^2/min	$m_v \times 10^3$ kPa^{-1}	$k_s \times 10^7$ mm/sec
0-24	0.26	5.15	2.23	0.33	3.20	1.76	0.29	1.40	0.68
24-48	0.41	1.45	1.00	0.54	0.54	0.50	0.52	0.57	0.49
48-96	0.52	0.90	0.78	0.68	0.35	0.40	0.63	0.30	0.32

TABLE 5.3 COMPRESSION PROPERTIES BEFORE AND AFTER TEST

Type of Test	At Start of Test	At End of 2nd Loading Stage (60 kPa)	At End of 1st Testing Programme	At End of 2nd Testing Programme
Triaxial				
(CU Test):				
C'	4.3	—	2.2	1.6
ø'	21.0	—	23.5	28.5
(UU Test):				
Cu (kPa)	6.25	—	16.4	24.2
Shear Box				
Clay-Brass				
(δ°)	20.7	—	22.0	25.3
Clay-Clay				
(ø°)	21.8	—	22.8	
Vane Shear				
Cu (kPa)	—	16.3	22.4	26.3
Density				
γ_w (kN/m³)	17.4	17.8	18.2	18.5
γ_d (kN/m³)	11.3	12.6	13.0	13.4
W%	54.5	41.6	40.0	38.0

TABLE 5.4 STRENGTH PROPERTIES BEFORE & AFTER TEST PROGRAMMES

CHAPTER (6)

NEGATIVE SKIN FRICTION - ANALYSIS AND PREDICTIONS

6.1 Introduction

A relative movement between a pile and a soil will produce a shearing stress along the interface of the pile and the soil. Such movement can be induced by a push load on the pile moving it down into the soil, or by a pull load moving it upwards. The same also applies when a soil moves relative to a pile, as in the case of downdrag or swelling. A number of model and field pile tests on different types of soils have shown that the maximum frictional resistance offered by a pile is developed very rapidly at vertical movements of a very low order, (Harris, 1964). Observations by Fellenius and Broms (1969) and Fellenius (1972) of negative skin friction on piles in a 40m thick clay layer indicated that the relative movement required can be smaller than 0.3% of the pile diameter. Such small relative movements can occur easily as a result of the large stiffness difference between the pile and the soil.

6.2 Mechanism of Negative Skin Friction Development

If continued movement of the pile relative to the soil takes place, the soil strength falls rapidly and reaches a fairly constant value which is known as the residual adhesion in the case of cohesive soils and residual frictional resistance in the case of a cohesionless soil.

To visualise the mechanism of load transfer between a pile and soil, three elements along a pile shaft are shown in Fig. 6.1a (Toma, 1984), element 1 near the ground surface, element 2 in the middle zone and element 3 near the pile base. As the effective overburden pressure and consequently the confining pressure increases with depth, it may be expected that the upper elements behave as a loose soil and the lower elements as a dense soil even though the soil is assumed homogeneous soil. For each of the three selected elements the expected stress-strain relationship is shown plotted in Fig. 6.1b. Due to a rigid body displacement, i.e., no elastic deformation of the pile body, the mobilised stresses at elements 1, 2 and 3 can be represented by points a, b and c in this figure. The mobilised shear stress at the lowest element 3, will be larger than that of the upper element 1. If the elastic deformation of the pile body is taken into consideration, then the mobilised shear stresses at elements 1, 2 and 3 will be larger and may be represented by points a', b' and c' respectively.

Generally, negative skin friction along a layer of

cohesive soil varies with time depending on both the amount and the rate of consolidation. As previously mentioned a residual adhesion applies where the soil has moved relative to the pile and the movement has been sufficiently great that the peak value of shaft adhesion has been passed. At some point along the pile it reaches the maximum shaft adhesion and would then drop off towards the bottom of the pile where the strain has not been sufficient to reach this value. As a result the peak value of the negative skin friction would travel down the pile with time.

6.3 Measured Negative Skin Friction And Relative Deflection Between Soil And Pile

In all stages within the test programme, it was evident that a significant build-up of negative skin friction had occurred under increasing consolidation pressure. The results also showed that the time-dependent accumulation of downdrag was controlled by the rate of consolidation of the clay stratum, or, alternatively, by the degree of dissipation of excess pore water pressure. The rate of downdrag increase reached a limiting value at the end of each consolidation stage. Measurements taken throughout and upon completion of the tests indicated that at the upper portion of the pile the clay layer, adhering to the pile wall, had experienced a large settlement. An

investigation of the profile of the clay surface, after the completion of each testing programme, showed that the soil within the upper region around the pile must have been subjected to considerable and complex shear forces. It is believed, from the settlement results, that relative deflections of the soil and pile along the pile surface may be well into the yield range, since a displacement of only 0.4-0.6 mm would have been needed for full mobilisation of shear strength based on the results of the direct shear tests, Figs. 4.13 5.9 4.20 and 4.21. & 5.10

Regarding the shear box test results, a slippage or failure seemed most likely to have taken place at the soil-pile interface for the particular material used in this experiment. This was expected as the angle of contact friction, δ is greater for the clay-clay tests than for the clay-brass tests, Figs. 4.12 4.13 4.20 and 4.21. The use of a roughened pile surface or porous material may cause a failure to occur within the soil rather than at the pile surface. Potyondy (1961) suggested that slippage usually occurs at the soil-pile interface for a wide range of construction materials. On the other hand, Chellis (1961) reported that a thin film of clay usually adheres to piles during pull-out tests, and consequently the skin friction resistance is higher than the shear resistance of the soil. However, it would seem that careful consideration must be given as to whether a slippage may occur at the soil-pile interface, in the soil or not at all.

The existence of an ultimate value of downdrag is

dependent upon the shear strength-displacement characteristics of the medium considered. The type of clay used in this project exhibits an elasto-plastic shear strength-displacement relationship. It is clearly shown in Figs. 4.13 to 4.20, 5.9 & 5.10 to 4.23, that as the relative displacement between soil and pile increases, the resistance also increases to a peak value and then drops slightly to an ultimate or residual value and maintains this value under an increasing shear strain. It is interesting to note that the upper portion of the pile would compress elastically by about 0.013mm under the 60 kPa surcharge pressure, which is very small (0.03% of pile diameter) compared to the measured settlements within the clay layer. It may therefore be suggested that this particular soil-pile system contained an incompressible pile, in contradistinction to a full-scale pile where the compression of the pile could be significant.

The curves of downdrag load versus time, for the 30 kPa stage and the 45 kPa stage revealed a reduction of load at the 30th day and the 14th day respectively followed by load increase, Figs. 5.3 and 5.13. On the other hand, Fig. 5.15 (90 kPa stage) shows a reduction of load only at the upper zone of the pile on the 2nd, 20th and 32nd days. Other loading stages showed similar tendencies at different times but of less significant load decrease. This suggests that the peak shear resistance was mobilised along a portion of the pile but that additional shear strains induced a slippage or failure at the interface

somewhere along the pile. As pore water pressures decreased, there was a gradual recovery of shear strength. At the 90 kPa stage, Fig. 5.39, high excess pore water pressures are thought to have been responsible for the early reduction of load at the 2nd day of that loading stage.

Test results for the 60 kPa loading stage revealed the existence of a neutral point approximately 80mm vertically above the bottom of the clay. It is conceivable that at this loading stage the pile might have experienced a small base settlement sufficient to cause the direction of relative movement between pile and soil to reverse and therefore, permit a positive skin friction to develop. If this did occur then it may have been attributed to sand accumulating on the ring plate (where the pile sat) before the installation of the pile in place. Unfortunately, there was no way of substantiating this.

It is helpful to view the experimental observations within a framework of three postulated mechanisms :

Case (a) : When both the pile and the bearing stratum are rigid, and a surcharge load is applied to the soil only, then according to Section 6.2 above a full mobilisation of skin friction will occur in the upper zones, whereas only a portion of the maximum resistance is mobilised near the bottom. The developed downdrag can be represented as in Fig. 6.2a.

Case (b) : When both the pile and the bearing stratum are flexible, (resulting in a compressive strain in the pile body and a compression in the bearing stratum), the resulting relative movement of the pile with respect to the surrounding soil will tend to relieve some of the downdrag load in the pile causing a less overall relative displacement in every point on the pile shaft. This, in fact, indicates that the upper zone points will not be so greatly affected as those at the lower zone. As the consolidation settlement decreases downwards near the bottom of the pile, it is possible that the deflection of the pile may exceed the deflection of the surrounding soil and this would correspond to a build-up of upward contact friction stresses on the pile surface which would relieve somewhat the downdrag force taken by the pile.

The most important feature here is that the downdrag force builds up to a maximum value at some point above the bearing stratum and the downdrag load which is transmitted to the bearing stratum is less than that in case (a) above, Fig. 6.2b. The point of maximum downdrag force is called the Neutral Point, (NP). This would correspond to the point at which there is no relative displacement between the pile and the soil at their interface.

Case (c) : When a structural load is applied to the top of a pile, as expected, there will be increases in the pile strain and compression of the bearing stratum which

together tend to decrease the build-up of downdrag at the bottom of the pile. The point of maximum force in the pile shifts upwards and the downdrag effect on the bearing stratum is reduced, Fig. 6.2c.

Observations from the experimental results have indicated that case (a) can be applied to the results of this study since both the pile and the bearing stratum are rigid. Results of all stages of the testing programme, Figs. 5.4, 5.8, 5.10, 5.12, 5.14, and 5.16, have shown an increasing rate of negative skin friction build-up down the pile length. This behaviour was expected as the settlement values of the clay were significant, 43.5mm, 75mm, 92mm and 129mm for the 15kPa, 30kPa, 45kPa and 90kPa surcharges respectively. By taking the 15 kPa stage as an example and considering a uniform settlement distribution along the clay bed, a settlement value of 0.6mm would result at a distance of 10mm vertically above the bottom of the clay layer. When comparing this value (0.6mm) with the displacement needed for full mobilisation of shear strength (0.4-0.6mm see Section 6.3) it can be said that for the 15kPa surcharge the neutral point might have generated somewhere within the 10mm distance mentioned above. The location of this neutral point could not be detected as the lower load cell was 12.5mm above the bottom of the clay.

The existence of the neutral point was clearly established at the 60kPa surcharge - see Fig. 5.6. This

loading stage, where the pile had experienced a small settlement sufficient to reverse the direction of frictional stresses to positive skin friction, can be represented by case (b).

It is realised that the existence of the drainage layers affects the location of the neutral point. For example, if drainage were to occur only at the top of the clay layer the location of the neutral point would be nearer to the bottom of the clay.

6.4 Application Of Test Results To Predictions Of Negative Skin Friction

It was shown in Section 6.3 that negative skin friction is primarily dependent upon the consolidation characteristics of the clay and also on the consolidation pressure acting on the surface of the clay. It follows that, as in most aspects of soil mechanics, the controlling factor is the effective stress acting on the pile shaft. It is therefore necessary to know about both the vertical and the horizontal effective stresses developed during the consolidation process from which to evaluate the shear strength of the soil close to the pile shaft in order to be able to assess the magnitude of downdrag developed.

Background:

The initial stresses σ_{v_o}' and σ_{h_o}' exist in the ground before settlement takes place. When these stresses increase due to surcharge loading, shear stresses develop around the pile accompanying the progress of consolidation. Fig. 6.3 shows a hypothetical relationship between the shear stress τ and the effective vertical stress σ_v' for soil. Also shown is a state of stress of an element of soil adjacent to the pile face before and after the progress of consolidation. In this figure the shear stress corresponds to $k.\tan\phi'(\sigma_{v_o}'+q)$, where k is the coefficient of lateral earth pressure and q is the surcharge pressure. The stress state in the soil near a pile due to the rotation of the principal stress axis is complicated and depends on factors such as soil type and stress history as well as the method of pile installation. Burland (1973) in his paper on applying the effective stress concept stated

> "the ultimate coefficient of earth pressure on the pile shaft may be expected to be close to the value k_o of driven piles in soft clays".

Burland adopted the empirical relationship, $k_o=1-\sin\phi'$ which implies that the lateral effective pressure, σ_{h_o}' does not change either during pile driving or pile loading. In fact, as rotation of the principal stress axes occurs in the vicinity of the pile accompanying the settlement, the stress state nearby the pile does change.

As a result, the directions of both vertical and horizontal effective stresses (σ_v', σ_h') do not correspond any more to the maximum and minimum effective principal stresses (σ_{vo}', σ_{ho}').

A derivation relating the changes of effective lateral pressure and k values has been proposed by Parry and Swain (1977a) who assumed that both pile loading and the subsequent settlement of the soil cause a new stress condition around the pile with the vertical and horizontal direct effective stresses, σ_v' and σ_h' retaining the same values of the principal effective stresses, σ_{vo}' and σ_{ho}', Fig. 6.4. Values of 'k' obtained by Parry and Swain according to that assumption were higher than the $k_o=1-\sin\phi'$ value by the ratio $(1+\sin\phi')/(1+\sin^2\phi')$.

Table 6.1 summarises some of the empirical values of k reported in the literature by different authors.

Depending on the test results of both testing programmes, an evaluation of the coefficient of earth pressure (k) for each loading stage along with other soil parameters, was made. Tables 6.2 to 6.5 summarise all test results for both testing programmes. Both total and effective stress analyses have been employed to predict negative skin friction.

6.4.1 Effective Stress Analysis

In this method the negative skin friction is calculated from the expression :

$$f_{ns} = \sigma_v'.k.\tan\delta'$$
$$= \beta.\sigma_v'$$

where

f_{ns} : Shear stress mobilised as negative skin friction

σ_v' : Vertical effective Stress

k : Coefficient of lateral earth pressure

δ' : Effective friction angle between soil and pile surface

The effective stress approach has been used by Burland (1973) to calculate the shaft resistance for piles in clay. For soft clay the coefficient β ($\beta=k.\tan\delta'$) was found to vary between 0.25 and 0.40. In the design of compression piles a value of 0.3 was proposed. For negative skin friction an upper limit of 0.25 was suggested.

Test data presented by Bjerrum et al (1969) from instrumented steel pipe piles indicated that the coefficient β for soft clay varied between 0.18 and 0.26.

Endo et al (1969) found that β varied between 0.20 and 0.35 for different types of steel piles.

Garlanger (1974) suggested, from an analysis of

available test results, the following values of the coefficient β that could be used for design purposes:

Soil Type	β Values
Clay	0.20-0.25
Silt	0.25-0.35
Sand	0.35-0.50

6.4.2 Interpretation Of Test Results By Effective Stress Analysis

Generally, for the case of a driven pile, excess pore water pressure generates around the pile shaft, the soil then regains its shear strength as the pore pressure dissipates. Since there is a continuous relative movement between pile and soil, then according to Zeevaert (1973) the shear strength of the remoulded material close to the pile shaft should be investigated. The value of tanδ' (δ'=effective angle of contact friction between pile and soil) is thought to be best determined in the laboratory in soil samples remoulded at constant water content and then consolidated by increasing the effective stresses and sheared under zero pore pressure. The average degree of consolidation of the soil close to the pile shaft can be either computed depending on the coefficient of consolidation as described by Zeevaert or directly measured from piezometers along the pile shaft as was the case in this research project. Figures 6.5 to 6.10 are

a set of graphs representing the determination of both β (β=k.σ_v') and k values for each loading stage.

As described in Chapter 4, a series of shear box tests of soil against brass were conducted in order to determine the shearing characteristics of the clay at the pile wall. A value of 20.7° for the angle of contact friction (δ') was observed which was used for the β and k values calculations.

In Figs. 6.5 to 6.10, effective stress curves were obtained by subtracting the pore water pressure developed close to the pile wall at specific periods from the total stress values which were calculated on the basis of a uniform distribution of the pressure along the clay bed. Beta values therefore were obtained by dividing the measured negative skin friction along the pile shaft by the effective vertical stress at each point. Finally, k values were determined by dividing β values by tanδ'. Sections 6.4.3 and 6.4.4 discuss these values for both testing programmes.

6.4.3 Effective Stress Parameters During 1st Testing Programme

Figure 6.5 indicates an average β value of 0.20 was obtained at the end of the 30 kPa loading stage corresponding to a degree of consolidation of 80%. For the 60 kPa stage with a degree of consolidation of 88%, an

average β value of 0.17 was obtained, see Fig. 6.6. The slight reduction in this latter value is thought to have been due to the consequent reduction of vertical stress due to "hanging up" in the manner described by Zeevaert (1973). "Hanging up" was defined as the tranferrence of part of the surrounding soil weight to the pile due to skin friction development at the pile shaft which results in a reduction of the confining effective stresses at the pile tip with a corresponding reduction in the point bearing capacity. By examining the trend of downdrag development for the 60 kPa stage, it can be clearly seen that the rate of increase of the drag load was lower than that of the 30 kPa stage, and particularly during the period between 4 and 16 days which would indicate that a failure or slippage might have occurred at the top of the pile at that period.

By considering Zeevaert's method to account for the reduction in effective stresses due to "hanging up" the new overburden pressure was redetermined and found to differ from the measured value, at the pile base, by 4%, see Appendix (I).

Average k values for both stages were found to be 0.51 and 0.46 respectively.

6.4.4 Effective Stress Parameters During 2nd Testing Programme

Figures 6.7 to 6.10 represent β and k values for all stages of the 2nd testing programme. Beta values showed wide variations between 7 and 35 days for the 1st stage compared to the following stages. Values of 0.20, 0.22, 0.20 and 0.16 were obtained at the end of each loading stage respectively. The average β values for both test programmes however showed a very good agreement with the published data. Average k values of 0.45, 0.54, 0.47 and 0.43 were obtained for the four stages respectively.

6.4.5 Total Stress Analysis

In a total stress analysis the maximum negative skin friction is evaluated from the undrained shear strength of the soil (C_u) by the following relation:

$$f_{ns} = \alpha . C_u$$

Where α is an adhesion factor that takes into account the properties of the pile material and of the surrounding soil (silt and clay) as well as the stress history of the soil (normally or over consolidated).

Tomlinson (1957) suggested different values of α depending on different soils and showed that α decreases as the undrained shear strength increases, i.e., α values

of 0.96 and 0.83 correspond to undrained strengths of 24 kPa and 48 kPa respectively.

Potyondy (1961) suggested values of α ranging between 0.5 and 1.0.

Burland (1973) pointed out that for compression piles the coefficient α can vary between 0.3 and 1.5 depending on the soil and the pile type.

It should be noted here that the time when the undrained strength is measured or acting should be taken into consideration. Test data reported by Bjerrum et al (1969) and Bozozuk (1970, 1972) indicated that for soft clays negative skin friction can be appreciably higher than the initial undrained shear strength mainly because of the increase of the shear strength that takes place with time due to consolidation of the soil and the reduction of the water content.

6.4.6 Interpretation Of Test Results By Total Stress Analysis

In this analysis adhesion factor values (α) were obtained by two different methods depending on the undrained shear strength of the clay layer. Calculated negative skin friction values were determined by using

1) the initial undrained shear strength (Cu_o).
2) the shear strength of the clay at the time when negative skin friction readings were taken (Cu).

The values for Cu_o were obtained from the initial value of the undrained shear strength of the clay which was determined at the time of placing the soil in the tank. The corresponding α values using initial undrained shear strengths have been referred to as $\alpha_{initial}$. The values Cu were obtained by using the calculated undrained shear strength at a given time during the consolidation process. Values for Cu could be calculated from the consolidated undrained triaxial test C-U results previously carried out on the clay. Knowing the vertical effective stress (σ_v') at each stage during the consolidation process, the horizontal effective stress (σ_h') was determined according to the C-U tests conducted with pore pressure measurements, Fig. 4.9 . Alpha values (α) corresponding to the calculated undrained shear strength have been referred to as $\alpha_{calculated}$.

The undrained shear strength of the clay was determined at the end of each testing programme using a manually operated vane on the end of threaded rods. Results from these tests revealed a good agreement with the calculated values, Table 5.4 ~~4.5~~.

Values for α were calculated by dividing the measured negative skin friction at each loading stage by the corresponding calculated (Cu) undrained shear strength at that stage. These values were plotted against both the degree of consolidation of the clay layer and the settlement ratio. The settlement ratio is defined as the settlement of clay surface divided by the depth of clay

layer.

It is useful here to view changing adhesion values with both the degree of consolidation and the settlement ratio. This is shown in Figs. 6.11, 6.12 and 6.13. From Fig. 6.11, a variation of 10% for the degree of consolidation resulted in a 5% increse of α based on the measured initial undrained shear strength. This rate (5%) decreases to 2% for α determined from the calculated values of undrained shear strength. It can also be seen from Fig. 6.11 that the adhesion values obtained assuming a constant initial undrained shear strength, ranged between 0.27 and 2.13 while those corresponding to the calculated undrained shear strength ranged between 0.29 and 0.58.

Regarding variation of α values with the settlement ratio, Fig. 6.12 indicates that the rate of increase of α based on the measured initial undrained shear strength ($\alpha_{initial}$) was approximately 25% for every 2% increase in the settlement ratio, while Fig. 6.13 shows that the rate of increase of α determined from the calculated values of undrained shear strength ($\alpha_{calculated}$) reached a limiting value of approximately 0.6 at a settlement ratio of 10%.

6.5 Relationship Of Measured Negative Skin Friction with Soil Parameters

In this section an attempt is made to relate the measured negative skin friction values with both the

effective stress and the undrained shear strength of the test clay. Fig. 6.14 illustrates the relation, on a log-log scale, between negative skin friction (N.S.F) and the following soil parameters:

1- Consolidation Pressure, P_c'

2- Initial undrained shear strength, Cu_o

3- Undrained shear strength, Cu

The ratios $N.S.F/Cu_o$ and Cu/P_c' represent the only two (main) parameters involved.

From Fig. 6.14,

$$\frac{\log_{10}(Cu/P_c') - \log_{10} 0.4}{\log_{10}(N.S.F/Cu_o) - \log_{10} 0.8} = \frac{\log_{10} 0.5 - \log_{10} 0.4}{\log_{10} 0.41 - \log_{10} 0.8}$$

$$\log_{10}(Cu/P_c') + 0.398 = -0.334 \log_{10}(N.S.F/Cu_o) - 0.0324$$

$$\log_{10}(N.S.F/Cu_o) = -[1.289 + 3 \log_{10}(Cu/P_c')]$$

or,

$$\log_{10}(N.S.F/Cu_o) = -[1.289 + \log_{10}(Cu/P_c')^3] \quad \ldots (6.1)$$

Values for Cu need to be known and/or determined for every stage at which negative skin friction is to be evaluated or measured. It is believed that a more general form of equation 6.1 could be obtained when relating Cu directly to the measured negative skin friction (N.S.F) values. The relation, N.S.F=m.Cu was introduced where m is

a factor determined from the experimental results of both testing programmes. These results are presented in Tables 6.2 and 6.4 from which an average value of m was found to be 0.495 for both testing programmes.

By substituting the above relation into equation (6.1), we obtain:

$$\log_{10}(m.\dot{Cu}/Cu_o) = -[1.289 + \log_{10}(Cu/Pc')^3]$$

$$\log_{10}(m.Cu/Cu_o) + \log_{10}(Cu/Pc')^3 = -1.289$$

$$\log\left[(m.Cu/Cu_o)(Cu^3/Pc'^3)\right] = -1.289$$

$$\left(\frac{m}{Cu_o}\right)\left(\frac{Cu^4}{Pc'^3}\right) = 0.0514$$

OR

$$Cu/Pc' = 0.476\ (1/m^{¼}).(Cu_o/Pc')^{¼} \qquad .... \quad (6.2)$$

Substituting Eq. 6.2 into Eq. 6.1, yields

$$\log_{10}(N.S.F/Cu_o) = -[1.289 - \log_{10}(0.476(1/m^{¼})(Cu_o/Pc')^{¼})^3]$$

$$\log_{10}\left[\frac{N.S.F}{Cu_o}(0.476/m^{¼})^3 . (Cu_o/Pc')^{3/4}\right] = -1.289$$

$$\frac{N.S.F}{Cu_o}(Cu_o/Pc')^{3/4} = 0.476\ m^{3/4}$$

$$\frac{N.S.F}{Cu_o} = 0.476\ m^{3/4}\ (P_c'/Cu_o)^{3/4} \qquad \ldots\ (6.3)$$

Equation 6.3 enables determining N.S.F by knowing both the effective pressure (P_c') and the initial undrained shear strength (Cu_o).

Figure 6.15 is a graphical representation of equation 6.3 with a value of m=0.495. The initial effective overburden pressure (P_o') is introduced herein and both axes expressed non-dimensionally in order to put the expression in a more generalised form.

Comparisons between field test results obtained by using this expression and the measured results are presented in Chapter (7).

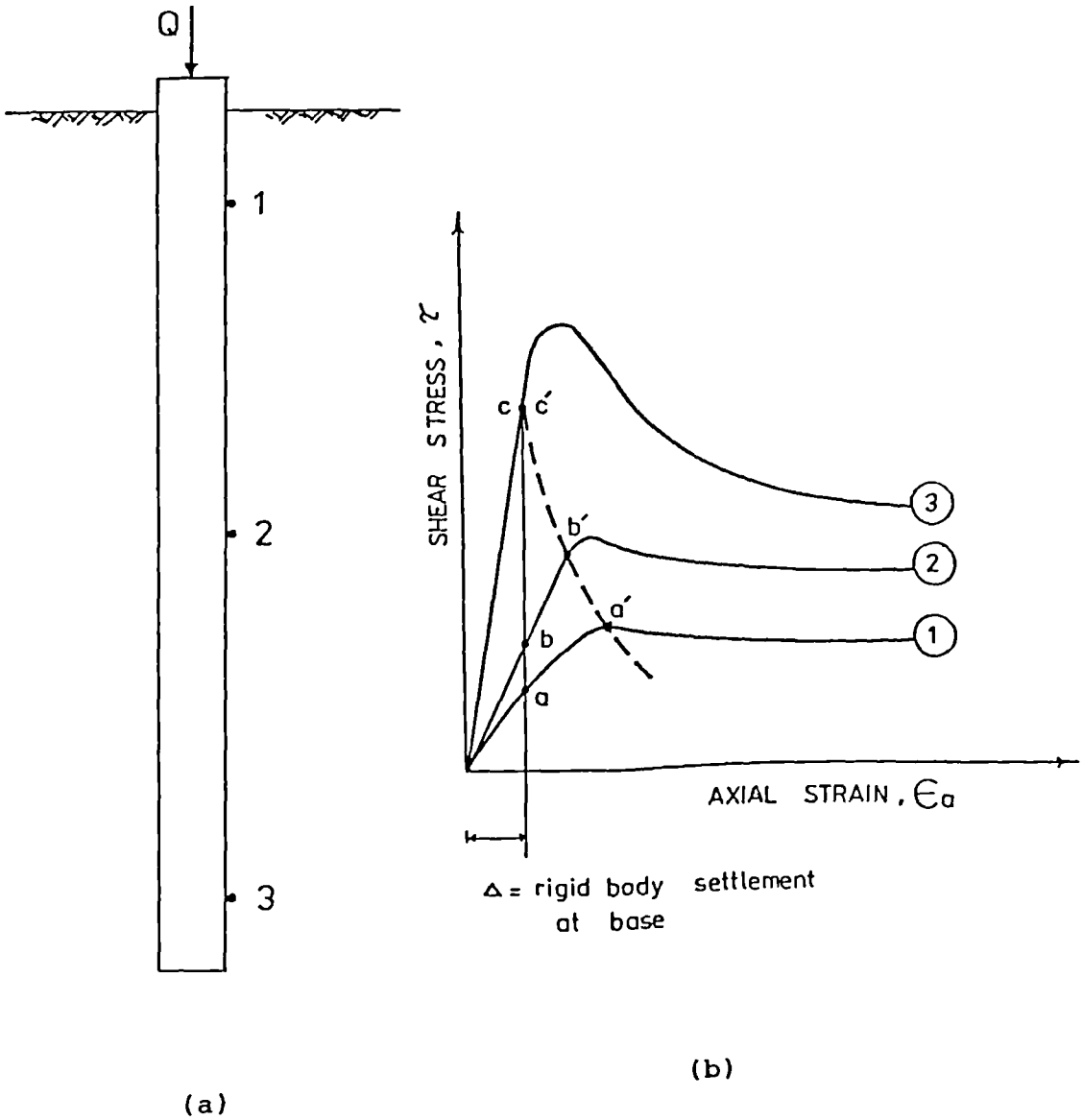

FIG. 6.1 THE EFFECT OF PILE BODY DEFORMATION ON THE LOAD TRANSFER CHARACTERISTICS OF A PILE (After TOMA, 1984)

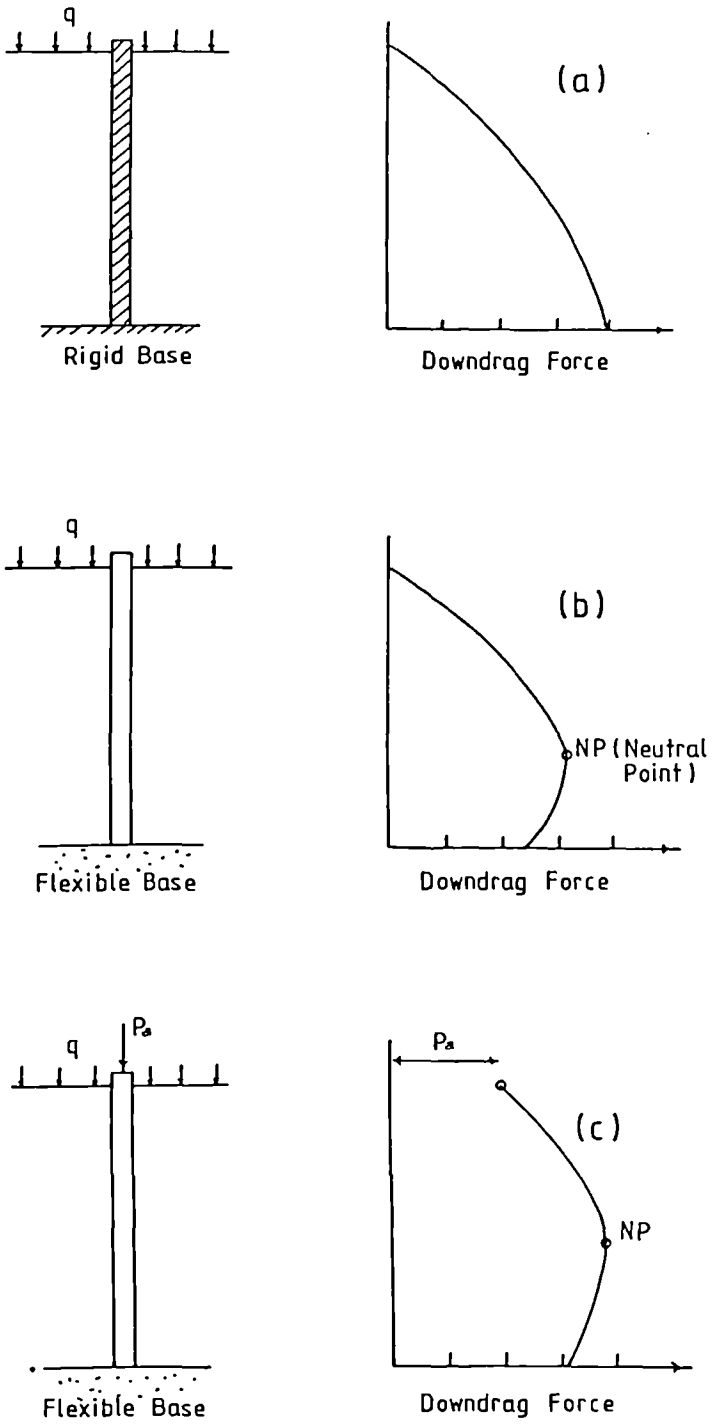

FIG. 6.2 DISTRIBUTION OF DOWNDRAG FORCE ALONG PILE FOR :

(a) RIGID PILE AND RIGID BASE

(b) FLEXIBLE PILE AND FLEXIBLE BASE

(c) FLEXIBLE PILE AND FLEXIBLE BASE WITH PILE LOADING

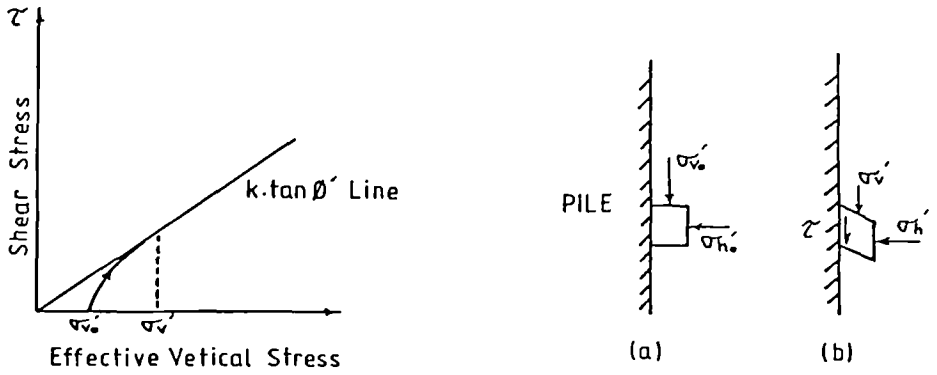

FIG. 6.3 DEVELOPMENT OF SHEAR STRESS WITH CONSOLIDATION

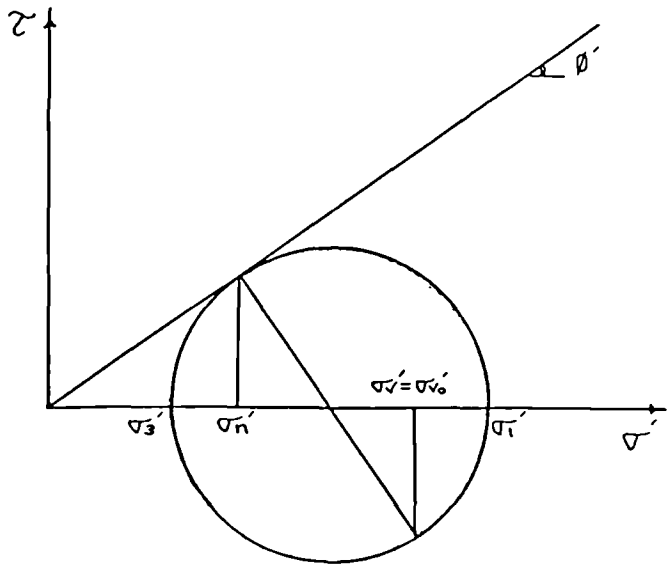

FIG. 6.4 STRESS CONDITION AFTER PILE DRIVING AND SUBSEQUENT SETTLEMENT

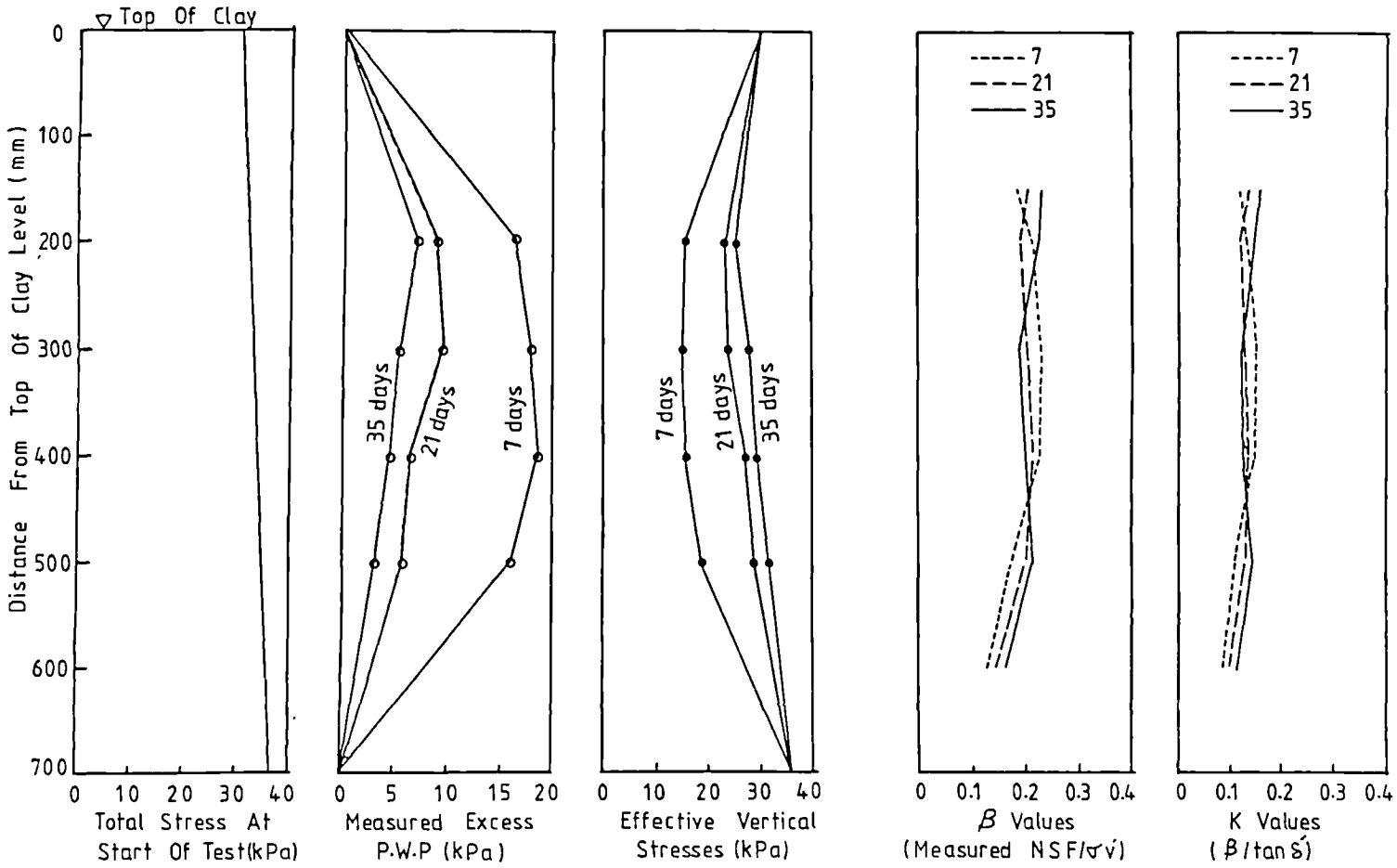

FIG. 6.5 DETERMINATION OF β AND K VALUES FROM TEST RESULTS, 1ST TESTING PROGRAMME. SURCHARGE PRESSURE=30 kPa

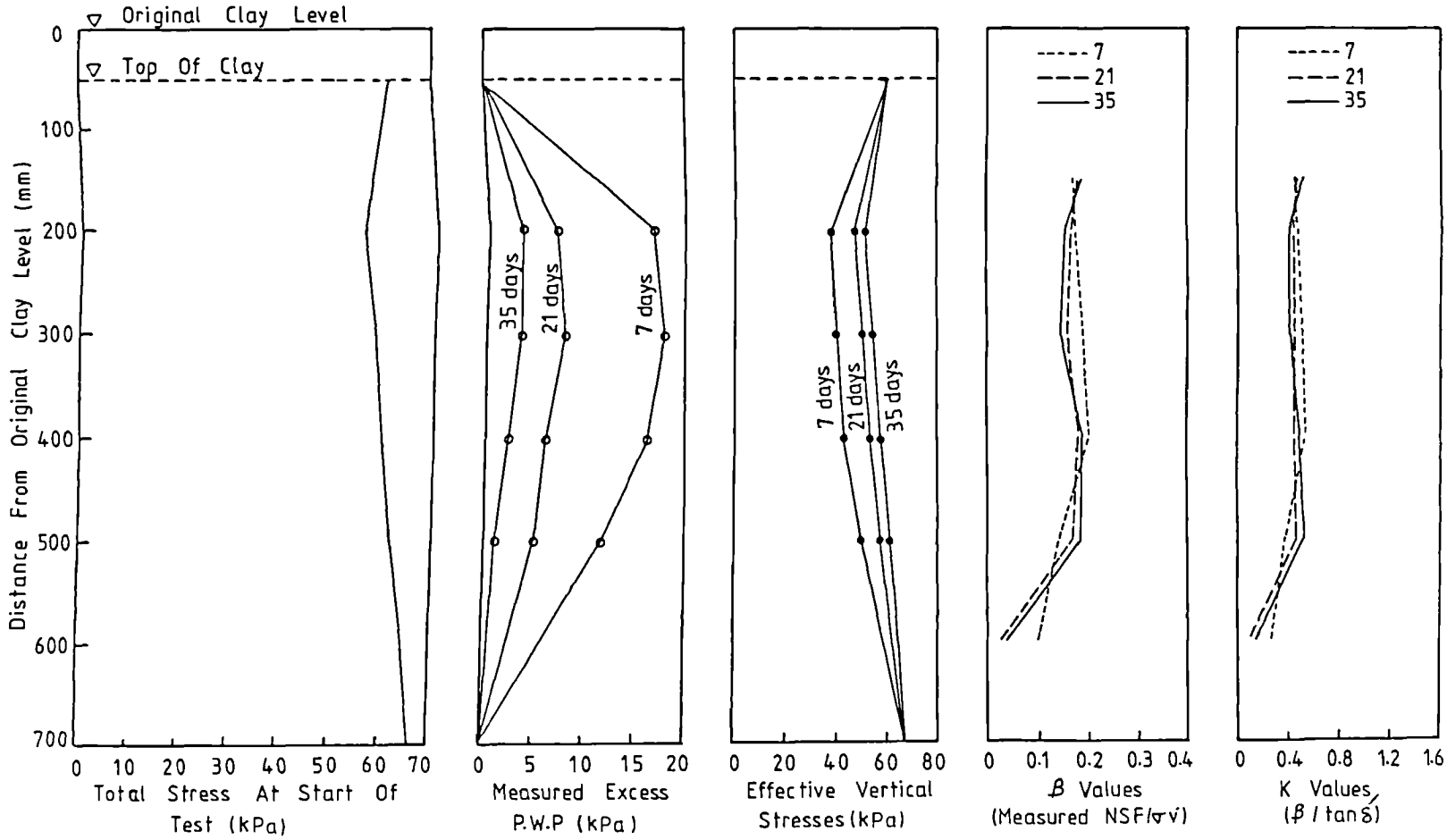

FIG. 6.6 DETERMINATION OF β AND K VALUES FROM TEST RESULTS, 1ST TESTING PROGRAMME. SURCHARGE PRESSURE=60 kPa

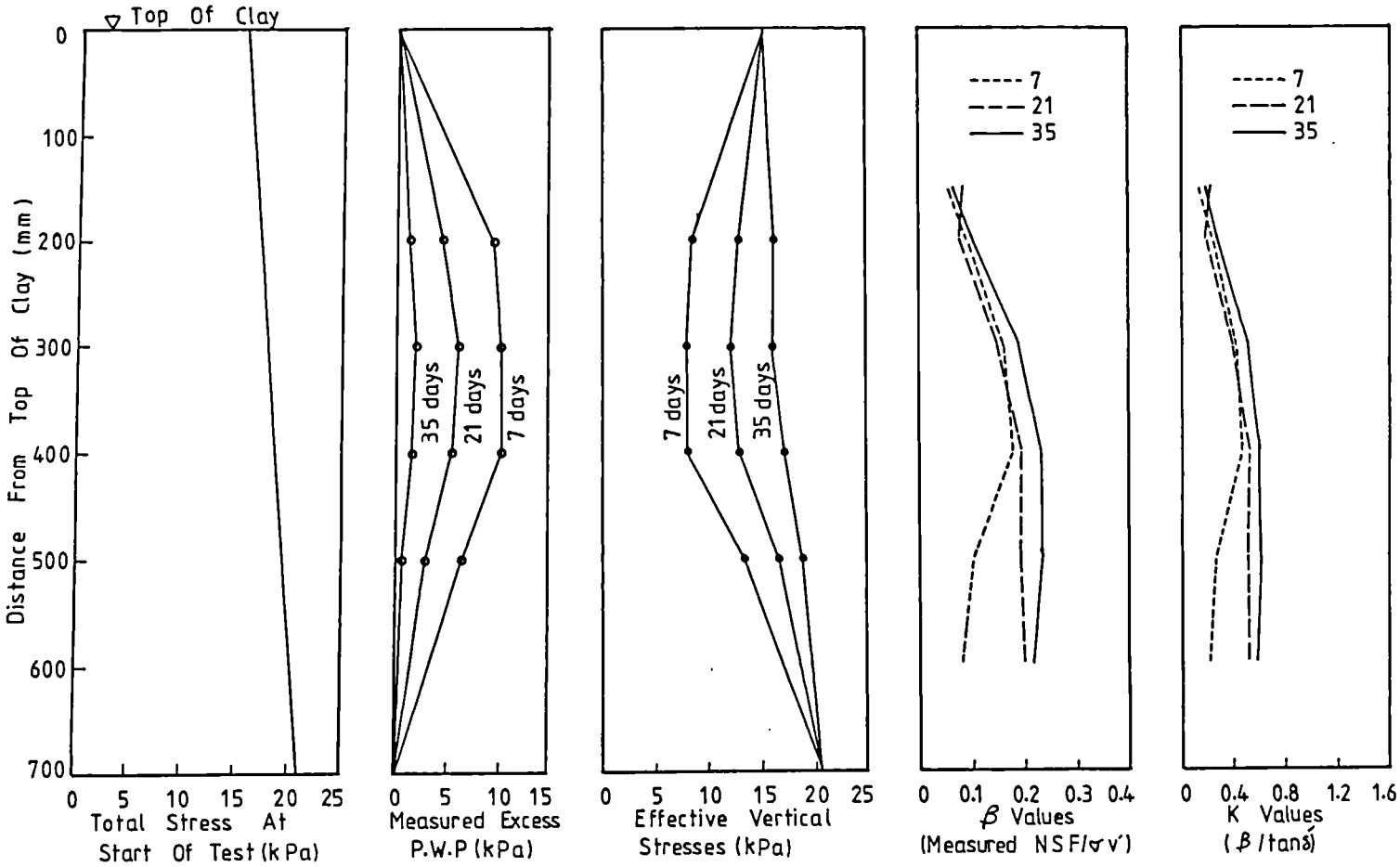

FIG. 6.7 DETERMINATION OF β AND K VALUES FROM TEST RESULTS, 2ND TESTING PROGRAMME. SURCHARGE PRESSURE=15 kPa

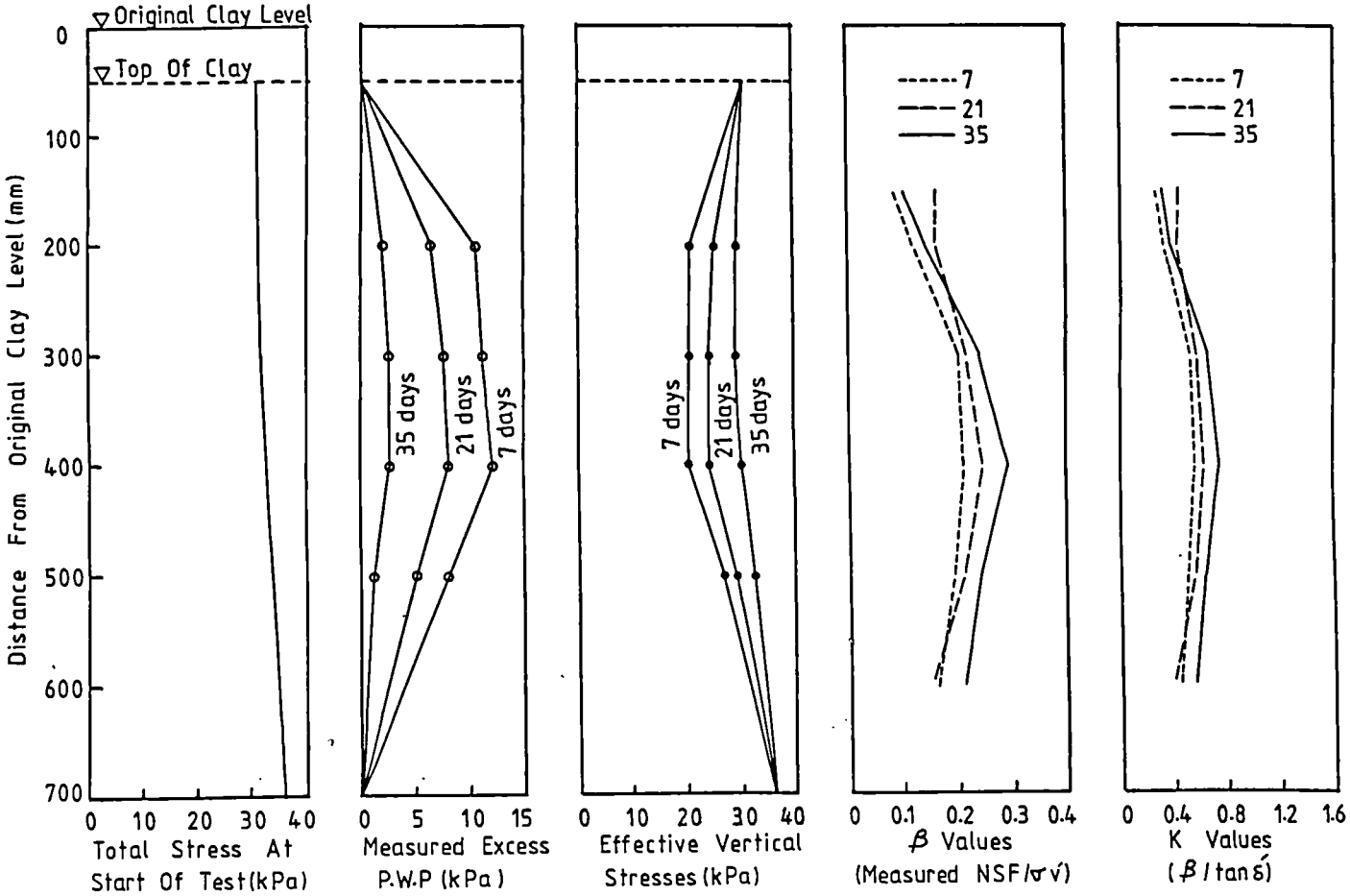

FIG. 6.8 DETERMINATION OF β AND K VALUES FROM TEST RESULTS, 2ND TESTING PROGRAMME. SURCHARGE PRESSURE=30 kPa

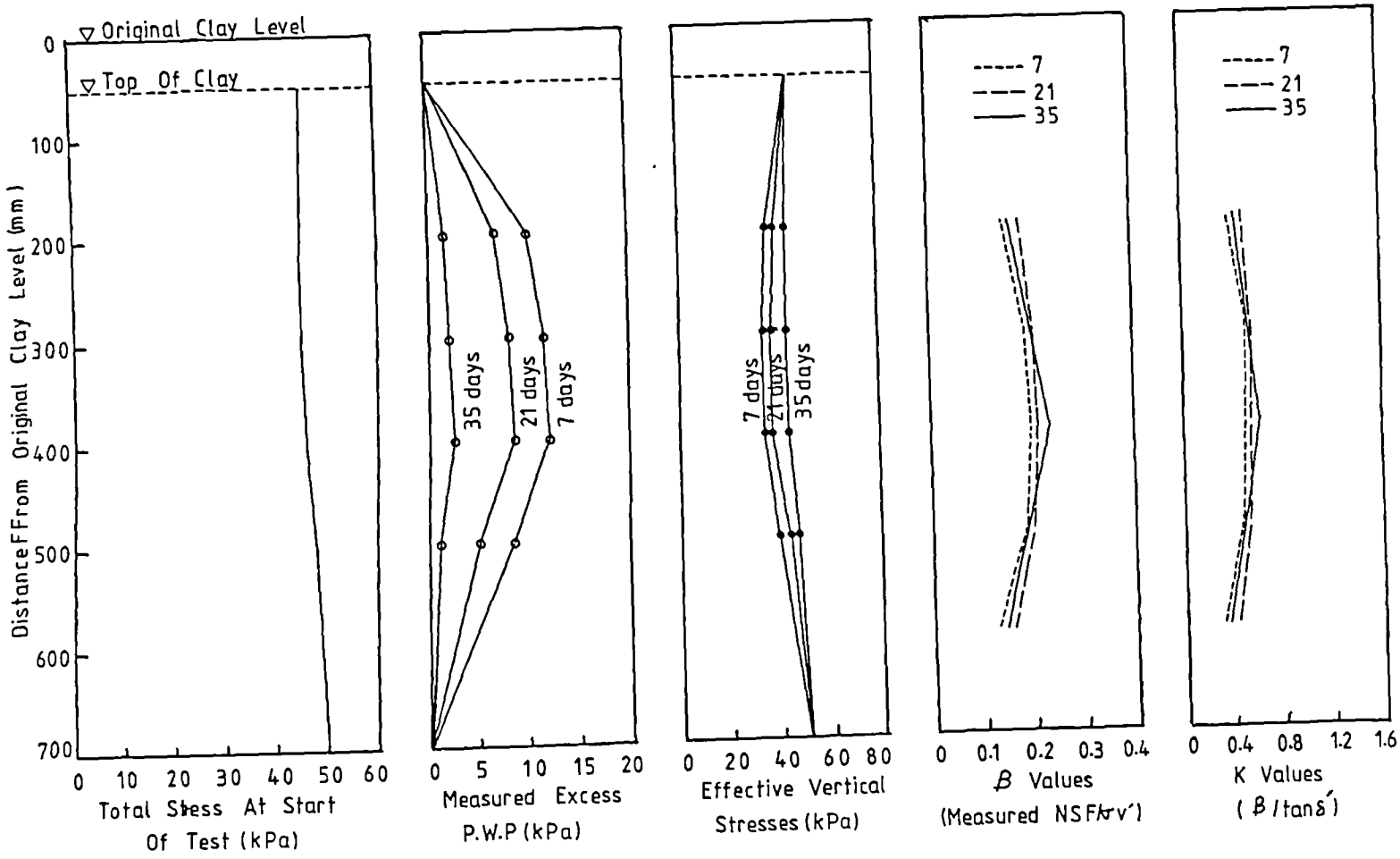

FIG. 6.9 DETERMINATION OF β AND K VALUES FROM TEST RESULTS, 2ND TESTING PROGRAMME. SURCHARGE PRESSURE=45 kPa

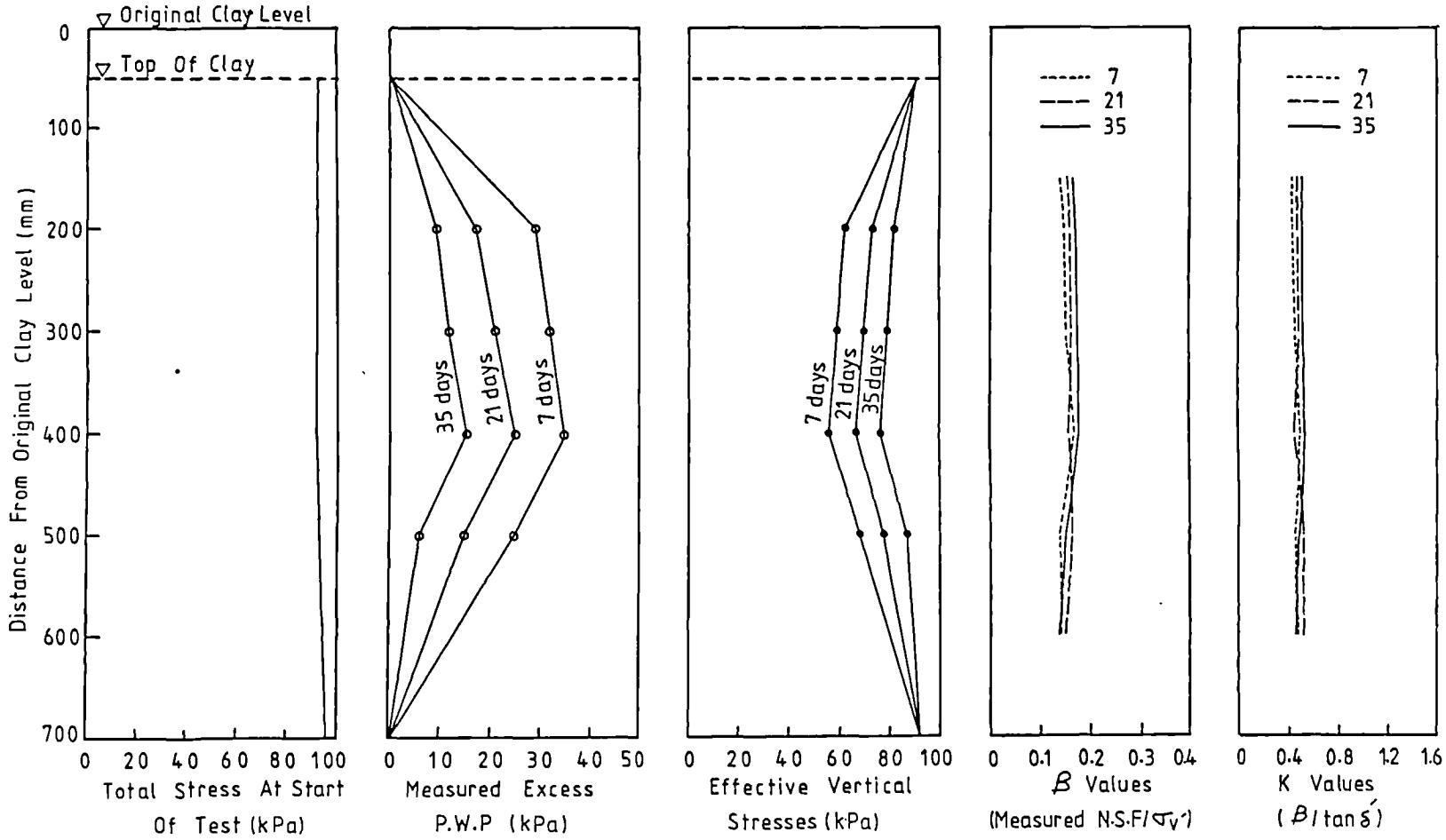

FIG. 6.10 DETERMINATION OF β AND K VALUES FROM TEST RESULTS, 2ND TESTING PROGRAMME. SURCHARGE PRESSURE=90 kPa

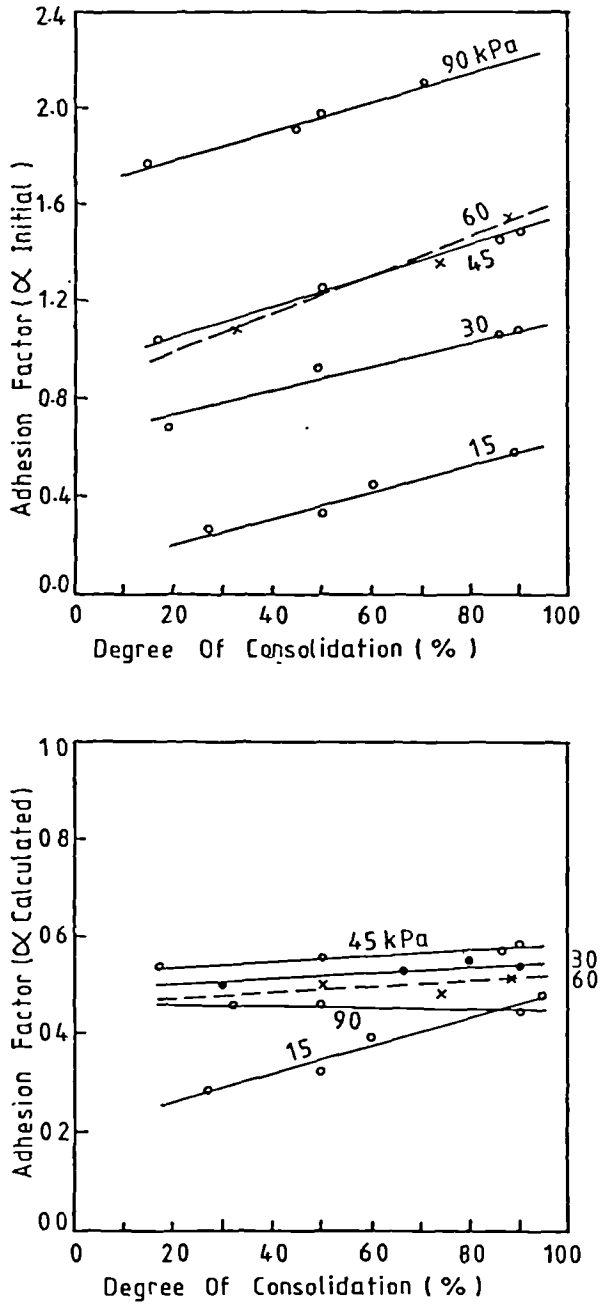

FIG. 6.11 ADHESION FACTORS Vs. DEGREE OF CONSOLIDATION

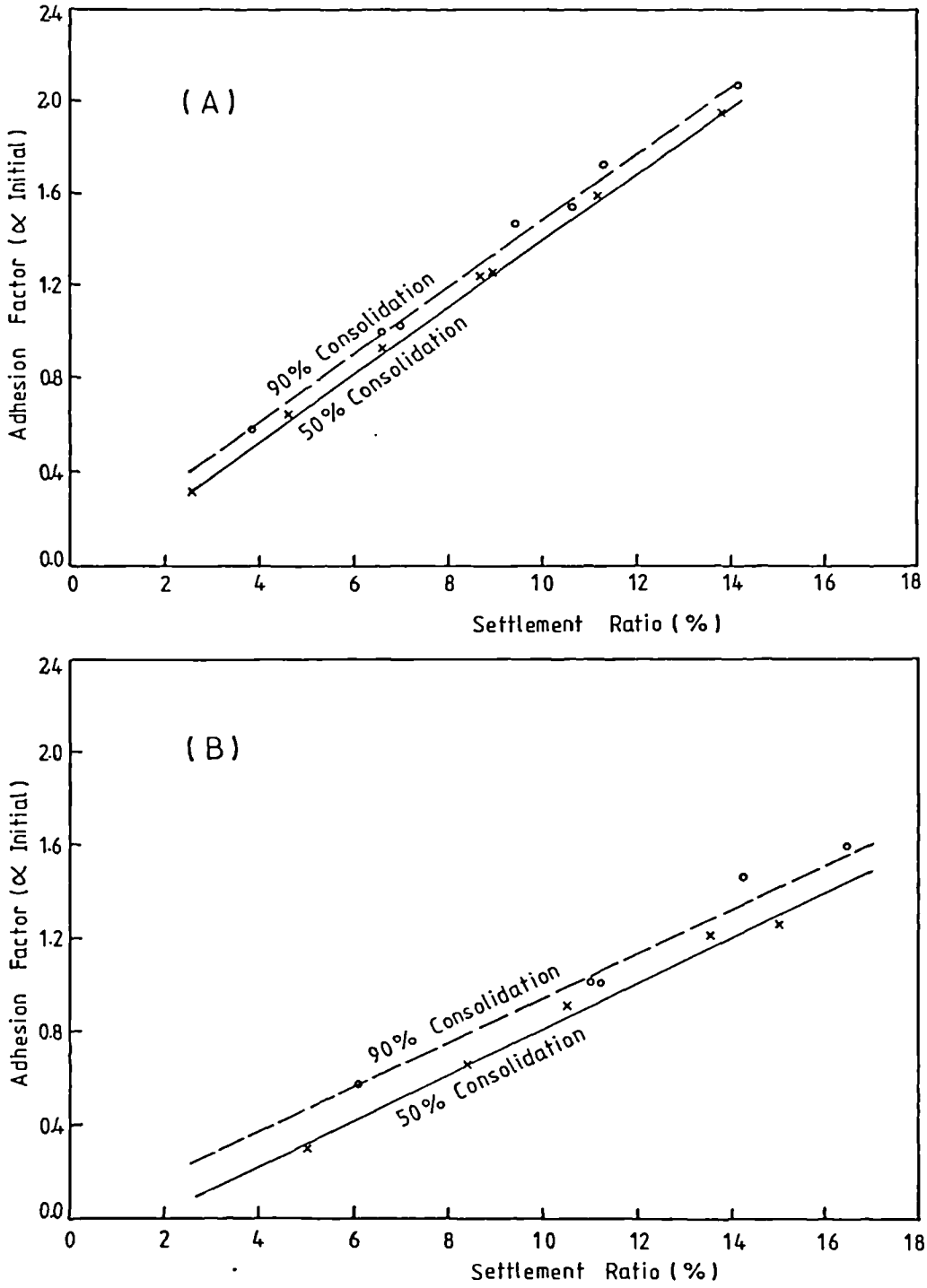

FIG. 6.12 ADHESION FACTOR ($\alpha_{initial}$) Vs. SETTLEMENT RATIO

A: SETTLEMENT BASED ON DRAINAGE RESULTS

B: SETTLEMENT BASED ON SLEEVE RESULTS

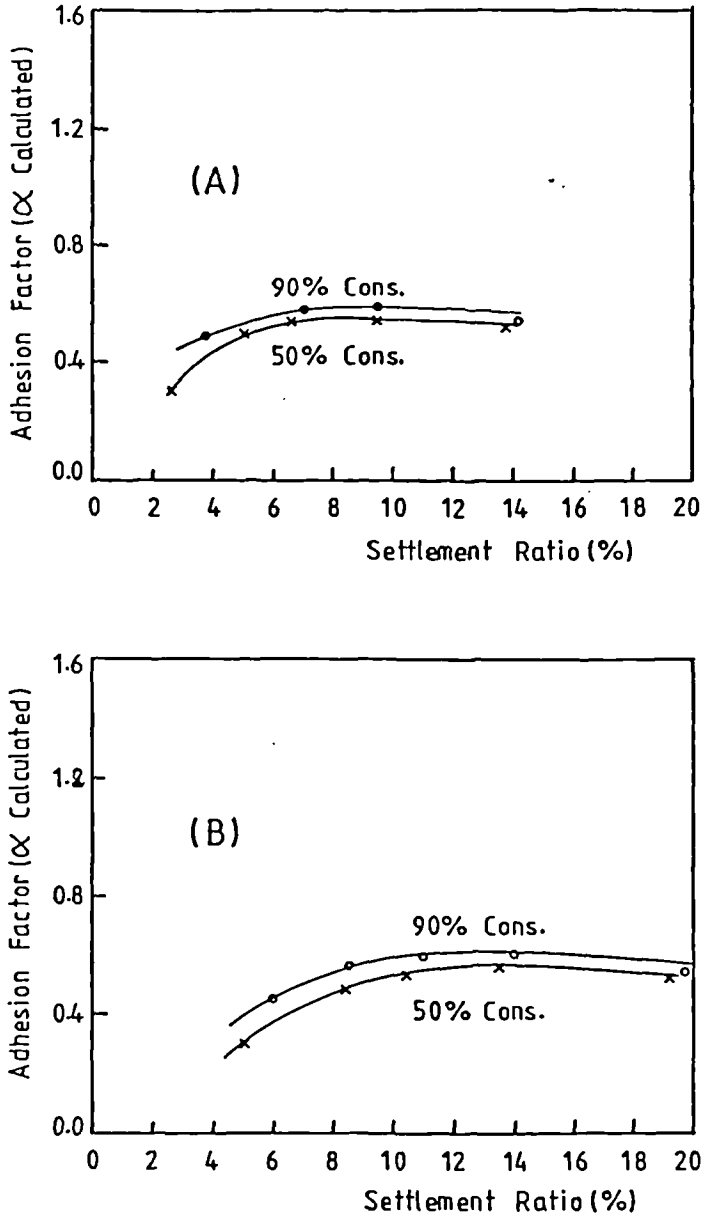

FIG. 6.13 ADHESION FACTOR ($\alpha_{calculated}$) Vs. SETTLEMENT RATIO

A: SETTLEMENT BASED ON DRAINAGE RESULTS

B: SETTLEMENT BASED ON SLEEVE RESULTS

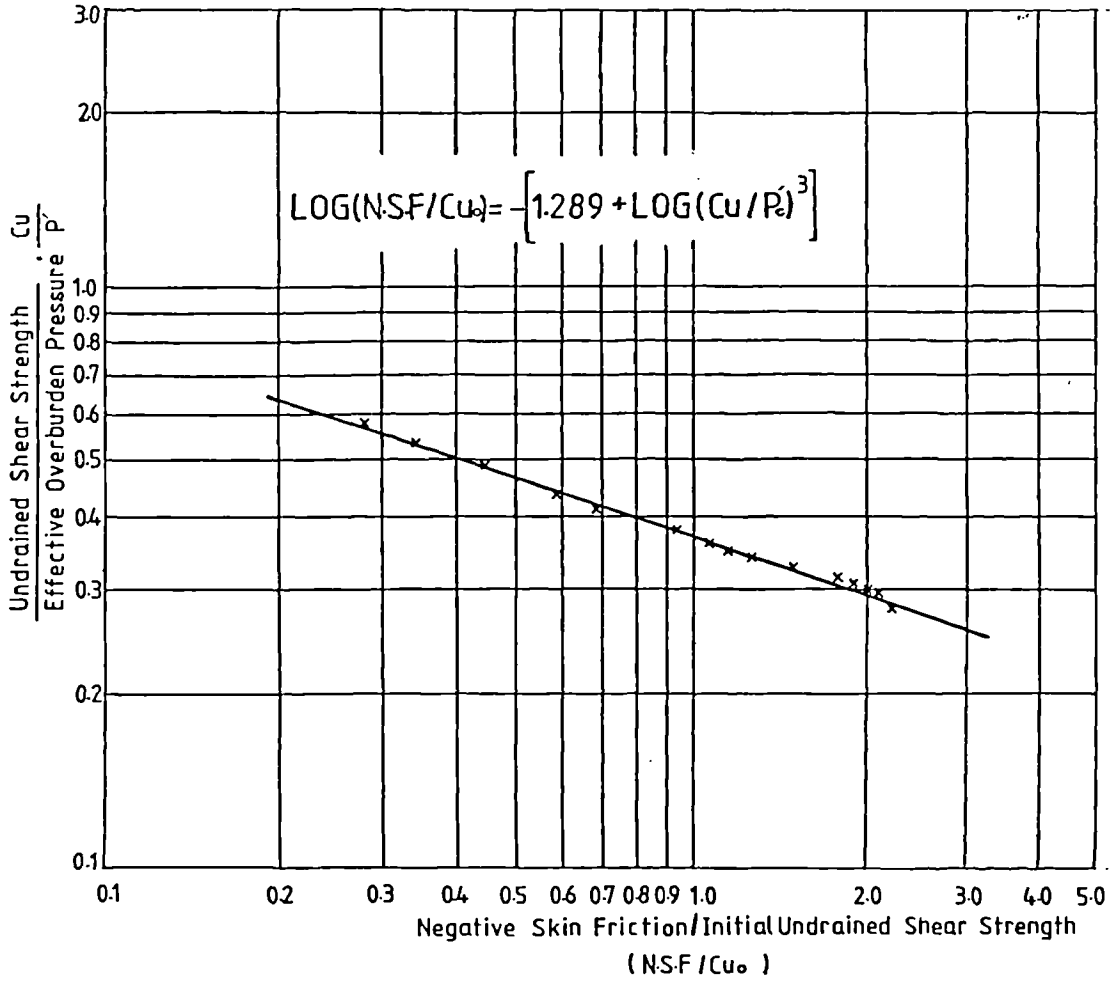

FIG. 6.14 N.S.F./Cu₀ - Cu/Pc' RELATION

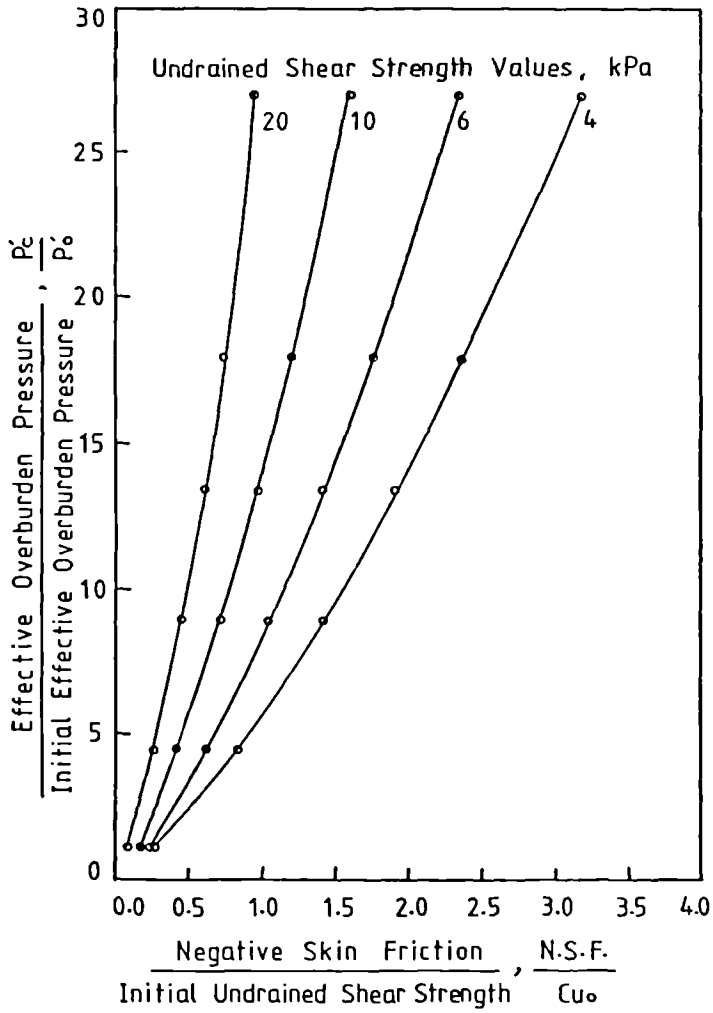

FIG. 6.15 VARIATION OF C_{u_o} WITH THE RATIOS P_c'/P_o' AND N.S.F./C_{u_o}

Authors	Expression	Notes
1.Jaky (1944)	$k=1-\sin\phi'$	Normally Consolida-ted Clay
2.Mislivec (1972)	$k=\tan^2(45-\phi'/3)$	Fills
3.Parry & Swain (1977,a)	$k=(1-\sin^2\phi')/(1+\sin^2\phi')$	Soft Clay
4.Parry & Swain (1977,b)	$k=(1-\sin\phi')/(1+\sin\phi')$	Stiff Clay
5.Holtz & Kovacs (1981)	$k=0.44+0.42(PI/100)$	PI= Plasticity Index

TABLE (6.1) DIFFERENT EMPIRICAL VALUES FOR K

Surcharge Pressure (kPa)	Elapsed Time (days)	Measured Negative Skin Friction (kPa)	Average Total Stress (kPa)	Average Pore Water Pressure (kPa)	Vertical Effective Stress, σ_v' (kPa)	Calculated * Undrained Shear Strength $C_{u\ calculated}$ (kPa)	Adhesion Factor α Calculated	Adhesion Factor α Initial	Degree of consolidation (%)	Total Settlement (mm)	
										Sleeve	Drainage
30	7	3.6	33.36	17.38	15.98	7.30	0.50	0.58	30	51	27
	21	5.2	33.36	7.93	25.43	9.80	0.53	0.83	66	70	40
	35	5.9	33.36	5.10	28.26	10.50	0.56	0.94	80	76	44
60	7	6.8	60.45	15.87	44.58	14.85	0.46	1.09	32	101	58
	21	8.4	60.45	6.50	53.95	17.32	0.48	1.34	74	109	70
	35	9.7	60.45	2.62	57.83	18.34	0.53	1.55	88	114	75

* refer to "Notes" in Table (6.3)

TABLE 6.2 RESULTS OF 1ST TESTING PROGRAMME

Degree of Consolidation (%)	Surcharge Pressure (kPa)	Time (days)	Measured Negative Skin Friction (kPa)	Pore water pressure (kPa)	Effective Overburden Pressure σ_v' (kPa)	Settlement Ratio (%)		$\alpha_{initial}$ N.S.F 6.25	$\alpha_{calculated}$ N.S.F $C_{u_{calc.}}$	β_{values} N.S.F σ_v'	Notes
						Sleeve	Drainage				
50	30	11	4.1	12.5	20.86	8.4	4.6	0.66	0.49	0.20	Calculated undrained shear strength values (Cu) are obtained from the results of triaxial tests with pore pressure measurement by applying the following relation: $\sigma_h' = \sigma_v'(1-\sin\phi')/(1+\sin\phi') - 2c'\cos\phi'/(1+\sin\phi')$ then $Cu = \frac{\sigma_v' - \sigma_h'}{2}$
	60	13	7.9	13.5	46.95	14.8	9.0	1.26	0.51	0.17	
90	30	44	6.3	2.4	30.96	11.2	6.6	1.00	0.53	0.20	
	60	38	9.7	2.6	57.85	16.4	10.7	1.55	0.53	0.17	

TABLE 6.3 RESULTS OF 1ST TESTING PROGRAMME FOR 50% AND 90% CONSOLIDATION

Surcharge Pressure (kPa)	Elapsed Time (days)	Measured Negative Skin Friction (kPa)	Average Total Stress (kPa)	Average Pore Water Pressure (kPa)	Vertical Effective Stress, σ_v' (kPa)	Calculated * Undrained Shear Strength $C_{u\ calculated}$ (kPa)	Adhesion Factor α Calculated	Adhesion Factor α Initial	Degree of consolidation (%)	Total Settlement (mm)	
										Sleeve	Drainage
15	7	1.64	18.36	8.78	9.58	5.6	0.29	0.27	27	25.0	11.5
	21	2.68	18.36	4.85	13.51	6.7	0.40	0.45	60	40.5	22.5
	35	3.46	18.36	1.13	17.23	7.6	0.46	0.58	89	43.5	27.0
30	7	4.03	32.53	10.52	22.01	8.9	0.45	0.68	19	63.0	38.5
	21	5.48	32.53	6.58	25.95	9.9	0.54	0.92	49	72.5	45.5
	35	6.31	32.53	1.83	30.70	11.2	0.56	1.06	86	75.0	48.0
45	7	6.80	46.76	10.32	36.44	12.7	0.54	1.14	17	85.0	53.0
	21	7.60	46.76	5.18	41.58	14.0	0.54	1.28	57	90.0	57.0
	35	8.70	46.76	1.85	44.91	14.9	0.58	1.46	86	92.0	58.0
90	7	10.65	91.93	32.73	59.20	18.7	0.57	1.79	15	118.0	82.0
	21	11.45	91.93	21.26	70.67	21.7	0.53	1.92	45	127.0	89.5
	35	12.70	91.93	10.91	81.02	24.5	0.52	2.13	71	129.0	92.5

* refer to "Notes" in Table 6.5

TABLE 6.4 RESULTS OF 2ND TESTING PROGRAMME

Degree of Consolidation (%)	Surcharge Pressure (kPa)	Time (days)	Measured Negative Skin Friction (kPa)	Pore water pressure (kPa)	Effective Overburden Pressure σ_v' (kPa)	Settlement Ratio (%)		$\alpha_{initial}$ N.S.F $\frac{}{5.95}$	$\alpha_{calculated}$ N.S.F $\frac{}{Cu_{calc.}}$	β_{values} N.S.F $\frac{}{\sigma_v'}$	Notes
						Sleeve	Drainage				
	15	14	2.04	6.3	12.06	5.0	2.6	0.34	0.32	0.17	Calculated undrained shear strength values (Cu) are obtained from the results of triaxial tests with pore pressure measurement by applying the following relation: $\sigma_h' = \sigma_v'(1-\sin\phi')/(1-\sin\phi') - 2c'\cos\phi'/(1+\sin\phi')$ then $Cu = \frac{\sigma_v' - \sigma_h'}{2}$
50	30	22	5.62	6.5	26.86	10.5	6.6	0.94	0.54	0.21	
	45	19	7.52	6.4	40.36	13.5	8.7	1.26	0.56	0.19	
	90	24	11.83	18.7	73.23	19.2	13.8	1.98	0.53	0.16	
90	15	36	3.46	1.1	17.26	6.1	3.8	0.58	0.46	0.20	
	30	44	6.43	1.3	32.06	10.8	7.0	1.08	0.56	0.20	
	45	42	8.90	1.2	45.56	14.2	9.4	1.50	0.59	0.20	
	90	50	13.10	3.8	88.13	19.8	14.2	2.20	0.52	0.15	

TABLE 6.5 RESULTS OF 2ND TESTING PROGRAMME FOR 50% AND 90% CONSOLIDATION

CHAPTER (7)

COMPARISON BETWEEN MEASURED AND CALCULATED RESULTS

7.1 Introduction

In this chapter, comparisons are made concerning the measured values of excess pore pressure, settlement and negative skin friction with those calculated using different methods attributed to various authors described in Chapter 2. Regarding negative skin friction, values obtained using Equation 6.3 are compared with those predicted according to the findings of others reported in the literature. Settlement results have been calculated in the usual way using the measured coefficients of compressibility obtained from oedometer consolidation tests on the soil. Finally, pore water pressure dissipation patterns have been generated numerically and compared with the measured values from the tests. Section 7.3 describes the numerical analysis technique and its application in predicting pore pressure dissipation.

7.2 Time-Consolidation Analysis

As the depth of the clay bed is large compared to the loading area, and due to the existence of a lateral flow in the tank's drainage system, it was more convenient to consider the case of three-dimensional consolidation rather than the more usual one-dimensional consolidation attributed to Terzaghi. Both theories, however, are included in the calculations for comparison purposes. As the piezometer tips were located adjacent to and along the pile shaft, it was possible to measure the distribution of pore water pressure as well as the degree of consolidation at any given time, and to compare these values with those obtained from a numerical analysis.

7.3 Numerical Solutions In Consolidation Theory

The partial differential equation governing the behaviour of the excess pore water pressure as a function of space and time can be solved using Finite Difference methods. These methods involve the replacement of the derivatives in the partial differential equations by finite difference approximations in terms of values at adjacent node or mesh points. The region is first subdivided by a rectilinear mesh having sides (in the case of a two-dimensional problem) of lengths dx and dy. Known

initial values of the pore water pressure are assigned to each node on the mesh, and the appropriate boundary conditions are inserted. From these initial values, the value of the pore water pressure at each node point is determined after successive time intervals, δt. The basic approaches of finite difference methods are discussed below.

7.3.1 Finite Difference Schemes Used For Consolidation Problems

Basically there are two types of representations available in finite difference schemes, namely the explicit and the implicit form. The explicit method has a limited region of stability (i.e. $\Theta < 1/2$ in one-dimensional consolidation problems, where $\Theta = C_v . \delta t/(\delta z)^2$, C_v =coefficient of consolidation, whereas the implicit method is a stable one (i.e. stable for all $\Theta > 0$). This requirement in the explicit method restricts the magnitude of the time step, and large time increments, δt, are not possible which in certain cases might be uneconomical. Morover, the explicit method involvs step-by-step computation while the implicit method requires the solution of a set of simultaneous equations (one for each node) at each time step.

Among the implicit schemes, the Alternating - Direction Implicit (A.D.I.) and the Locally One-Dimensional (L.O.D.)

methods are two recently developed techniques. Details of these methods can be found in Murray (1971). Murray analysed a test embankment using various methods, namely the explicit, the A.D.I. and the L.O.D. scheme. He reported that these three methods yield virtually identical results.

7.3.2 Prediction Of Pore Water Pressure Using Numerical Analysis

An attempt was made herein, using the explicit method, to examine its reliability in assessing the distribution of pore water pressure which developed during surcharge load application and also to compare the results with those measured. The method employed for the one-dimensional consolidation problem is based on a depth-time grid shown in Fig. 7.1. In a radial symmetry condition (as in this case) the grid becomes two dimensional with time being the third dimension, Fig. 7.2.

The governing three dimensional differential equation is expressed (Gibson and Lumb, 1953) in ~~polar~~ cylindrical coordinates form as :

$$\partial u / \partial t = C_v . (\partial^2 u / \partial z^2 + 1/r \; \partial u / \partial r + \partial^2 u / \partial r^2) \quad ...(7.1)$$

The following finite difference approximations as described by Mitchell (1969) can be derived from Taylor's

theorem as follows:

$$\partial u/\partial t \triangleq 1/\delta t.(U_{i,j,t+1} - U_{i,j,t})$$

$$\partial^2 u/\partial z^2 \triangleq 1/(\delta z)^2.(U_{i-1,j,t} + U_{i+1,j,t} - 2U_{i,j,t})$$

$$\partial^2 u/\partial r^2 \triangleq 1/(\delta r)^2.(U_{i,j-1,t} + U_{i,j+1,t} - 2U_{i,j,t})$$

$$1/r.\partial u/\partial r \triangleq 1/2r(\delta r).(U_{i,j+1,t} - U_{i,j-1,t})$$

Substituting in equation 7.1 above and putting dz=dr, the finite difference approximation yields :

$$U_{i,j,t+1} = \Theta.(U_{i-1,j,t} + U_{i+1,j,t} - 4U_{i,j,t} + U_{i,j-1,t} + U_{i,j+1,t} + 1/2\Omega.(U_{i,j+1,t} - U_{i,j-1,t}) + U_{i,j,t} \quad \ldots(7.2)$$

where

$\Omega = r/\delta r$

$U_{i,j,t+1}$ = predicted pore pressure at the node i,j for the first time step

This equation cannot be used on the axis r=0 where $\Omega=0$, and it is necessary only to note that as r--»0 then:

$$(\partial^2 u/\partial r^2 + 1/r\ \partial u/\partial r) \text{ --» } 2\ \partial^2 u/\partial r^2$$

Or

$$1/r\ \partial u/\partial r \text{ --» } \partial^2 u/\partial r^2$$

The governing equation will then have the form:

$$\partial u/\partial t = 2C_v(\partial^2 u/\partial r^2 + \partial^2 u/\partial z^2)$$

Therefore on the axis r=0, the numerical form of the equation becomes :

$$U_{i,j,t+1} = \Theta.(U_{i-1,j,t} + U_{i+1,j,t} - 6U_{i,j,t} + 2U_{i,j-1,t} + 2U_{i,j+1,t}) + U_{i,j,t} \quad \ldots(7.3)$$

Equations 7.2 and 7.3 are a complete numerical solution of a three-dimensional consolidation problem.

The accuracy of the solution depends on the number of intervals into which the mesh is divided, and upon the value chosen for Θ. Errors due to neglecting higher order derivatives in Taylor's theorem are reduced to a minimum when the value of Θ is 1/6 (Scott, 1963).

7.3.3 Numerical Solution Of A Three-Dimensional Consolidation Problem

The finite difference (explicit) method is employed in solving the partial differential equation 7.1 for three dimensional consolidation. A computer programme, using FORTRAN IV, was generated by adopting the finite difference approximations of equations 7.2 and 7.3. The reason for chosing the explicit method was that it can be programmed easily. The mesh used in the analysis contained 25 nodes, see Fig. 7.3. The size of the mesh was chosen such that the resulting Θ value would comply with

the stability restrictions suggested by Scott (1963), i.e. $\Theta<1/6$. Two stages of surcharge pressures were included in this analysis, 30 kPa and 60 kPa. A value for $\Theta=0.15$ was used for both stages. It should be noted here that in order to maintain a fixed value of Θ for both loading stages, the time interval (dt) for these stages should be different according to the difference in the coefficients of consolidation (C_v) for each loading stage. Appendix II presents the computer programme along with specimen solutions of the numerical analysis for the two stages. A graphical comparison between these results and those measured are presented in Fig. 7.4.

It was concluded from Fig. 7.4, that the numerical analysis approach overpredicts the size of the initial excess pore pressure and underestimates its rate of dissipation by approximately 40%. This means that at any given time through the consolidation process, excess pore pressure according to the numerical analysis is 1.4 times larger than those recorded or measured. However, this difference may be justified when bearing in mind that some assumptions were made in the analysis in order to simplify the solution. These are:

1) variation of consolidation parameters, C_v and C_r, with time and depth was not taken into account.

2) an equivalent value of the coefficient of consolidation was assumed, i.e., $C_v=C_r=C$.

3) soil parameters (especially C_v and C_r) which were obtained from laboratory tests by the conventional

oedometer tests (where no provision is made for radial drainage) do not represent the actual values that should be incorporated when using three-dimensional analysis.

It is believed that the variation of C_v and C_r with depth can be incorporated in the analysis by dividing the soil layer into a number of layers each with constant values of C_v and C_r.

7.3.4 Rigorous Solution Of Three-Dimensional Consolidation

In order to compare the results from the exact solution given by Terzaghi and Peck (1967) with those obtained by the numerical analysis, when considering the settlement curve of the clay surface in the three-dimensional case, it becomes necessary to solve the equation of consolidation in three-dimensions . The rigorous solution of this equation is arduous and difficult (Aboshi,1955). However, researchers experiences with three-dimensional model tests have shown that three-dimensional consolidation can be validly approximated by assuming that there exists a cylindrical drain of appropriate diameter. By considering consolidation of a cylinder of clay with the drainage permitted only in the radial direction, Equation 7.1 in 7.3.2 becomes:

$$\partial u / \partial t = C_r \left(\partial^2 u / \partial r^2 + (1/r) \, \partial u / \partial r \right)$$

This equation was solved by Silveira (1953), the amount of consolidation being given by:

$$U.J_n^2 = 1 - 4 \sum_{n=1}^{\infty} (1/J_n^2).\ \exp(-C_r.t/r^2\ .\ J_n 2)$$

where

r = radius of the sample

C_r = coefficient of consolidation in radial direction

J_n = the nth root of the equation $B_o(J)=0$,

B_o = the Bessel function of order zero

From this relation, U as a function of $Tr=C_r.t/r^2$ is plotted in Fig. 7.5. Also plotted are curves of the ordinary consolidation test (vertical drainage only). A three-dimensional drainage case was therefore obtained by setting $T_r=T_v$ and applying the relation,

$$U_{av}\ \% = 1-(1-U_z).(1-U_r).$$

As shown in Fig. 7.5, a case of end drainage was considered and the time required to achieve certain amounts of consolidation was calculated and compared with the measured values, the one-dimensional condition and also with the numerical analysis. Table 7.1, summarises these results.

It can be concluded from Table 7.1 that the existence of a radial drainage had a significant effect on the time required for 90% consolidation, i.e., when considering one dimensional consolidation, the time needed for the soil to reach 90% consolidation was approximately 3.5 times larger than the measured value, while a very good agreement was obtained when employing the three-dimensional consolidation analysis.

When considering numerical analyses, an overestimation of the measured values by 24% was obtained. This in fact, was expected as these analyses overpredicted the size of excess pore pressure by 40%, refer to Section 7.3.3.

7.4 Settlement Analysis

For each loading stage within the two testing programmes, settlement calculations were carried out according to the measured compression properties of the clay obtained from the consolidation tests. The clay was divided into seven layers of 10mm thick and then applying the conventional equation $S_o = m_v . H . dP_c'$. A typical calculation of the clay settlement, for a surcharge loading of 45 kPa, is presented in Table 7.2. Results of all stages together with pore pressure calculations are summarised in Table 7.1.

Regarding total settlement calculations of the clay layer, the predicted values by the conventional equation,

$S_o = m_v . H . dP_c'$, showed an underestimation of the measured settlement values by 27%. It is believed that the use of a constant value of the compressibility coefficient, m_v, along the clay bed could explain this difference between the measured and the calculated values. Moreover, m_v values were obtained from the one-dimensional oedometer apparatus which may not represent the actual values that should be used in cases where three-dimensional problems are present.

Based on the results of laboratory tests on various types of clays, Barden and Berry (1969) indicated that the simple Terzaghi approximation of a constant m_v can result in a predicted rate of consolidation approximately twice as rapid as in the case of a constant C_c, where C_c is the compression index for the voids ratio-logarithm of effective stress relation.

In view of the above discussion it is suggested that for settlement calculations in three-dimensional consolidation, different m_v values should be used according to the stress distribution along the clay bed and that m_v values should be determined from more representative tests (other than the oedometer tests) where the three-dimensional consolidation case prevails.

7.5 Comparisons Between Measured Results And Findings Of Others For Negative Skin Friction Predictions

In this Section negative skin friction values are calculated according to several different theories and authors mentioned in the literature. Comparisons are then made with the measured results.

Downdrag force P_n on a single pile, length L, diameter d, is taken as the perimeter area multiplied by the contact shear strength, f_s, of the soil;

$$P_n = f_s . \pi . d . L$$

Using the effective stress parameters from the shear box results, Fig. 4.~~21~~13, the average shearing resistance becomes:

$$f_s = k . \sigma_v ' . \tan(20.7°)$$

Table 7.3 shows the calculated f_s values for each loading stage according to Terzaghi's method. Also shown are the measured values obtained through the two testing programmes. A value of k=0.5 was used through all the calculations.

It should be noted that in Terzaghi's method, the maximum shear resistance at the soil-pile interface, is

assumed to be mobilised on the entire length of embedment implying that the method does not take into account the existence of a neutral point. Bearing this in mind, the calculated downdrag by Terzaghi's method showed lower values in comparison with the measured values for all loading stages except for the 60 kPa and the 90 kPa surcharges. An increase of approximately 12% of the calculated downdrag compared to that measured was evident at the 60 kPa stage where the neutral point existed at 80mm above the bottom of the clay. It is interesting to note that the position of the neutral point was calculated (depending on both the calculated and the measured results) and was found to occur at 72mm above the bottom of the clay.

Regarding the 90 kPa loading stage, the calculated downdrag values showed 20% increase over the measured values. This difference is thought to be due to the incomplete consolidation of the clay layer, i.e., only 71% of the excess pore pressure had dissipated at that loading stage compared to approximately 90% for other loading stages.

Hansen (1968) considered a case where a surcharge pressure (q) being applied on a compressible layer after the piles were placed in position. The presence of this surcharge causes an increase in the effective vertical stress throughout the layer. Hansen indicated that due to

the "hanging up" tendency caused by the presence of the pile, a reduction in the vertical effective stress should occur close to the pile shaft. The amount of this reduction in the effective stress was regarded as an upper limit of the negative skin friction generated on the pile shaft.

The resulting negative skin friction on a pile within the group was given as an upper limit by the expression:

$$f_s = q / (4 + 6.8d/s)$$

Where

f_s = frictional stress along the pile shaft

q = surcharge pressure

d = pile diameter

s = centre to centre spacing of piles within the group

$6.8d/s = 0$ for a single pile.

Therefore

$$\text{Downdrag } (P_n) = \pi.d.L.q/4$$

Table 7.4 shows the calculated P_n values for each loading stage according to Hansen's method. Also shown are the measured values obtained through the two testing programmes. As shown from the above table, the difference in value between the consolidation pressure and the surcharge pressure is due to the existence of excess pore pressure at the end of each loading stage. Values of this

pressure at mid-depth of the clay have been deducted from the values of the surcharge pressure, the self-weight of the soil was then added to obtain the actual consolidation pressures.

With the exception of the 60 kPa and the 90 kPa loading stages, Hansen's approach would appear to overestimate the downdrag values by 25% compared with the measured results. Generally this can be regarded as in good agreement with the measured results when bearing in mind that the semi-empirical expression by Hansen was expressed as an upper limit for negative skin friction predictions.

Regarding the 60 kPa and the 90 kPa stages, the presence of the neutral point in the former and the incomplete consolidation for the latter explains the large differences (54% and 59%) between the calculated and the measured results.

Garlanger and Lambe (1973) conducted a symposium at the Massachusettes Institute of Technology. Different methods of predicting negative skin friction by six prominent engineers were encountered, Section 2.2 in Chapter 2.

It was noticed that all of the predictors who participated in the symposium assumed that full slip had occurred along the entire length of the pile. Moreover, the same approach for negative skin friction prediction was adopted by the predictors, i.e., $f_s = k.\sigma_v'.\tan\delta'$. However, there were differences of opinion concerning the

evaluation of the Beta factor, $\beta=k.\tan\delta'$. Below is the different assumptions used by the predictors:

a) In the fill and sand, Focht used an empirical relationship between f_s and the standard penetration resistance : $f_s=1.9N$ (kPa). In the clay he set f_s equal to the undrained triaxial compression strength.

b) Davis and Poulos chose a value of $k.\tan\delta'$ equal to 0.3 for fill, the sand and the clay.

c) Esrig used a value of $k.\tan\delta'$ for sand on steel equal to 0.15 and for clay on steel equal to 0.21 for the normally consolidated layer and 0.25 for the overconsolidated layer.

d) Garlanger adjusted the equation for determining f_s to include a factor (ä) to account for that part of the soil weight being carried by the pile, i.e. $f_s = k.ä.\sigma_v'.\tan\delta' = \beta.\sigma_v'$ and determined β from published case histories. A value of $\beta=0.2$ was chosen for normally and overconsolidated clay while $\beta=0.33$ for the fill.

e) Perez-Guerra also empirically adjusted for the weight of soil being carried by the pile by decreasing k until the values of $k.\tan\delta'$ in the clay were compatible with its undrainred strength. He chose values of $k.\tan\delta'$ equal to 0.2 for the sand, 0.25 for the overconsolidated clay and

0.12 for the normally consolidated clay.

From the above presentation, it is evident that results of the predictors showed a difference of approximately 100% between their estimated values of β. When comparing the Beta value obtained from the experimental results of the present study (β=0.20) with those mentioned above, good agreement was found with both Esrig's and Garlanger's estimations.

The maximum downdrag force predicted using the elastic solutions of Poulos and Davis (1972), was obtained using Equation 2.21 and Fig. 2.23. Table 7.5 presents the parameters required for downdrag computation for the four stages of surcharge pressure. A value of Poisson's ratio (μ=0.45) for the soil was assumed in the calculations.

First, the influence factor (I_n) was determined from Fig. 2.23. The maximum downdrag force (P_n) was then calculated according to Equation 2.21. The predicted results (in terms of stresses) are presented in Table 7.5 together with the measured results.

The predicted values revealed an underestimation of downdrag of 51%, 22% and 11% for the first three loading stages respectively and an overestimation of 80% for the 90 kPa loading stage.

In addition to the major effect of both K, $K=E_p/E$ and L/d on the calculated results, values of negative skin

friction appeared to be also sensitive to the assigned value of Poisson's ratio (μ). For example, a decrease of μ by 0.01 resulted in a 14% increase in the calculated value of negative skin friction. It is believed that both the lateral restraint of the container and the degree of consolidation of the clay layer are two important factors which directly affect the value of μ. In these calculations a value of 0.45 for μ was adopted for all loading stages as there was no attempt to evaluate the μ value at different consolidation stages. Therefore, it becomes very crucial in these analysis to employ representative parameters for the medium considered. It is interesting to note that if a value of 0.49 for μ was assigned for the 90 kPa stage, a good agreement would have been obtained with the measured results.

It should be mentioned that, in this analysis, the time between pile driving and surcharge application was short (6 days) compared to the time needed for 90 % consolidation which was about 35 days, a value of N_T of 0.95 was therefore used in these calculations.

7.6 Application Of The Suggested Expression For Negative Skin Friction Prediction To Results From Model And Field Observations :

In this section an examination of Equation 6.3 is made with respect to two model studies and a field study.

These are Elmasry (1963), Silva (1966) and Fellenius (1972). For each case study, a brief description is given followed by presentation of the necessary soil data needed for negative skin friction predictions. Finally, a discussion related to the outcome of this evaluation study is presented in Section 7.7.

Elmasry (1963) conducted a series of experimental tests on a 50mm diameter model pile imbedded in 500mm deep silty clay soil. The experimental apparatus consisted of a 320mm diameter steel tank. The clay was surcharged by means of a plate on its upper surface. Different soil parameters were used in order to achieve a formula for the determination of the net downdrag load was found to be a linear function of the surcharge pressure $(P_c)'$, the thickness of the clay layer (H), the dry unit weight of soil (γ_d) and the moisture content (W), refer to Chapter 2, p.30. Below is a list of the experimental data:

Measured Negative Skin Friction = 15.5 kPa

Consolidation Pressure, P_c' = 32.0 kPa

Initial Overburden Pressure, P_o' = 2.60 kPa

Initial Undrained Shear Strength, Cu_o = 9.40 kPa

Saturated Unit Weight, γ_s = 18.8 kN/m^3

Thickness of Soil Layer, H = 500 mm

Soil Classification:

Clay : 9%

Silt :35%

Sand :56%

In evaluating the results, the parameters P_c'/P_o' and Cu_o are introduced in Fig. 6.15 from which the predicted negative skin friction ratio $N.S.F/Cu_o$ is determined. It is shown from Table 7.6 that the predicted negative skin friction value amounted to 11.3 kPa while that measured was 15.4 kPa. This indicates that an underestimation of the measured value by 27% was obtained by Elmasry's method.

Silva (1966) investigated the negative skin friction of a clayey silt with an aluminium pile of 76mm diameter. The experiments were carried out in a 1.34m diameter steel tank. The soil was surcharged incrementally by means of a pressurised rubber bag. Negative skin friction was measured at each consolidation stage, refer to Chapter 2, P.33. The relevent data and soil parameters are listed below:

Measured Negative Skin Friction = 16.2 kPa

Consolidation Pressure, P_c' = 61.7 kPa

Initial Overburden Pressure, P_o' = 4.30 kPa

Initial Undrained Shear Strength, Cu_o = 8.60 kPa

Saturated Unit Weight, γ_s = 18.5 kN/m^3

Thickness of Soil Layer, H = 1.00 m

Soil Classification:

Clay :33.4%

Silt :66.5%

Sand :0.6 %

As shown in Table 7.6, the predicted negative skin friction was 12.1 kPa corresponding to 16.2 kPa which was obtained by Silva, a difference of 25%.

Fellenius (1972) carried out a test programme on Two 330mm diameter instrumented precast concrete piles driven through 40m of soft clay and 15m into underlying silt and sand. The build-up of negative skin friction due to clay consolidation was observed through a period of 495 days. Results obtained from that study together with the soil properties are listed below :

Average Negative Skin Friction	= 12.8 kPa
Consolidation Pressure, P_c'	= 336 kPa
Initial Overburden Pressure, P_o'	= 136 kPa
Initial Undrained Shear Strength, Cu_o	= 32.0 kPa
Saturated Unit Weight, γ_s	= 16.8 kN/m^3
Thickness of clay Layer, H	= 40.0 m
Surface Area of the Pile	= 42.0 m^2

It is shown from Table 7.6 that the predicted negative skin friction according to Fellenius amounted to 6.4 kPa while that measured was 12.8 kPa, a difference of 50%.

7.7 Discussion

The interesting feature of the proposed expression (Equation 6.3) is its simplicity and the dimensionless terms it contains. It also combines parameters from both the total stress and the effective stress methods for negative skin friction predictions. These are the consolidation pressure, P_c', and the undrained shear strength, Cu_o.

In examining Equation 6.3, it can be shown that the effect of varying the consolidation pressure, P_c', on the resulting negative skin friction is larger than varying the undrained shear strength (Cu_o), i.e., an increase in negative skin friction of only 18% would result when the value of Cu_o is doubled, while doubling P_c' would result in a 70% increase in the predicted negative skin friction. By considering the relation $f_s=\beta.\sigma_v'$ for the effective stress analysis, values of β usually range between 0.2-0.3 for most types of clayey soils (Bjerrum et al, 1969). The controlling parameter is therefore the effective overburden pressure. On the other hand, when considering the total stress analysis, $f_s=\alpha.Cu$, the increase in Cu has less effect on f_s as the adhesion factor α decreases when Cu increases (Tomlinson, 1975).

However, in all three cases considered in this section, the predicted negative skin friction, using equation 6.3 and Fig. 6.15, generally showed values less than those

measured or observed. The difference was greatest for the field study. This is not surprising in view of the fact that clays of different natures have been encountered coupled with the fact that the formulation of the parameters encountered in Equation 6.3 was achieved depending on a very special case where a rigidly supported pile is surrounded by a remoulded clay which was consolidated under a uniform applied pressure. The simple formula outlined here is however, intended to identify some of the important factors which should be accounted for in any theoretical treatment of the problem of negative skin friction. It is recognized that a considerable amount of additional experimental work and study must be undertaken using different pile materials and a variety of soil types in order to accomodate all soil parameters that would influence the value of negative skin friction.

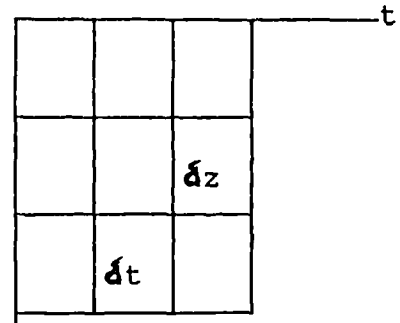

t=time , i=r/δr
z=depth j=z/δz
r=radial distance
i,j=co-ordinates of the node points in x and y direction respectivaly

FIG.(7.1) TIME - DEPTH GRID FOR ONE-DIMENSIONAL CONSOLIDATION PROBLEM

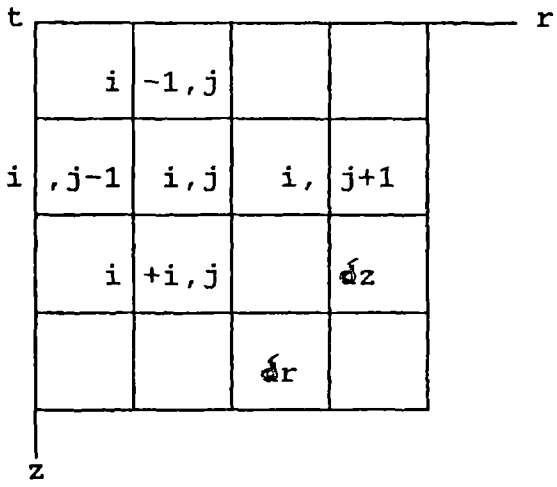

FIG.(7.2) TIME - DEPTH GRID FOR TWO-DIMENSIONAL CONSOLIDATION PROBLEM

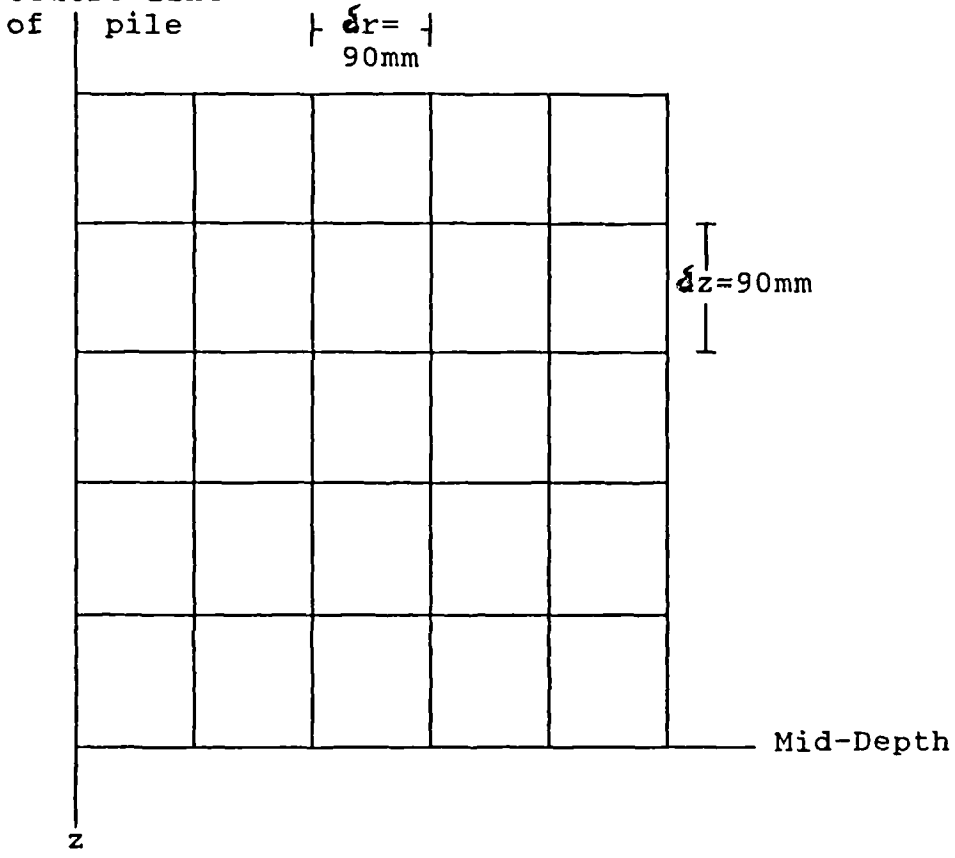

FIG.(7.3) TWO-DIMENSIONAL MESH USED FOR NUMERICAL ANALYSIS

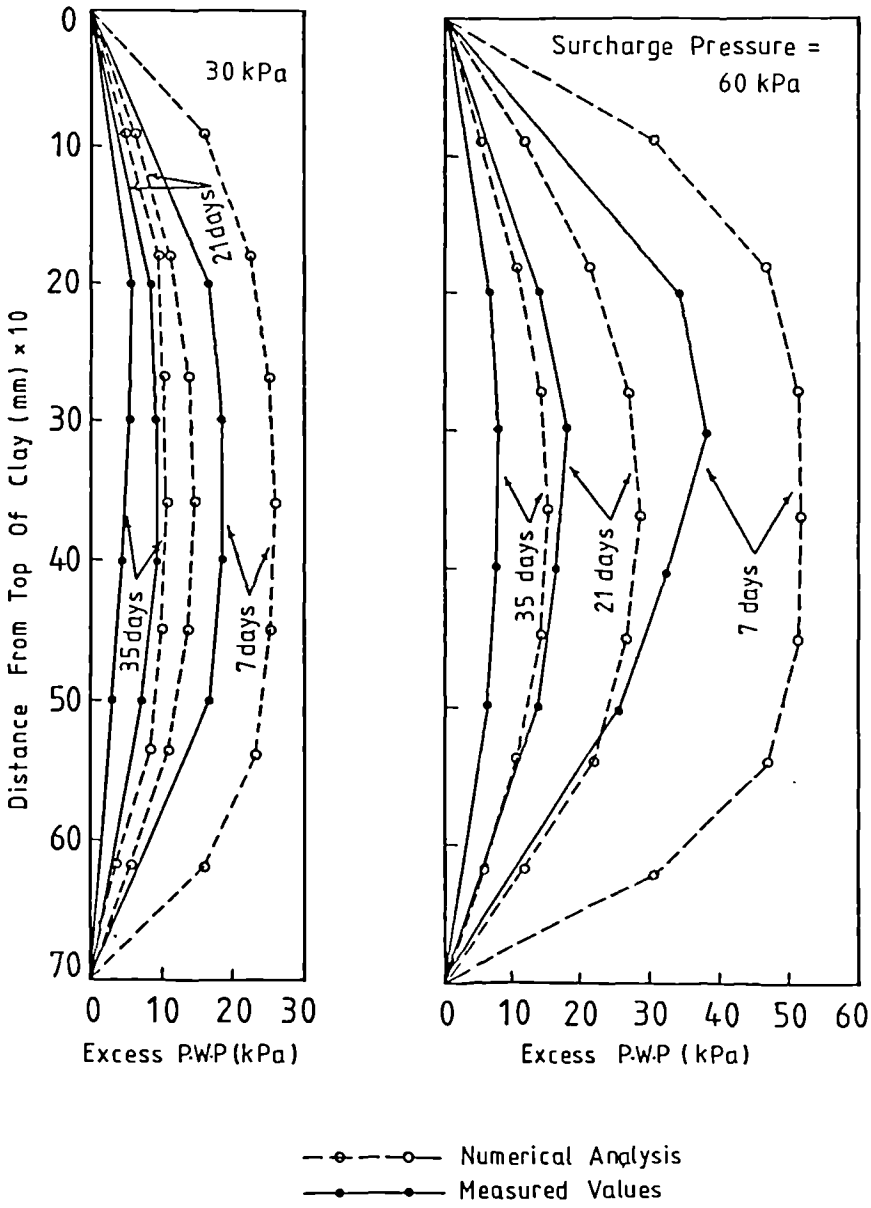

FIG. 7.4 COMPARISONS OF EXCESS PORE WATER PRESSURE DISSIPATION PATTERNS FOR TWO LOADING STAGES WITH THOSE PREDICTED BY NUMERICAL ANALYSIS

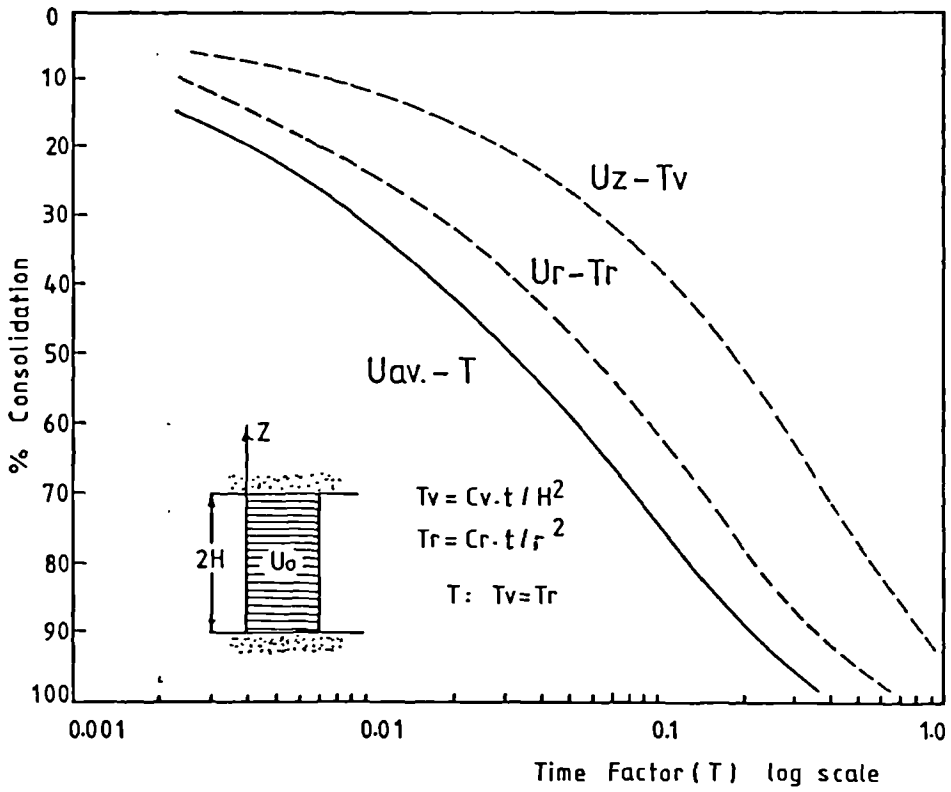

FIG. 7.5 AVERAGE DEGREE OF CONSOLIDATION, Uav Vs. TIME FACTOR (T) CURVES FOR THREE DIMENSIONAL CONSOLIDATION

Applied Surcharge Pressure (kPa)	Measured						Calculated $S_c = m_v . H . dP_c$		Numerical Analysis	1-Dimensional Consolidation	3-Dimensional Consolidation
	Average % Of Consolidation At End Of Loading Stage	Time Required to reach 90 % Consolidation (Days)	Total Settlement (mm)* 1	2	Average Pore Water Pressure * 1 (kPa)	2	Total Settlement (mm)* 1	2	Time Required to Reach 90 % Consolidation (Days)	Time Required to Reach 90 % Consolidation (Days)	Time Required to Reach 90 % Consolidation (Days)■
30 (1st)	80	44	44	46	5.1	2.4	31.7	33.2	55	159	48
60 (1st)	88	38	75	76	2.6	2.6	55.8	57.4	48	121	30
15 (2nd)	89	36	27	27	1.1	1.1	17.8	18.6	--	190	47
30 (2nd)	86	44	48	49	1.8	1.3	31.1	33.8	53	176	44
45 (2nd)	86	42	58	59	1.8	1.2	43.3	44.5	--	141	42
90 (2nd)	71	50	72	92	10.9	3.8	86.5	94.2	49	105	26

* (1) : At end of Loading Stage .
(2) : At 90 % Consolidation .

(■) : Refer to Figure (7.5) .

(1st) : 1st Testing Programme .
(2nd) : 2nd Testing Programme .

TABLE 7.1 SUMMARY OF PORE WATER PRESSURE AND SETTLEMENT ANALYSIS

Depth (m)	Height to mid depth (m)	Pressure at mid depth (kPa)		Compression of layer, mm		Total settlement (mm)	
		1	2	1	2	1	2
0.00-0.11	0.055	45.0	44.0	7.2	7.0	44.5	43.3
0.11-0.22	0.165	44.8	43.3	7.1	6.9	37.3	36.3
0.22-0.33	0.275	45.0	43.0	7.2	6.9	30.2	29.4
0.33-0.44	0.385	46.5	44.5	7.4	7.1	23.0	22.5
0.44-0.55	0.495	48.4	47.8	7.7	7.6	15.6	15.4
0.55-0.66	0.605	49.5	49.2	7.9	7.8	7.9	7.8

1: At 100% consolidation
2: At end of loading stage

TABLE 7.2 CALCULATED SETTLEMENT DUE TO A SURCHARGE PRESSURE OF 45 kPa - 2nd LOADING STAGE
$m_v = 1.45 \times 10^{-3}$ kPa^{-1}

	Surcharge pressure (kPa)	Average effective stress, kPa	f_s (kPa)	L (m)	$\pi.d.L$ (m^2)	$P_n = f_s .\pi.d.L$ (kN)	Measured value (kN)
1st T.P	30	28.26	5.34	0.70	0.110	0.59	0.65
	60	57.83	10.93	0.66	0.104	1.09	0.97
2nd T.P	15	17.23	3.26	0.70	0.110	0.36	0.38
	30	30.70	5.80	0.67	0.105	0.58	0.63
	45	44.91	8.49	0.65	0.103	0.87	0.90
	90	81.02	15.31	0.64	0.101	1.55	1.28

T.P = Testing Programme

TABLE 7.3 COMPARISON BETWEEN MEASURED AND CALCULATED NEGATIVE SKIN FRICTION OBTAINED BY TERZAGHI

	Surcharge pressure (kPa)	Consolidation pressure (kPa)	$\pi.d.L$ (m^2)	P_n (kN)	Measured value (kN)
1st T.P	30	28.26	0.110	0.78	0.65
	60	57.83	0.104	1.50	0.97
2nd T.P	15	17.23	0.110	0.47	0.38
	30	30.70	0.105	0.80	0.63
	45	44.91	0.103	1.16	0.90
	90	81.02	0.101	2.04	1.28

TABLE 7.4 COMPARISON BETWEEN MEASURED AND CALCULATED NEGATIVE SKIN FRICTION OBTAINED BY HANSEN

Surcharge Pressure (kPa)	Young's Modulus of the Soil, E_s (kPa) *	Maximum Settlement S_o, (m) **	Depth of soil layer L, (m)	L/d	E_p/E	μ	$R=\frac{(1-2\mu)(1+\mu)}{(1-\mu)}$	I_s ***	Calculated N.S.F (kPa)	Measured N.S.F (kPa)
15	0.58×10^3	0.027	0.70	14.0	184×10^3	0.45	0.26	0.40	1.64	3.46
30	1.60×10^3	0.048	0.67	13.5	67×10^3	0.45	0.26	0.41	4.94	6.31
45	2.10×10^3	0.058	0.63	12.5	51×10^3	0.45	0.26	0.43	7.72	8.70
90	4.20×10^3	0.093	0.57	11.3	25×10^3	0.45	0.26	0.44	22.9	12.7

N.S.F=negative skin friction
* : refer to Fig.(4.10)
** : see Table (6.4)
*** : see Fig.(2.23)

TABLE 7.5 COMPARISON BETWEEN MEASURED AND CALCULATED NEGATIVE SKIN FRICTION OBTAINED BY POULOS AND DAVIS

Reference	Cu_o (kPa)	P_c'/P_o	Predicted N.S.F/Cu_o	Predicted N.S.F kPa	Measured N.S.F kPa
Elmasry,1963	9.4	11.5	1.2	11.3	15.4
Silva, 1966	8.6	14.3	1.4	12.1	16.2
Fellenius, 1972	32	2.50	0.2	6.4	12.8

Cu_o = Initial undrained shear strength
P_c' = Consolidation pressure
P_o = Initial overburden pressure
N.S.F = Negative skin friction

TABLE 7.6 A COMPARISON OF RESULTS UTILISING EQUATION (6.3) ON CASE STUDIES REPORTED IN THE LITERATURE

CHAPTER (8)

FINITE ELEMENT ANALYSIS

8.1 Introduction

With the advent of digital computers, numerical methods such as the finite element method have become increasingly important. The sophistication of these methods now allows for the realistic stress analysis of complex problems.

Since these methods can incorporate non-linear material properties, they have great potential in the analysis of all kinds of structures, including pile foundations. For the past twenty years, finite element methods have been used to solve a wide range of soil-structure interaction problems (Baguelin and Frank, 1979), (Walker and Dravall, 1973), (Balaam et al, 1975), (Desai and Christian, 1977), (Nishi and Esashi, 1982).

This chapter describes the application of the finite element technique to the study of negative skin friction on the model pile and consolidating surrounding soil described in Chapter 3 and subsequently. Specifically, it was hoped that numerical predictions of negative skin friction might be obtained which could then be compared with the measured values.

8.2 The Finite Element Programme (LUSAS)

LUSAS (London University Structural Analysis System) has been developed and is marketed by Finite Element Analysis Ltd. The latest version was completed in August 1987 and was released in January 1988.

The main reason of using this computer programme was its capability of dealing with joint elements, i.e., elements providing connections between the structure and rigid supports, or between a soil and a pile,...etc. A detailed description of the theory of joint elements or thin layer elements can be found in Desai et al (1982).

8.3 Modelling Of Pile-Soil System By LUSAS

In this analysis, four different element types are used in conjunction with the Mohr-Coulomb yield criterion. These are:

1. plane strain element
2. axisymmetric solid element
3. plane strain membrane element
4. plane stress membrane element

The effects of other parameters were also considered, i.e., different yield criteria and different values of

Young's modulus and Poisson's ratio.

This section provides a description of both the finite element mesh used in the analysis and the material properties of pile and soil incorporated into the finite element model, while Sections 8.4 and 8.5 present the results obtained from the finite element analysis together with a comparison discussion comparing these predictions with measured values.

8.3.1 Finite Element Mesh

The two dimensional finite element mesh adopted is shown in Figs. 8.1, 8.2 and 8.3. The mesh comprised a total of 100 isoparametric - eight noded type elements. The dimensions of the pile and the container correspond to those of the models used in the experimental investigation. The boundaries of both the axis of symmetry of the pile and the wall of the container were assumed to be rigid; free movement being only allowed in the vertical direction. On the other hand, the boundary corresponding to the base of the container was assumed to be smooth (frictionless) and rigid, thus no movement was allowed in the vertical direction.

Thin layer elements or interaction elements were incorporated at the boundary between the pile and the soil and also between the soil and the container's wall. The thickness of the interaction elements (0.75mm) was chosen

in such a way that it complies with the limits suggested by Desai et al (1982).

The finite element mesh consisted of 341 nodes, 10 pile elements, 10 container's elements, 60 soil elements and 20 interface elements.

8.3.2 Modelling of Material Load-Deformation Characteristics

As the stress-strain relation or the load-deformation curve for a particular point in the soil is not a straight line, a non-linear problem is usually considered. However, as different problems vary according to the degree of non-linearity, and because a direct solution of the non-linear equations is not possible, an incremental-iterative model or solution was used by LUSAS, Fig. 8.4.

Four loading stages or surcharge pressures are involved in this analysis, 15 kPa, 30kPa, 45 kPa and 90 kPa. The maximum applied pressure for each loading stage was divided into ten equal steps or increments. The number of load increments was decided as a result of trial runs previously performed in order to achieve convergence of the solution process.

Concerning the state of stresses in the soil at start of test, a value of $k_o=0.5$ (k_o is the coefficient of lateral earth pressure at rest) was assumed in the analysis. With respect to the material properties input,

the shear strength parameters, c' and ϕ' were effective stress parameters since a 100% consolidation was considered. Young's modulus (E) and Poisson's ratio (μ) for clay vary over a wide range depending upon several factors such as clay plasticity and stress level. Two sets of E and μ values were therefore used in this analysis. Young's modulus values obtained from the results of consolidated undrained triaxial tests were adopted, Fig. 4.10. Values of E, for each loading stage, were introduced into LUSAS in the form given by Fig. 8.5, i.e. the stress-strain curve, for a certain surcharage pressure, is approximated by three straight lines. The slope of these lines E_1, C_1, C_2 together with L_1 and L_2 are essential input information required by LUSAS.

8.3.3 Elastic-Plastic Behaviour At Interface Elements

As the mobilisation of load transfer is caused by relative movement between the soil and the pile, thin layer elements or interface elements were incorporated along both the soil-pile and the soil-container interfaces. Different soil properties were given at each interface element, i.e. contact angle of friction (δ'), obtained from the direct shear tests, was used for the pile side while a soil-soil effective angle of friction (ϕ') was used for the soil-wall side. The reason behind assigning ϕ' value at the wall side was the existence of a

filter fabric material at the tank's wall which a soil-soil failure is anticipated to occur.

Both the relative movement and load transfer are dependent on the shear or tangential stiffness of the interface elements. The important factor which affects the shear stiffness is the rigidity modulus (G). Values of (G) for the interface element were determined by the consolidated drained direct shear tests and according to the relation below:

$$G = \frac{\tau . t_i}{S_{u\,l\,t}}$$

where

τ= ultimate shear strength (kPa)

t_i = 0.75 mm =thickness of the interface element

$S_{u\,l\,t}$ = displacement required to reach the ultimate shear strength value (mm).

8.4 Presentation And Discussion Of The Results

This section offers presentation and comments on the results obtained while Section 8.5 deals with the discussion. Results of the finite element analysis are presented in Figs. 8.6 through 8.14. In all these figures, the negative skin friction distribution curves, obtained from the finite element analysis, are plotted together with the experimentally observed curves to facilitate comparison. Different runs have indicated that

the developed negative skin friction along the pile length is influenced by several factors such as the type of element used, the yield criterion and also by the material properties assigned. The following sections provide an insight into the effects of various parameters that were included in this study on the predicted results.

8.4.1 Effect Of Element Type

As previously mentioned, four different element types were conducted in conjunction with the MOHR-COULOMB yield criterion. Figs. 8.6 to 8.13 show the results for all four loading stages of surcharge pressure, i.e. 15, 30, 45 and 90 kPa. It can be seen that the PLANE STRAIN element produced better results in comparison to other element types. The distribution of negative skin friction did not agree well with that observed in the experimental programme at the upper regions of the pile while there was a reasonably good agreement at mid-depth and in the lower parts of the pile. The average predicted values were over the measured values by 25-40 %.

Regarding settlement results, Table 8.3 summarises settlement values obtained by the four different element types. The maximum slip at the pile interface and the average settlement of clay surface are both included together with the measured settlement of the clay surface. It is shown from Table 8.3 that the PLANE STRAIN elements

have produced the greatest difference in settlement when compared with the measured results while values obtained from the MEMBRANE PLANE ELEMENT STRAIN appeared to be in a very good agreement with the measured values.

8.4.2 Effect Of Different Yield Criteria

In view of the fact that different classes of materials exhibit different elastic-plastic characteristics, two yield criteria, other than the MOHR-COULOMB criterion, were used in the analysis basically for comparison purposes. These were the TRESCA yield criterion and the VON-MISES yield criterion. The latter two criteria are usually used to approximate metal plasticity behaviour while Mohr-Coulomb criterion is applicable to concrete, rocks and soils. A detailed description of the various yield criteria can be found in Hinton and Owen (1978).

Figs. 8.10 to 8.13 give the predicted shear stress distribution as negative skin friction for the aformentioned three different criteria along with the measured values for all loading stages. It can be concluded from these figures that the results were affected by the type of yield criterion used. The Mohr-Coulomb criterion appeared to be more appropriate for this analysis. The difference between all three yield criteria diminshes at the lower part of the pile.

8.4.3 Effect Of Young's Modulus And Poisson's Ratio On The Distribution Of Negative Skin Friction

Both Young's modulus and Poisson's ratio of clays can vary over a wide range, therefore the influence of changing these parameters on the developed shear stress is desirable. Several computer runs were conducted using different values of E and μ. Table 8.1 gives the values of E and μ used in three such runs. In all of the runs, the Young's modulus of the pile, E_p was 107×10^6 kPa while its Poisson's ratio, μ_p was 0.33. These values were taken from the manufacturer's data sheet supplied.

Fig. 8.14 presents the distribution of negative skin friction along the pile shaft for two different values of E and μ, i.e., 1) under a constant E value for each loading stage, and 2) under a constant μ value. The results of only one surcharge pressure (30 kPa) have been given since the effect of varying E and μ was found to be the same for the other loading stages.

It can be concluded from Fig. 8.14 that upon varying the Young's modulus (E) a slight effect was noticed on the resulting negative skin friction, i.e., doubling the E values resulted in a reduction of the negative skin friction values along the pile surface by only 14% while in reducing the Poisson's ratio (μ) by 0.05, the resulting negative skin friction along the pile shaft increased by

25%. This is to be expected as the Poisson's ratio is representative of the tendency of the material to expand laterally when it strains vertically. A high μ value indicates large lateral expansion under conditions of no lateral constraint, or high lateral stresses under conditions of complete restraint as in the case of the model used.

8.4.4 Effect Of Young's Modulus And Poisson's Ratio On The Settlement Of The Clay Bed

Table 8.2 gives the average surface settlement of the clay layer for two different values of E and μ. It can be seen from Table 8.2 that the settlement of the clay layer increases upon reducing the value of μ. This is to be expected since Poisson's ratio is a function of the degree of horizontal restraint. Regarding the influence of Young's modulus, the results show that settlement is significantly affected by the variation of E, i.e. doubling the E values resulted in a 50% reduction of the settlement. This is also expected as displacements reduce with increasing stiffness of the soil elements.

8.5 Discussion of Results

Different computer runs have indicated that the

magnitude of negative skin friction is influenced by several factors, i.e. the type of element used, the yield criterion and also by the material properties assigned.

The material properties used for the first increment of loading and the subsequent increments were obtained according to the measured results from laboratory tests. Concerning the state of initial stresses assigned for the model used in this study, the initial vertical stresses (σ_v') were given by (γz) while the initial confining stresses (σ_h') were calculated using the relation $\sigma_h' = k_o . \sigma_v'$. It is believed that the results obtained from this analysis were largly controlled by the magnitude and distribution of these initial stresses together with the values assigned for the material properties.

Figs. 8.6 to 8.9 show that the predicted results, especially in the upper part of the pile, are consistently higher than the experimental data. For example, at the first loading increment of 15 kPa, the measured negative skin friction recorded along the top half of the pile was 3.4 kPa while the finite element analysis yielded a value of 5.8 kPa.

Regarding the application of the interface or joint element to soil-structure interaction problems, many authors (i.e., Zienkiewicz, 1970; Ghaboussi et al, 1973; Katona, 1981) have indicated that the shear stress distribution along the interface element depends on the assigned shear stiffness values and the relative displacement of adjacent nodes in each of the interface

elements. The interface shear stiffness is, in turn, dependent on the normal stress and the ratio of shear stress to shear strength. The magnitude and distribution of the skin friction is therefore largely controlled by the magnitude of the confining pressures acting on the pile shaft, and the mechanisms used in modelling yield in the clay as well as slippage in the soil-pile interface.

An investigation was carried out by Siah (1980) to develop and apply a non-linear finite element programme for the analysis of the behaviour of a model pile driven into medium dense sand. Five different shear stiffness values were assigned along the interface elements. After conducting several runs Siah concluded that the distribution of skin friction didn't agree with that obtained from the experimental programme. He also observed that there existed a non-zero shear stress at the top of the pile. This was attributed, according to Siah, to the use of a coarse mesh and a finite shear stiffness value for the top interface element.

In view of the above discission and the results obtained in this analysis, it is believed that the results are greatly influenced by the correctness of the interface parameters among the other factors mentioned earlier. The following suggestions are therefore made:

1) A modification of LUSAS that computes the tangent modulus is required in order to simulate the available soil shear strength after soil failure occurs along the

interface, i.e. the way in which the tangent or shear modulus is computed should be modified to account for the available shear strength on the interface after the elements reach failure. It is believed that as lower shear stiffness values will give rise to larger relative displacement in the interface elements and consequently lower skin friction stresses, a more reasonable distribution of negative skin friction would be obtained if a limited value of shear stiffness is assigned for the interface element at the time of failure, i.e., the relative displacements between two adjacent nodes are checked against a limiting value. If the limiting value is exceeded, the shear stiffness of the interface element is then set to a failure value (a sliding type of failure).

2) It is realised that the accuracy of the solutions could be improved by reducing the size of the mesh used. On the other hand, as the number of elements is increased, the computational efforts required to reach a solution also increases. However, this was not explored due to the limited time available.

From the finite element study carried out in this chapter and the results so obtained, it is recognised that the behaviour of the pile-soil interface has not been modelled entirely successfully. The work conducted to date however, would provide a good starting point for

further research, thus permitting the use of more appropriate models and so producing more conclusive findings.

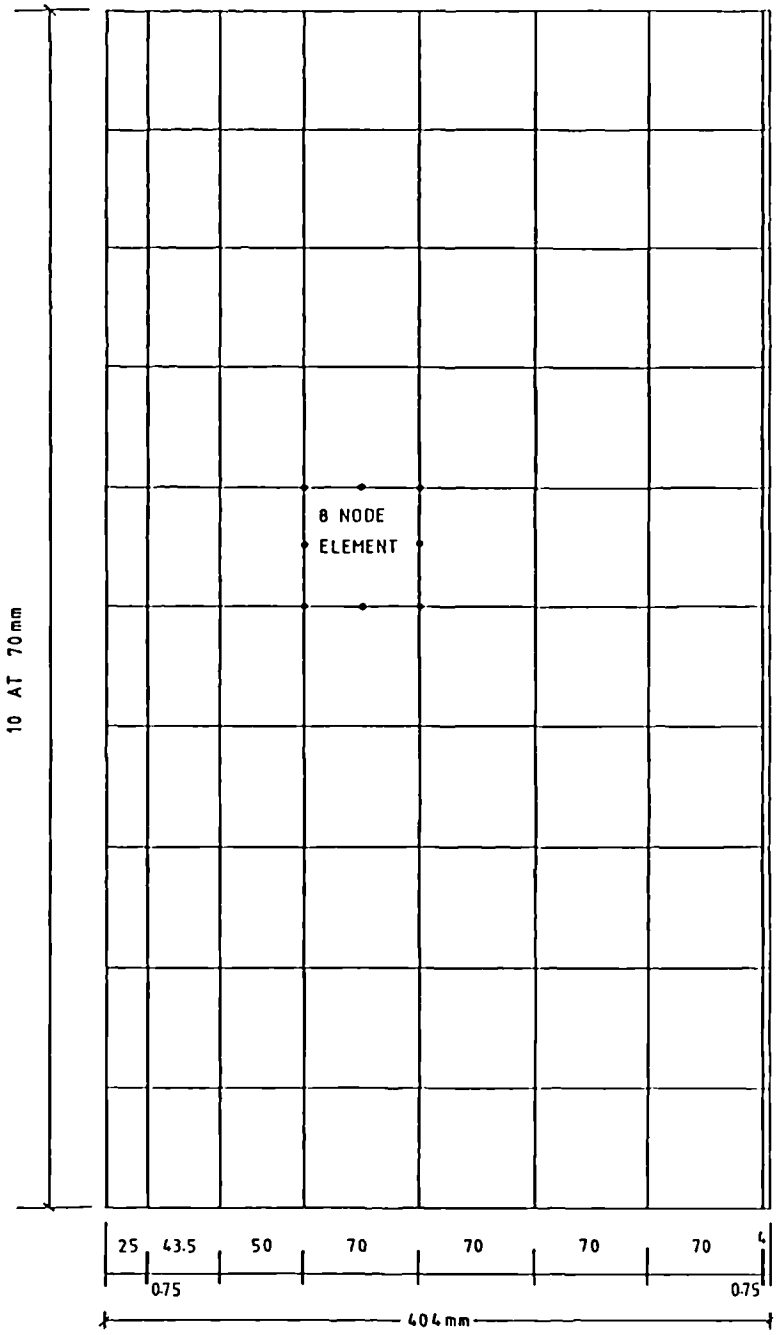

FIG. 8.1 FINITE ELEMENT MESH FOR PILE-SOIL SYSTEM SHOWING ELEMENT DIMENSIONS

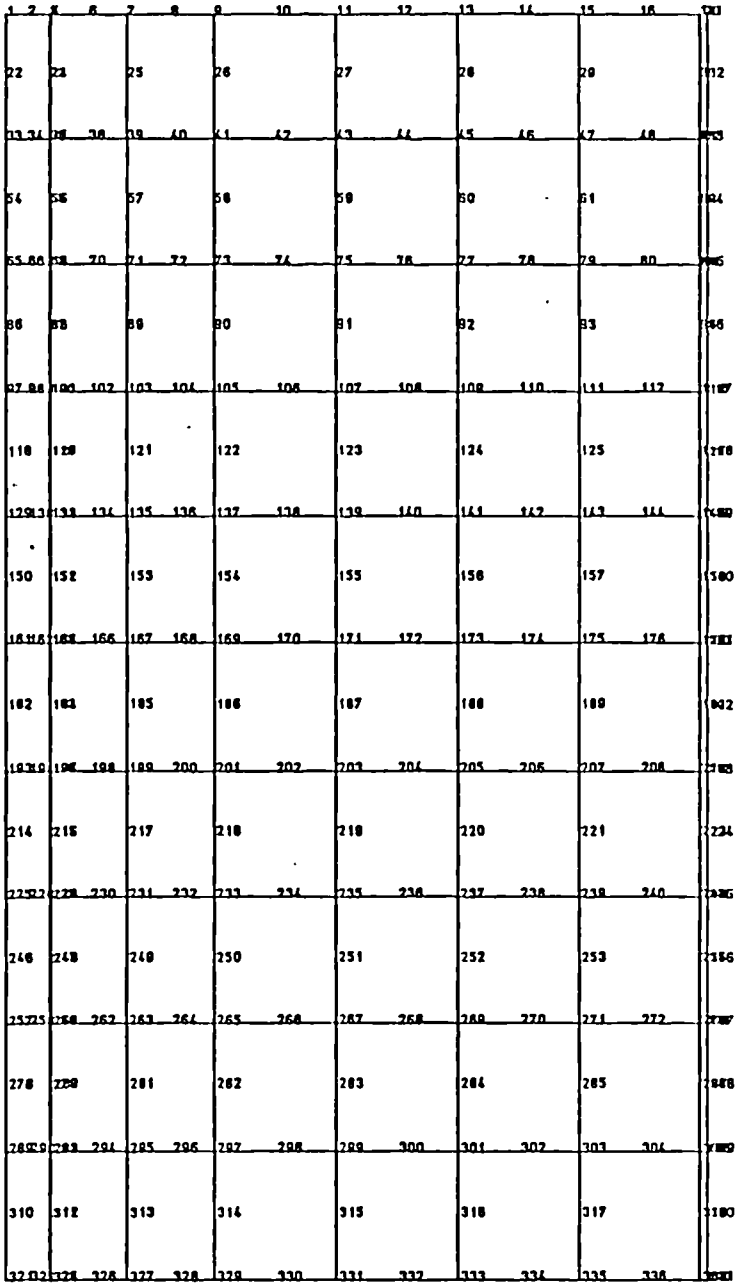

FIG. 8.2 FINITE ELEMENT MESH FOR PILE-SOIL SYSTEM SHOWING NODES NUMBERS

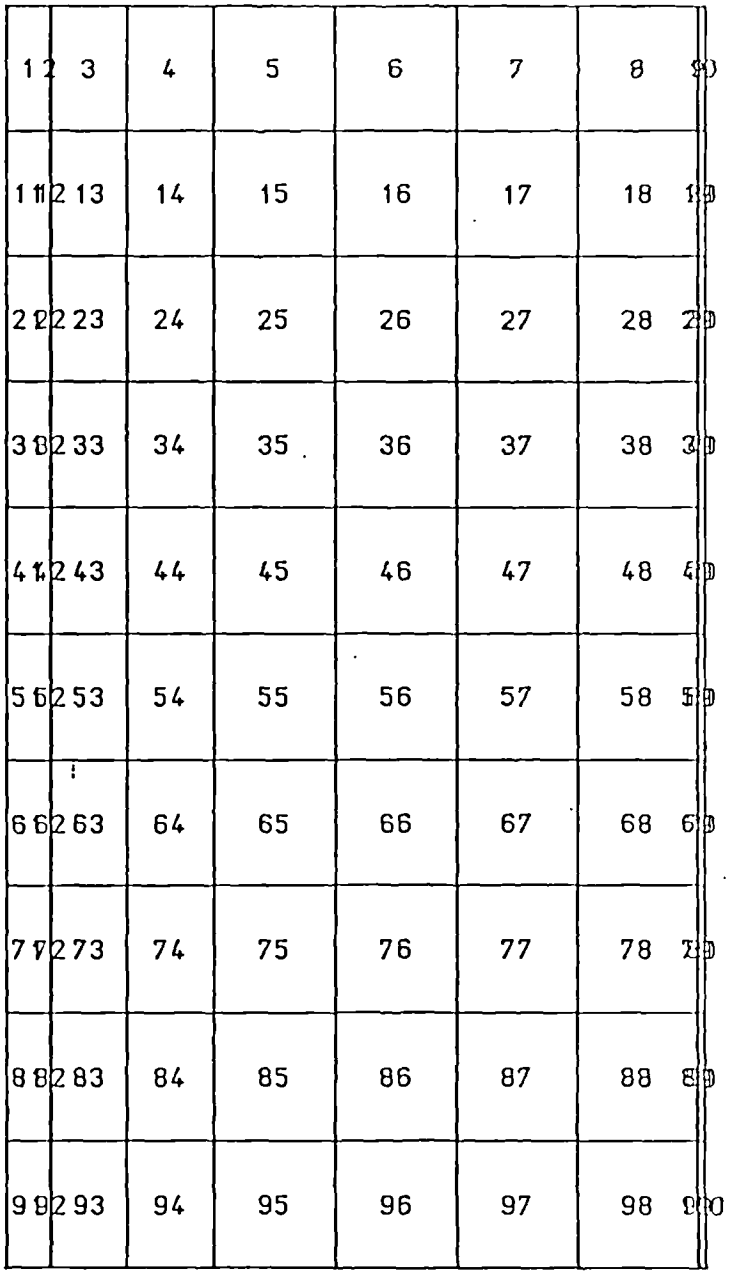

FIG. 8.3 FINITE ELEMENT MESH FOR PILE-SOIL SYSTEM SHOWING ELEMENTS NUMBERS

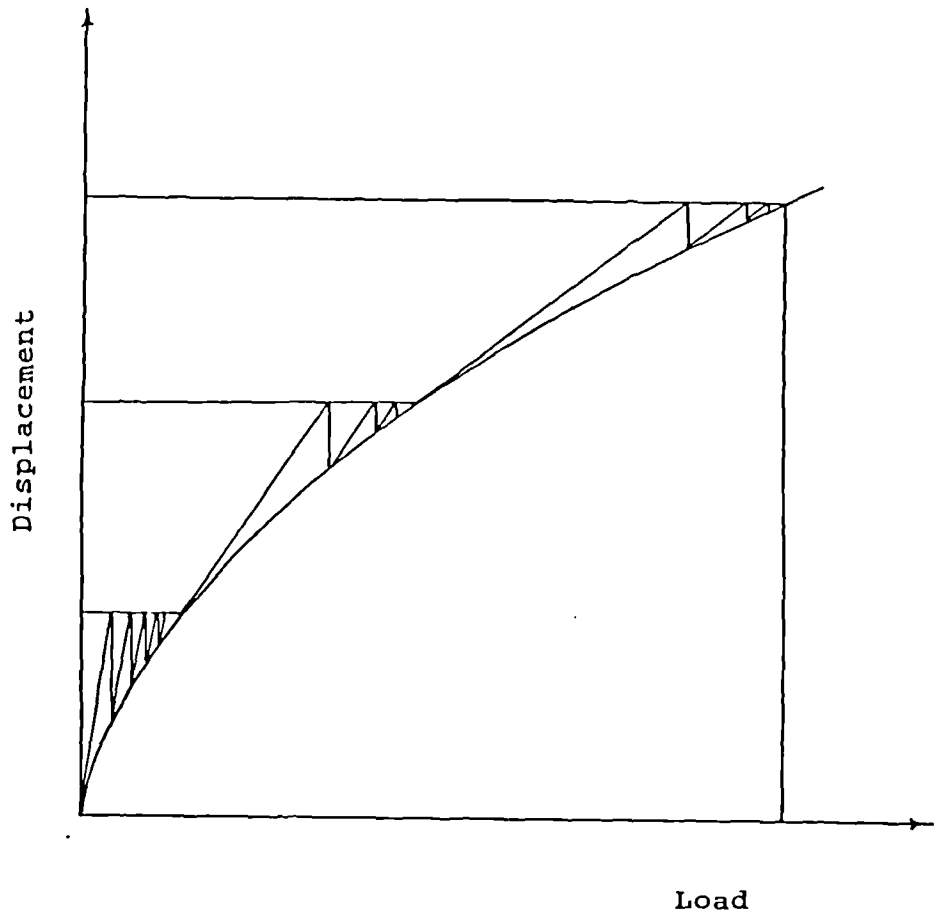

FIGURE 8.4 INCREMENTAL-ITERATIVE METHOD

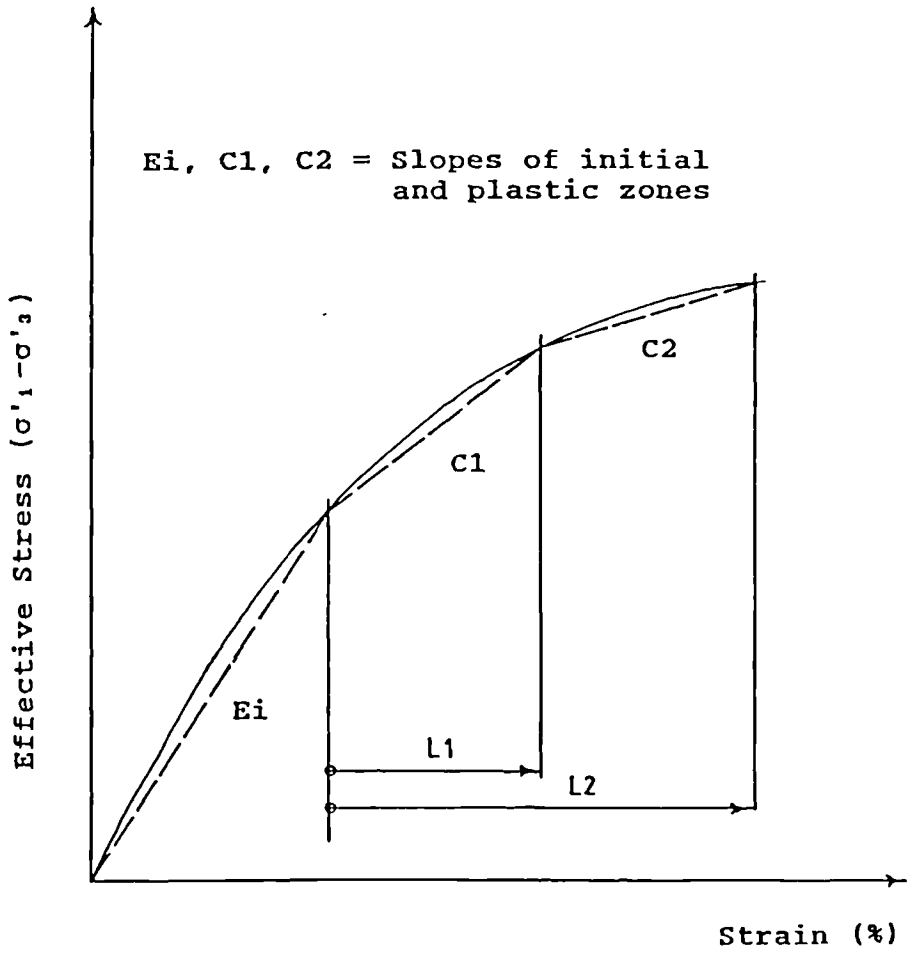

FIG. 8.5 STRESS-STRAIN RELATIONSHIP FOR NON-LINEAR MATERIAL MODELS

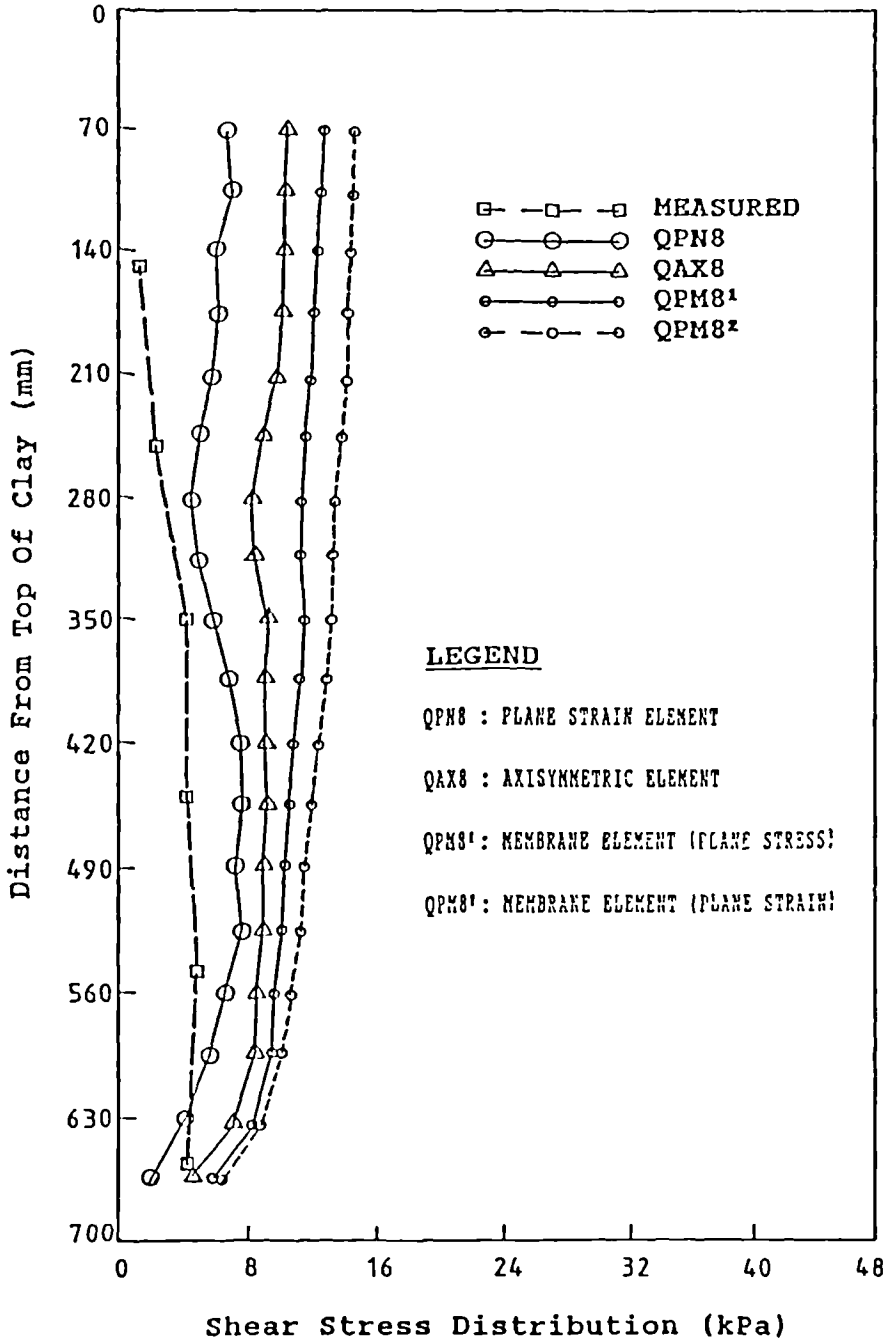

FIG. 8.6 FINITE ELEMENT SOLUTIONS FOR DIFFERENT ELEMENT TYPES COMPARED WITH MEASURED VALUES. (SURCHARGE PRESSURE =15kPa)

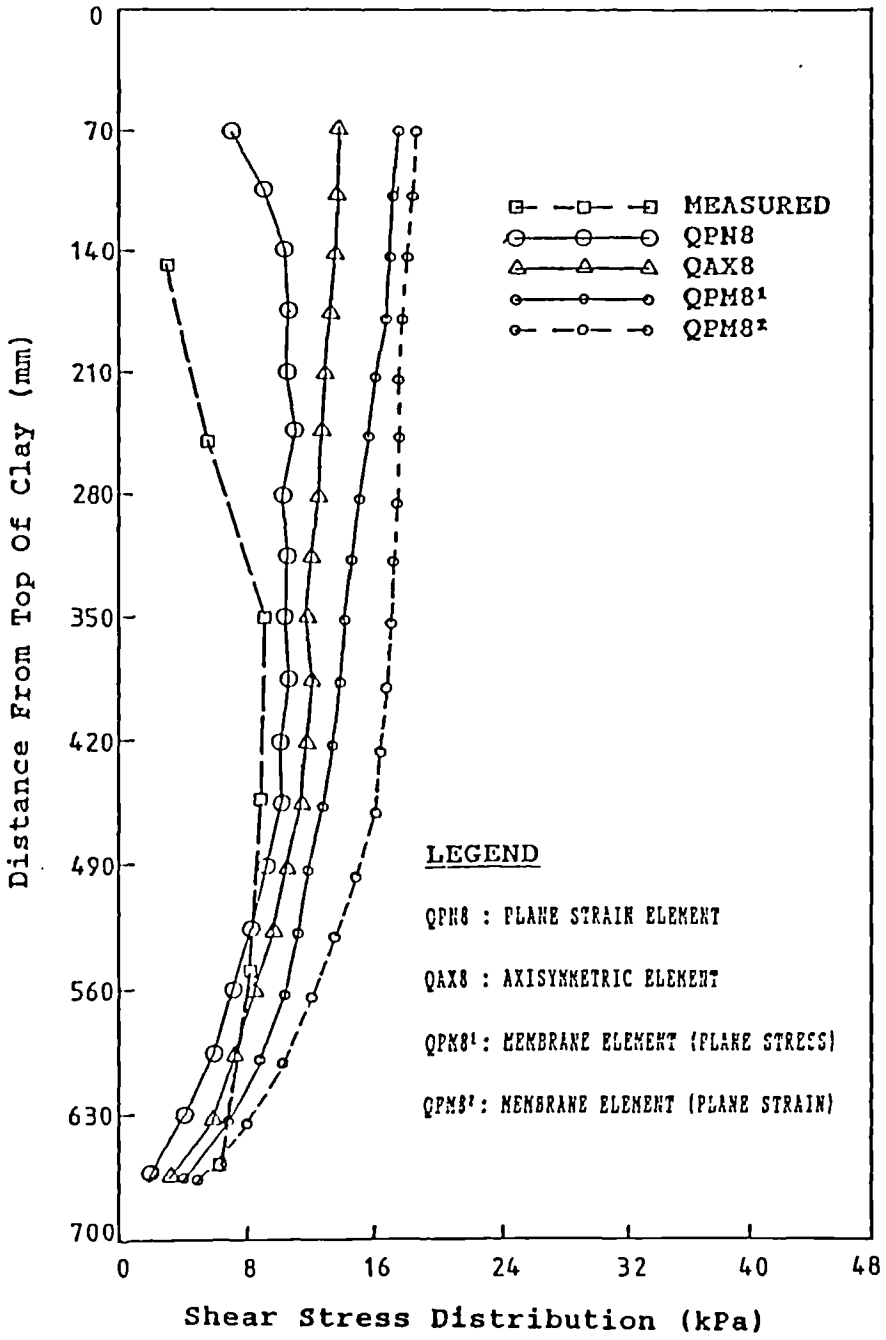

FIG. 8.7 FINITE ELEMENT SOLUTIONS FOR DIFFERENT ELEMENT TYPES COMPARED WITH MEASURED VALUES. (SURCHARGE PRESSURE =30kPa)

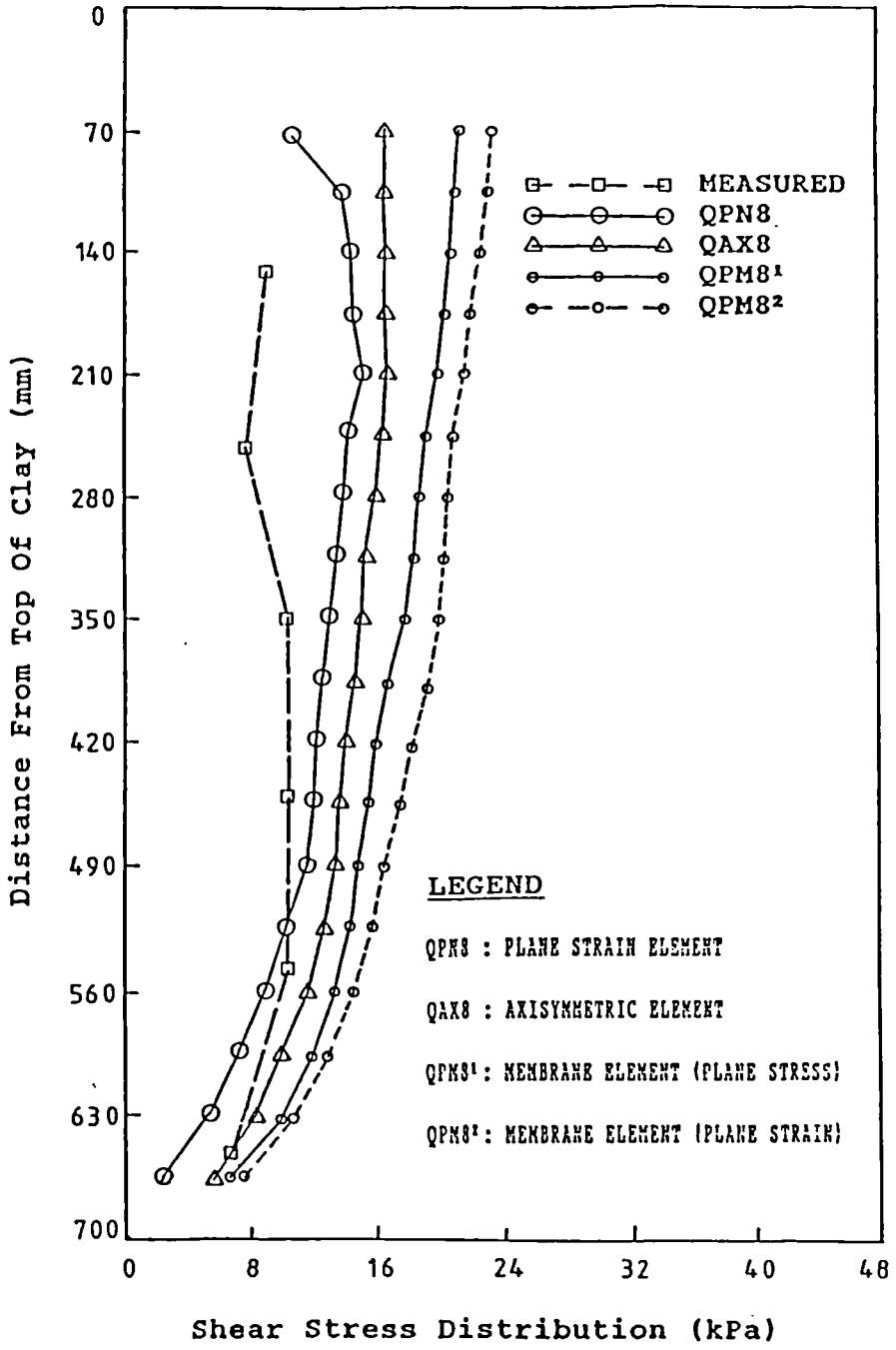

FIG. 8.8 FINITE ELEMENT SOLUTIONS FOR DIFFERENT ELEMENT TYPES COMPARED WITH MEASURED VALUES. (SURCHARGE PRESSURE =45kPa)

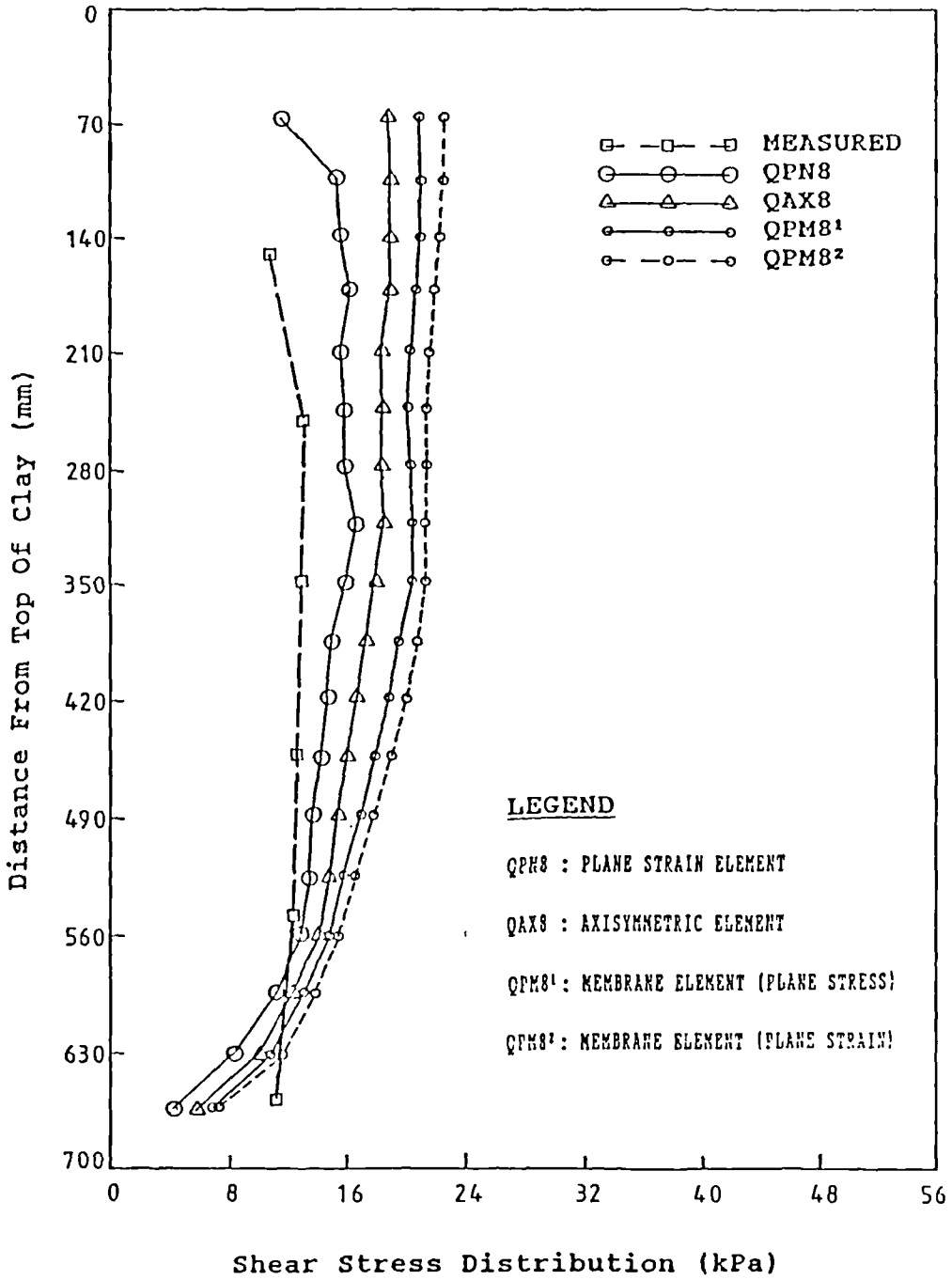

FIG. 8.9 FINITE ELEMENT SOLUTIONS FOR DIFFERENT ELEMENT TYPES COMPARED WITH MEASURED VALUES. (SURCHARGE PRESSURE =90kPa)

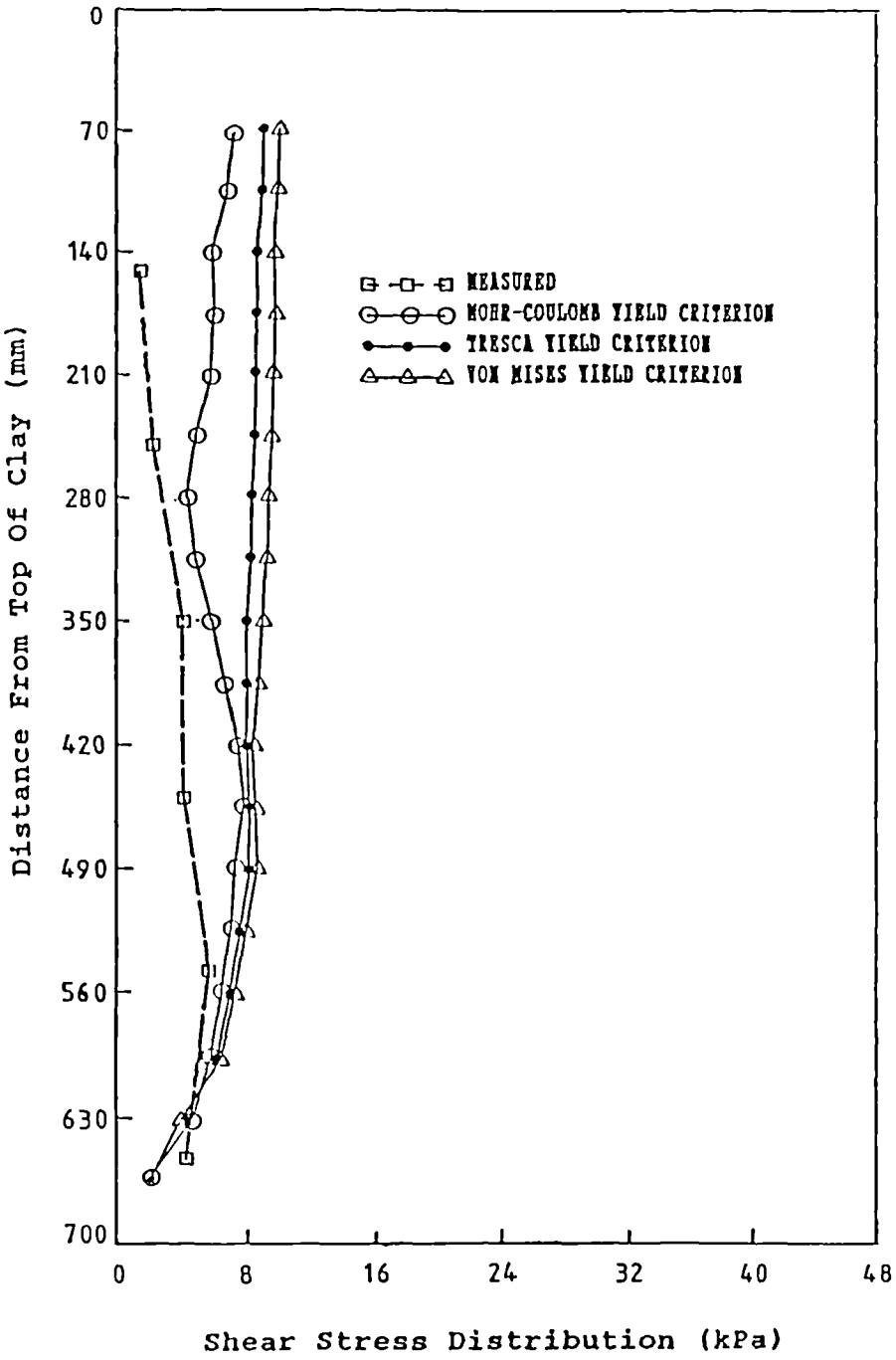

FIG. 8.10 FINITE ELEMENT SOLUTIONS FOR DIFFERENT YIELD CRITERIA COMPARED WITH MEASURED VALUES. (SURCHARGE PRESSURE =15kPa)

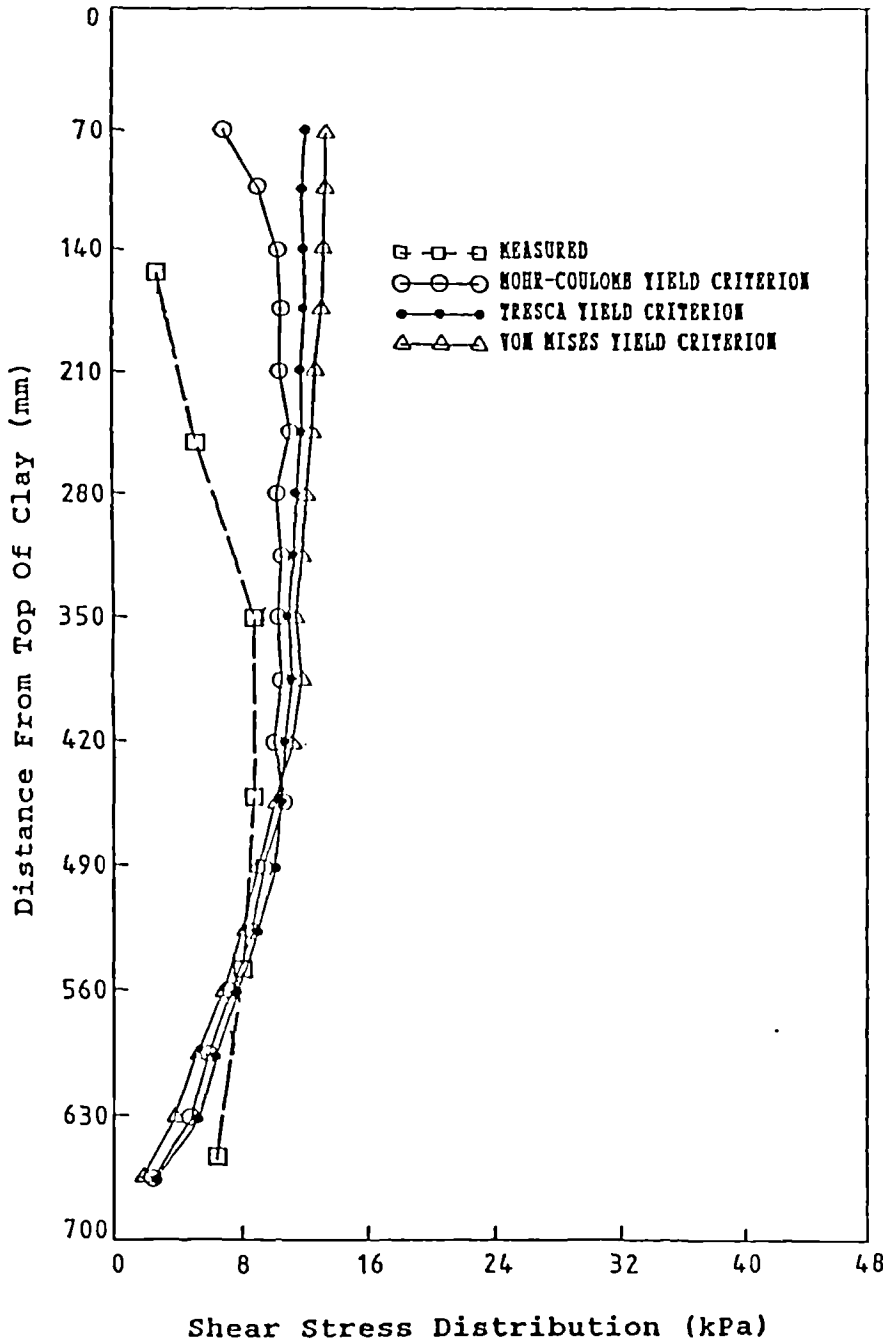

FIG. 8.11 FINITE ELEMENT SOLUTIONS FOR DIFFERENT YIELD CRITERIA COMPARED WITH MEASURED VALUES. (SURCHARGE PRESSURE =30kPa)

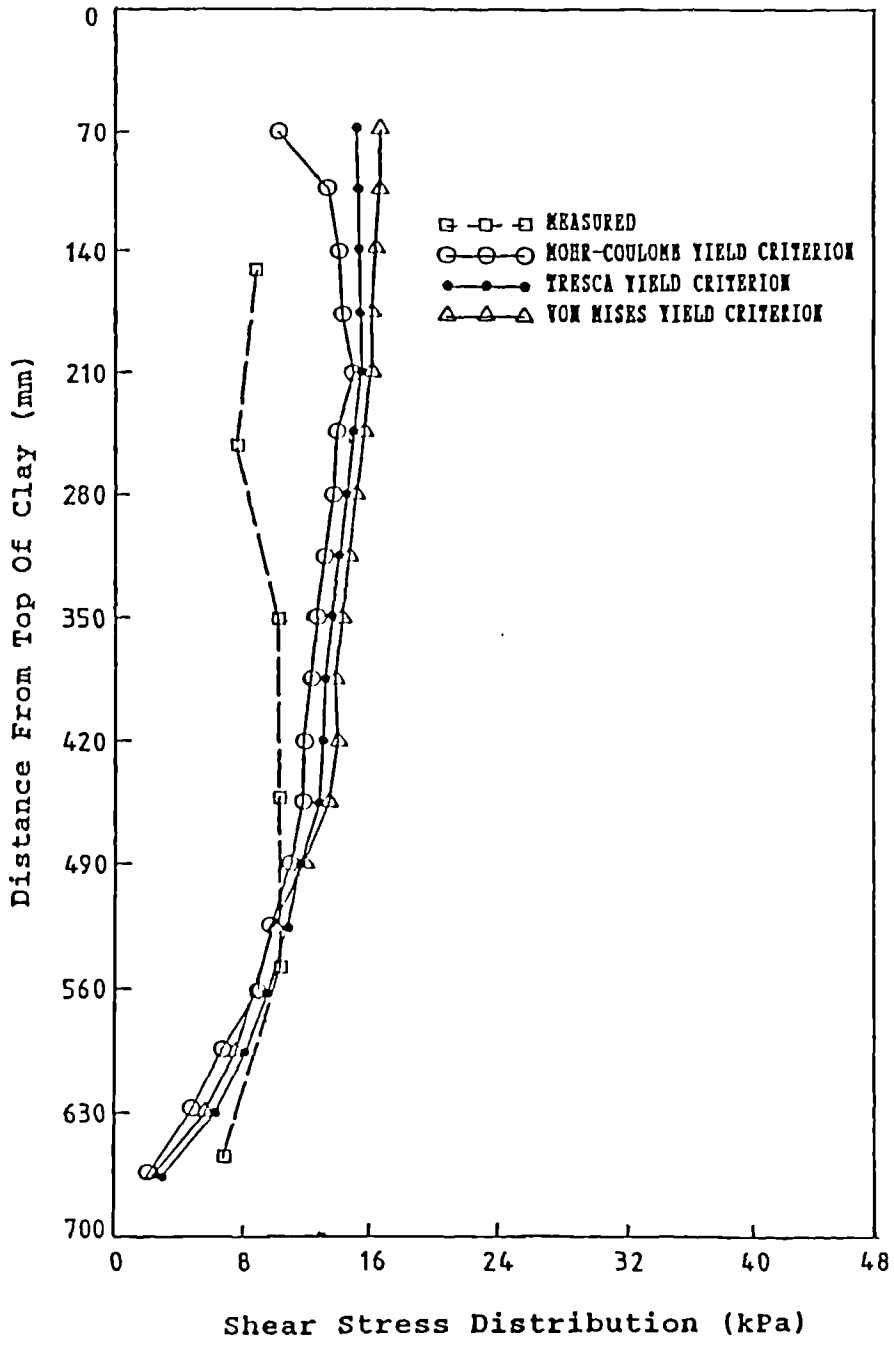

FIG. 8.12 FINITE ELEMENT SOLUTIONS FOR DIFFERENT YIELD CRITERIA COMPARED WITH MEASURED VALUES. (SURCHARGE PRESSURE =45kPa)

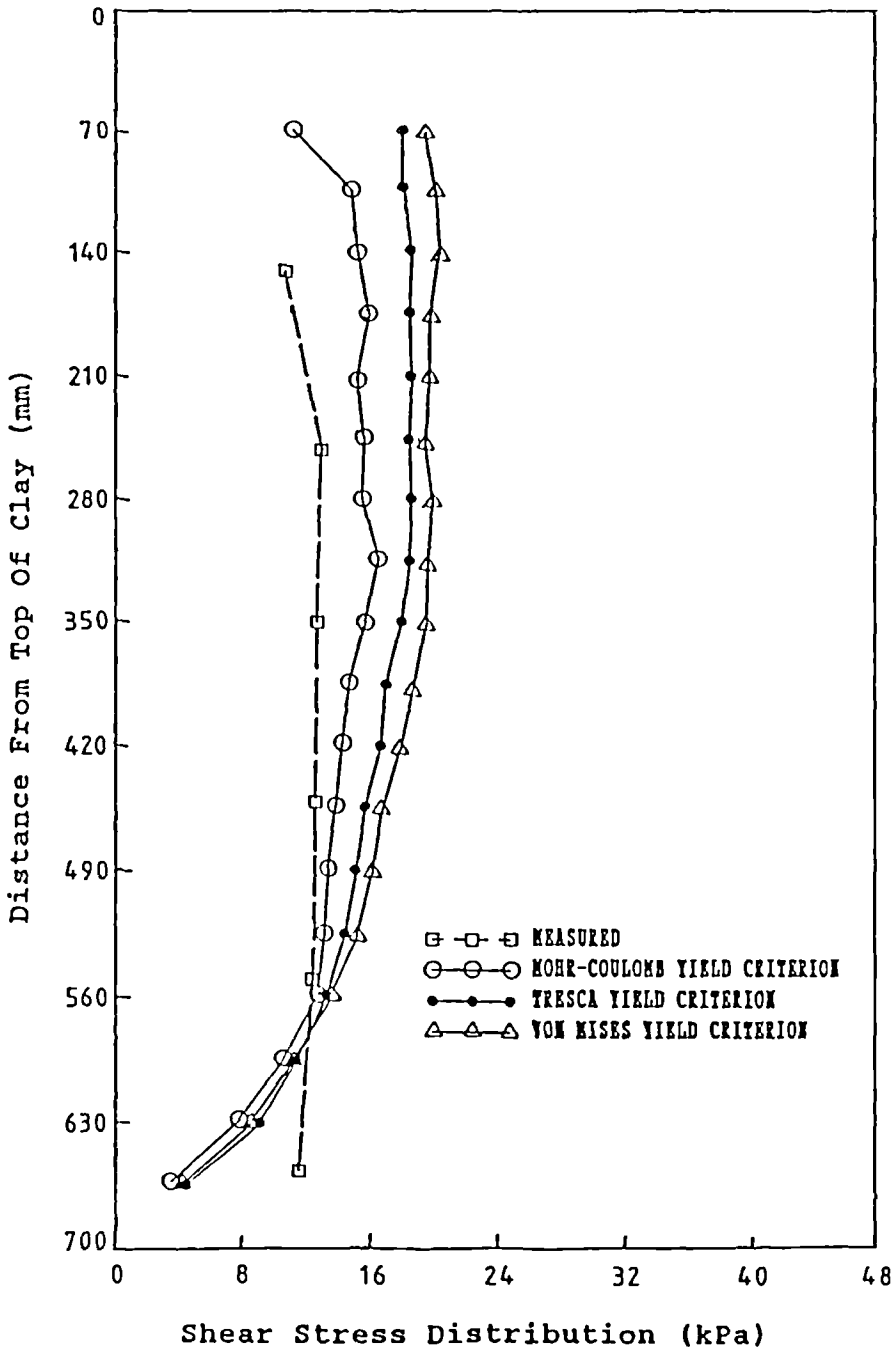

FIG. 8.13 FINITE ELEMENT SOLUTIONS FOR DIFFERENT YIELD CRITERIA COMPARED WITH MEASURED VALUES. (SURCHARGE PRESSURE =90kPa)

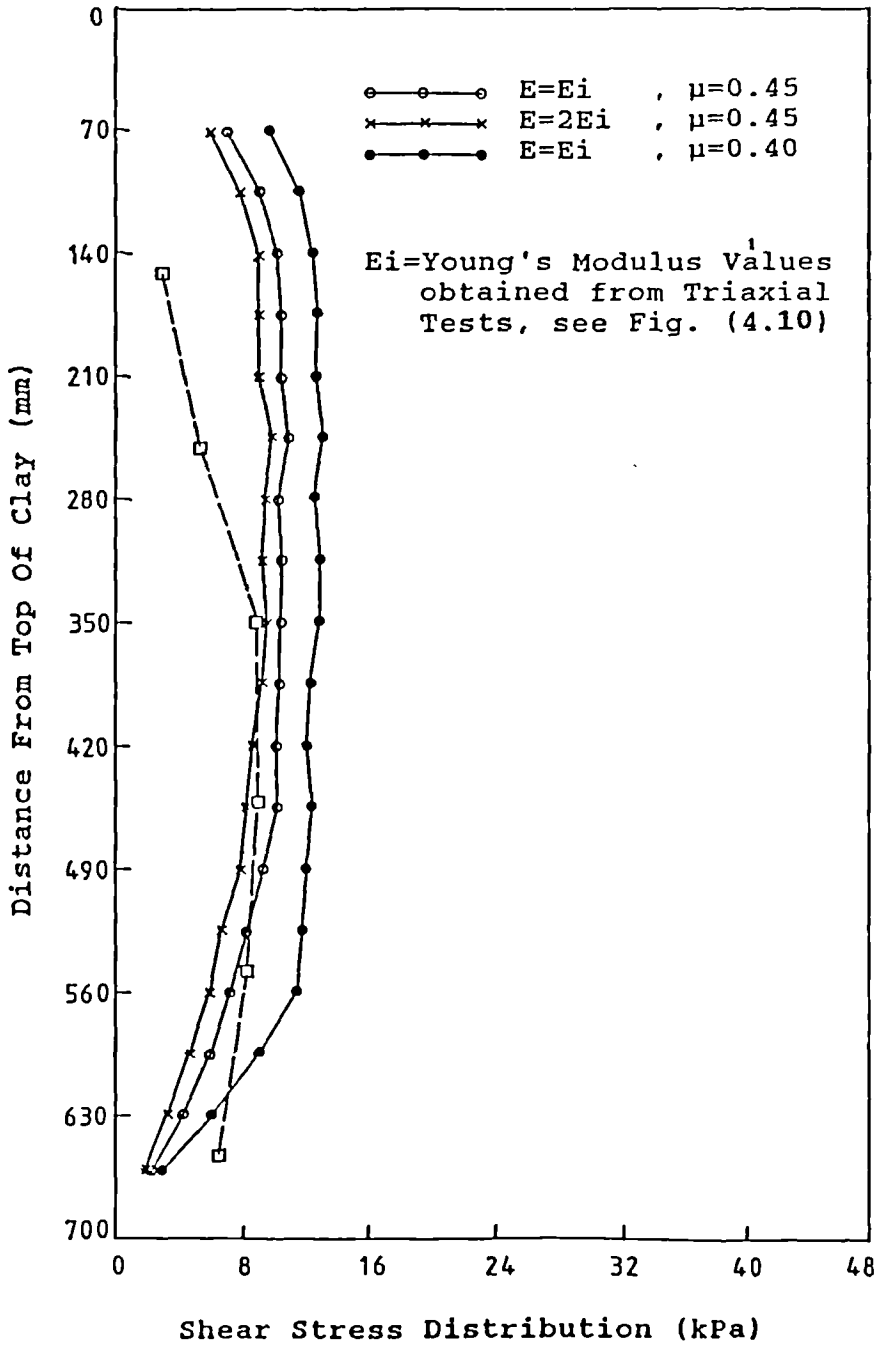

FIG. 8.14 FINITE ELEMENT SOLUTIONS FOR TWO DIFFERENT VALUES OF YOUNG'S MODULUS, E AND POISSON'S RATIO, μ. (SURCHARGE PRESSURE =30kPa)

Run No.	Material Properties Ei & μ	Surcharge Pressure (kPa)			
		15	30	45	90
1	Ei (kPa) μ	0.58×10^3 0.45	1.60×10^3 0.45	2.10×10^3 0.45	4.20×10^3 0.45
2	Ei (kPa) μ	0.58×10^3 0.40	1.60×10^3 0.40	2.10×10^3 0.40	4.20×10^3 0.40
3	Ei (kPa) μ	1.16×10^3 0.45	3.20×10^3 0.45	4.20×10^3 0.45	8.20×10^3 0.45

TABLE 8.1 YOUNG'S MODULUS, E AND POISSON'S RATIO, μ VALUES FOR THREE DIFFERENT RUNS

		Predicted Settlement (mm)			
Run No.	Material Properties	Surcharge Pressure (kPa)			
		15	30	45	90
1	E =Ei μ =0.45	6.2	9.5	12.8	15.3
2	E =Ei μ =0.40	9.4	14.5	22.7	26.6
3	E =2Ei μ =0.45	3.4	5.2	7.0	8.3

TABLE 8.2 AVERAGE SETTLEMENT OF CLAY SURFACE FOR THREE DIFFERENT RUNS

Element Type	Surcharge Pressure (kPa)	Average Settlement of Clay Surface (mm)	Maximum Slip At Pile Interface (mm)	Measured Settlement (mm)
QPN8	15	6.2	2.2	27.0
	30	9.5	3.6	48.0
	45	12.8	4.7	58.0
	90	15.3	5.3	92.5
QAX8	15	7.3	3.0	27.0
	30	11.2	4.9	48.0
	45	15.0	6.3	58.0
	90	17.9	7.1	92.5
QPM8[1]	15	23.7	4.4	27.0
	30	38.8	7.5	48.0
	45	60.3	9.2	58.0
	90	76.6	10.5	92.5
QPM8[2]	15	21.2	4.1	27.0
	30	34.5	7.0	48.0
	45	54.3	9.6	58.0
	90	68.8	10.9	92.5

TABLE 8.3 PREDICTED SETTLEMENT OF CLAY SURFACE FOR FOUR ELEMENT TYPES COMPARED WITH MEASURED RESULTS

CHAPTER (9)

CONCLUSIONS AND RECOMMENDATIONS

9.1 Introduction

In this research study an investigation of negative skin friction has been made through a model scale laboratory test on an instrumented end bearing pile in soft clay. Two testing programmes have been conducted. Each testing programme consisted of applying loading increments on the soil up to 90 kPa. Pore pressure, settlement and pile load were monitored until 90% consolidation had been achieved. The purpose of this was to:

(i) establish the magnitude and distribution of negative skin friction along the pile length for different surcharge pressures,

(ii) to monitor pore water pressures and their pattern of dissipation during the consolidation process.

Thus it was hoped that expressions relating surcharge

pressure and soil shear strength with the developed negative skin friction might be obtained. It was also hoped to numerically model excess pore pressures generated as well as the onset of negative skin friction and to test these predictions against the measured values.

Conclusions resulting from this study have been grouped into three subject areas, i.e., pore water pressure, negative skin friction, and finite element analysis. The following conclusions may be drawn for each subject:

9.2 Pore Water Pressure

(i) Driving the pile into the clay bed caused an excess pore water pressure of 35% of the overburden pressure or in terms of undrained shear strength (Cu), to 0.5Cu. The highest value was registered by the piezometer near the pile tip.

(ii) A knowledge of the magnitude and distribution of the induced pore pressures with respect to both depth and distance from the pile is essential in calculating the distribution of effective overburden pressure along the clay bed and then to estimate the magnitude of negative skin friction along the shaft. As one row of piezometers was located along the pile shaft, it was possible to calculate the distribution of vertical effective stresses

with depth according to the results of pore water pressure dissipation at different loading stages which could then be utilised in the negative skin friction calculations.

(iii) An analysis of the pore pressure readings of all loading stages revealed continous dissipation of pore water pressure with time, a maximum value being at the mid- depth of the clay bed. On the other hand, plots of pore pressure readings versus horizontal distance from the pile surface revealed significant lateral variation at some of the loading stages, i.e. a maximum difference between points along the pile shaft and at 200mm apart from it was of the order of 2.0 kPa. It is realized that this value, in absolute terms, is small but when considered relative to the other values of pore water pressure, it becomes significant in this respect.

(iv) Numerical analysis using a finite difference approximation method for the three dimensional process of consolidation has led to the conclusion that the size of the initial excess pore pressure is overpredicted. This was attributed to the assumptions made in order to simplify the solution, namely, a) an equivalent value of the coefficient of consolidation was assumed in the analysis which was determined from the one dimensional oedometer test, and b) the variation of the consolidation parameters C_v, C_r with depth and time were not taken into account.

9.3 Negative Skin Friction

(i) In all stages within the testing programmes, it was shown that a significant build-up of downdrag has occurred under increasing consolidation pressure. A value of 1.3 kPa (0.2 Cu) was registered due to the self-weight of the soil layer and approximately 60% of the maximum negative skin friction was developed during the first 7 days after surcharge application.

(ii) The results clearly show that the time-dependent build-up of downdrag is controlled by the rate of consolidation of the clay bed or, alternatively, by the degree of dissipation of excess pore water pressure. The time required for 90% consolidation ranged between 35-40 days for all loading stages.

(iii) At early stages of surcharge application, the maximum negative skin friction was registered at mid-depth of the clay bed. As surcharge increased additional negative skin friction was measured at the lower region of the pile until a limiting value was reached at the end of the consolidation stage. The existence of an ultimate value of downdrag is dependent upon the shear strength-displacement characteristics of the medium considered. The type of soft clay used exhibited an elastic-plastic shear strength-displacement relationship. The ultimate or

residual value of downdrag was therefore maintained under an increasing shear strain.

(iv) The soil-pile system was such that the pile was relatively incompressible in contrast with full-scale piles where the compression of the pile could be significant. The model pile used herein will compress, under a surcharge pressure of 60 kPa, only 0.013mm which is very small compared to the settlements within the clay stratum. It may therefore be concluded that the relative deflection between the pile and the soil, in this project, was due only to the clay settlement.

(v) Both effective and total stress methods were employed for negative skin friction predictions. For the effective stress analysis, values of β ($\beta=K.\tan\phi'$) were obtained by dividing the measured negative skin friction by the effective vertical stress at each point along the pile shaft. A set of graphs representing the determination of β values for each loading stage within the testing programmes have been presented. An average value of 0.20 for β was determined which is believed to be consistent with the findings of others.

For the total stress analysis, adhesion factor values (α) were obtained by two different methods depending on the undrained shear strength of the clay layer, i.e., 1) based on the initial undrained shear strength (Cu_o), and 2) based on the shear strength of the clay at the time

when negative skin friction readings were taken (Cu).

Adhesion values (α) by both methods were plotted against the degree of consolidation of the clay layer and against the settlement ratio (defined as the settlement of clay surface divided by the depth of clay layer). Results showed that a variation of 10% for the degree of consolidation would produce an increase of 2% and 5% of α values based on the calculated and the initial undrained shear strengths respectively.

The rate of increase of α based on the initial undrained shear strength was approximately 25% for every 2% increase in the settlement ratio, while the rate of increase of α determined from the calculated values of undrained shear strength reached a limiting value of approximately 0.6 at a settlement ratio of 10%.

(vi) An expression has been presented relating negative skin friction with both the consolidation pressure and the initial undrained shear strength. An application of this expression to model and field studies revealed an underestimation of the negative skin friction values in comparison with the measured results. However, this expression tended to identify some of the important factors which should be accounted for in any theoretical treatment of the problem of negative skin friction.

9.4 Finite Element Analysis

The aim of the finite element analysis described in this research study was to determine whether the finite element method would yield comparable results with respect to those measured when input from the experimental pile-soil model and the related material properties were used.

A two-dimensional finite element model was adopted in this analysis using an existing computer programme, LUSAS. Thin layer elements or interaction elements were incorporated at the boundary between the pile and the soil. The thickness of each element was chosen in such a way that it complied with the limits suggested by Desai (1982). Many computer runs were performed using different parameters which would have an influence on the results of both negative skin friction and settlement:

(a) Four various element types were used, those are (i) plane strain element, (ii) axisymmetric element, (iii) membrane plane strain element and (iv) membrane plane stress element. Regarding the distribution of negative skin friction, results obtained by the PLANE STRAIN ELEMENT showed good agreement with the measured results. On the other hand, when considering settlement results, values obtained using the MEMBRANE PLANE STRAIN ELEMENT produced good agreement with the measured results.

(b) Several runs were also conducted using different values of Young's modulus, E and Poisson's ratio μ.

Results have shown that varying μ values has a significant effect on both the negative skin friction values and on the settlement values, i.e., reducing μ by 12% resulted in a 25% and 38% increase in negative skin friction and settlement respectively. On the other hand changing E values showed a large influence on the settlement but only little effect on the negative skin friction values, i.e., doubling E values resulted in 50% reduction in settlement and 14% reduction in negative skin friction.

(c) It was shown that the results can also be affected by the type of yield criterion used, i.e., Mohr-Coulomb criterion appeared to be most suitable for the problem considered than other criteria (Von-Mises or Tresca).

9.5 Recommendations For Future Work

It was felt, during and after this research study, that the following recommendations are necessary :

1) It would be valuable to extend the present investigation to large field scale study.

2) As piles are seldom installed singly in practice, the understanding of negative skin friction of group behaviour should be investigated.

3) Instrumentation for future research should be designed

to accomodate the ability of measuring the effective lateral stresses and also monitoring pore water pressure in the vicinity of the pile.

4) Research is needed to explore the effect of pile material, shape, diameter and type of soil on the developed negative skin friction.

5) Regarding numerical analysis, finite element and finite difference methods, a desirable starting point for further research will be to account for all the factors that have a direct effect on negative skin friction and also to include or model the dissipation of pore water pressure as the pattern of dissipation of this pressure controls the stress conditions in the soil mass and accordingly affects the distribution of negative skin friction.

6) Finally, it is suggested that the finite element method should be used in conjunction with a detailed full-scale testing programme.

APPENDIX (I)

REDUCTION OF EFFECTIVE OVERBURDEN PRESSURE DUE TO NEGATIVE SKIN FRICTION, BY ZEEVAERT (1973)

The procedure suggested regarding reduction of effective stresses due to a "hanging up" effect is outlined below :

Assuming the pile is rigid compared to the soil, the transfer of pressure is expressed by the following formula:

$$d(P_{oz}' - P_{vz}')/dz = c.\tau_{p-s} \quad \ldots \quad 1$$

where

P_{oz}' = initial effective vertical pressure in soil

P_{vz}' = reduced effective vertical pressure in soil

z = depth below ground ~~surface~~ surface

c = perimeter of pile

τ_{p-s} = ultimate shear resistance along the pile shaft

The shear resistance (τ_{p-s}) was assumed to be a function of P_{vz}' as follows:

$$\tau_{p-s} = \tan\phi'.k.P_{vz}'$$

By introducing $P_{oz}' = P_o' + \gamma'_s \cdot z$ (where γ'_s = submerged

unit weight of the soil), then equation 1 becomes :

$$dP_{vz}'/dz + M1\ P_v' = \gamma'_s \qquad \ldots \quad 2$$

where M1 = c.k.tanδ'

The solution of equation 2 must fulfil the boundary condition P_{vz}' (at z=0) = P_o'

By differentiation, equation 2 becomes:

$$P_{vz}' = (\gamma'_s/M1)\ (1-\exp^{-M1 \cdot z}) + P_o'.\exp^{-M1 \cdot z} \qquad \ldots \quad 3$$

Equation 3 above represents the reduced vertical pressure in the soil after the load transfer due to consolidation of the soil surrounding the pile has taken place.

Numerical Example:

To calculate the % reduction of vertical stress at the pile tip due to "hanging up", the following example demonstrates this for a surcharge pressure of 30 kPa where the value of effective stress at the pile tip is 36.02 kPa, refer to Fig. 6.5.

γ'_s = 17.6 kN/m³ , z=0.7m , P_o'=30.7 kPa

M1 = 0.05.π.(0.5).tan20.7°

= 0.0297

$$\exp^{-M.z} = \exp^{-0.0297 \times 0.7} = 0.9704$$

By applying equation 3,

$$P_{vz}' = 17.6/0.0297\ (1.0-0.9794) + 30.7\ (0.9794)$$

$$=35.34 \text{ kPa}$$

$$\% \text{ Reduction} = (36.02-35.34)/35.34(100)$$

$$= 4\%$$

APPENDIX (II)

NUMERICAL SOLUTION COMPUTER PROGRAMME AND SPECIMEN RESULTS FOR THREE DIMENSIONAL CONSOLIDATION

```
100$RESET FREE '
110       DIMENSION U(11,11,50)
120       WRITE(6,1)
130     1 FORMAT(' M , N , Uo , α , T , Cv , H '//)
140       READ/,M,N,Uo,α,T,Cv,H
150       DT1=(α*H**2/Cv)*365*24
160       TT=DT1/24
170       WRITE(6,2)
180     2 FORMAT(71H NUMERICAL SOLUTION PROGRAMME OF A THREE
          'DIMENSIONAL CONSOLIDATION PROBLEM/)
190       WRITE(6,3)Uo,α,Cv,DT1,H
200     3 FORMAT(' Uo(kPa)=',F5.2/,'ALPHA  =',F4.2/,' Cv(M²/Yr)
210       '=',F4.2,' DT1(hrs)   =',F5.2,' H(m)     ='/F4.2//)
220       DO 20 I=1,M
230    20 U(1,I,1)=0.0
240       DO 30 I=2,N+1
250    30 U(1,M,1)=0.0
260       DO 40 I=2,N+1
270       DO 40 J=1,M-1
280    40 U(I,J,1)=Uo
290       DO 70 IT=2,T
300       DO 60 IR=2,M-1
310       DO 60 JZ=2,N
320       RO=FLOAT(IR-2)
330       IF(RO.LE.0.0)GO TO 45
340       U(JZ,IR,IT)=α*(U(JZ,IR+1,IT-1)+U(JZ-1,IR,IT-1)+U(JZ,
350       'IR-1,IT-1)+U(JZ+1,IR,IT-1)-4.*U(JZ,IR,IT-1)+(U(JZ,IR
360       '+1,IT-1)-U(JZ,IR-1,IT-1))/(2.0*RO))+U(JZ,IR,IT-1)
370       U(JZ,1,IT)=U(JZ,3,IT)
380       U(N+1,IR,IT)=U(N-1,IR,IT)
390       GO TO 60
400    45 U(JZ,IR,IT)=α*(2.*U(JZ,IR+1,IT-1)+U(JZ-1,IR,IT-1)+2.
410       '*U(JZ,IR-1,IT-1)+U(JZ+1,IR,IT-1)-6.*U(JZ,IR,IT-1))+U
420       '(JZ,IR,IT-1)
430       U(N+1,IR,IT)=U(N-1,IR,IT)
440    60 CONTINUE
450    70 CONTINUE
460       DO 90 K=1,T
470       IF(K.EQ.1)GO TO 72
480       DT=DT+DT1*(K-1)
490       TT=DT/24
500       GO TO 75
510    72 DT=0.0
520       TT=DT/24
530    75 WRITE(6,81)TT
540       DT=0.0
550       TT=0.0
560    81 FORMAT(10H T(DAYS)  =,I3)
570    90 WRITE(6,95)((U(I,J,K),J=2,M),I=1,N)
580       STOP
590    95 FORMAT(1X,5F9.2,///)/////)
600       END
```

NUMERICAL SOLUTION PROGRAMM OF A THREE
DIMENSIONAL CONSOLIDATION PROBLEM :
Uo (kPa) = 30.00
⊙ = 0.15
Cv (m^2/yr) = 0.21
DT1 (Hrs) = 50.68
H (m) = 0.09

T(DAYS) = 0

0.00	0.00	0.00	0.00	0.00
30.00	30.00	30.00	30.00	0.00
30.00	30.00	30.00	30.00	0.00
30.00	30.00	30.00	30.00	0.00
30.00	30.00	30.00	30.00	0.00

T(DAYS) = 2

0.00	0.00	0.00	0.00	0.00
25.50	25.50	25.50	20.25	0.00
30.00	30.00	30.00	24.75	0.00
30.00	30.00	30.00	24.75	0.00
30.00	30.00	30.00	24.75	0.00

T(DAYS) = 4

0.00	0.00	0.00	0.00	0.00
22.35	22.35	21.37	15.00	0.00
29.32	29.32	28.34	20.40	0.00
30.00	30.00	29.02	21.08	0.00
30.00	30.00	29.02	21.08	0.00

T(DAYS) = 6

0.00	0.00	0.00	0.00	0.00
20.04	19.82	18.12	11.73	0.00
28.38	28.16	26.02	17.11	0.00
29.90	29.68	27.54	18.28	0.00
30.00	29.78	27.64	18.38	0.00

T(DAYS) = 8

0.00	0.00	0.00	0.00	0.00
18.15	17.73	15.58	9.52	0.00
27.22	26.67	23.63	14.60	0.00
29.55	29.00	25.83	16.08	0.00
29.84	29.28	26.11	16.29	0.00

T(DAYS) = 11

0.00	0.00	0.00	0.00	0.00
16.54	15.96	13.56	7.95	0.00
25.88	25.04	21.40	12.63	0.00
28.91	28.02	24.07	14.29	0.00
29.42	28.53	24.54	14.60	0.00

NUMERICAL SOLUTION PROGRAMM OF A THREE
DIMENSIONAL CONSOLIDATION PROBLEM :
Uo (kPa) = 60.00
⊙ = 0.15
Cv (m^2/yr) = 0.26
DT1 (Hrs) = 40.94
H (m) = 0.09

T(DAYS) = 0

0.00	0.00	0.00	0.00	0.00
60.00	60.00	60.00	60.00	0.00
60.00	60.00	60.00	60.00	0.00
60.00	60.00	60.00	60.00	0.00
60.00	60.00	60.00	60.00	0.00

T(DAYS) = 2

0.00	0.00	0.00	0.00	0.00
51.00	51.00	51.00	40.50	0.00
60.00	60.00	60.00	49.50	0.00
60.00	60.00	60.00	49.50	0.00
60.00	60.00	60.00	49.50	0.00

T(DAYS) = 3

0.00	0.00	0.00	0.00	0.00
44.70	44.70	42.73	30.00	0.00
58.65	58.65	56.68	40.80	0.00
60.00	60.00	58.03	42.15	0.00
60.00	60.00	58.03	42.15	0.00

T(DAYS) = 5

0.00	0.00	0.00	0.00	0.00
40.09	39.64	36.25	23.46	0.00
56.76	56.32	52.04	34.23	0.00
59.80	59.35	55.07	36.56	0.00
60.00	59.56	55.28	36.76	0.00

T(DAYS) = 7

0.00	0.00	0.00	0.00	0.00
36.31	35.47	31.16	19.05	0.00
54.45	53.34	47.27	29.20	0.00
59.11	58.00	51.66	32.15	0.00
59.67	58.57	52.22	32.58	0.00

T(DAYS) = 9

0.00	0.00	0.00	0.00	0.00
33.08	31.92	27.12	15.90	0.00
51.76	50.08	42.80	25.27	0.00
57.83	56.04	48.14	28.59	0.00
58.84	57.05	49.08	29.21	0.00

FOUNDATIONS & TUNNELS-89

PROCEEDINGS

SECOND INTERNATIONAL CONFERENCE on FOUNDATIONS AND TUNNELS

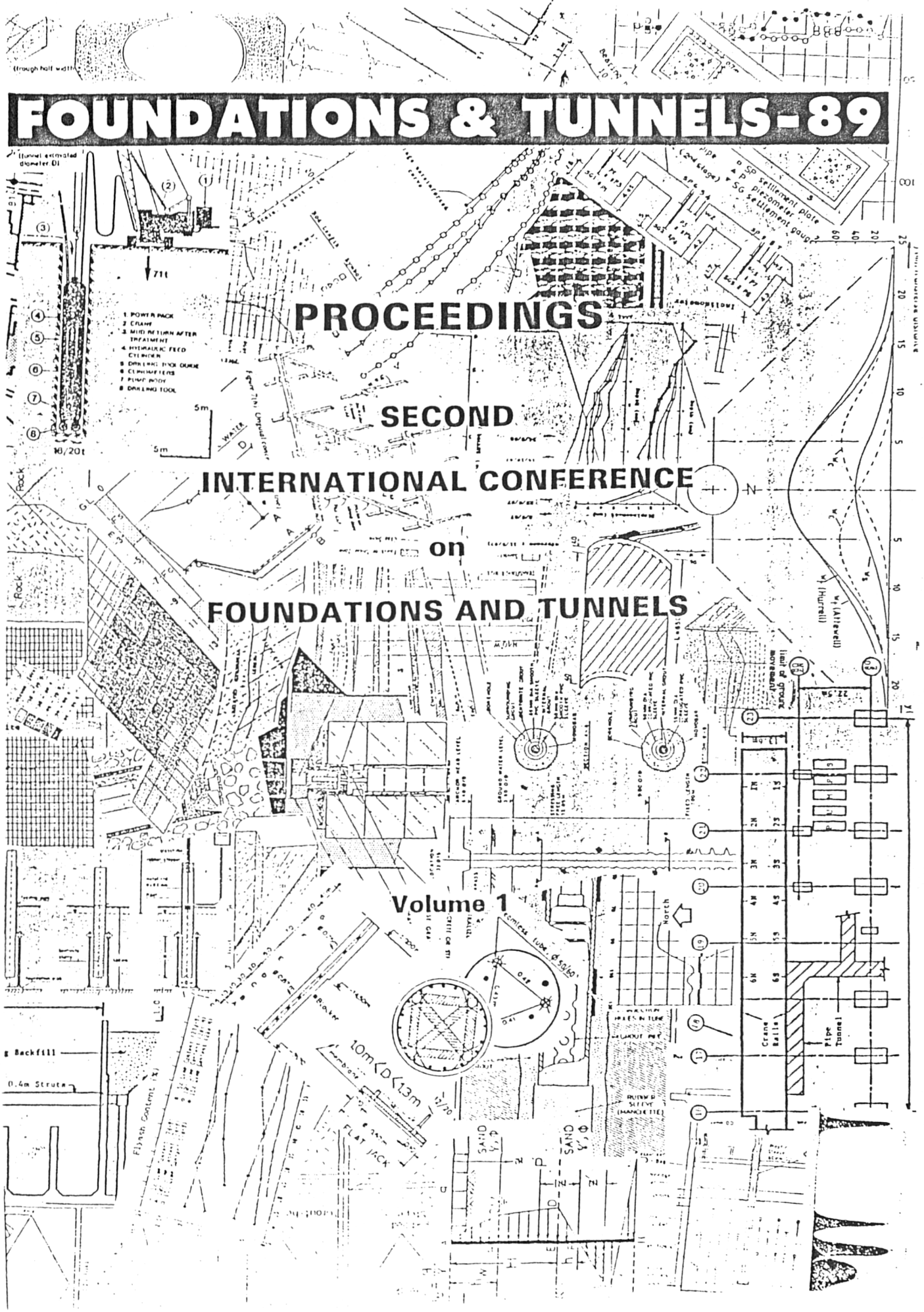

Volume 1

THE DEVELOPMENT OF SHAFT ADHESION WITH ONSET OF NEGATIVE SKIN FRICTION FOR A FIXED BASE MODEL PILE

J. A. Little, BSc, MSc, PhD, CEng, MICE, FGS,
Department of Civil Engineering, Heriot-Watt University, Edinburgh
and T. M. Toma, BSc, MSc, Department of Civil Engineering, Heriot-Watt University, Edinburgh

Synopsis

The paper describes a laboratory study on an instrumented pile embedded in soil undergoing surcharge-induced consolidation causing negative skin friction. Instrumentation consisting of miniature piezometers and electrical resistance strain gauges is described which has enabled the progression of negative skin friction with soil consolidation to be monitored. The variation of downdrag force vertically and with surcharge pressure is described and values for the calculated adhesion coefficients determined with respect to both total and effective stresses are reported.

Introduction

Pile negative skin friction, when neither recognised nor sufficiently accounted for in design can lead to serious foundation failures, eg. Chellis (1961), and a number of such failures in different parts of the world attributed to negative skin friction have been reported by Broms (1979). While in some of these reported cases structural damage was not severe, in other cases complete structural collapse occurred.

The onset of negative skin friction is due to consolidation of soil immediately adjacent to a pile. The magnitude of such consolidation is governed by factors such as the properties of the soil around the pile or pile group, the size of any surcharge load present, and changes in the level of the groundwater table.

Conservative methods have been developed eg the total and effective stress methods for prediction of pile load values for positive friction situations, and these methods have also been used in the estimation of negative skin friction.

In a total stress analysis the maximum negative skin friction (Fns) is evaluated from the undrained shear strength of the soil (cu) according to equation 1.

$$Fns = \alpha \, cu \qquad ....(1)$$

In this expression α is an adhesion factor (Tomlinson, 1977) which expresses the mobilised pile /soil adhesion as a ratio of the undrained shearing resistance of the soil. The value of α will depend on the method of pile installation and pile material as well as soil type.

In the effective stress method (the so-called Beta method) the maximum negative skin friction is calculated according to equation 2.

$$Fns = Ko \; \sigma vo' \; \tan\phi' \qquad ....(2)$$

where Ko = coefficient of lateral earth pressure at rest

$\sigma vo'$ = effective overburden pressure

$\tan\phi'$ = tangent of the effective stress friction angle for the soil.

Writing β for $K_o \tan\phi'$ equation 2 may also be written:

$$F_{ns} = \beta \sigma_{vo}' \quad ....(3)$$

Garlanger (1973) quoted values for β in the range 0.2 (clay) to 0.5 (sand). Test data presented by Bjerrum et al (1969) from instrumented steel pipe piles indicated that the coefficient for soft clay varied between 0.18 and 0.26, whilst Endo et al (1969) found that varied between 0.2 and 0.35 for different types of steel piles.
The Beta method is regarded as providing an upper bound estimate of the downdrag load acting on a single vertical pile. It is applicable when significant relative movement or slippage occurs between soil and pile. An overestimation of the negative skin friction will occur when surface settlement is not sufficient to produce full slippage. The method is also applicable when the pile group spacing is less than 4 to 5 times the pile diameter. An overestimate of downdrag occurs when the spacing exceeds this.
Broms (1979) reported that both the effective stress and total stress methods give similar results for soft normally consolidated silts and clays.
The literature indicates that other approaches have been suggested for calculating negative skin friction and downdrag forces on piles based on the results of laboratory and field tests. At the present time however there is no single ideal solution available. The approach to the problem is still therefore largely empirical with reliance on the results of model or full-scale tests. The latter provide particularly valuable information but tend to be very expensive.
Laboratory-scale studies are far less expensive and can be readily designed to investigate specific aspects. The shearing stress - displacement characteristics required for the effective stress method for example can readily be determined in laboratory studies on soil samples remoulded at constant water content and then consolidated by increasing the effective stresses and sheared off under zero excess pore pressure. The average degree of consolidation of the soil close to the pile shaft can then either be computed from known consolidation characteristics or, preferably, can be measured directly using implanted piezometers. In this context there is a particular need for studies which add to the growing bank of data relating to particular soil and pile types.

The study

The Forth Estuary in Scotland presents a set of challenging foundation conditions to the geotechnical engineer due mainly to the considerable thickness of glaciomarine and postglacial sediments present, particulary near to Grangemouth. Gostelow and Browne (1986) reported an average thickness of between 50-60m for these soft sediments, increasing locally to over 190m north of Bo'ness.
The majority of the large structures asssociated with the petroleum refining industry of Grangemouth are therefore piled either to gravel or to till underlying the clay .
The problems already mentioned concerning the design of such foundations from the point of view of negative skin friction are therefore also extremely pertinent here.
With this in mind a laboratory study was commenced in 1986 to investigate the mechanisms of negative skin friction in the postglacial 'carse' clay of the Forth Estuary .
Specifically, the aims of the study were:

(i) to study the interaction between a fixed base pile and surrounding soil undergoing consolidation induced by surcharge.

(ii) to examine and quantify the distribution and size of the negative skin friction and hence the total downdrag force generated.

(iii) to relate the changing effective stresses in the soil at the pile soil interface to the developed negative skin friction.

A convenient landsite was chosen in the upper Forth from which a sufficient quantity of soil could be sampled.
The results of basic soil classification tests in accordance with BS1377 indicated a soil with a liquid limit of 55 and a plastic limit of 30. The natural water content was 55% ; the liquidity index was therefore 1.20. A grain size determination showed 0.5% by weight fine sand, 61.5% silt and 38% clay ; the activity of the soil was therefore 0.66 (cf 0.74 quoted by Skempton, 1953, for Grangemouth Late Glacial Estuarine clay). The bulk unit weight was 17.4 kN/m3 and the particle specific gravity 2.62. In the study described the soil was used in its remoulded state, at its natural water content.

Testing apparatus

Fig. 1 shows the apparatus used in the study. The basic features were a steel circular tank of dimensions 1.0m height, 0.8m diameter containing a thin-walled brass pipe pile of 50mm outer diameter and 1.0mm wall thickness. This pile was made up in six sections instrumented internally with electrical resistance strain gauges. Following its calibration, the instrumented pile was introduced into the soil by displacement. Drainage was permitted at the top and bottom surfaces of the soil by sand layers and radially by 2mm thick filter fabric.
Consolidation was induced in the soil by application of pressure to the top surface of the soil through a water filled cylindrical rubber bag (800mm dia. by 150mm deep) bearing against a lid adjustable either up or down by means of four long tie bolts.

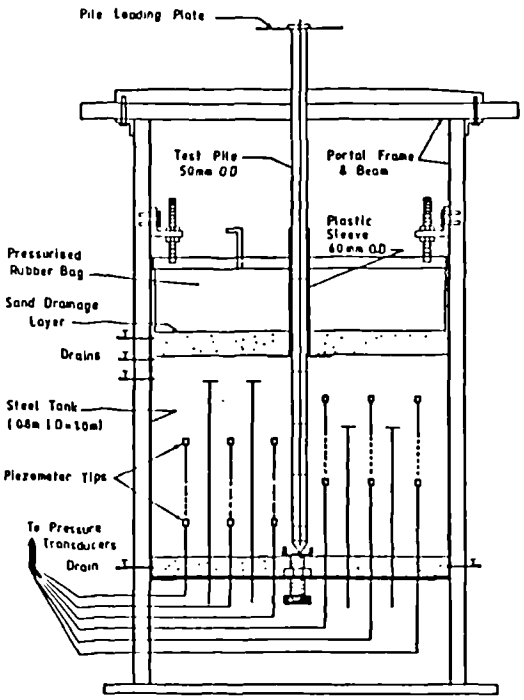

Fig. 1 Experimental apparatus

Soil instrumentation

Twelve piezometers were embedded at four different levels and four settlement plates at two different levels in order to monitor both pore pressure and settlement during the consolidation process. The miniature piezometers were of the high air entry hydraulic type and were designed and fabricated within the workshops of the Department of Civil Engineering. The piezometer tips measured 15mm length by 12mm in diameter; water pressure on each tip was read via a digital strain meter. The settlement plates consisted of 30mm diameter by 2mm thick stainless steel discs attached to 1.5mm sleeved steel rods fed through water-sealed apertures formed in the base of the chamber.

Pile instrumentation

Axial load was measured at nine vertical positions on the pile shaft, Fig. 2. The pile was divided into six sections, five of which were instrumented with foil type bi-directional electrical resistance strain gauges. These were mounted on the inside surface of the pile. Each load cell comprised four active and four dummy strain gauges configured to form a full bridge circuit.

Experimental procedure and testing programme

Prior to filling the testing chamber with soil the piezometer lines, settlement rods and peripheral filter fabric were fixed in position.

The clay was thoroughly mixed at natural water content using a large bowl mixer and then carefully placed by hand into the chamber. A saturated layer of sand provided drainage on the top surface of the clay.
Before starting the testing programme a time period of 40 days was found necessary for equilibration of pore pressures due to self - weight consolidation . At the end of the period required for the soil to consolidate, the rubber bag and its retaining plate were placed in position and the pile was carefully pushed from the top through a guide collar until the required depth had been reached and the pile tip had located itself onto a bearing plate positioned centrally on the base of the chamber.
The testing programme comprised increasing the surcharge pressure in four successive stages: 15, 30, 45, and 90kPa. Readings of pore water pressure, settlement and pile axial load were commenced immediately after pile driving. The duration of the testing programme was approximately six months.

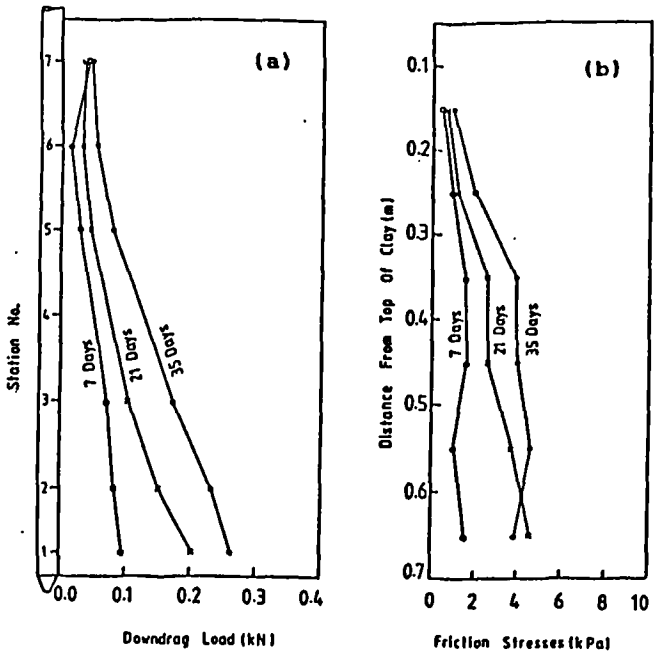

Fig. 2 Distribution of downdrag load and contact friction stresses surcharge pressure 15kPa

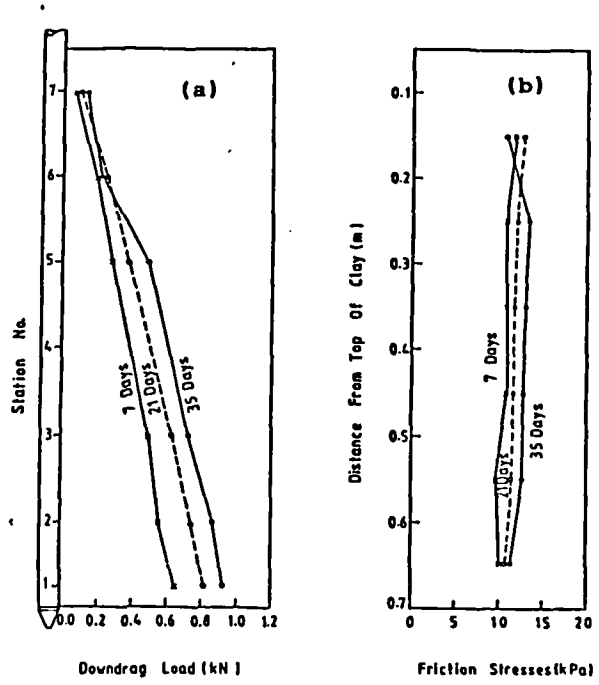

Fig. 3 Distribution of downdrag load and contact friction stresses surcharge pressure 90kPa

Results

(i) Pile axial force

The vertical distributions of axial force in the test pile at the end of the 15kPa and 90kPa loading stages are shown in Figs. 2 and 3.
Each point plotted on these figures represents the average value derived from four strain gauge readings. The difference in load between each measuring station represents the increased loading caused by the consolidating clay.
Considering Fig.2, an increase in downdrag was noticeable at day 21 on stations 1,2 . The distribution of negative skin friction shown in Fig. 2b indicated a slight decrease in frictional stress at day 35. This may be explained by the development of a small amount of positive frictional stress at the lower end of the pile. Fig. 3b indicates that a constant negative skin friction value of approximately 13 kPa was attained at the 90 kPa stage.
For both loading stages the axial force in the pile increased with depth along the pile shaft with the maximum force registered near to the pile tip.

(ii) Pore water pressure.

Dissipation of excess pore water pressure with time is shown in Figs. 4,5 for the 15 kPa and 90 kPa loading stages.
During the 15 kPa loading stage an excess pore pressure of 14 kPa was recorded at approximately 400mm from the top of the clay.
A relatively slow and steady rate of pore water pressure dissipation was evident during the 90 kPa loading stage. Readings on the four piezometers were 41 kPa, 37 kPa, 33 kPa and 30 kPa from top to bottom respectively.

(iii) Settlement

During the 15 kPa stage settlements of 44mm (settlement at the centre of the clay surface) and 27mm (average settlement of the clay bed obtained from measurements of drainage) were recorded, Fig. 6. This same difference in settlement was not evident during the 90 kPa loading stage where a total settlement of between 35mm and 40mm was recorded, Fig. 7.

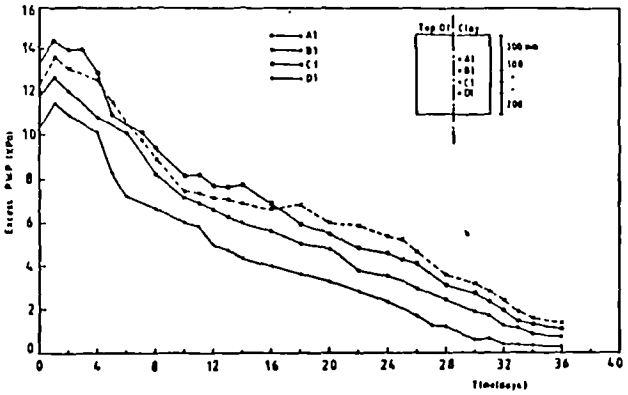

Fig. 4 Excess pore pressure versus time, surcharge pressure 15kPa

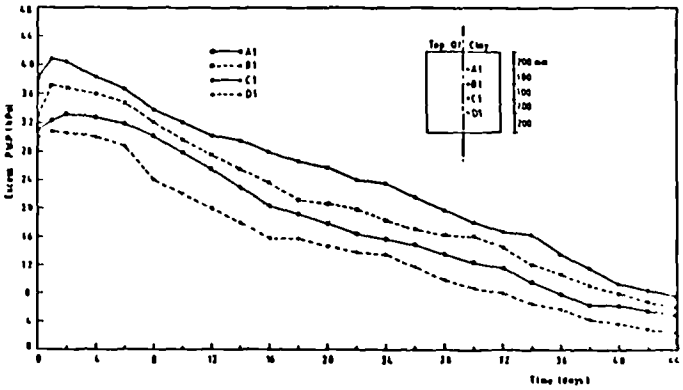

Fig. 5 Excess pore pressure versus time, surcharge pressure 90kPa

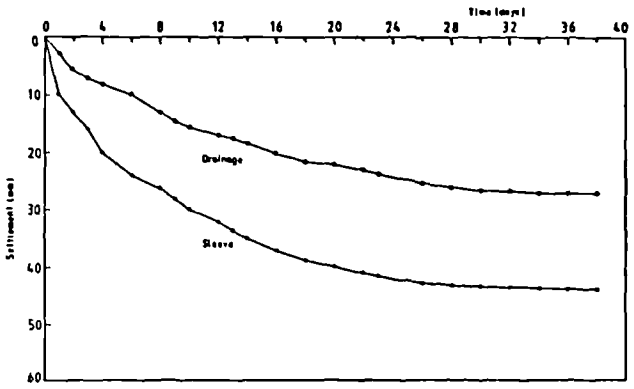

Fig. 6 Settlement versus time, surcharge pressure 15kPa

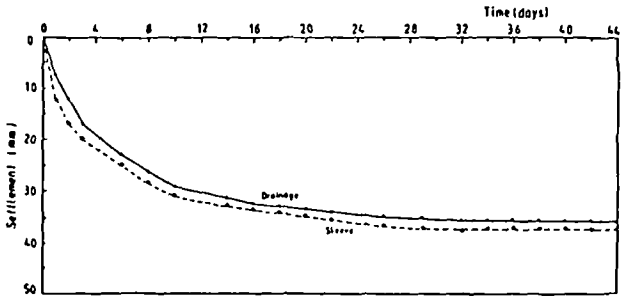

Fig. 7 Settlement versus time, surcharge pressure 90kPa

Discussion

A combination of the average measured axial forces on the pile shaft for each stage of the testing programme with the properties of the soil obtained from laboratory testing has enabled values for K and β to be evaluated, Figs. 8, 9. The average values for thus indicated (in the range 0.1 to 0.2) are very similar to those reported by Bjerrum et al (1969) and Endo et al (1969). Values for the adhesion factor α indicated from the results have been calculated in two ways: from the initial α measured undrained shear strength of the soil at the beginning of each loading stage, and from the calculated value of the undrained shear strength appropriate to the changing degree of consolidation.
The adhesion values obtained assuming a constant initial undrained shear strength ranged between 0.27 and 2.13. Taking into account the changing shear strength due to consolidation resulted in calculated adhesion values in the range 0.29 to 0.58.
It is useful to view changing adhesion values with settlement ratio, Figs. 10, 11. Fig. 10 indicates that the rate of increase of α based on the measured initial undrained shear strength was approximately 25% for every 2% increase of the settlement ratio, while Fig. 11 shows that the rate of increase of α determined from the calculated values of undrained shear strength reached a limiting value of approximately 0.6 at a settlement ratio of 10% .

Conclusions

1. Negative skin friction was found to increase with time after application of surcharge pressure and then to attain a limiting value.

2. The time dependent build-up of negative skin friction is controlled by the rate of consolidation of the clay bed and therefore the degree of dissipation of excess pore pressure.

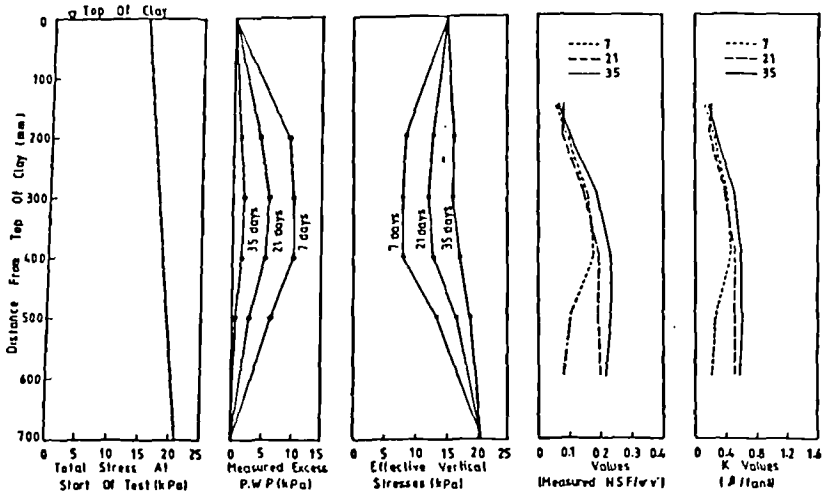

Fig. 8 Evaluation of β and K values, surcharge pressure 15kPa

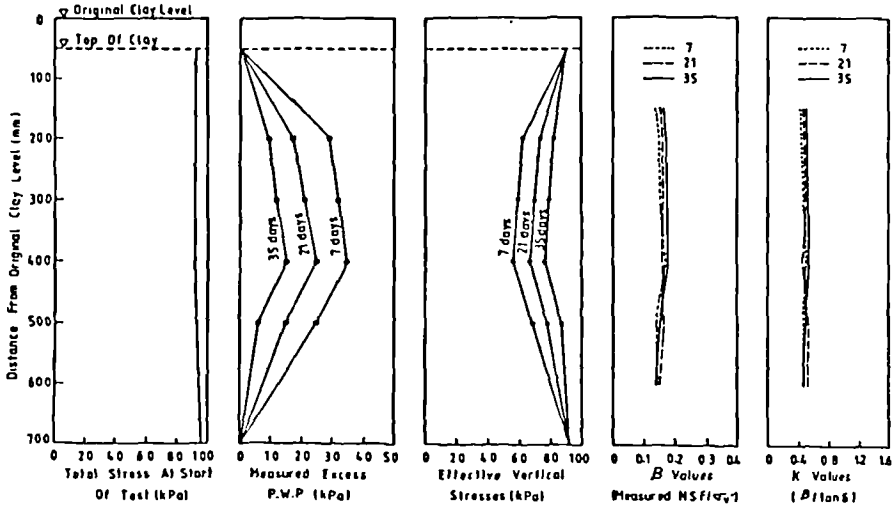

Fig. 9 Evaluation of β and K values, surcharge pressure 90kPa

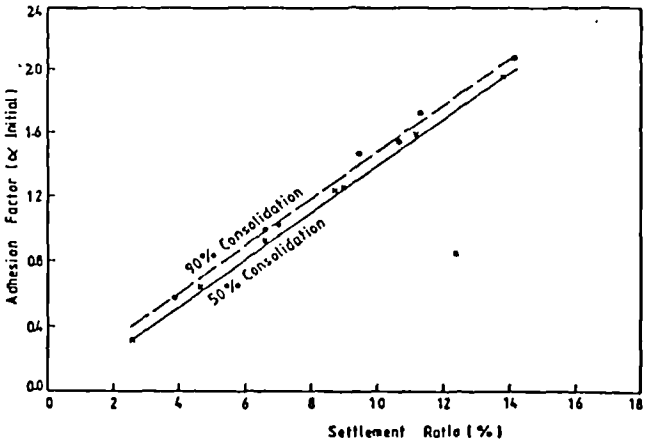

Fig. 10 Variation of adhesion factor α (initial) with settlement ratio

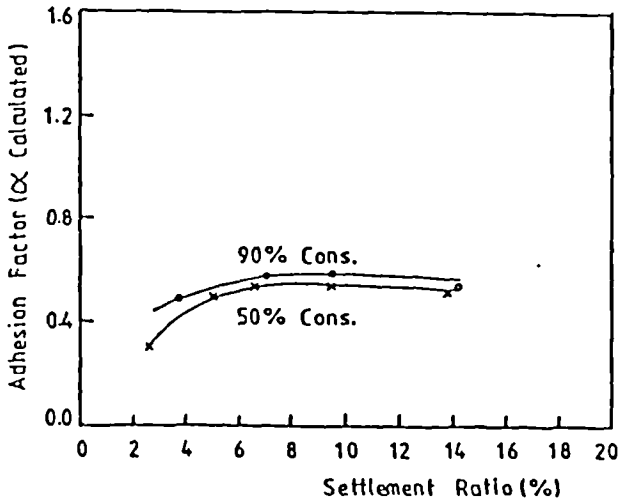

Fig. 11 Variation of adhesion factor α (calculated) with settlement ratio

3. An effective stress analysis gave values for β in the order of 0.2, values consistent with the findings of others.

4. A total stress analysis revealed a wide range of values for α when based on the initial undrained shear strength of the clay. An alternative method utilising calculated values for changing shear strength produced values in the range 0.29 to 0.58.

Acknowledgements

The work described in this paper was carried out in the Department of Civil Engineering, Heriot-Watt University. The authors are therefore grateful to the Head of the Department of Civil Engineering for the provision of facilities to enable its completion. The authors also thank Mr.E.L.Pole and Mr. H.Barras for their valuable assistance in this work.

References

Bjerrum, L., Johannessen, I.J. and Eide, O. (1969). Reduction of negative skin friction on steel piles to rock. Proc. 7th. Int.Conf. Soil Mech. Found. Eng., Mexico, Vol. 2, 27-33.

Broms, B.B. (1979). Negative skin friction, state-of-the-art report. Proc. 6th. Asian Regional Conf. Soil Mech. Found. Eng., Singapore, Vol. 2, 41-75.

Burland, J. (1973). Shaft friction of piles in clay. Ground Engineering, Vol.6, No.3, 30-42.

Chellis, R.D. (1961). Pile Foundations, McGraw-Hill, 2nd. Ed., 704pp.

Endo, M., Minov, A., Kawasaki, T. and Shibata, T. (1969). Negative skin friction acting on steel pipe piles in clay. Proc. 7th Int. Conf. Soil Mech. Found. Eng., Mexico, Vol. 2, 85-92.

Garlanger, J.E., (1973). Prediction of the downdrag load at Cutler Circle Bridge. In: Garlanger and Lambe (eds), Proc. Symp. on Downdrag of Piles, M.I.T., Cambridge, Massachusetts. (Research Report R73-56, Soil-331, Department of Civil Engineering, M.I.T.)

Gostelow, T.P., and Browne, M.A.E., (1986). Engineering geology of the upper Forth Estuary. British Geological Survey Report, Vol. 16, No.8, 56pp.

Skempton, A.W., (1953). The colloidal activity of clays. Proc. 3rd. Int. Conf. Soil Mech. Found. Eng., Switzerland, Vol. 1, 57-61.

Tomlinson, M.J. (1977). Foundation Design and Construction, Pitman Publishing, 3rd. Ed., 785pp.

REFERENCES

ABOSHI, H., (1955)," Measurement of pore water pressure during consolidation of fine grained soil", Bulletin of the faculty of engineering, Hiroshima Univ., Vol. 4, PT.1, PP.1-12.

ALDRICK, JR., H.P. (1970), "Back Bay, Boston- Part 1," Journal of the Boston Society of Civil Engineers, Vol. 57, No.1 .

AUVINET, G. and HANELL, J.J. (1981), "Negative skin friction on piles in Mexico City clay," Proc. Of the 10th Conf. SMFE, Stockholm, Sweden, Vol. 2, PP. 599-604.

BAGUELIN, F. and FRANK, R., (1979), " Theoretical studies of piles using the finite element method", Numerical Methods in Offshore Piling Conf., ICE. PP.65-74.

BALAAM, N.P., POULOS, J.R., and BROOKER, J.R.,(1975), "Finite element analysis on the effects of installation on pile load-settlement behaviour", Geotechnical Eng., Proc. ASCE, Vol. 6, p. 33-48.

BARDEN, L. and BERRY, L., (1969), " Consolidation of

normally consolidated clay", Journal of the SMFE Div., SM5, PP. 15-35.

BEGEMANN, H.K.S.P. (1969), " Negative skin friction of a single pile," Proceedings, Specialty Session on Negative Skin Friction and Settlement of Piled Foundations, 7th Int. Conf. SMFE, Mexico, 3 PP.

BJERRUM, L., JOHANNESSEN, I.J. and EIDE, O. (1969), "Reduction of negative skin friction on steel piles to rock," Proceedings, 7th. Int. Conf. SMFE, Mexico, Vol. 2, PP. 27-33 .

BOZOZUK, M. (1970), " Field observations of negative skin friction loads on long piles in marine clay," Proc. Conf. on Design and Installation of Pile Foundations and Cellular Structures, Lehigh Univ., PP. 273-280

BOZOZUK, M. (1972), " Downdrag measurements on a 160- ft floating pipe test pile in marine clay," Canadian Geotechnical Journal, Vol. 9, No. 2, PP. 127-136.

BOZOZUK, M. (1981), " Bearing capacity of pile preloaded by downdrag," Proc. of the 10th Conf. SMFE, Stockholm, Sweden, Vol. 2, PP. 631-636.

BRAND, E.W. and LUANGDILOK, N. (1975), " A long-term failure caused by dragdown on piles," Proceedings, 4th.

Southeast Asian Conf. Soil Engng., 4.15-4.24 .

BURLAND, J. (1973), "Shaft friction of piles in clay," Ground Engineering, Vol. 6, No. 3, PP. 30-42 .

BUTTERFIELD, R. and BANERJEE, P.K. (1978)," The elastic analysis of compressible piles and pile groups", Geotechnique, Vol. 21, PP. 43-60.

CHELLIS, R.D. (1961), " Pile Foundations," McGraw-Hill Co., 2nd Ed., 704 PP .

LEMENT, F.M.JR., (1984), " Downdrag, negative skin friction and bitumen coatings on prestressed concrete piles," Ph.D Thesis Submitted to the University of Tulane, 325 PP.

DESAI, C.S. and CHRISTIAN, J.T., (1977), " Numerical methods in geotechnical engineering", McGraw-Hill Co., NewYork.

DESAI, C.S., LIGHTNER, J.G. and SARGAND, S., (1982), " Mixed and hybrid procedures for non-linear problems in geomechanics", Proc. 4th Int. Conf. on Numerical Methods in Geomechanics, Univ. of Alberta, Edmonton, Canada.

ELMASRY, M.A. (1963), " The negative skin friction of bearing piles," Ph.D Thesis, Swiss Federal Institute of

Technology, Zurich, 115 PP.

ENDO, M., MINOV, A., KAWASAKI, T. and SHIBATA, T., (1969), " Negative skin friction acting on steel pipe-piles in clay," Proc., 7th. Int. Conf. SMFE, Mexico, Vol. 2, PP. 85-92 .

ELLENIUS, B.H. (1969), " Negative skin friction on piles in clay - A literature Survey," Proc., Specialty Session, Negative Skin Friction and Settlement of Pile Foundations, 7th. Int. Conf. SMFE, Vol. 2, 8 PP

FELLENIUS, B.H. (1972), "Downdrag on piles in clay due to negative skin friction," Can. Geotechnical Jour., Vol. 9 , No. 4 , PP. 325-337.

FELLENIUS, B.H. and BROMS, B.B. (1969), " Negative skin friction on long piles driven in clay," Proc. 7th Int. Conf. SMFE, Mexico, Vol, 2, PP. 93-98.

GANT, E.V., STEPHENS, J.E. and MOULTON, L.K. (1958), " Measurement of forces produced in piles by settlement of adjacent soil," Highway Research Board, Bull. 173, Analysis Of Soil Foundation Studies, PP. 20-37.

GARLANGER, J.E. and LAMBE, T.W. (1973), "Proceedings of a Symposium on Downdrag of Piles," Mass. Inst. Techn., Cambridge, Mass., Research Report, No. 73-56, 104 PP.

GARLANGER, J.E. (1974), " Measurement of pile downdrag beneath a bridge abutment," Highway Research Board, Transp. Research Record, No. 517, PP. 61-69 .

GHABOUSSI, J., WILSON, E.L. and ISENBERG, J., (1973), "Finite element for rock joints and interfaces", Jour. of Soil Mech. and Found. Div., ASCE, 99, (SM10), PP. 512-535.

GIBSON, R.E. and LUMB, P. (1953), " Numerical solutions of some problems in the consolidation of clay", Proc., ICE, Part 1, Paper No. 5877.

GOSTELOW, T.P., and BROWNE, M.A.E., (1981), " Engineering geology of the upper Forth Estuary", British Geotechnical Survey Report, Vol. 1, 57PP.

HANSEN, J.B. (1968), "A theory for skin friction on piles," Danish Geotechnical Institute, Bulletin No. 25, PP. 5-12.

HARRIS, M.C. (1964)," Model pile behaviour in a clay soil," M.Sc. thesis, University Of Alberta, 164pp.

HINTON, E. and OWEN, D.R.J. (1978)," Finite Element Programming," Academic Press.

HOLTZ, R.D. and KOVACS, W.D. (1981), "An Introduction to

Geotechnical Engineering," Prentice Hall Inc., Englewood Cliffs, New Jersy .

JAKY, J., (1944), " The coefficient of earth pressure at rest," Magyar Mernokes Epitesz Egyiet Kozlonye.

JOHANESSEN, I.J. and BJERRUM, L. (1965)," Measurement of the compression of a steel pile to rock due to settlement of the surrounding clay,"Proc. 6th Int. Conf. SMFE, Vol.2, Montreal, PP. 261-264.

KATONA, M.G., (1981), " A simple contact-friction interface element with applications to buried culverts", Proc. Symp. on Implications of Computer Procedures and Stress-Strain Laws in Geotech. Eng., Chicago, Illinois, Vol. 1, PP. 45-63.

KERISEL, J. (1965)," Vertical and horizontal capacity of deep foundations in clay," Symposium On Bearing Capacity And Settlement Of Foundations, Duke University, USA, PP. 45-61.

KERISEL, J. (1976), "Deep foundations-basic experimental facts," Proc. North American Conf. on Deep Foundations, Mexico City, PP. 121-137.

KOERNER, R.M. and MUKHOPADHYAY, C. (1972), "Behaviour of negative skin friction on model piles in medium plasticity

silt," Highway Research Record, No. 405, PP. 34-44.

MILLER, R.M. (1938), "Soil reactions in relation to foundations on piles,"Trans. ASCE, Vol.103, PP. 1193-1236.

MINDLIN, R.D., (1936), " Force at a Point in the Interior of a Semi-Infinite Solid ", Physics, PP.532-547

MISLIVEC, A. (1972)," Pressure at rest of cohesive soils," Proc., 5th Europ. Conf. SMFE, Madrid, Vol. 1, PP. 63-67.

MITCHELL, A.R., (1969)," Computational methods in partial differential equations", John Wiley and Sons, New York.

MURRAY, R.T. (1971), " Embankments constructed on soft foundations: settlement study at Avonmouth, TRRL Report LR 419.

NARASIMHA, R.S. and KRISHNAMURTHY, N.R. (1982), "Studies of negative skin friction in model piles," Indian Geotechnical Eng. Vol. 13, Part 1 (June), PP. 83-91.

NISHI, K. and ESASHI, Y., (1982), " Field measurement and prediction of negative friction on piles", Int. Symp. on Numerical Models in Geomechanics, Zurich, PP. 776-784.

NICHOLLS, R.A. (1973), "Negative friction on piled foundations," Ph.D thesis, University of Wales, UWIST.

PARRY, R.H.G. and SWAIN, G.W. (1977a)," Effective stress methods of calculating skin friction on driven piles in soft clays," Ground Eng., Vol. 10, No.3, PP. 24-26.

PARRY, R.H.G. and SWAIN, G.W. (1977b)," A study of skin friction on piles in stiff clay," Ground Eng., Vol. 10, No.5, PP. 33-37.

PERLOFF, W.H., BALADI, G.Y. and HARR, M.E. (1967)," Stress distribution within and under long elastic embankments. Embankments And Their Foundations, Highway Res. Rec., No. 181, PP. 12-40.

POTYONDY, J.G., (1961), "Skin friction between various soils and construction materials," Geotechnique, Vol. 11, PP. 339-353 .

POULOS, H.G. and DAVIS, E.H. (1972)," The development of negative friction with time in end-bearing piles," Australian Geomechanics Jour., Vol. C2, No. 1, PP. 11-20 .

POULOS, H.G. and DAVIS, E.H. (1975), "Predictions of downdrag forces in end-bearing piles," Jour. of the Geotechnical Eng. Division, ASCE, Vol. 101, No. GT2, February, PP. 189-204.

POULOS, H.G. and MATTES, N.S. (1969)," The analysis of

downdrag in end-bearing piles," Proc. 7th Int. Conf. SMFE, Mexico City, Vol. 2, PP. 203-209.

SALAS, J.A. and BELZUNCE, J.A (1965)," Resolution Theorique de la distribution des forces dans des pieux," Proc. 6th Int. Conf. SMFE, Vol. 6, Montreal, PP. 309-313.

SCOTT, R.F. (1963), "Principles of Soil Mechanics ," Addison-Wesley Pub. Co.

SIAH, B.S. (1980)," A study of pile-sand interaction," Ph.D thesis, University Of Leeds, 417PP.

SILVA, A.J. (1966), " Downdrag on piles," Ph.D thesis, University of Connecticut, 123 PP.

SILVEIRA, I.D. (1953), "Consolidation of a cylindrical clay sample with external radial flow of water," Proc. 3rd Int. Conf. SMFE, Vol. 1, PP. 83-86.

TERZAGHI, K. and PECK, R.B. (1948), " Soil mechanics in engineering practice, John Wiley and Sons, New York, 566PP

TERZAGHI, K. and PECK, R.B. (1967)," Soil mechanics in engineering practice, John Wiley and Sons, New York, Second Edition, 729PP.

TOMA, T.M. (1984), " Base-shaft interaction of an insitu

axially loaded pile," M.Sc thesis, University of Baghdad, Iraq.

TOMLINSON, M.J. (1957)," The adhesion of piles driven in clay soils," Proc., 4th. Int. Conf. SMFE, London, Vol. 2, PP. 66-71 .

VAN WEELS, A.F. (1964)," Negative skin friction on pile foundations in Holland," Symposium on Bearing Capacity of Piles, Roorkee, India, PP. 1-10 .

WALKER, L.K. and DRAVALL, P.L.P. (1973), "Dragdown on coated and uncoated piles," Proc., 8th. Int. Conf. SMFE, Moscow, Vol. 2.1, PP. 257-262 .

ZEEVAERT, L. (1973), "Foundation Engineering for Difficult Subsoil Conditions," Van Nostrand Reinhold Co. New York, 652 PP.

ZIENKIEWICZ, O.C. (1970)," Analysis of non-linear problems with particular reference to joined rock systems", Proc. 2nd Int. Conf. Society of Rock Mech., Belgrade, Vol. 3, PP. 501-509.